NBSIR 84-2852

RADC/NBS Workshop Moisture Measurement and Control for Semiconductor Devices, III

U.S. DEPARTMENT OF COMMERCE
National Bureau of Standards
National Engineering Laboratory
Center for Electronics and Electrical Engineering
Semiconductor Materials and Processes Division
Washington, DC 20234

May 1984

U.S. DEPARTMENT OF COMMERCE
NATIONAL BUREAU OF STANDARDS

NBSIR 84-2852

RADC/NBS WORKSHOP MOISTURE MEASUREMENT AND CONTROL FOR SEMICONDUCTOR DEVICES, III

Proceedings of the RADC/NBS Workshop
held at the National Bureau of Standards
Gaithersburg, MD

November 2-4, 1983

Benjamin A. Moore and Stanley Ruthberg, Editors

U.S. DEPARTMENT OF COMMERCE
National Bureau of Standards
National Engineering Laboratory
Center for Electronics and Electrical Engineering
Semiconductor Materials and Processes Division
Washington, DC 20234

This activity was sponsored by:

Rome Air Development Center
RBRE
Griffiss AFB, NY 13441

and

National Bureau of Standards

May 1984

U.S. DEPARTMENT OF COMMERCE, Malcolm Baldrige, *Secretary*
NATIONAL BUREAU OF STANDARDS, Ernest Ambler, *Director*

Table of Contents

Preface

A third workshop on Moisture Measurement Technology for Semiconductor Devices was held at the Gaithersburg, Maryland, facility of the National Bureau of Standards on November 2 to 4, 1983, under the co-sponsorship of the Rome Air Development Center (RADC) and the National Bureau of Standards (NBS). It was another in a series of workshops that have been conducted as part of the Semiconductor Technology Program of the NBS. These workshops have been dedicated to the furtherance of the measurement technology needed by the semiconductor device industry in its attempt to provide to its customers products that are based on the most advanced technology, yet have high reliability and the affordable costs which result from high yields. Representatives from industrial, governmental, and academic organizations concerned with device manufacture, analysis, and instrument design participated.

These workshops have provided a forum for reporting the continuous progress that has been made in the measurement of moisture in hermetic semiconductor devices, in the correlation between measurements by different procedures, in determining the sources of moisture, in test environments, and in process control. Thirty-four formal presentations were given.

The workshop was co-chaired by Benjamin A. Moore of RADC and Stanley Ruthberg of NBS; Sara R. Torrence and Kathleen D. Kilmer of NBS coordinated workshop arrangements; Pamela M. Baker of NBS was responsible for fiscal matters and registration; E. Jane Walters of NBS provided editorial assistance and supervised processing of these Proceedings; and Brenda L. Kefauver, Marilyn L. Stream, Jennifer L. Allen, and Josephine S. Halapatz assisted in operational details.

Disclaimers

The views and conclusions expressed are those of the authors and do not necessarily represent the official policies of the Department of Defense, Department of Commerce, or the United States Government.

Certain commercial equipment, instruments, or materials are identified in papers published in this report in order to adequately specify the experimental procedure. In no case does such identification imply recommendation or endorsement by the National Bureau of Standards, nor does it imply that the material or equipment identified is necessarily the best available for the purpose.

Papers in this volume have not been edited by the National Bureau of Standards. Non-NBS authors are solely responsible for the content and quality of their submissions.

RADC/NBS Workshop
Moisture Measurement and Control for Semiconductor Devices, III

- A Workshop Report -

Benjamin A. Moore (RADC) and Stanley Ruthberg (NBS)

The workshop, one of a series concerned with measurement problems in integrated circuit processing and assembly, served as a forum to examine the continuing progress that has been made in the measurement and control of moisture in hermetically packaged semiconductor devices. Thirty-four presentations are included which contain detailed information for securing hermetic packages with low moisture content. Agreement in measurement has been obtained with the mass spectrometer for cerdip and metal packages at the 5000 ppmv level of moisture through the use of suitable moisture generators, a 3-volume calibrator, calibrated dewpoint hygrometers, and appropriate operational procedures. An approach is given for a reproducible and reliable transfer package. However, the increased use of organic materials in new and rapidly expanding technologies such as VLSI/VHSIC and hybrid packaging presents new and more complex challenges to accurate measurement of interior moisture.

Key words: analysis of moisture content; hermetically packaged semiconductor devices; hybrid packages; mass spectrometer measurements; moisture; organic package materials; moisture generators; moisture sensors; quality control; reliability of semiconductor devices; semiconductor devices.

1. Introduction

A workshop on Moisture Measurement and Control for Semiconductor Devices was held at the National Bureau of Standards in Gaithersburg, Maryland, on November 2 to 4, 1983, co-sponsored by the Rome Air Development Center and the National Bureau of Standards. It was another in a series concerned with measurement problems related to integrated circuit processing, assembly, and reliability. This was the third workshop at NBS concerned with the moisture measurement and control problem. The first workshop was sponsored by Defense Advanced Research Projects Agency/National Bureau of Standards (DARPA/NBS) on March 22 to 23, 1978 (see NBS Special Publication 400-69, Semiconductor Measurement Technology: ARPA/NBS Workshop V, Moisture Measurement Technology for Hermetic Semiconductor Devices, May 1981). The second workshop was sponsored by NBS/RADC on November 5 to 7, 1980 (see NBS Special Publication 400-72, Semiconductor Measurement Technology: NBS/RADC Workshop, Moisture Measurement Technology for Hermetic Semiconductor Devices, II).

Progress has continued in the measurement and control of moisture in hermetically packaged semiconductor devices. At the time of the first workshop in 1978, interlaboratory measurement precision was poor, although it appeared that individual laboratory precision of mass spectrometer measurements could

be adequate. It also appeared that the use of moisture sensors was becoming practical, but correlation to the mass spectrometer was low. Now, however, as presented in the third workshop, agreement in measurement has been obtained with the mass spectrometer for cerdip and metal packages at the 5000 ppmv level of moisture through the use of suitable moisture generators, a 3-volume calibrator, calibrated dewpoint hygrometers, and specific operational procedures. The procedures by which such agreement can be obtained, including extended computer control and data processing, are presented.

A reproducible and reliable transfer standard, i.e., a simulated package of known volume and moisture control, could be a very helpful device. Achievement of such a structure has been elusive. An approach for this was presented as based upon a demountable metal seal over a machined volume.

Nondestructive measurement techniques such as a capacitance-ratio method on the IC die and internal moisture sensors of both the oxide and surface conductivity types have become useful for production control and for diagnostics of materials behavior. The thermal and the aging characteristics of the oxide sensor, which affect the sensor's precision, are better known.

The sorption of water on package components and its effect on corrosion and performance along with allowable levels within packages are topics that were addressed. Of primary concern now is the increased use of organic materials such as epoxies, polyimides, dessicants, etc. in new and rapidly expanding technologies such as VLSI/VHSIC and hybrid packaging which present new and more complex challenges to the accurate measurement of moisture.

The workshop included 34 presentations in 7 sessions on topics such as Method 1018.2 of MIL-STD-883, measurement methods, sensors, hermeticity, moisture physics, organic materials, and moisture control.

2. SESSION I METHOD 1018.2 MOISTURE ANALYSIS

2.1 WHAT'S HAPPENING AT RADC

BENJAMIN A. MOORE
ROME AIR DEVELOPMENT CENTER
GRIFFISS AFB NY 13441
(315)330-4055

ABSTRACT

The following information was initially prepared to be presented as informal comments during a "rump" session or question/answer period during the Moisture Workshop. Therefore, no formal text was prepared. However, due to a paper withdrawal, the information was presented during the Method 1018.2 Moisture Analysis Session (I). A brief discussion of the accompanying tables and figures follows.

DISCUSSION

Table I outlines current efforts at RADC to improve the quality and scope of moisture measurements while anticipating and meeting the challenges of new (VHSIC) and burgeoning technologies (hybrid). Issues of concern with accompanying current and planned activities to address them are presented.

The results of an in-house experiment to determine the feasibility of producing an organic containing standards are presented in Table II. The potential is demonstrated. However, work must be done to evaluate the moisture uptake in epoxies and the best methods (i.e., pre-analysis bake) of assuring acceptable analytical accuracy.

Figures 1-7 present some of our current efforts in advanced software development. When completed, the software will provide the capabilities of evaluating moisture desorption from package materials, temperature and sample volume effects, and specie related phenomena (i.e. hydrogen pumpout characteristics). Though not shown on the accompanying figures, date and experimental information is now included.

As shown in Figure 1, any single mass scan from an analysis may be examined. Figures 2 and 3 detail sample pressure measurement and pumpout curves. Unusual pumpout phenomena can be detected using these features. Figure 4 shows the pumpout curve for a typical "ideal" acting gas (N_2) in contrast to moisture as shown in Figure 5. The option now exists to extrapolate the moisture curve until it reaches background. The effects of moisture desorbing materials on a mass spectrometric gas analysis can be seen in Figures 6 and 7. It should be noted that Figures 5-7 present both the raw data points and a "best-fit" polynominal to the data. This information is used in comparing discrete (point-to-point) and integrated (Simpson's Rule) gas analysis.

A recent in-house comparison of plating processes is detailed in Figure 8-11. Examination of this data shows that gold over electrolytic plating will yield the minimum package effect on microelectronic device ambients.

CONCLUSIONS

A very brief overview on current efforts at RADC has been presented. While much of the material is self-explanatory, questions or comments concerning these areas are encouraged and should be directed to the author.

TABLE I

MOISTURE MEASUREMENTS & EFFECTS

PROBLEM: ELIMINATION OF MOISTURE AIDED & ABETTED FAILURES

ISSUE	ACTIVITIES
• QUALITY MEASUREMENT ASSURANCE	O NEW GENERATION STANDARDS
• ACCEPTABLE MOISTURE LEVELS	O INDEPENDENT STANDARD-JPL
• LABORATORY RECERTIFICATION	X RECERTIFICATION VIA DEWPOINT HYGROMETER
• NEW TECHNIQUES	O COMMERCIAL LASER SPECTROMETER SYSTEM
	O CAPACITANCE-RATIO/MASS SPEC CORRELATION
	X NEW PROCEDURES IN 1018
• MATERIALS EFFECTS VLSI/VHSIC & HYBRIDS	O IN-HOUSE EVALUATION OF ANALYTICAL TECHNIQUES AND CONDITIONS
• INCREASING SAMPLE VOLUMES	O IN-HOUSE DEVELOPMENT IMPROVED SOFTWARE
	X CHANGES TO 1018 (PRE-ANALYSIS BAKE, ETC.)

O CURRENT ACTIVITIES X=PLANNED (JEDEC COORDINATION REQUIRED)

TABLE II

IN HOUSE STANDARD DEVELOPMENT

CONDITIONS	SEAL H_2O, ppm_v	ANALYZED H_2O, ppm_v BAKED	NON-BAKED
N_2	2620	2110	2130
N_2, 1 MG EPOXY	2620	19770	6740
N_2, AIR	5720	8580	5080
N_2, AIR 1 MG EPOXY	5720	59490	57540 (~2 μ GRAMS)

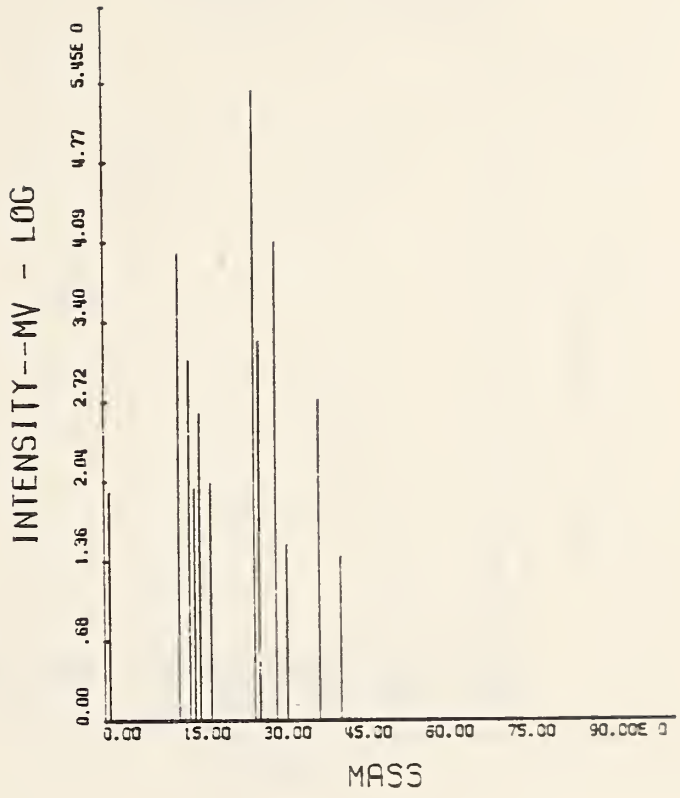

FIGURE 1

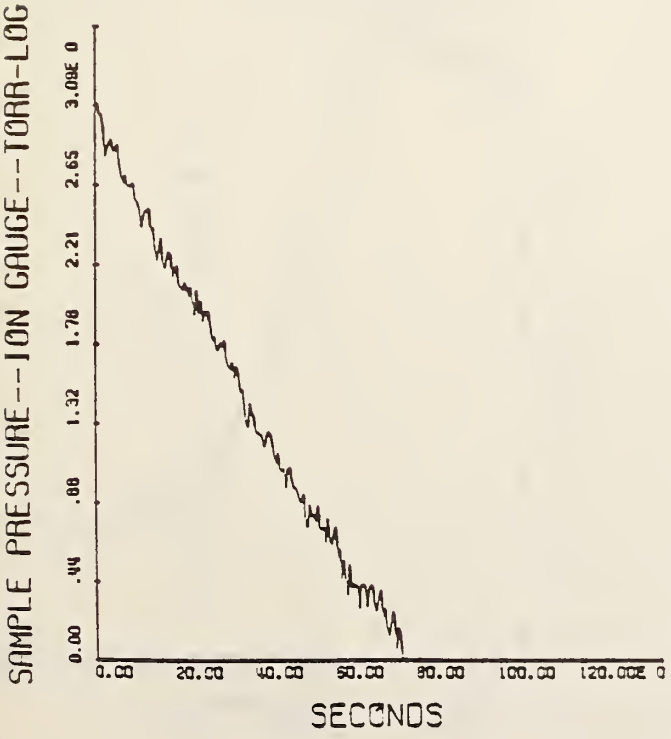

FIGURE 2

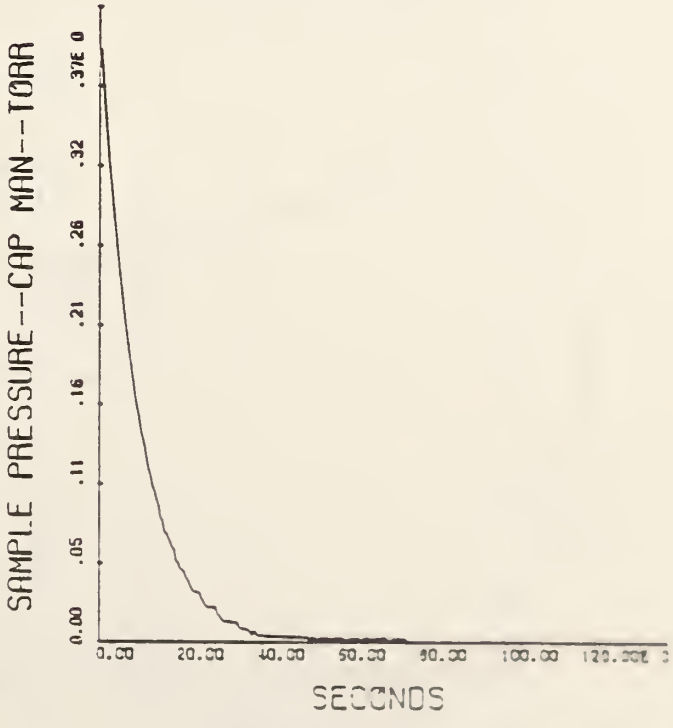

FIGURE 3

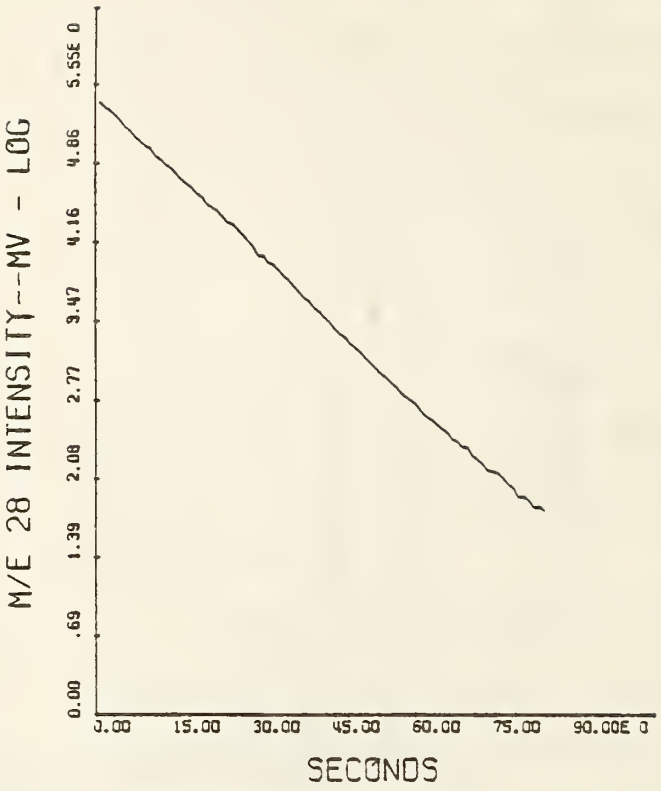

FIGURE 4

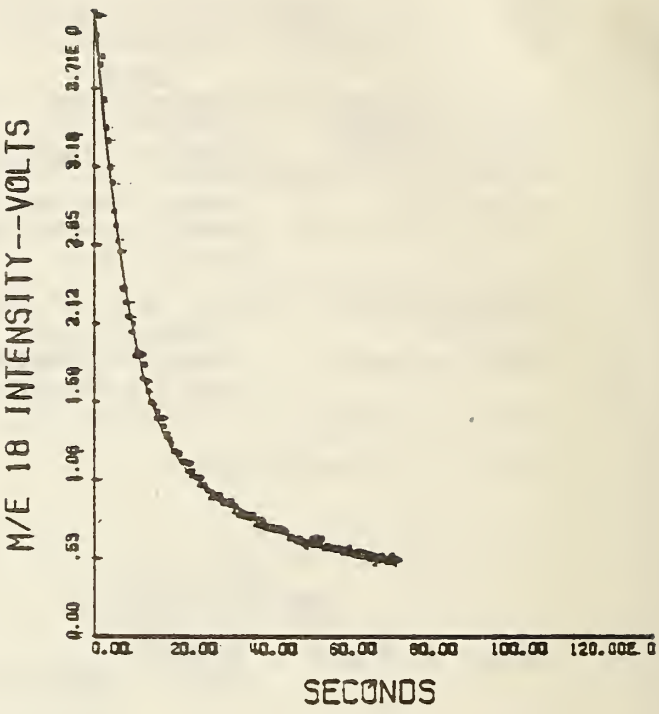

FIGURE 5

FIGURE 6

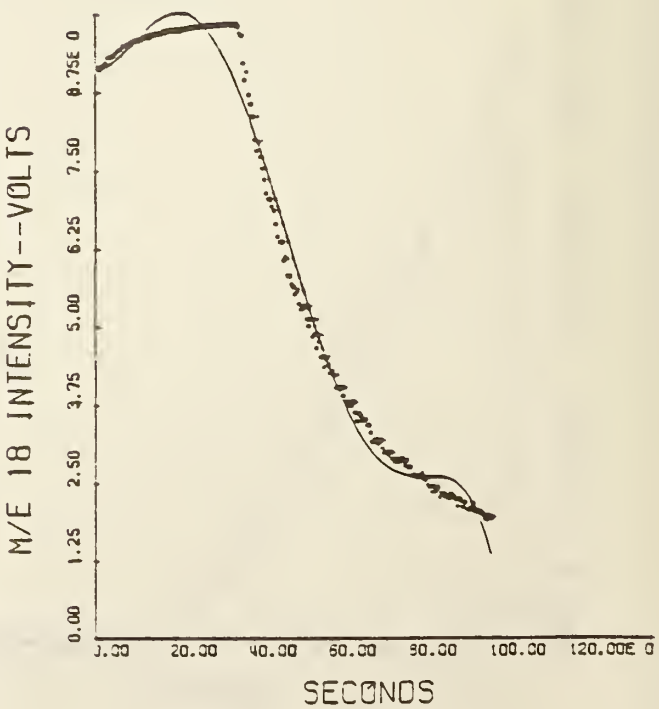

FIGURE 7

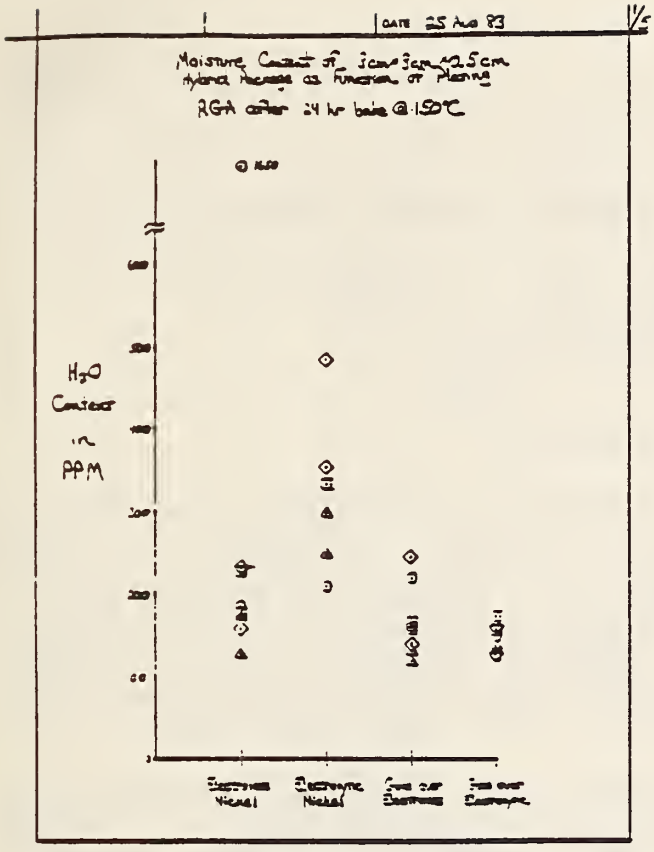

FIGURE 8

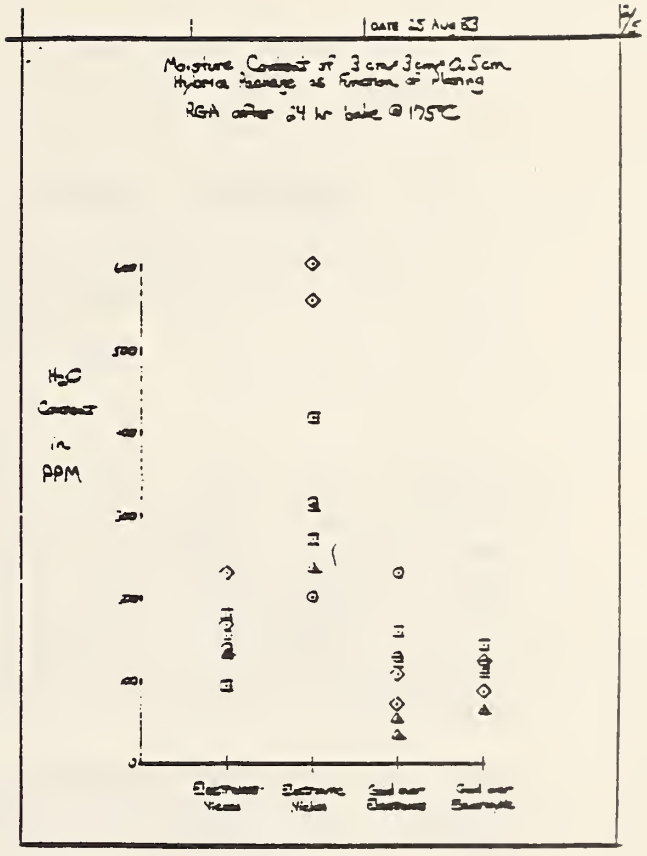

FIGURE 9

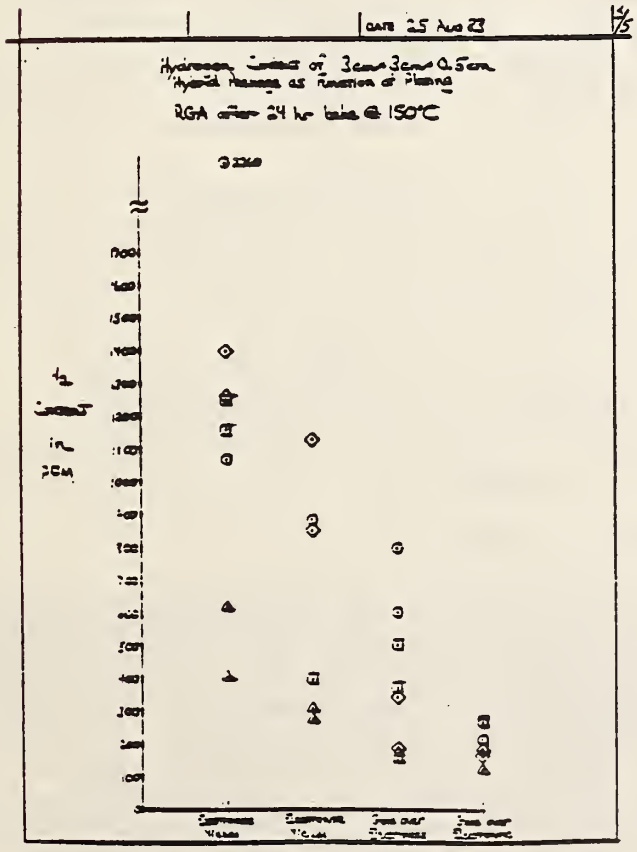

FIGURE 10

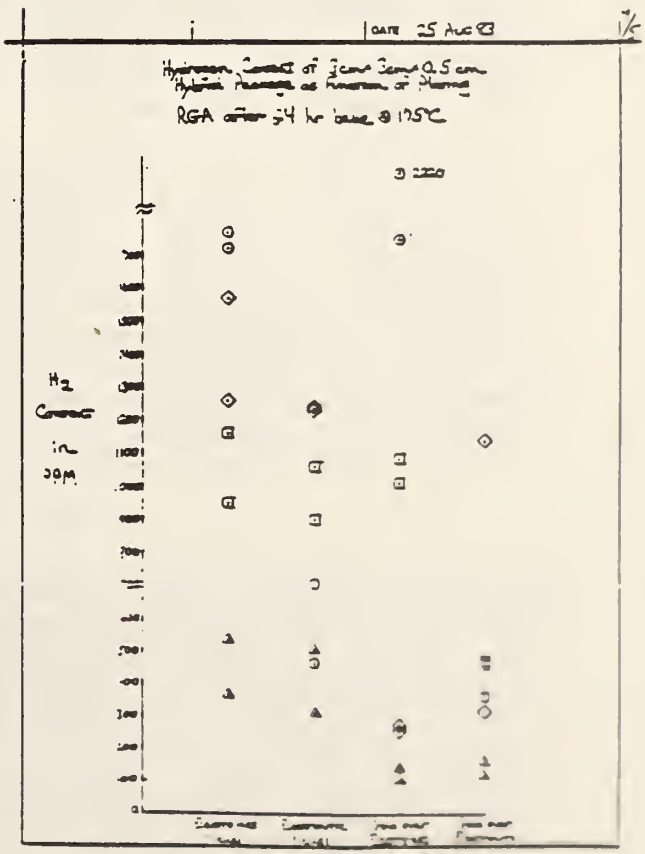

FIGURE 11

2.2 MOISTURE ANALYSIS AT ONEIDA RESEARCH SERVICES, INC.

Thomas J. Rossiter and Diane Feliciano-Welpe
Oneida Research Services, Inc.
3 Ellinwood Court
New Hartford, NY 13413

INTRODUCTION

For the past five years, Oneida Research Services, Inc., has been offering as a standard service Residual Gas Analysis via the Mass Spectrometric method outlined in Procedure 1 of MIL-Std 883, Method 1018. During that time, ORS has had a continuing program to develop methods that accurately and reproducibly measure gases sealed in electronic devices. Primary focus has been placed on developing a method that measures moisture and other gases without achieving steady state conditions in the mass spectrometer.

There are several reasons for developing a Dynamic Method. The primary reason is that moisture is a bipolar molecule and easily adsorbs on surfaces, such as a mass spectrometer's chamber walls. The rates of adsorption are a function of many variables such as temperature, surface conditions of the mass spectrometer, pressure, and other gases present. Surface conditions, themselves, are very difficult to control because it depends on the content of prior samples, time between samples, pumping efficiency and vacuum integrity. Rather than trying to develop elaborate techniques to control the large number of variables, a method was developed that was less sensitive to the adsorption properties.

The objective of a Dynamic Method is to measure adsorbent gases very quickly, before they have time to significantly adsorb on the chamber surfaces. The rates of adsorption still have to be controlled, but now to a much lesser degree. Because we are an independent testing laboratory, we are faced with the task of performing RGA (Residual Gas Analysis) on a wide variety of device types ranging in size, construction, and gas content. Therefore, it is essential that the proposed test method be reproducible and easy to control. The Dynamic Method offers this ability plus other interesting advantages.

THE DYNAMIC METHOD

The fundamentals behind the Dynamic Method of measurement require an understanding of the dynamic behavior of residual gases. We must start by looking at the physical design of the sample chamber and inlet path to the mass spectrometer. A cross-section of a rapid cycle mass spectrometer system is shown in Figure 2. The sample is held in place on the sample mount by suction from a small vacuum pump. The lid of the sample is sealed against a viton O-ring. This mounting procedure places most of the surface of the IC device outside of the realm of the mass spectrometer

analyzer, thus minimizing the effect of the exterior of the package as one of the major adsorption variables. The mount is sealed against the wall of the inlet block leaving a hermetic cavity around the sample in which a vacuum may be maintained. This vacuum around the exterior of the package is needed for equipment protection in case the package should fracture, and is unrelated to the vacuum in the inlet block itself. The puncture pin mechanism, which is manually operated, guides the puncture pin through the center of the small O-ring to pierce the lid of the sample. The cavity gas is released into a transfer passage or inlet and travels through a fixed orifice. This fixed orifice provides for a slower and more controlled flow into the mass analyzer. The pumping mechanism is maintained by a direct drive turbomolecular pump which achieves background levels of $1x10^{-8}$torr.

In order to derive the dynamic behavior of gases in a mass spectrometer, we can use a simple diagram shown below. The system takes on three major components: the sample, the inlet chamber, and the analyzer chamber. Prior to puncturing the sample, the inlet and the analyzer are at $1x10^{-8}$torr while the sample is generally at 1 atm. (less than 1 atm. for cerdips).

The conductance path (σ_2) between the inlet and the analyzer chamber is set by the fixed orifice described earlier. When the sample is punctured, a conductance path is created (σ_1) between the sample and the inlet chamber.

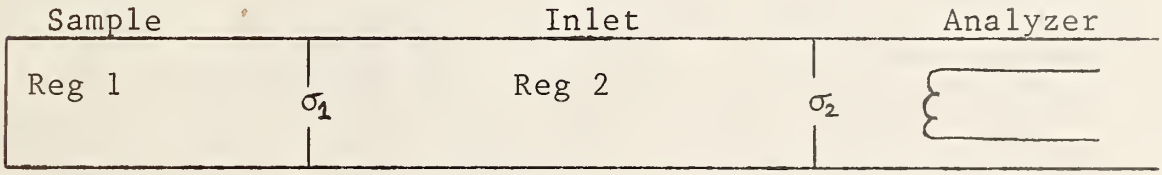

1.) Ideal Gas Law

$$P = \frac{NRT}{V}$$

2.) Fluid Movement

$$\frac{dN_2}{dt} = \sigma_1(P_1 + P_2) - \sigma_2(P_2)$$

3.) Conservation of Matter

$$N = N_1 + N_2 + N_3$$

P = pressure (torr)
N = number of molecules
T = temperature (^oK)
V = volume (cm^3)
R = Universal Gas Constant
σ = conductance
t = time (sec)

By using three fundamental laws of physical behavior, an equation representing the flow of nonadsorbent molecules through the fixed orifice (σ_2) into the analyzer may be derived (Eq. 1). This equation represents the value which is actually being measured by the analyzer during pumpout.

$$\frac{dN_3}{dt} = N\left[k_2(1 - e^{-k_1 t})e^{-k_2 t} + k_1(1 - e^{-k_2 t})e^{-k_1 t}\right] \qquad \text{(Eq. 1)}$$

where: $k_1 = \frac{T_1}{V_1}\sigma_1 R$ $\qquad k_2 = \frac{T_2}{V_2}\sigma_2 R$ $\qquad k_1 \sim 100{,}000 \times k_2$

Since: $V_1 \ll V_2$

$\sigma_1 \gg \sigma_2$

Because the sample puncture hole size is much larger than the size of the fixed orifice and because the volume of the package is smaller than the volume of the inlet chamber, k_1 is several orders of magnitude greater than k_2. Application of this equation shows that shortly after a sample is punctured, the term $e^{-k_1 t}$ will essentially be equal to 0, leaving Eq. 2:

$$\frac{dN_3}{dt} = Nk_2e^{-k_2 t} \qquad \text{(Eq. 2)}$$

Equation 2 is the mathematical representation of an exponential pumpout rate. A linear plot of Equation 1, as shown in Figure 3, illustrates the predicted behavior of residual gas (as measured by the quadrupole analyzer) when the sample lid is punctured. The gas rises instantaneously (50-100 microsec.) to a sharp and stable maximum and begins to decline at an exponential rate. Actual pumpout curves from the RGA systems have reproducibly followed this theoretical exponential plot which when displayed on a semilog scale will yield a straight line. A pumpout curve for nitrogen (mass 29) is shown in Figure 4 on a semilog scale. As seen theoretically, when burst into the system, the nitrogen rises instantaneously to a sharp and stable maximum and begins to decrease at a characteristic pumpout rate which is proportional to the square root of the molecular weight. The larger the molecular weight of a gas, the slower the pumpout rate.

These curves have shown such a great degree of reproducibility that, in effect, they may be used as quality control curves for the given RGA system. In the case of the nitrogen pumpout curve in Figure 4, the sharpness of the peak at the maximum indicates that the ion source is properly tuned. The fact that the curve can be fitted to a straight line (correlation coefficient = 0.9999) demonstrates the quality of the fixed orifice, the linearity of the analyzer over a dynamic range, and the signal to noise of the detector.

Given this dynamic behavior of ideal gases (nonadsorbent gases), what is the best way to acquire the data and quantitate the results? Contemporary methods acquire data over the full curve or until 95% of the gas is pumped out of the inlet chamber. Data is then summed or integrated for quantitation. Summation or

integration techniques usually result in higher peak-to-background ratios, but this is not true when integrating under conditions of a rapidly decreasing exponential data curve. If we evaluate the peak-to-background levels of various sections of the dynamic curve, we find that the peak-to-background is highest at the maximum of the curve. Thus, by making several measurements at the peak of the curve (before 10% of the gas is allowed to pump away) a 2 to 1 improvement in peak-to-background can be achieved as compared to the integration method which sums data (and background noise) over the entire curve. Clearly, the advantages to this form of analysis is a more accurate method for measuring peak intensities.

Up to this point, we have only discussed ideal or nonadsorbent gases, and find an improvement in signal processing by using a dynamic measurement. When we consider the behavior of adsorbent gases, moisture in particular, we find that the Dynamic Method provides even more advantages than the 2 to 1 peak-to-background improvement described earlier. Figure 5 displays various moisture pumpout curves on a semilog scale.

Matrix effects such as adsorption, desorption and outgassing of moisture must be taken into account since the pumpout of moisture changes radically with chamber surface conditions, the presence of organic materials in the IC cavity, and the presence or absence of gases such as hydrogen in the ambient. If one were to measure moisture peak amplitude along any one of the curves presented in Figure 5 to arrive at an integrated quantitative analysis, several problems would result. In some cases, we would be faced with integrating the moisture signal (and background) to infinity since moisture does not always reach background levels within the given measurement period. Since moisture background levels are non-trivial, this would result in a very poor statistical averaging method even if it could be assumed that the moisture background remained constant, which it does not.

The Dynamic Method overcomes a great number of the problems encountered with integrated measurement by taking the required measurements at the peak of the pumpout curve where there is minimum adsorption effects, peak-to-background is substantially large and there is confidence in background measurements for accurate quantitation.

To make all these measurements within a short period of time (~3 seconds) requires computer technology with high-speed interfacing. A PDP11-23 system with 256K memory is used to acquire data. An elaborate data acquisition routine and quantitation program has been written to maximize accuracy and reproducibility.

PERFORMING THE ANALYSIS

ORS operates two mass spectrometer systems dedicated specifically to RGA analysis. The sample is loaded into the mass spectrometer and allowed to reach thermal equilibrium at 100°C for a minimum

of ten minutes. During this time, the vacuum system pumps down the inlet and sample chamber to 1×10^{-8} torr. An automated computer data acquisition program is activated which collects a background spectra, checks for minimum background requirements, then goes into an Auto-Start routine. This routine monitors the nitrogen peak (or any other selected peak) and triggers the data acquisition program when it senses a rise in signal from the package puncture. Immediately following the release of residual gas through a puncture hole in the sample lid, the Dynamic Method incorporates an initial set of repetitive moisture measurements followed by several full scale scans (0-100 AMU) to measure all other residual gases. One of the advantages of the automated data acquisition routine is that it controls the time frame of the analysis which is a critical parameter.

Quantitation is calculated in % concentration as shown in the following equation:

$$\frac{(\text{peak intensity})(\text{sensitivity factor})}{\text{total gas}} \times 100\% = \% \text{ concentration}$$

$$\text{total gas} = \sum_i (\text{peak intensity})_i \ (\text{sensitivity factor})_i$$

CALIBRATION

The calibration and determination of sensitivity factors are equally as important as the actual test method. The key to accuracy, in this case, is to perform the actual calibration under the same conditions as the test method. To accomplish this, calibration of each RGA system uses a Multi-Volume Calibrator which is shown in Figure 6. This unit is mounted in close proximity to the sample and simulates a sample burst into the inlet and mass analyzer using various calibration gases. Three volume sizes (.01cc, .1cc, and .8cc) are available within the unit with two additional extension volumes (1.8cc and 4.0cc) that may be fitted for larger calibration bursts. By purging a given calibration gas through the Multi-Volume Calibrator, an operator may simulate sample bursts for several package sizes. A schematic illustrating the Multi-Volume Calibrator with the calibration hardware is shown in Figure 7. In the case of moisture, a General Purpose Humidifier is used to generate a known moisture level which is confirmed by an NBS Traceable Dew Point Hygrometer. For the calibration of other gases, room air and special gas mixtures are used.

SUMMARY

An advantage of the Mass Spec method of analysis is that all other gases present in the ambient are measured as well as the moisture. Clearly, this is more than just a pass-fail moisture measurement test and can offer valuable information about the history of the device. Data on other ambient gases can lead to the identification

of fine and gross leakers, leak test escapes, poor process control, internal chemical reactions, and effects of organic materials and dessicants.

The Dynamic Method, also referred to as the instantaneous method, provides improved sensitivity and reproducibility in measuring moisture while minimizing adsorption effects as a measurement variable. The method more closely measures the ambient gas in the package because it precludes measuring outgassing products from the package after the device is punctured. When the device is punctured, the interior of the package is suddenly under vacuum. This in itself is a stress condition which can result in outgassing and mechanical stress on the device. It is our opinion that an analytical method that measures gas content should not also be a stress test on the device. Stress tests should be performed prior to analysis so as to generate realistic, worst case conditions in the product. The mass spectrometer should then be able to measure those conditions as they exist without introducing additional stress. By collecting data within a very short period of time, the Dynamic Method essentially accomplishes this.

The Dynamic Method has been utilized by ORS since 1978. In that time, a number of the supporting factors in this method have been revised (for example, upgrading the software and the computer system) but the basic fundamentals presented in this paper have remained unchanged. Throughout the years, this instantaneous method of measurement has offered a data base with both accuracy and reproducibility.

MINIMUM REQUIREMENTS OF MIL-STD 883, METHOD 1018, PROCEDURE 1

Accuracy	±10% at 5000 ppm
Volume Range	.01cc - 10cc
Temperatures	Sample - 100°C for ten minutes Inlet - 125°C
Puncturing	Puncture a hole, do not break seal
Sample	Ceramic Lids may be thinned Prebake at 100°C for 12-24 hours if unit contains dessicants or organics.
Measure	Chamber Pressure, Moisture Content, All Other Gases.

TABLE 1

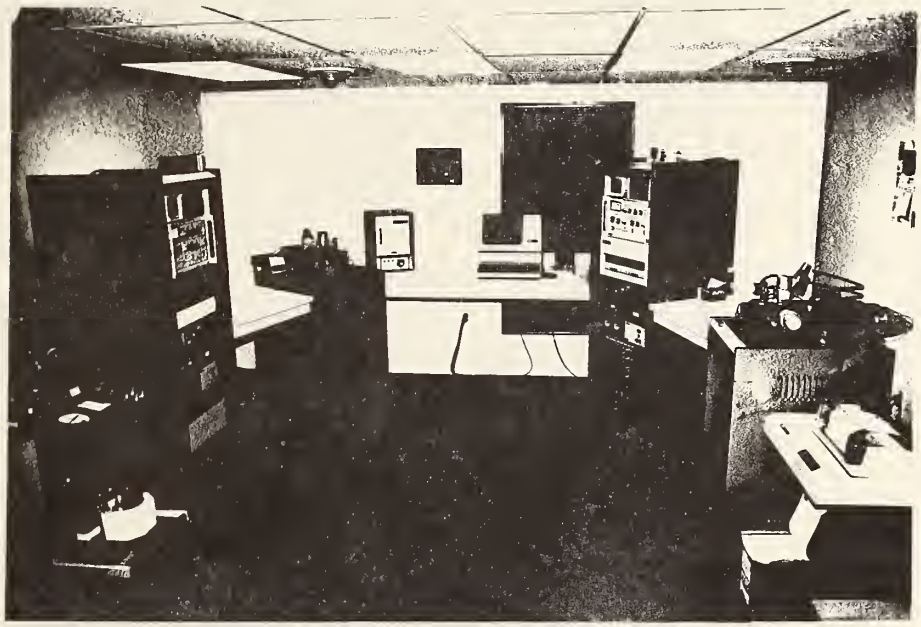

Fig. 1: Two adjoining mass spectrometer systems

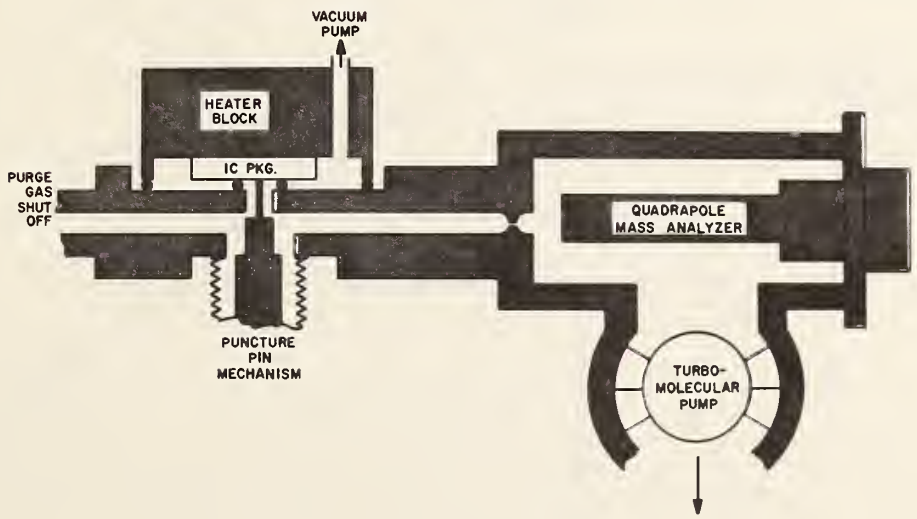

Fig. 2: Cross-section of sample block and analyzer

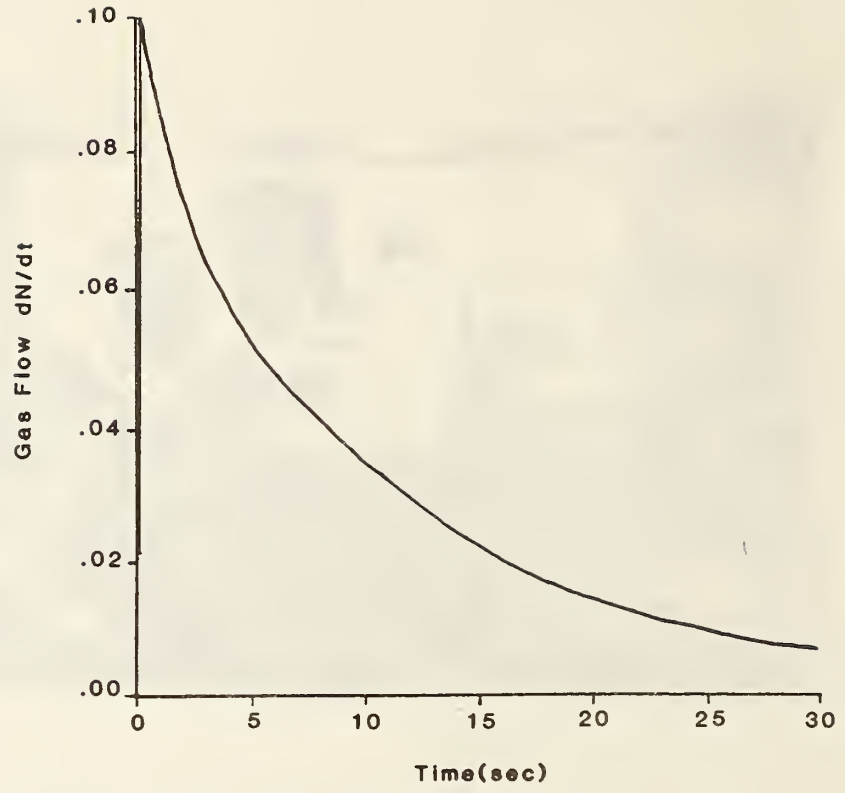

Fig. 3: Signal Intensity vs. Time from Puncture

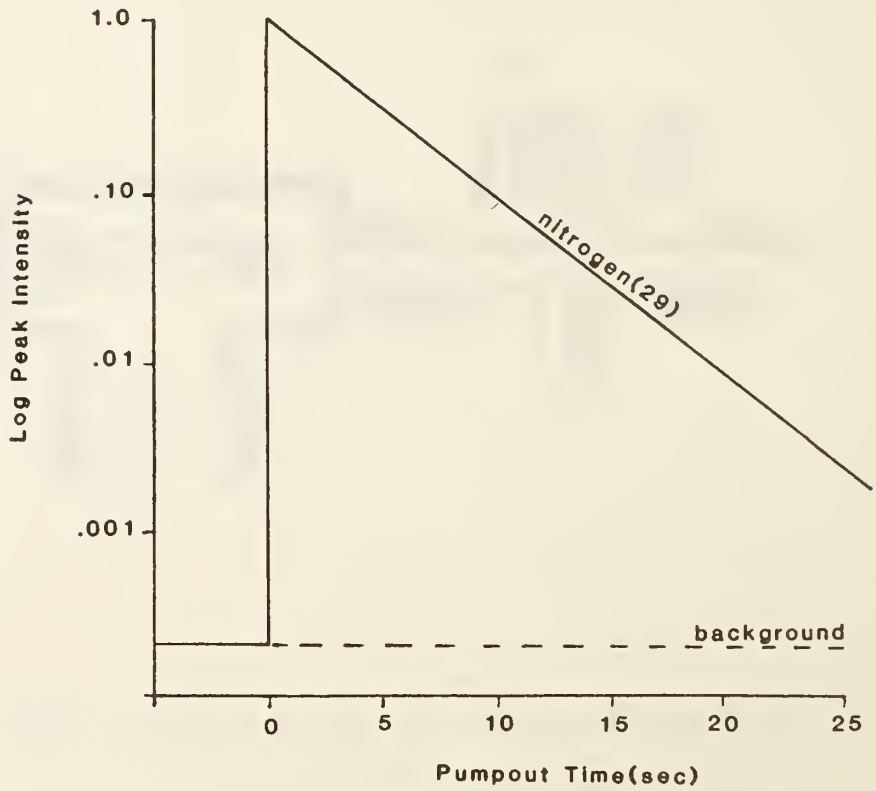

Fig. 4: Nitrogen(29) Pumpout Curve

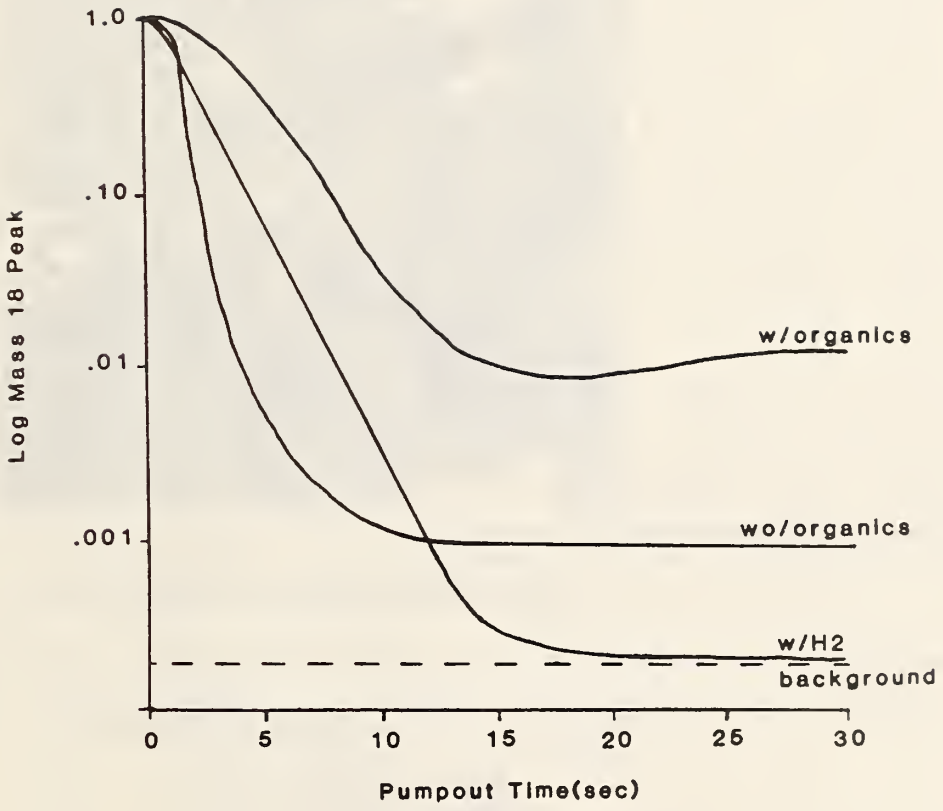

Fig. 5: Moisture Pumpout Curves

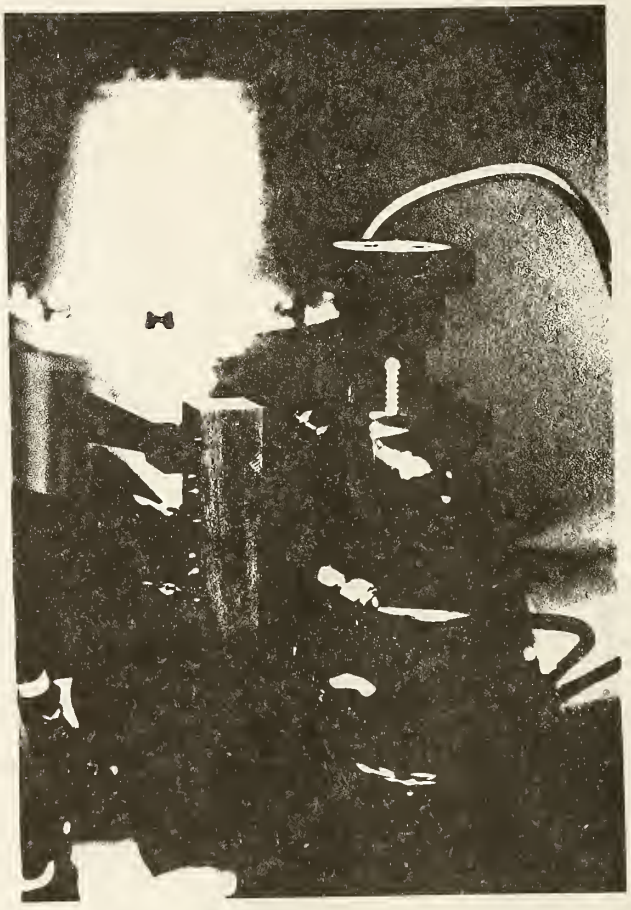

Fig. 6: Multi-Volume Calibrator

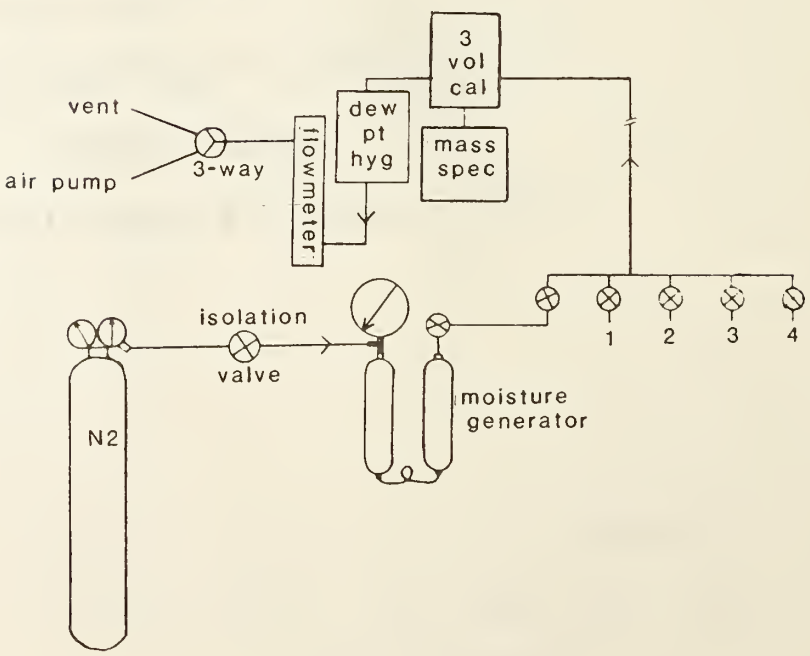

Fig. 7: Schematic of calibration system

2.3 GAS ANALYSIS AT GOLLOB ANALYTICAL SERVICE

Fred Gollob
Gollob Analytical Service
47 Industrial Road
Berkeley Heights, NJ 07922
(201) 464-3331

ABSTRACT

This discussion is concerned with the analysis of the gas content of hermetic packages, as per Method 1018.2 ,Mil Std 883B. After an introductory statement about the need for the method and the background of its development, the equipment used at G.A.S. for the performance of the procedure will be described. This will include a schematic of the mass spectrometer showing conventional sample system, including vacuum system and data acquisition system. Modifications to the mass spectrometer for the performance of Method 1018.2 will then be discussed. The design of universal puncturing chambers, with provision for calibration and puncturing will be described. Two accessories to this system, the three volume calibrator and the controlled humidity generator complete the equipment needed for the analysis.

After the description of equipment, the detailed analytical procedure will be presented. Initially, conventional analytical procedures will be described. This includes background and regular scan analyses. Procedures specific for 1018.2 will then be described, covering wet and dry gas "burst" calibrations, specific measurement of the water peak (using the instantaneous reading technique), and the sample volume measurement.

The final portion of the discussion will be concerned with the data handling and calculation. It will include data storage and interpolation of the background water correction.

INTRODUCTION

This discussion is concerned with the analysis of the gas content of hermetic packages as per Method 1018.2 of MIL STD 883B. The impetus for the development of this procedure came over ten years ago from studies performed by Ben Moore and Bob Thomas at RADC. Failure analysis showed a correlation between corrosive failure and excessive moisture content. Initial analyses were performed at RADC using a mass spectrometer with a "cookie cutter" sampling inlet. This unique inlet was effective in determining water content at a time when it was generally considered to be not feasible to perform that determination by mass spectrometer. The reason for difficulties with the determination was the strong adsorption of water on surfaces within the analytical instrument, and the reason for success at RADC was their unique sampling procedure, which provided dynamic sampling and analysis and overcame this problem.

The basic problem is that relatively large amounts of moisture adsorb on the surfaces of the gas sample handling equipment, and establish a dynamic equilibrium with the gas phase. Inasmuch as

100 ppm of water in .01 cc of gas at .5 atmospheres pressure (the long term goal for the lower limit for subject specification) is only about 0.0004 micrograms, careful conditioning of the analytically active surfaces must be performed to minimize interference from this equilibrium.

If the walls of the system contain too much moisture, appreciable amounts of moisture will desorb and produce a falsely high value for the water content of the sample. In addition, slight variations in temperature and technique can cause large variations in this false contribution. On the other hand, if the conditioning cycle of heat and evacuation is too effective in removing moisture from the walls, the walls can act as a getter, adsorb moisture from the sample, and produce a falsely low result. Therefore, the conditioning must be controlled so that desorption from the walls contributes an amount of moisture that is small compared to the amount that is actually present in the sample. As can be seen by a consideration of the numbers,this desorption factor becomes much less important as the sample size increases, and as the goal value for moisture increases. Thus, a desorption of 0.01 micrograms of moisture from the walls would destroy the accuracy of a 0.01 cc sample at 100 ppm, would still be a major factor vis-a-vis 0.01 cc at 5000 ppm , and would be insignificant when considering a 1.0 cc sample at 5000 ppm.

For the fixed gases (nitrogen,oxygen,hydrogen,etc.),the sorption problem is so small that it does not have a significant effect on their determination. These inorganic gases are much less polar than water. This means that 1) smaller amounts of these gases would normally adsorb on surfaces, and 2) water will displace them. Thus, omni-present water effectively covers all the surfaces and helps eliminate a similar analytical problem for these other gases.

Although we cannot eliminate this adsorption problem, we can minimize it and learn to control it. Materials of construction should be smooth and not be moisture absorbant, and should be free from moisture absorbing contaminants. Our systems are constructed of stainless steel, heli-arc welded, with minimum amounts of Teflon, where needed. As far as techniques are concerned, all surfaces that contact the sample gas are thermostatically maintained at 100 C.,or 125 C., to minimize the amount of adsorbed moisture and to minimize equilibrium excursions that are caused by temperature fluctuations. In addition, we minimize the exposure of these surfaces to atmospheric moisture, by keeping the system sealed whenever feasible, and by using a dry nitrogen backflush when the system is open.

CALIBRATION

Before I describe the specific equipment we use, and the calculation procedures, I should like to discuss calibration. In any analytical procedure, the only legitimate verification of the accuracy of the results is to analyze a known standard using the same conditions of analysis for the standard and the unknown. In many situations, where all the variables that may affect the analysis are known and understood, it is acceptable to calibrate the equipment on an absolute basis. However, where it is known

that adsorption-desorption phenomena are significant, or where system memory effects are large, standards must be analyzed. In the present case, the ideal situation would be to analyze packages (of the same type as the real samples) but which contain known amounts of moisture in them. Many attempts have been made to produce these standards, but these efforts have met with only limited success.

In the absence of a large supply of package standards, we developed a "burst" calibration procedure in which we tried to simulate the puncturing of an ic package, and the subsequent release of its gaseous contents. A "burst" valve was attached to the far end of the sample puncturing chamber and connected to an external system which supplied a flowing stream of nitrogen containing a controlled amount of moisture. The moisture level of this flowing stream, which could be accurately measured using a refrigerated mirror dewpointer, could be continuously adjusted by varying the amounts of a dry gas stream and a water saturated gas stream that were blended. The "burst" valve could then be manually operated to introduce a small amount of this gas stream. A skilled mass spectrometrist could, with a very high success ratio, introduce, in a fraction of a second, an amount of gas, of known moisture content, that was very similar to the amount of gas in the real sample. Although this procedure required a lot of operator skill, it did result in increased precision.

Subsequently, the well-known Three Volume Calibration Valve (TVCV) and the NBS General Purpose Humidifier (GPH) were developed elsewhere and have become available through Pernicka Corporation. The TVCV and the GPH permit burst calibration to be performed with excellent reproducibility and have resulted in the achievement of acceptable correlation among the various analytical laboratories and with the standards that have been circulated.

MASS SPECTROMETER EQUIPMENT

At Gollob Analytical Service, we perform this test procedure using a modified DuPont 21-614 cycloidal focussing mass spectrometer. This instrument is equipped with a relatively conventional static gas sample system that we built ourselves. The system permits us to introduce known amounts of the various stable gases into the analyzer and to establish sensitivities for these gases, in terms of divisions of peak height on the recorder per micron of each gas that is present in the sample system. As mentioned earlier, the adsorption problems associated with water render this calibration procedure inaccurate for water, and the separate "burst" procedure is used for that gas. Our conventional gas sample system is operated at room temperature. However, as referred to earlier, it is advisable to maintain those systems used for water determination at a constant and elevated temperature. We therefore constructed a separate system for the Method 1018 work and connected it to the conventional sample system as close as feasible to the analyzer. Provision is made, using valves, to connect either the regular or the 1018 system to the source. All surfaces exposed to the sample gas in the 1018 system, from the breaking chamber through to the gold leak entrance to the source are temperature controlled; the breaker is maintained at 100 C and the sample transfer passages are

maintained at 125 C. The TVCV and the GPH are connected to a port at the far end of the breaker, so that the "burst" calibration gas must travel the full length of the gas transport system. This ensures that the calibration gas will see all surfaces, and experience all aberrations that might affect the sample. This is part of the approach that the best calibration really is a package of the same size and structure as the real sample, but with a known gas content. In the absence of the standard, the analyst must use his ingenuity to insure as complete simulation between the calibration procedure and the sample analysis procedure as imaginable.

UNIVERSAL BREAKING CHAMBERS

Over the years, we have designed and constructed a number of breaking chambers, all of which are capable of providing analysis as per Method 1018.2. These chambers can accomodate a wide variety of samples, from tiny crystal carriers, through a variety of TO cans, cerdips, flat-paks, hybrids, to other structures, such as pacemakers, infra-red scanners, gyroscopes, implantable medical devices, reed switches, resistors, capacitors, spark gaps, surge arrestors, and the list goes on. Basically, the universal approach used in building the chambers has permitted us to analyze the gas content of devices , glass or metal, with internal gas content from 0.00001 to 1000 cc. What is universal about these chambers is that they all have the same three connector fittings. One fitting is of the size to connect to the mass spectrometer sample system. The second fitting, at the other end of the chamber,accepts the TVCV. The third fitting, which must be precisely located over the sample at the spot to be punctured, mates with the puncturing actuator. For our universal actuator, we modify an all stainless steel bellows valve and have a special fitting machined on the bonnet. The mate of this fitting is then welded onto the breaker. There are a variety of interchangable breaking, puncturing and smashing tips than can be mounted in this actuator. After the appropriate chamber and accessories are assembled and connected to the mass spectrometer, the breaker is enclosed in a temperature controlled environment. We thus wind up with a system in which we can puncture a sample, collect all the gaseous contents (at 100 C) without loss or contamination, transfer the gas (at 125 C) to the analyzer, and "burst" calibrate. A puncture can usually be made within 1/16 of an inch of the desired puncture point.

ANALYTICAL PROCEDURE AND CALCULATIONS

The analytical procedure used to perform this analysis is based upon standard analytical procedures, as follows. On the day prior to analysis, the samples are loaded into a suitable chamber. After the chamber is attached to the mass spectromter, initial leak test analyses are performed to insure that the system is free of leaks and that no unusual gases are being evolved from the samples. The next morning, usually sixteen hours later, final leak tests are performed. The mass spectrometer is tuned to mass 18, and that peak is monitored with the pump valve closed to be sure that rate of increase of that peak is suitable. At this point, bursts of dry gas are introduced, in order to establish how much moisture will be desorbed into the system when the walls are hit with a burst of gas

similar in amount to the sample. Bursts can be introduced with volumes of .01,.10,1.0 cc and larger, and are chosen to bracket the sample size. Sample analysis then proceeds in a similar fashion. The mass spectrometer is tuned to mass 18 and the sample is punctured. There is an almost instantaneous rise in the water peak. After the initial rise, the water value may then continue on its previous slope, or may establish a new one. The value used for the calculation of the water content is the instantaneous change which occurred at the moment of puncture. This value correlates with the true water value because it is measured before any of the sorption effects (other than the burst effects) have had the opportunity to influence it. After the water value has been read, the mass spectrometer is scanned in the conventional manner and all of the other gases present are measured. Suitable blank analyses are performed periodically. After all samples have been analyzed, burst dry gas analyses, and burst wet gas analyses (the bursts contain about 5000 ppm water as produced by the GPH) are performed. Finally, the mass spectrometer is calibrated in the normal fashion for nitrogen, hydrogen, oxygen and other gases of interest. All of the data is fed into a computer for the calculation. The computer program corrects the water value of the sample for the dry burst gas contribution and interpolates for differences in sample volume. Then, using a sensitivity for moisture calculated from the wet burst gas analyses, the partial pressure of water in the breaking chamber is calculated. The partial pressure of all other gases is calculated from their individual sensitivities, and the over-all composition of the gas released from the sample is calculated. Inasmuch as the sample gas is contained in a fixed calibrated volume and is slowly bled into the analyzer through a fixed leak, the analysis yields the actual partial pressure, and, therefore, the total amount of each gaseous constituent. Thus the actual total amount of gas that was present in the sample can be determined accurately. This added bit of information is often of great value in studying unusual samples.

In summary, at GAS, we use a mass spectrometer to analyze the gases released from various electronic packages. The water is determined by measuring the instantaneous change in the water peak that occurs when the sample is punctured. This procedure has been shown to produce good correlation with the other mass spectrometer laboratories and with package standards from RADC.

2.4 CONTROL CHART ANALYSIS OF MOISTURE IN CERDIPS

by

Robert B. Elo, Ph.D. and Arnold M. Massoletti
American Microsystems, Inc.
3800 Homestead Road
Santa Clara, California 95051

INTRODUCTION

Beginning 3rd quarter of 1980, a development effort was undertaken to produce a state of the art, very low moisture cavity, cerdip package. The 1st phase task was evaluation of the then current AMI package moisture level. The 2nd phase task was development of alternative processes which would produce lower cavity moisture. The 3rd phase was selection and implementation of the optimum low moisture process. Cavity moisture was continuously monitored during the implementation of this process as it phased into manufacturing production.

Control chart methodology was selected as the format for the process monitor. The data gathered by and the interpretation of these control charts is the subject of this paper.

The piece parts of cerdip construction used at AMI are common to the industry (see Table 1). The manufacturing assembly process flow is shown in Table 2.

For the purpose of evaluation and subsequent monitoring of cavity moisture, the following sampling methodology was used. A weekly sample of ten adjacent units were taken from the belt after exiting from the furnace. A secondary monitor of ten units with minimized processing was assembled using electrical reject die (dummy).

The dummy packages were put into seal on the belt beside normal product. Both product and dummy samples were then processed through post seal assembly flow with the exception of the tin plate operation.

Low Moisture Evaluation and Development

Results of the development phase of 1981 are presented in Figures 1 and 2. The data in control chart format is shown with typical MEAN and RANGE values representing progress made as a result of various evaluations. The $\overline{\overline{X}}$ and control limits for the various time periods was obtained from actual data.

It is seen that $\overline{\overline{X}}$ and control limits are decreasing for each successive time period.

The Jul/Sep plot represents a projection from a limited sample, completed near the end of the 2nd quarter. Actual start-up in the 3rd Quarter proved to be better than this projection, as can be seen in later figures.

Assembly Process Monitor

In addition to the unit sampling for mass spectrometer moisture measurement, manufacturing performs read and record monitors on a daily or shift basis (see Table 3).

Process Capability

We found in the evaluation studies that experiments would need to be repeated over time to arrive at a statistically valid conclusion that a change had been effected.

It was decided that control chart methodology was the best tool to provide long-term assessment of changes, and to provide a process control monitor. One half of the weekly product and dummy sample was sent to a DESC certified lab for cavity moisture measurement. The product and dummy measurement sample size was three units each with the remaining two units acting as spares. The other five units were archived.

At the initiation of ramped volume production in the 3rd Quarter 1981 the original process capability study was made (see Table 4). With the passage of time the process appeared to move into tighter control than that of the original study. A second study was performed in the 3rd and 4th Quarters of 1982. In the second study $\bar{\bar{X}}$, the average of the MEANS, remains constant. However, the average RANGE has decreased to less than one-half its original value.

The process stability in this period of time is shown in Figures 3 and 4. These are the MEAN and the RANGE control charts of product for 1982. The RANGE chart shows only two points above the upper control limit (weeks 24 and 50). One of these, week 24, is coincident with a MEAN point above its upper control limit.

The MEANS chart shows four points above the upper control limit and five points below the lower control limit. The 1982 process period generally appears to be in control with signs of instability.

Whenever data that plotted above the upper control limits occurred, process information and other monitors were reviewed by engineering for assignable causes. No assignable causes were found in the four instances where the upper control limit was exceeded.

A histrogram was generated from individual product measurements. This histogram includes all data from the initiation of ramped product volume through the first quarter of 1983.

The plot, shown in Figure 5, is skewed. It has a tail of high values, usually associated with sports. The low value side is truncated because of a measurement limit at one-hundred PPMV. Overlayed on the bar graph is a plot of an ideal normal Gaussian distribution, created from the MEAN and Sigma of the actual distribution. It can be seen that, the tail of the distribution has shifted the Gaussian MEAN to a value higher than the Median.

The population statistics of product sampled from 1981 through third quarter 1983 are summarized in Table 5. The number of observations in this distribution is 372. The MEAN is 623 PPMV. This should be compared with the Median of 555 PPMV and the 1982 Control Chart $\bar{\bar{X}}$ of 555 PPMV. The Control Chart $\bar{\bar{X}}$ is derived from process capability studies. Sport measurements were excluded from these studies. The 1982 upper control limit of 712 PPMV (555 + 157 PPMV) is defined as three Sigma of the sample $\bar{X}$ above $\bar{\bar{X}}$. For large populations the following relationship is valid.

$$\sigma_X = \sqrt{N}\ \sigma_{\overline{X}}$$

Assuming: $3\sigma_{\overline{X}} = 157$ PPMV,

then, $\sigma_X = 91$ PPMV

The actual spread (σ_X) with sports included is 300 PPMV. The question then arises, on what basis can we determine that a measurement is a sport. The DESC lab estimates, based on calibration data and internal controls, that they should be able to reproduce ± 100 PPMV at an average moisture level of 500 PPMV. If we assume this 100 PPMV reproducibility value is between the 1σ and 2σ limit of the measurement then the conrol chart may be reflecting only measurement scatter. The sports could be then, either measurement error or actual moisture level change in the package. There does not appear to be any way, at the present, to discriminate between the two alternatives.

Shift of the Process Average

As the process continued into 1983 a sudden change of the average of the MEANS in the product samples was observed. It appeared, based on the measurements after this change that the process average had shifted up from 555 PPMV to 815 PPMV.

A view of this change is given by a 26 week period from 4th Quarter 1982 to 2nd Quarter 1983. It is shown with an arbitrary weekly numbering system (see Figure 6).

The product RANGE chart (Figure 7) shows two values above the upper control limit from week 18 through 26. From this there is no evidence to reason that most of the above control limit points on the MEANS chart are invalid.

The dummy samples monitor shows a similar pattern to the product sample, in that the pattern seems to have shifted upward after week 17 (see Figure 8).

It was observed that the RANGE values here (Figure 9) typically stayed below the upper control limit, with only one of 8 points above the RANGE upper control limit after week 17. Again, there are no indications that the data was not valid.

After a pattern was established we began to resample product and dummy date codes. We first resampled date codes after week 17. The MEANS data showed general agreement with the original data. We then resampled date codes before week 17. The ranges of all resampled data showed fewer points above the upper control limit than original data (see Figure 11).

The MEANS of resampled product and dummy after week 17 confirmed a shift to a higher value. However, the resample of the MEANS before week 17 showed a gradual trend upwards in marked contrast to the original data (see Figures 10, 12).

Now the Dilemma

The initial product monitor and its back-up the dummy monitor, indicated a sudden change in moisture level had occurred. The resample of this out of control period seemed to confirm this out of control regime. However, when we resampled the "IN" control period just prior to week 18, it too was shifted up and out of control.

The question was then raised what changed, the process or the measurement, since all measurements made after week 17 seemed to have moved up by 200 to 300 PPMV.

During this period of resampling, a thorough engineering review was undertaken both in Santa Clara and in the Korean manufacturing facility. Attempts were made to correlate the apparent change in moisture to a specific change or to a drift in monitors, production practices, and a variety of other probable and improbable factors. The combination of resample results and our own failure to turn up any clue as to the cause of a change, led us to consult with the DESC lab performing the measurements.

The data and our general lack of success was discussed with the lab. They then reviewed their own methodology to see if anything had changed.

An elaborate software program is used by the DESC lab to acquire data and to perform quantitative calculations of the data. On April 16, 1983, a typographical error was inadvertently introduced into the quantitative portion of the program. The error resulted in occasional incorrect background subtraction. The error was in a section of the program that is only accessed when quantitating for small packages that have about 500 PPMV moisture. Because of the limited use of this portion of the program, the error may have gone undetected for an indefinite length of time had not a review been requested.

Background effects are usually insignificant because the signal from testing the sample is orders of magnitude higher than the background signal. But for small packages, the background is significant and background subtraction errors can produce substantial errors in the quantitation for moisture.

Calibration for moisture is done at 500 PPMV by the lab, but not routinely. The major interest in the industry is between 1000 PPMV and 6000 PPMV. Calibration outside this range is only performed occasionally. A method to obtain tighter tolerances at 500 PPMV would be more frequent calibration. Another method would be the calibration procedure using the RADC standards now in development.

After requantitation of the data, the corrected values were plotted with the original and resampled measurements. This correction of data affected some but not all of the control chart points after the apparent sudden change (shown in Figure 13).

There was no correction for the very high peak of week 18. There were two small corrections for weeks 19 and 21. Starting in week 22 there were more substantive changes.

There were no corrections to the resample data prior to the week 18 "sudden change". However, week 19,20,21 have very substantial decreased values, bringing that portion of the chart below the upper control limit.

The original dummy data (Figure 14) shows no change in the high peak for week 18. There are substantial corrections for week 21, 22, and 24. The resampled data has no correction for week 18, but for weeks 19 through 21 there are substantial shifts downward.

SUMMARY

A single consistent phenomena throughout this analysis is that week 18 is consistently a high, above control limit, measurement. It is less clear whether the period from week 19 through 25 is in or out of control. The general appearance of the process is that there is evidence of instability. This indicates the process is probably subject to a complex combination of causes. One possible cause is the substantial correction factor used to arrive at measurement values. For example, the average difference between data before and after correction is 383 PPMV out of a 555 PPVM process average. These control charts show a process in control for a period of 85 weeks, followed by a period of increased instability. A sudden change in $\bar{\bar{X}}$ during this period of instability was the result of at least one assignable cause. This was a data quantitation problem caused by a typographical error.

Control Chart Methodology has been useful to monitor and assess a cerdip seal process. Measurements, less than 1000 PPMV, for small cavity packages can be subject to the instabilities from complex causes. These instabilities could be reduced by: increased frequency of calibration and further refinements in measurement technique. This will provide the necessary confidence for further process improvements, or proper responses to apparent out of control points.

References

1. "Statistical Quality Control Handbook", by Western Electric Co., Inc., second edition 1958, fourth printing 1970.

Acknowledgements

1. The authors wish to "thank" Mr. Tom Rossiter and Oneida Research for their cooperation and contribution to this paper.

TABLE 1: Cerdip Package Part Materials

1. Pressed alumina ceramic base and cap.
2. Commercially available low temperature non-devitrifying glass.
3. Gold/glass frit die-attach pad
4. Alloy 42 lead frame with spot aluminum bonding fingers.
5. Cavity desiccant
6. Cavity volume ~.06 cubic centimeters

Table 2: Assembly Process Flow

1. Infrared frame attach
2. Die attach
3. Lead Bond
4. Desiccant
5. Seal
6. Tin plate
7. Mark
8. Temperature cycle
9. Lead trim and tube load

Table 3: Manufacturing Monitors

1. Air dryer dew point
2. Seal furnace dew point
3. Seal furnace gas flow rate
4. Work area relative humidity
5. Work area temperature

TABLE 4

Process Capability Studies

	ORIGINAL STUDY PRODUCT DATA 10 WEEKS 1981	SECOND STUDY PRODUCT DATA 20 WEEKS 1982
	PPMV	PPMV
$\overline{R}$ = SUM R/N	400	154
UCLR = $D4\overline{R}$	1020	396
LCLR = $D3\overline{R}$	0	0
$\overline{\overline{X}}$ = SUM $\overline{X}$/N	550	555
UCLX = $\overline{\overline{X}}+A2\overline{R}$	970	712
LCLX = $\overline{\overline{X}}-A2\overline{R}$	130	398

TABLE 5

CERDIP MOISTURE MONITOR

BASIC STATISTICS

NUMBER OF SAMPLES		372
STANDARD ERROR OF THE MEAN		15.6
MEAN		623
COEFFICIENT OF VARIATION		48 %
VARIANCE		89966
STANDARD DEVIATION		300
SKEWNESS		1.6
KURTOSIS		7.4
95% CONF. INTERVAL FOR THE MEAN	UPPER	654
	LOWER	592
MEDIAN		555
.25 QUANTILE		441
.75 QUANTILE		706

FIGURE 1

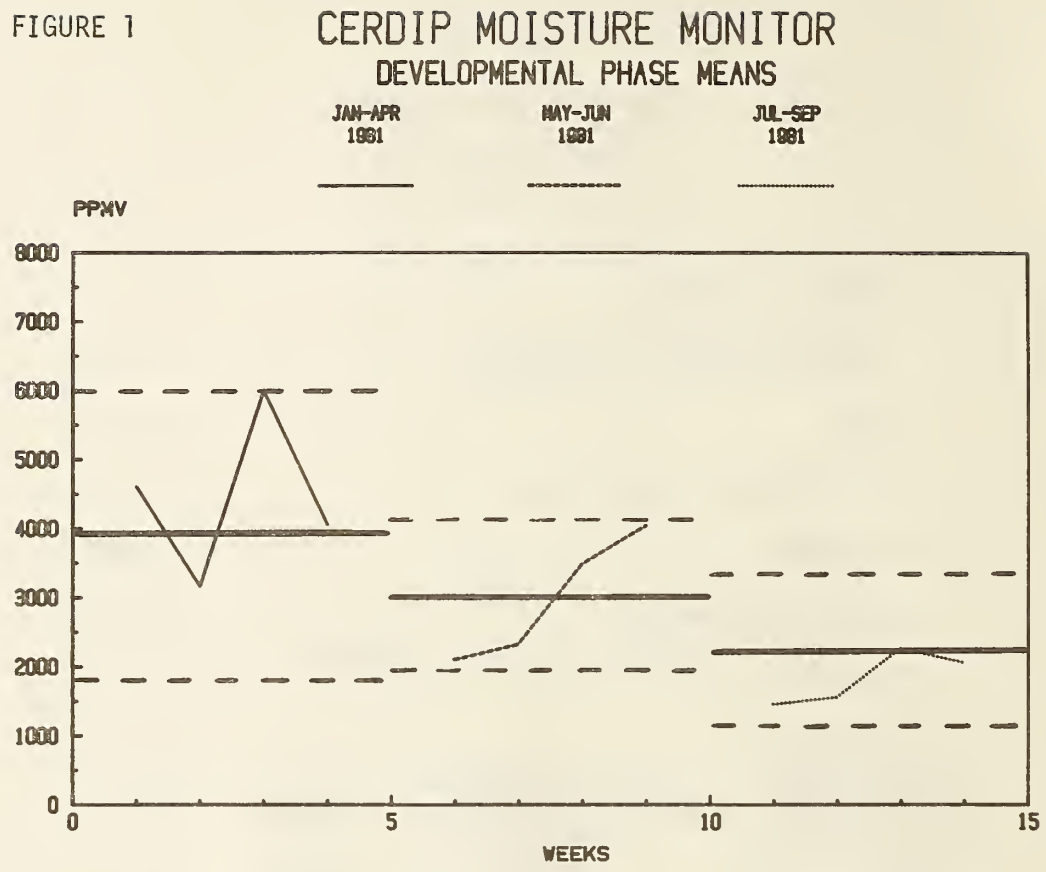

FIGURE 2

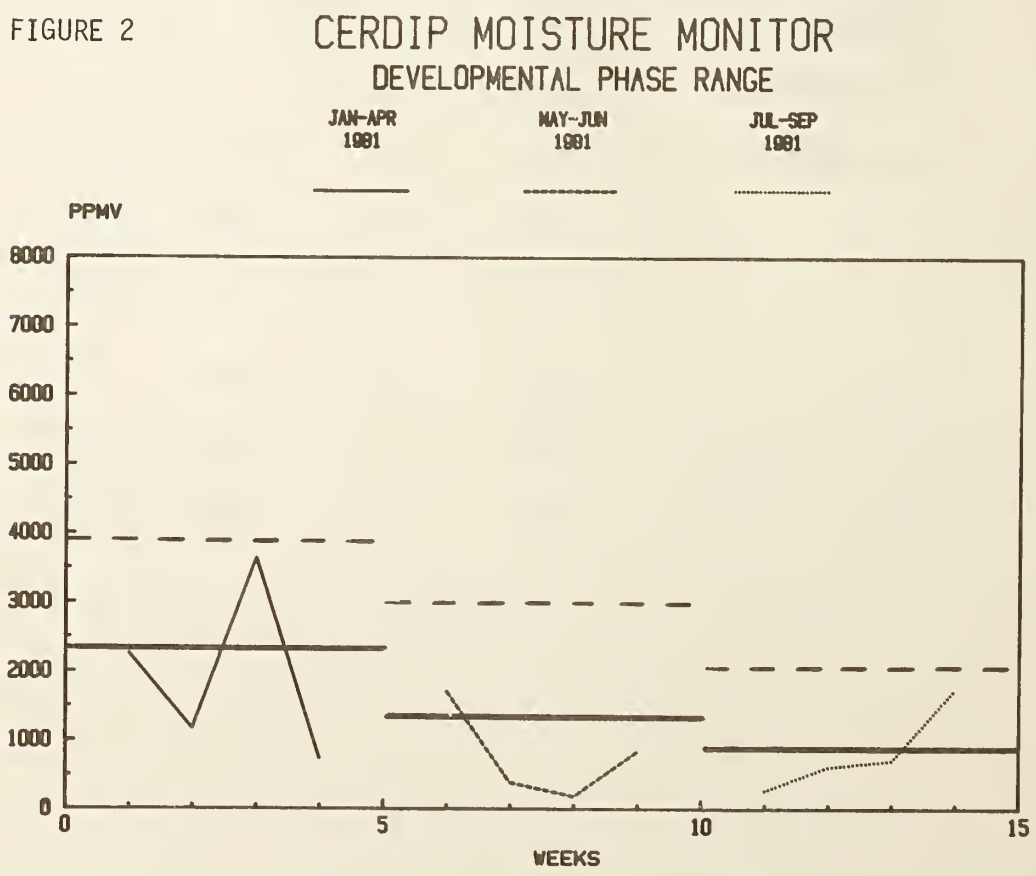

FIGURE 3

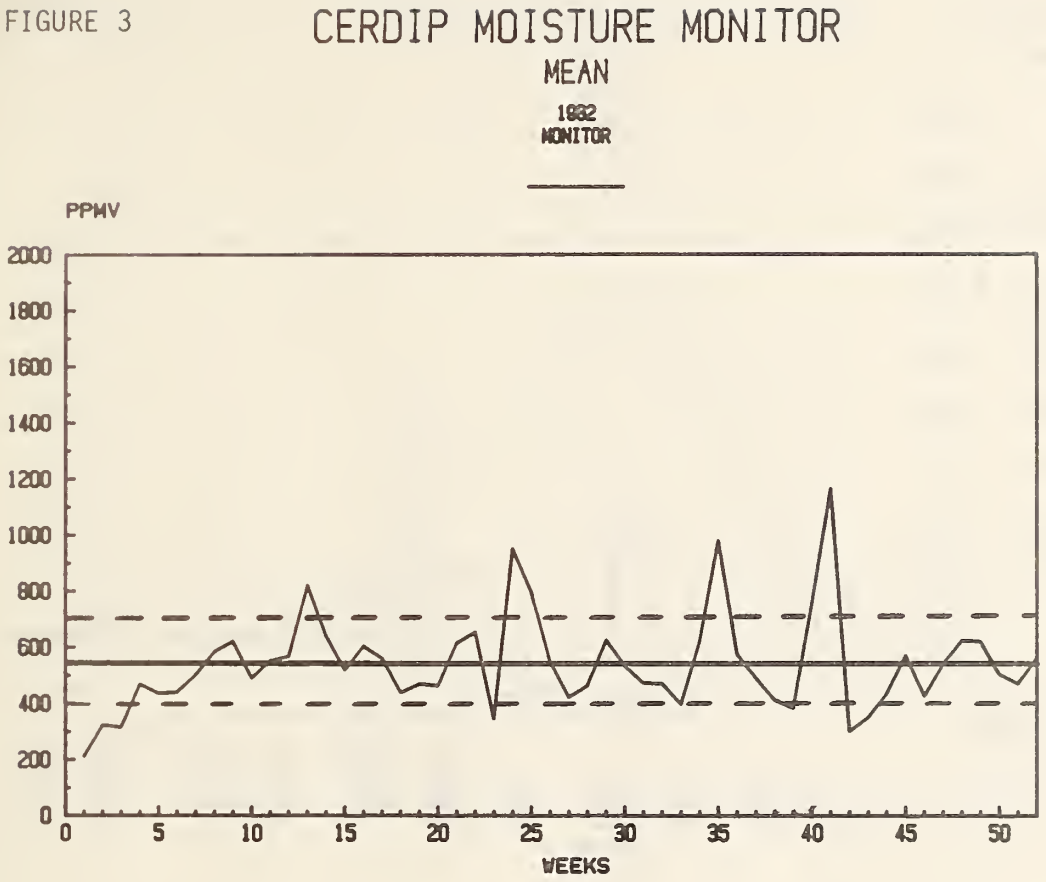

FIGURE 4

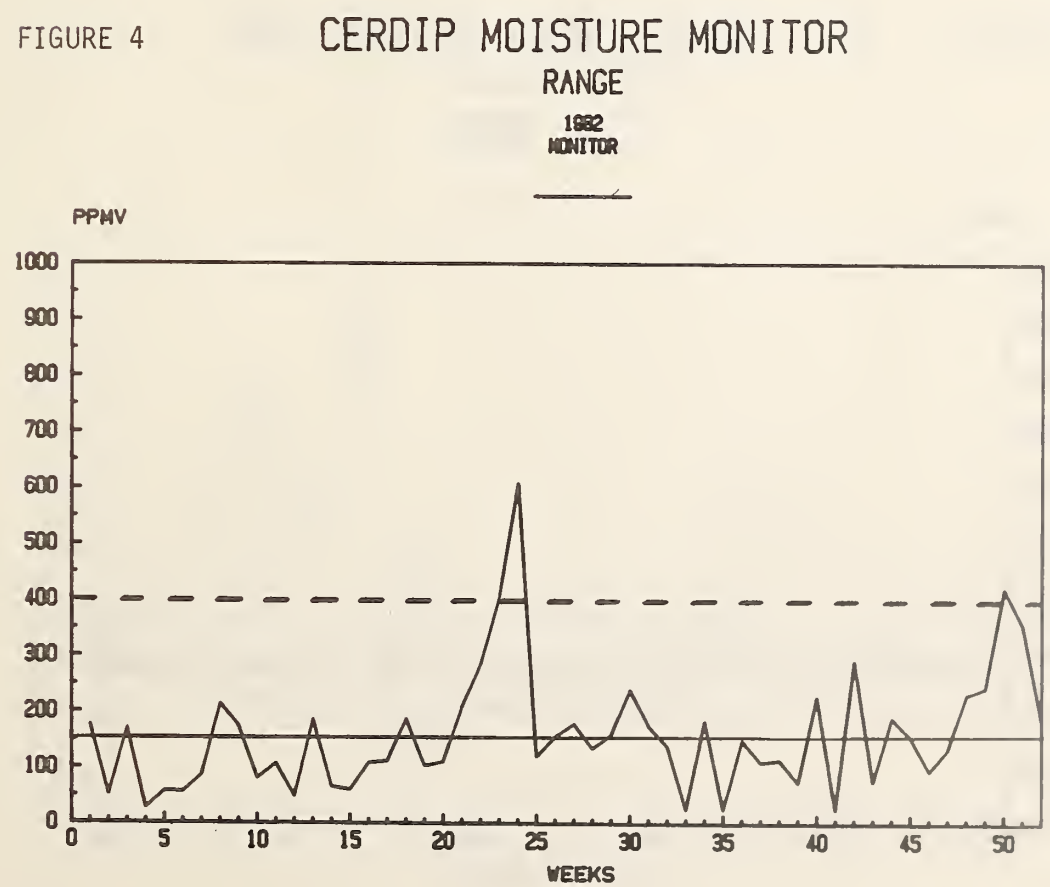

FIGURE 5

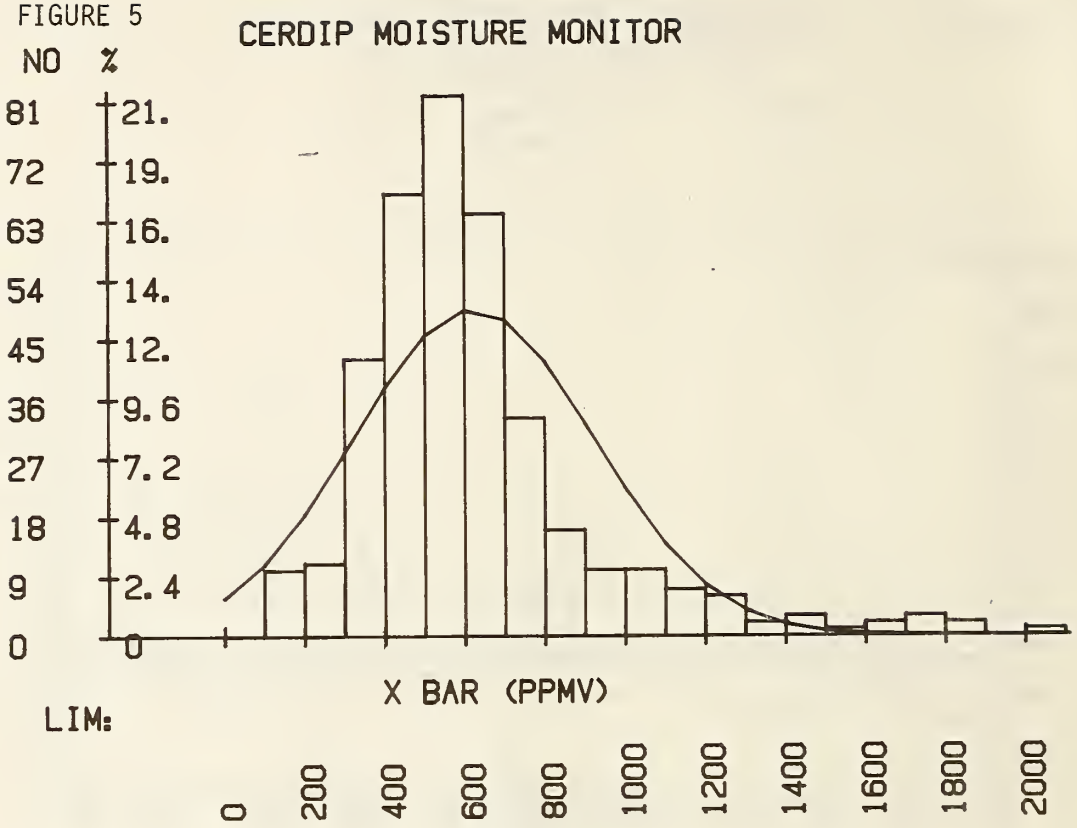

FIGURE 6

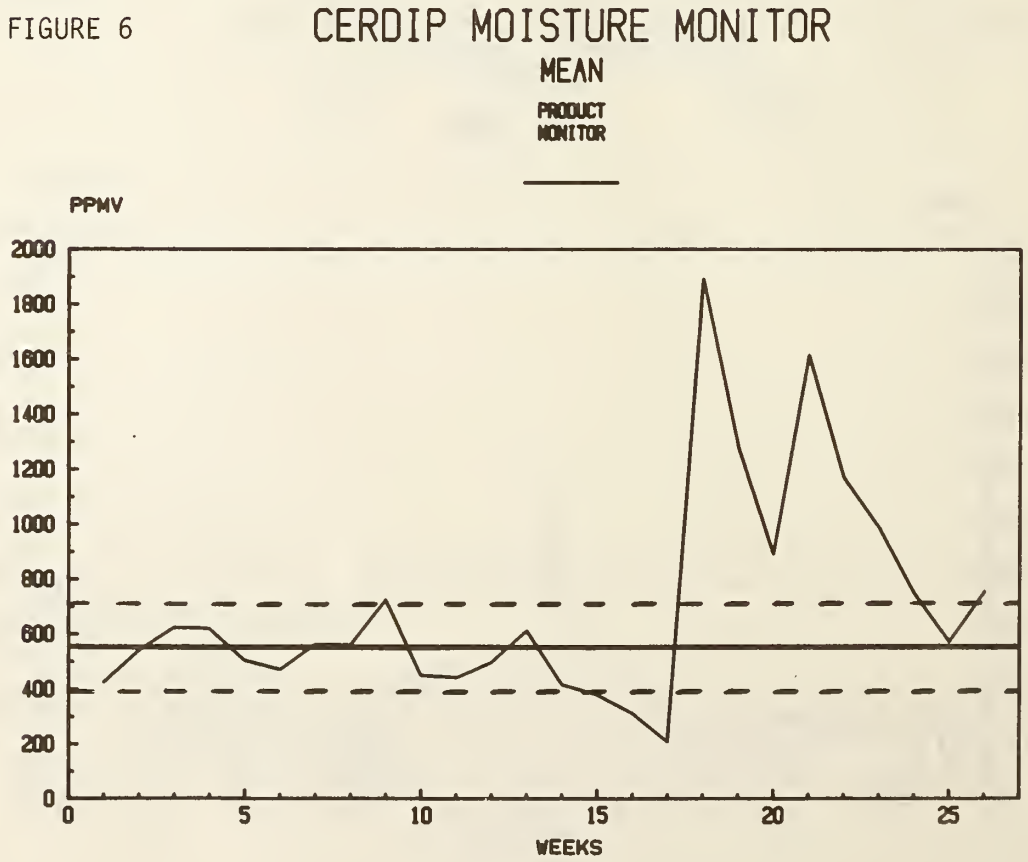

FIGURE 7

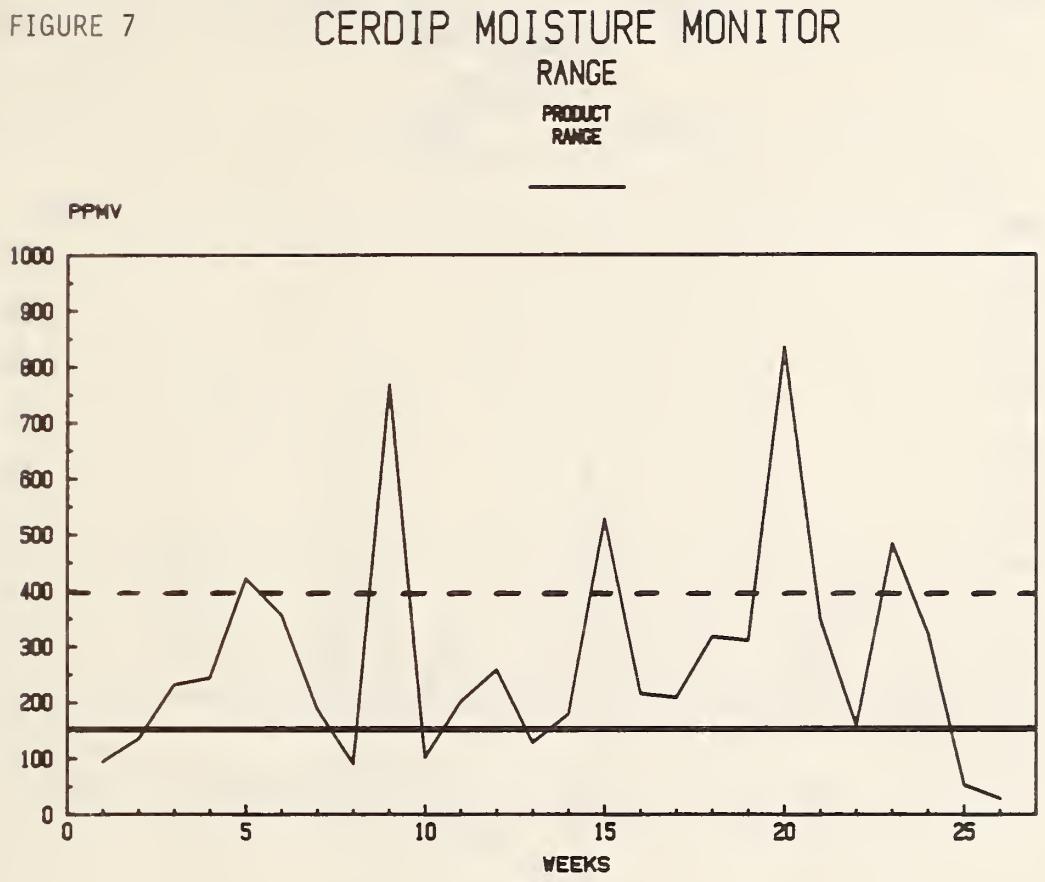

FIGURE 8

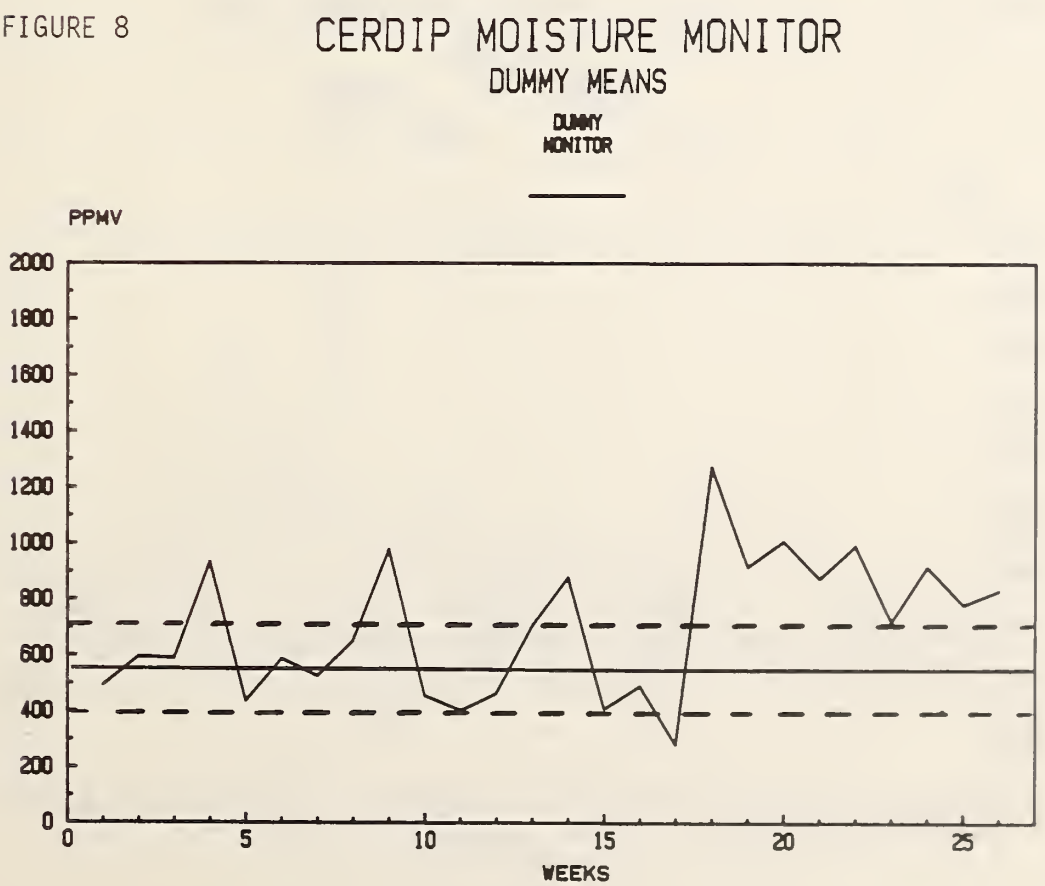

FIGURE 9

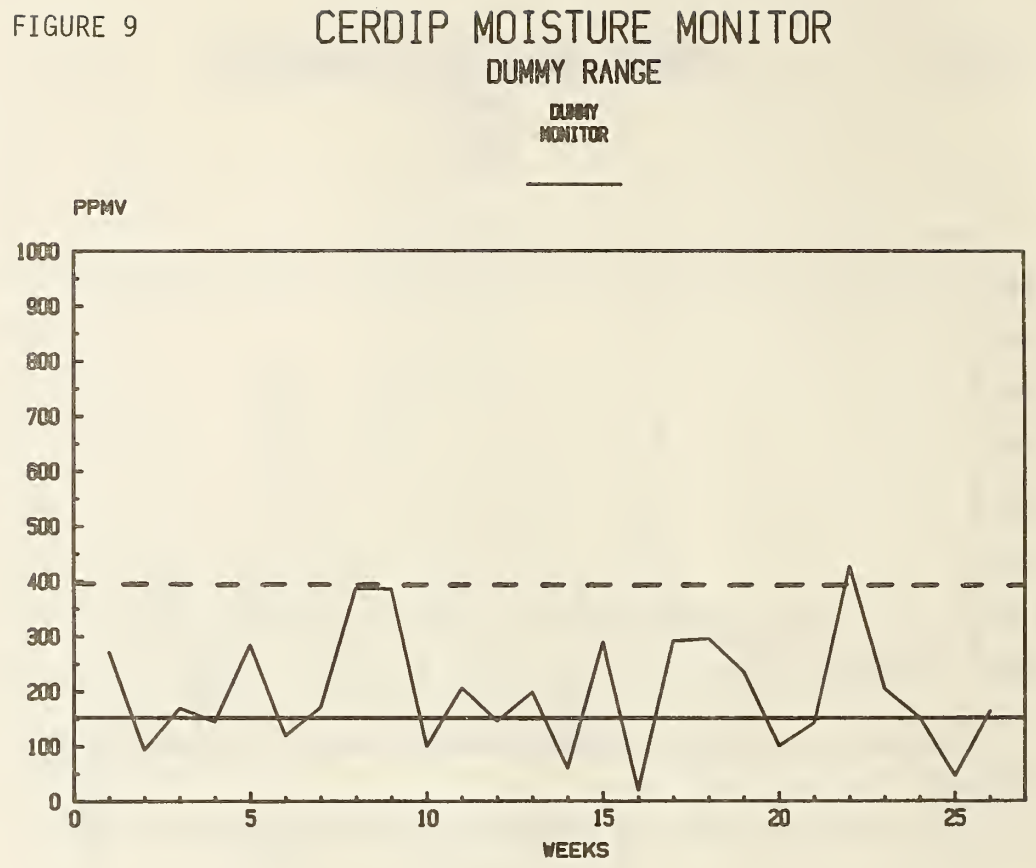

FIGURE 10

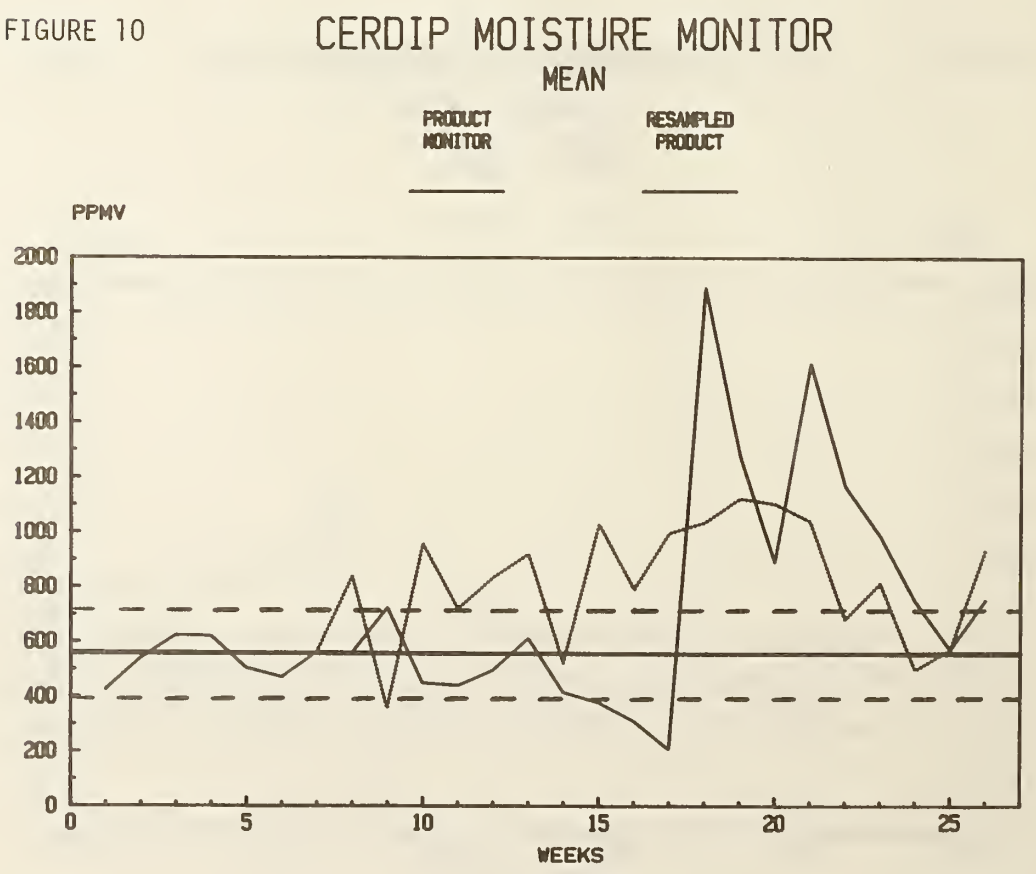

FIGURE 11

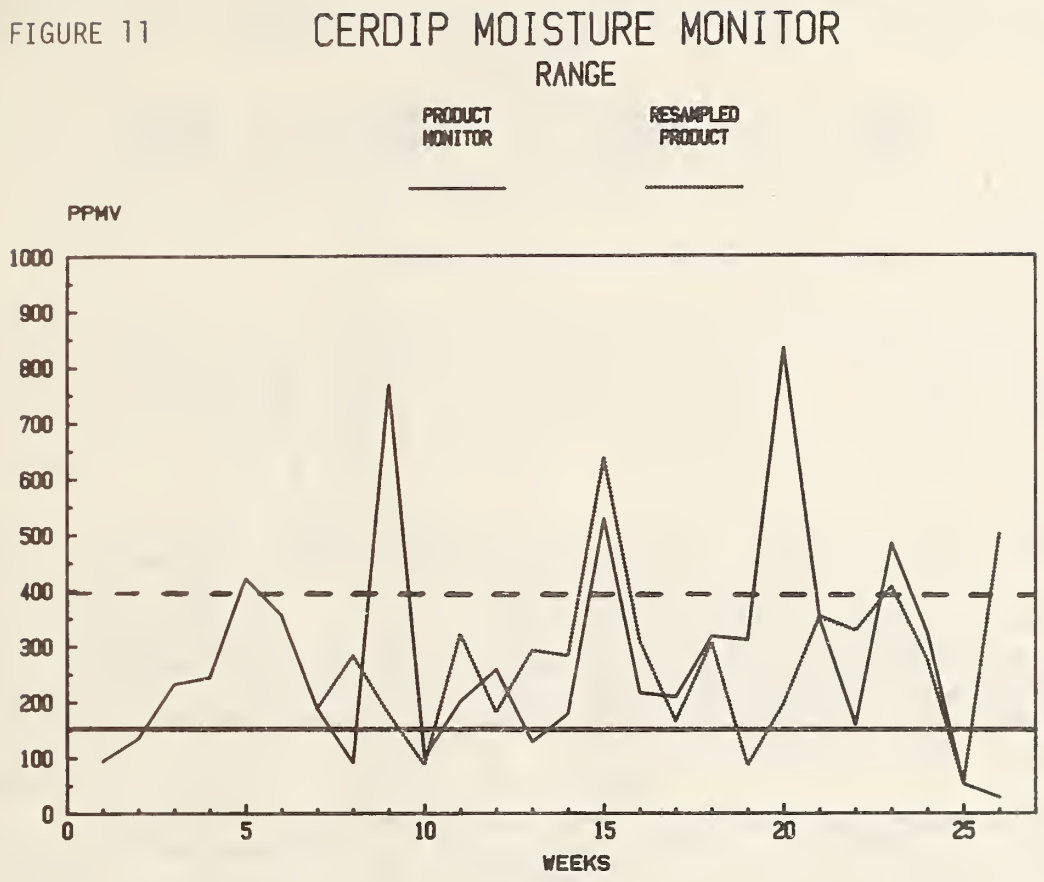

FIGURE 12

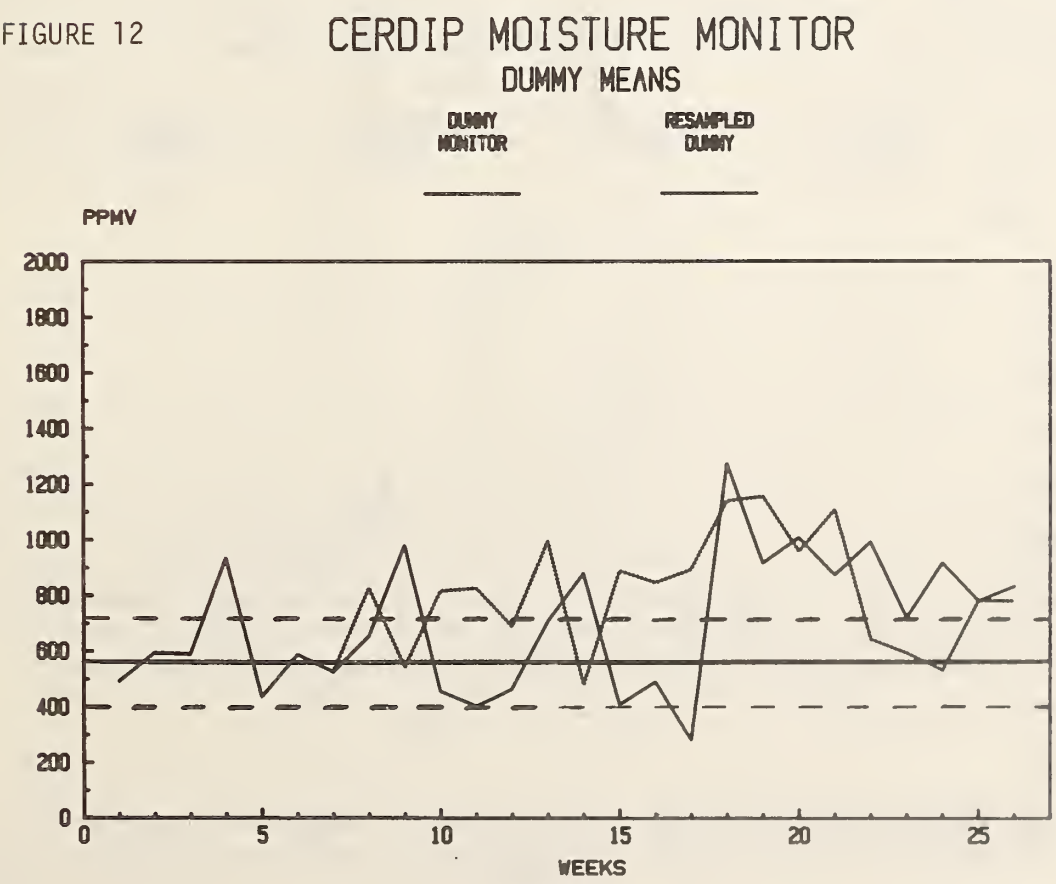

FIGURE 13

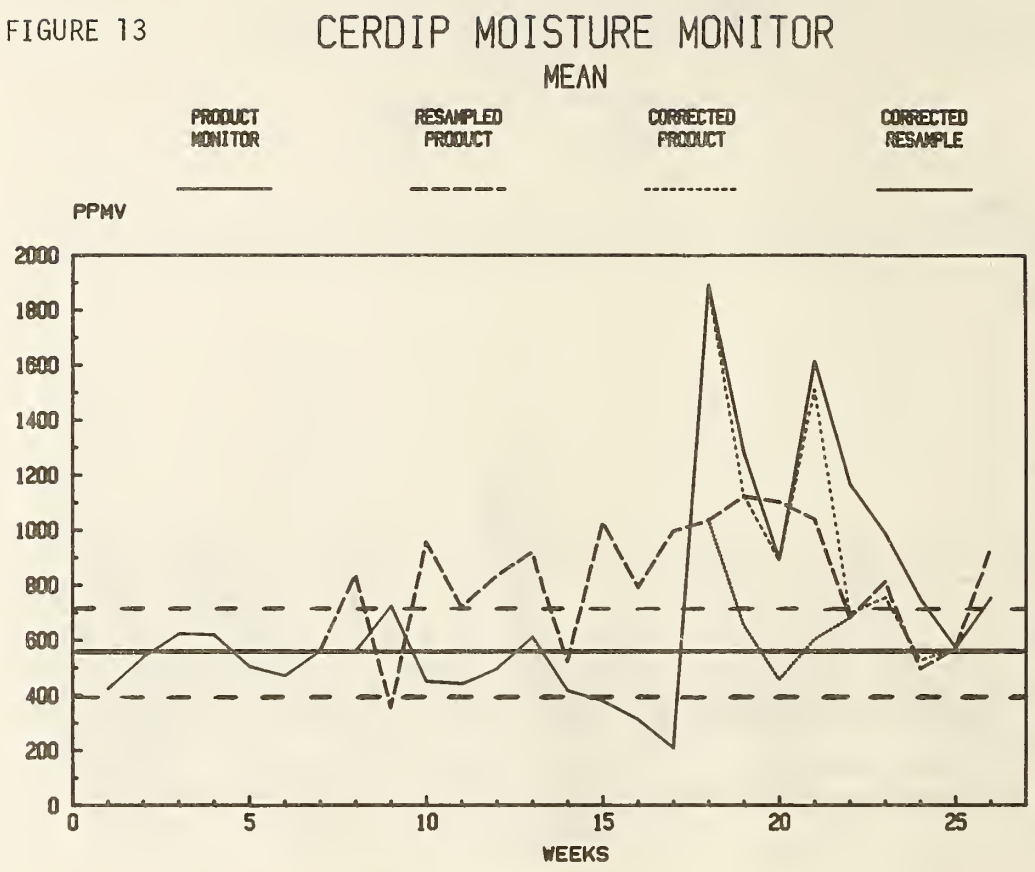

FIGURE 14

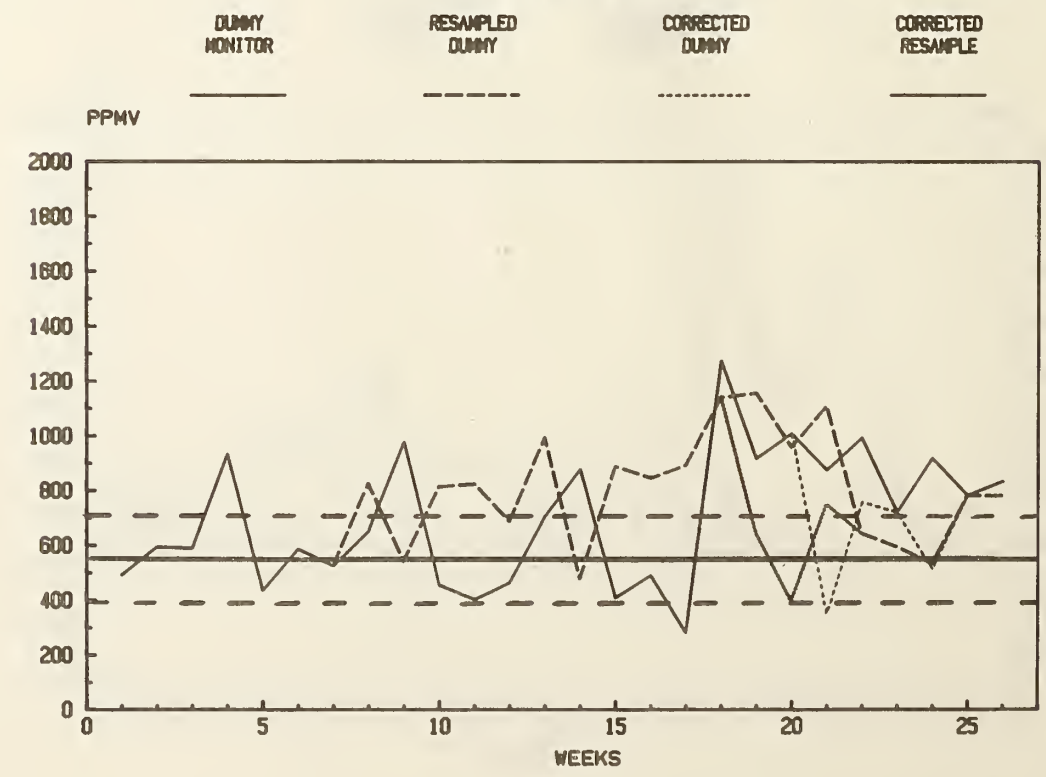

2.5 A MOISTURE STANDARD FOR IC PACKAGE GAS ANALYSIS*

Ray F. Haack
Jet Propulsion Laboratory
California Institute of Technology
4800 Oak Grove Drive, M/S 122-123
Pasadena, CA 91109

ABSTRACT

Moisture determination of IC package gas by the mass spectrometric method requires a carefully controlled analysis sequence and a standard for calibration. The availability of a well-defined standard at present is lacking. In order to provide a reproducible and reusable standard package, an investigation was begun to test a prototype model.

The standard consists of a stainless steel body with threads, brass cap, and aluminum disc. A pressure seal is made by applying suitable torque to the assembled unit. The disc enables one to access (via puncture) the trapped gas. The body of the unit has a machined cavity which provides the desired calibration volume of "moist" gas for a respective IC package gas analysis. The standard not only duplicates the sample volume, but also allows the introduction of the standard gas for calibration in identical manner to that for the IC package gas. Therefore, the dynamic method for moisture analysis of IC packages using the mass spectrometer has comparable calibration and analysis parameters.

Feasibility of the standard has been determined in two stages: (1) hermeticity testing and (2) analysis of the trapped gas. Gas analyses of sealed units having a leak rate less than 1×10^{-8} atm·cm^3/s He have shown no helium. Since the unit can be assembled and sealed at ambient conditions in an atmosphere of known moisture content, the trapped sample represents the total of surface moisture and moisture in the gaseous state at the time of sealing. For the prototype used, the effects of sealing disc material, surface area, and gas used are being investigated. Ambient air has been the principal sealing environment since its moisture content can be accurately determined and the package can be readily assembled under such conditions.

INTRODUCTION

Water and other contaminants have been of concern to the electronics industry and to customers requiring high reliability integrated circuit packages for applications in space, defense, and medicine. As a consequence of necessary qualification, test methods and procedures for analysis of moisture have been developed, as outlined in MIL-STD-883B, Method 1018.2. The mass spectrometric method and its development have been described by Thomas [1] and also outlined by this author [2,3]. Considerable progress has been made in standardization among different testing laboratories using empty parts from the electronics industry, but availability, consistency, and necessary sealing equipment have been limiting factors. A reusable moisture standard package promises reproducible volumes, ambient sealing conditions, and availability for the analyst. This investigation was undertaken to provide such a standard.

---

* This paper represents one phase of research performed by the Jet Propulsion Laboratory, California Institute of Technology, sponsored by the National Aeronautics and Space Administration, Contract NAS7-918.

EXPERIMENTAL

Fabrication

The fixture designed for containing a fixed volume of moist gas is shown in Figure 1. Stainless steel #304 was selected as the material for the body containing the cavity volume and for the cap. Initial tests produced galling of the threads, and consequently brass was used for the cap material. Cold-rolled aluminum alloy #1100 of 5 mil thickness was used for the pressure seal when torque was applied to the body, disc, and cap assembly. The type B fixture (courtesy of Pernicka Corp., Mountain View, CA) utilizes a variation of the pressure seal. It differs from type A in that it contains a stainless steel washer which transmits the pressure from the cap to the sealing disc.

Part Surface Treatment and Assembly

The surface of the cavity and the seal area were progressively worked with finer grades of grit paper and finally polished with alumina (1 micron); all steps were performed using the concentric motion of a lathe. The parts of the package were cleaned with sonication in a series of washes (water, 2-propanol, methanol). A microscopic examination of the seal area was made in order to check for any transverse scratches. The parts were dried in air at 110°C for two hours and then equilibrated at ambient conditions for 1 hour prior to assembly in the same area.

Leak Test

Within hours of assembly, the unit was subjected to a 20-hour helium pressurization test at 15 psig (2 atmospheres absolute), and then fine leak tested using a model MS-170 VEECO tester. The test method is described in MIL-STD-883B, Method 1014.4, and its application to large hybrid packages is detailed by Ruthberg [4].

Package Gas Analysis

A 20-hour high vacuum bakeout at 100°C was used prior to puncture and analysis at 100°C. The batch inlet system is interfaced with a Finnigan Model 3200 quadropole mass spectrometer. This system, which is also used for IC package gas analysis for moisture and other volatile contaminants, has been discussed in detail with respect to operation, procedure, and results, as mentioned earlier [2,3].

RESULTS AND DISCUSSION

Hermeticity Testing

The first criteria for a candidate moisture standard is a level of hermeticity which prevents a change in its composition due to external conditions. Since the package contents must maintain their integrity during a vacuum bakeout at 100°C and also at ambient conditions, helium pressurization was used so that the mass spectrometer would detect any inward diffusion of helium. Initially, this would assist in determining the minimum leak rate necessary for this type and size of package. Representative leak rates and helium analyses are shown in Figure 4. A variation of torque values was used for assembling the package and achieving an optimum seal. Although 150 in-lb_f torque produced some good seals, the torque is mechanically excessive for the thickness (5 mil) of the disc, the threads, and for the metal hex. Several trials are not shown here because either the leak rate was of the order of 10^{-7} atm·cm^3/s or helium in the package gas was in excess of 10% (volume/volume). A decreased torque of 50 in-lb_f was not sufficient to produce a seal significantly hermetic in the case of helium. Finally, for the 75-90 in-lb_f torque, several units

had measured leak rates better than $1x10^{-8}$ atm·cm^3/s He. Gas analysis for these packages did not indicate any presence of helium (<0.1%).

Gas Analysis

It is possible to reasonably predict the pressure produced upon puncture of the sealed package (burst pressure) when the cavity dimensions, sealing conditions, and batch inlet chamber volume are known. The measured and predicted values for burst pressures of some units are shown in Table I. For packages of ~0.1 cm^3 volume, good agreement was found except for S/N 4-0216 (gas analysis indicated 7% helium!). Unit S/N 6- was sealed at two different times and gave almost identical burst pressures. The units of ~0.02 cm^3 volume were generally higher in burst pressure than expected. It has been observed that the sealing disc (5 mil) does not always remain flat while the unit is assembled. The curvature of the "cap" for the 0.02 cm^3 cavity would significantly affect the total volume.

A complete set of physical measurements and gas analysis results for several packages (all sealed in air at ambient conditions) are shown in Table II. The following items should be recognized:

- For leak rates <$1x10^{-8}$ atm·cm^3/s He, helium was not detected (<0.1%) upon analysis of the package gas.
- The analyzed %H_2O represents the total moisture (includes adsorption), whereas the %H_2O (theory) is calculated using the relative humidity measurement of ambient air.
- S/N 26- and 27- were sealed on the same date but analyzed by two different laboratories. Agreement with regard to helium and to moisture levels measured is encouraging.

The gases evolved upon puncture of the package are analyzed in their entirety by the mass spectrometer. Since the burst pressures for known cavity volumes are measured in a calibrated volume at 100°C, it is possible to express the moisture content in units of total micrograms (µg). These moisture units are more pertinent than % volume/volume when some variation in burst pressure is observed and when discussing adsorbed surface moisture effects. The measured moisture (µg) for packages of 0.1 cm^3 and 0.02 cm^3 volumes is given in Table III. The corresponding theoretical values listed do not include adsorbed moisture. An approximation of this factor can be made using physical constants for the water molecule [5,7]. If the geometric area for S/N 24-0816 has a surface monolayer, the total µg would be 0.0338. At ambient conditions (40-50% relative humidity), 10 monolayers could actually be present, and furthermore, the geometric area would be considerably less than the true surface area. Consequently, even a geometric area with 10 monolayers of water for this package could contain at least 0.338 µg of water.

The preceding discussion concerning adsorbed moisture has applications in this respect: the stability and measured value of moisture for a sealed package must be established. A reusable package (known history and surface condition) should decrease significantly the surface characteristics influence as discussed by Singh et al. [6].

CONCLUSIONS

These packages can be sealed and analyzed at a later time. Results thus far indicate that the hermeticity and moisture can be maintained until time of analysis

after a conventional vacuum bakeout at 100°C for a period of 20 hours. Although the degree and role of adsorbed moisture has not yet been determined, changes in surface/volume ratios and sealant gas should elucidate these factors. Inward diffusion of moisture and/or argon which could occur upon storage of the packages at ambient conditions can be adequately determined later when nitrogen is used as the sealant gas. The detection at low ppm level for inward argon diffusion is reasonably accurate.

More precise moisture control, as is possible with a gas humidification system and an optical dew-point hygrometer, will aid in determining the adsorbed moisture effect. Further study involving either nitrogen or air at the 0.5% volume/volume level and an effort to control the surface finish should provide a basis for determining the stability of the amount of total moisture present.

The second phase of this investigation will consider some of the aforementioned aspects such as surface nature and lower, more precisely controlled moisture levels. Presently, it appears that the package is also suitable as a container for testing outgassing characteristics of small amounts of materials at temperatures from ambient to 100°C.

The author wishes to acknowledge the assistance of W.W. Reilly with the design of the package and B. Moore of RADC for suggestions and analysis results.

REFERENCES

1. Thomas, R.W., "Moisture Myths and Microcircuits", Proceedings 26th Electronic Components Conference, pp. 272-276, San Francisco, CA, April 1976.

2. Haack, Ray F. and Shumka, Alex, "Microcircuit Package Gas Analysis", ARPA/NBS Workshop V, Moisture Measurement Technology for Hermetic Semiconductor Devices, NBS SP 400-69, May 1981, pp. 43-57.

3. Haack, Ray F. and Shumka, Alex, "Moisture and Other Contaminants in Hybrid Packages", 1978 International Microelectronics Symposium, September 25-27, 1978, Minneapolis, MN, pp. 128-133.

4. Ruthberg, Stanley, "Hermetic Testing of Large Hybrid Packages", 1982 International Microelectronics Symposium, November 15-17, 1982, Reno, NV, International Journal for Hybrid Microelectronics, Vol. 5, No. 2, November 1982, pp. 215-232.

5. Brunauer, Stephen, The Adsorption of Gases and Vapors, Volume I., Physical Adsorption, Princeton University Press, Princeton, NJ, 1945.

6. Singh, Avtar et al, "Effects of Surface Condition on Nucleation and Boiling Characteristics", Technical Report prepared for Army Research Office, National Technical Information Service, AD/A-007 275 (Report No. ARO-9731.2-E), September 1974.

7. Vasofsky, R., Cyanderna, A., Cyanderna, K., "Mass Changes of Adhesives During Curing, Exposure to Water Vapor, Evacuation, and Outgassing. Part I: Abelfilms 529, 535, and 550", IEEE Transactions on Components, Hybrids, and Manufacturing Technology, Vol. CHMT-1, No. 4, December 1978.

S/N	CAVITY VOLUME (cm^3)[a]	STORAGE TIME (days)[b]	BURST PRESSURE (Torr)	
			theory	measured
4-0216	0.1125	2	0.429	0.500
3-0221	0.1125	3	0.426	0.474
6-0221	0.1125	3	0.426	0.459
6-0301	0.1125	9	0.426	0.462
26-0823	0.0225	17	0.085	0.118
26-0913	0.0225	17	0.084	0.122
28-0913	0.0225	17	0.084	0.092

a Calculated using cavity dimensions and assuming flat sealing disc
b Ambient conditions

Table I. Burst Pressures for Sealed Packages

S/N	CAVITY VOLUME (cm^3)	STORAGE TIME (days)	BURST PRESSURE (torr)	FINE LEAK RATE ($atm \cdot cm^3/s$ He x 10^{-8})	ANALYSIS (% volume/volume)[b]			$\%H_2O$	
					He	H_2O	Ar	(theory)[c]	actual/ theory
1-0316	0.1125	90	0.410	0.14	ND[a]	1.48	0.94	0.93	159
1-0725	0.1125	2	0.414	0.15	ND	1.70	0.94	1.25	136
3-0221	0.1125	3	0.474	0.14	ND	1.40	1.05	0.86	163
6-0221	0.1125	3	0.459	0.54	ND	1.14	1.10	0.86	133
23-0816	0.0232	2	0.134	0.70	<0.02	3.05	1.04	1.28	238
24-0816	0.1125	2	0.490	0.16	<0.02	1.24	0.95	1.28	97
25-0816	0.0225	2	0.123	0.70	<0.02	3.42	1.07	1.28	267
26-0823	0.0225	17	0.118	0.30	<0.1	1.19	0.94	1.39	87
27-0823	0.0225	~30	NA[d]	0.30	ND	1.424[e]	0.887	1.39	102
26-0913	0.0225	17	0.122	0.05	<0.1	1.90	1.05	1.33	143
28-0913	0.0225	17	0.093	0.03	<0.1	2.41	1.01	1.33	181

a ND = None Detected
b The results for oxygen and nitrogen are omitted for the purpose of simplicity.
c Calculated from ambient relative humidity measurement (psychrometer); does not include surface adsorbed moisture
d NA = Not Available
e Analysis courtesy of RADC, Griffiss AFB, Rome, N.Y.

Table II. Gas Analysis of Prototype Moisture Standards

S/N	CAVITY VOLUME (cm^3)	SURFACE AREA (cm^2)[a]	MOISTURE (µg)	
			theory[b]	measured
24-0816	0.1125	1.302	1.154	1.128
23-0816[c]	0.0237	2.419	0.243	0.759
25-0816	0.0211	0.544	0.217	0.781

a Calculated geometric area. The true surface area (dependent upon surface finish) could vary several fold from the calculated geometric area; e.g., the ratio of true surface/ apparent surface for rolled new nickel is 5.8, newly polished 13.3, newly activated 46 [5].

b Calculated from ambient relative humidity measurement (psychrometer); does not include surface adsorbed moisture

c Contains cylindrical insert (0.0893 cm^3 volume; 1.1133 cm^2 area), original cavity volume was 0.1130 cm^3.

Table III. Package Cavity Moisture (micrograms) and Surface Area

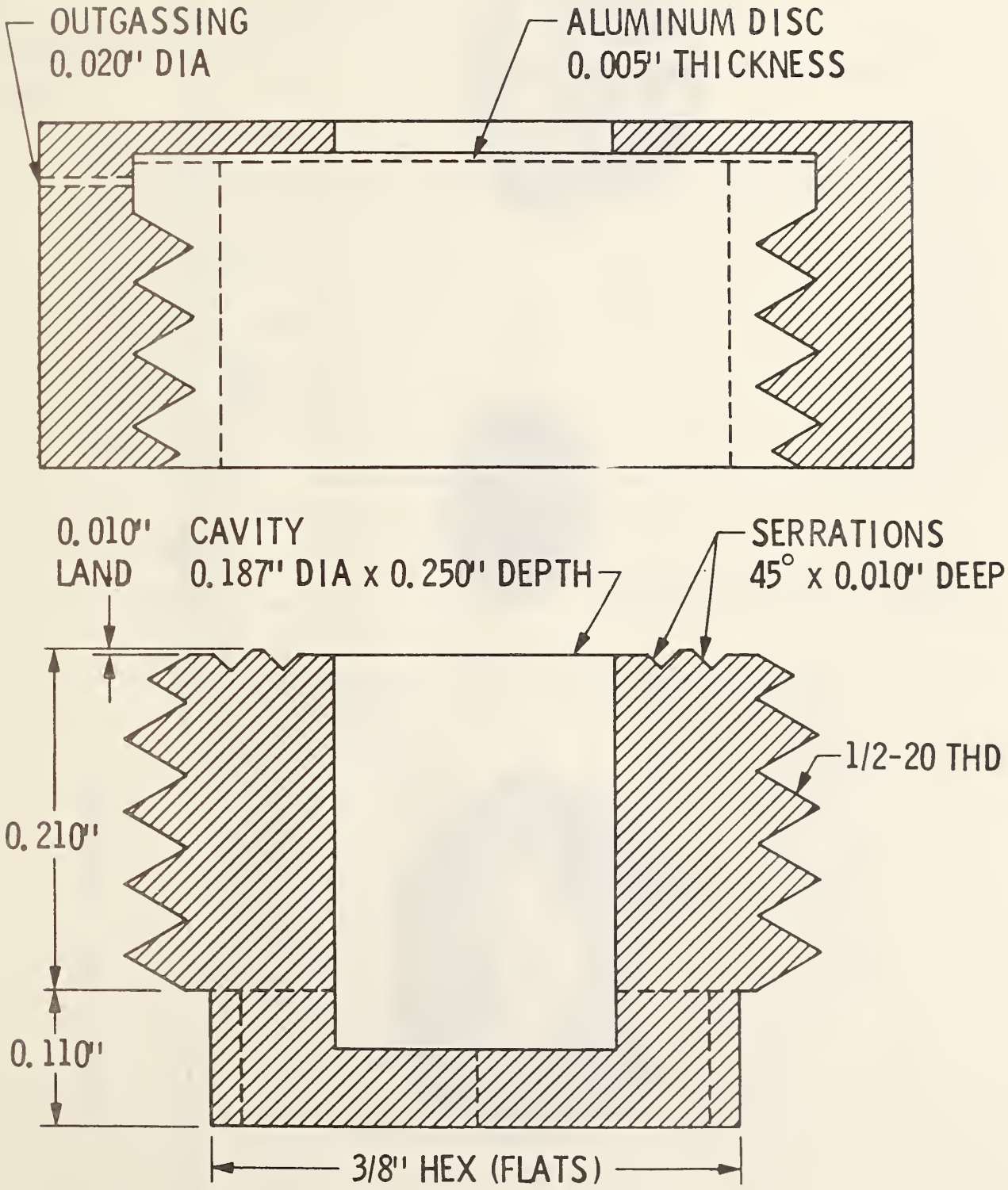

Figure 1. Package Schematic - Type A

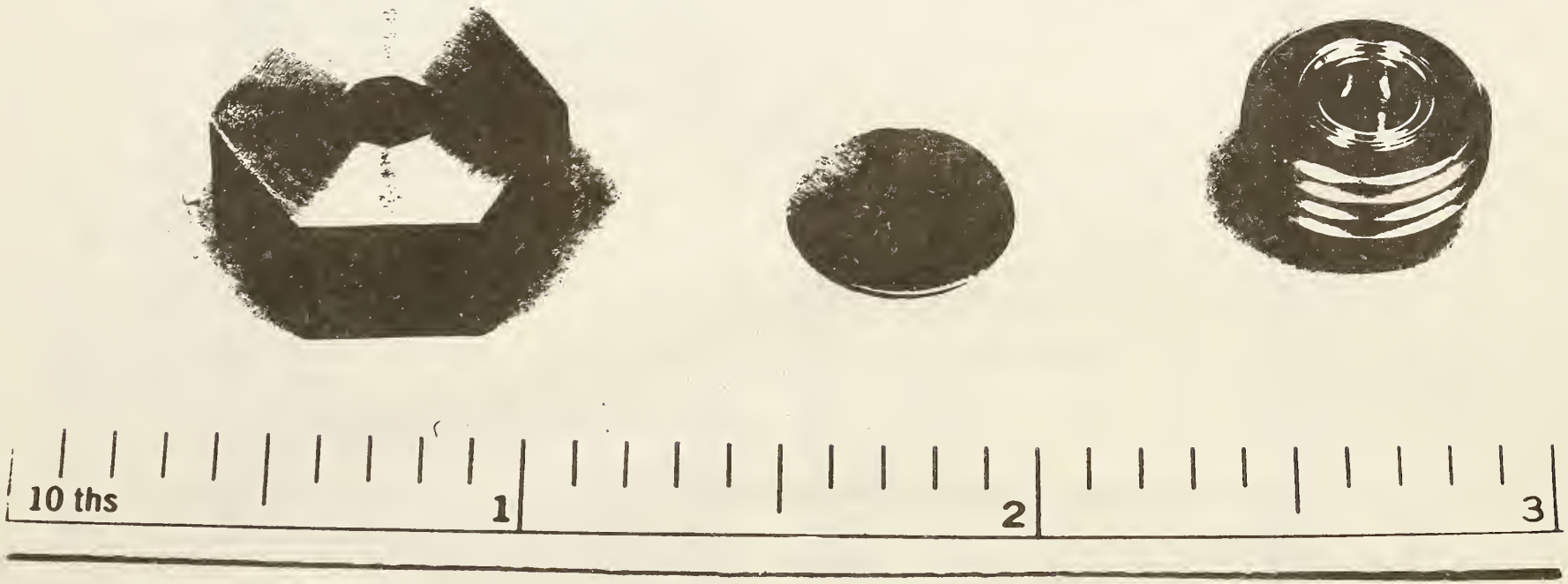

Figure 2. Package - Type A - Photograph

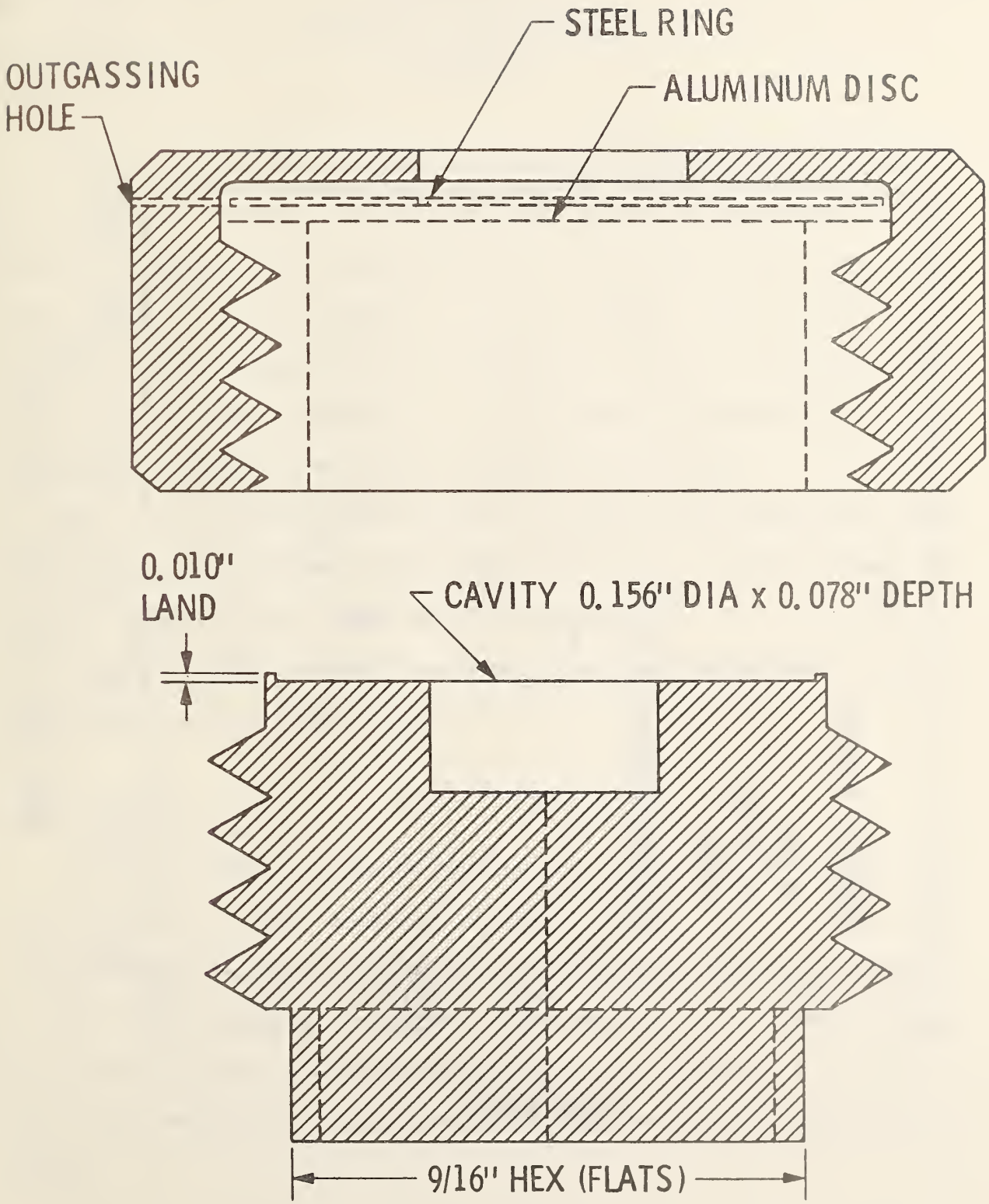

Figure 3. Package Schematic - Type B

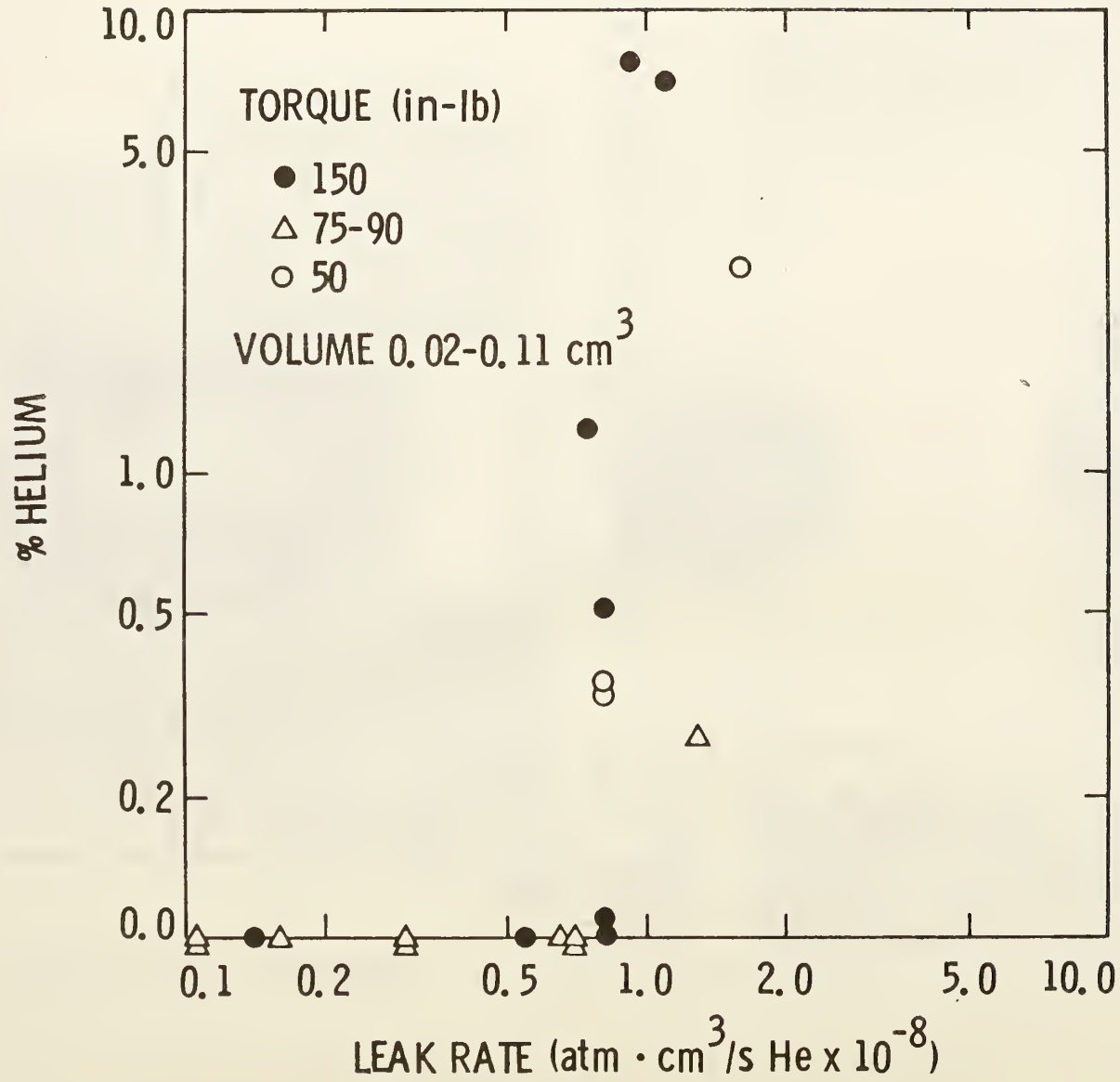

Figure 4. Seal Permeability: Gas Analysis (helium) vs. Assembly Torque Value

2.6 THE EVOLUTION OF METHOD 1018

Robert W. Thomas
Rome Air Development Center
Griffiss AFB NY 13441
(315)330-3730

Method 1018.2 is not, at present, a universal test method which can be applied to any hermetic enclosure. It was specifically tailored to measure the internal ambient of packages such as CERDIPs and metal TO-5 cans that contain eutectically bonded chips. A further constraint is that the package interior be free of any outgassing sources (epoxies, desiccants, devitrifying sealing glass). Since this covers 95% of the JAN military qualified parts that are produced, the specification can then be judged as successful at least as far as the military is concerned.

With the introduction of MIL-STD-1772 to qualify hybrid manufacturers there will have to be major revisions to Test Method 1018.2 that will take into account the variety of outgassing sources used to fabricate hybrid parts.

In order to better understand the necessary changes, it may be useful to review what a test method is and what it isn't.

What is Method 1018?

The method defines the desired measurement as the amount of moisture in the vapor state at 100°C under equilibrium conditions. The parts must be prepared for analysis so that the results are reproducible. The method describes a method of puncture that will give valid results and specifies the range of volume and moisture levels that may be measured accurately based on current availability of standards. It offers three methods that may be used for analysis and sets the temperature of analysis.

What it isn't!

It is not a detailed cookbook that anyone can use to do moisture analysis. There is a great deal of technique and hardware required in order to meet the Defense Electronic Supply Center (DESC) suitability requirements. As was said before, it is not universally applicable to all hermetic enclosures. For instance, it does not apply to parts which are either evacuated or filled with an inert liquid.

There are many questions left unanswered by the test method that must be established by the analytical laboratory customer. The customer must specify whether the sample being tested to Method 1018 is a JAN, DESC controlled, Qualified Parts List (QPL) test sample. The analytical lab is required to record and report the results of these tests in a specific way. Essentially, for JAN samples the data from a Method 1018 test becomes the property of the government. DESC controls, through the application of MIL-STD-5004, how and when the samples are pulled from the production line, establishes the failure criteria and grants suitability status to the analytical labs by quality source inspection (QSI). For JAN parts, DESC requires the test apparatus to be set up to maximize ambient moisture as opposed to someone performing a epoxy adhesive study to optimize bakeout time. The latter might require extended bakeout prior to analysis to insure that moisture has been adequately removed from the adhesive material.

To summarize the problems associated with invoking Test Method 1018 for non-JAN devices, refer to Figures 1 and 2. In the case of JAN devices, the system is a self-contained set of specifications, and surveillance that is controlled at each stage by a government agency. For non-JAN analysis, any lab can do a 1018-like analysis, however, the vendor must perform his own suitability evaluation and laboratory surveillance to assure that the laboratory complies with Method 1018 requirements. The vendor must also call out specific sections in Method 5004 or 5008 depending on the device type (ie, IC or Hybrid). This will insure that the method of sampling and

the failure criteria are adequately specified. It is also the responsibility of the parts supplier or systems house to indicate in the service contract information which will assist the analytical lab in setting up the analytical conditions that will insure optimum results. It is required that the manufacturer notify the laboratory if the samples submitted are to be analyzed for JAN qualification. It is also necessary to notify the laboratory that the samples contain either desiccants or known absorbing/desorbing material such as polyimides, epoxy or silicone. Information on unusual ambients, such as 100% helium, greater than 20% oxygen, or greater than 1% condensible gases like freon, alcohol, MEK or acetone should be supplied to the analytical laboratory. It is also helpful to indicate a preferred or optimum place to puncture the package. If the package is fragile (like some cerpacks) this will prevent unnecessary seal breakage which invalidates the analysis. The point of puncture may be necessary to control in samples that are destined for failure analysis where an undamaged chip is high priority requirement. Giving the analytical laboratory as much information about the analysis as is possible will insure that the customer gets his money's worth.

Recent Changes

To insure that organic containing parts are analyzed in a uniform manner, RADC is in the process of establishing a moisture standard that will contain an absolute amount of water. The purpose of the total water standard will be to provide a correlation standard that will allow the analytical laboratories to establish their own data analysis procedures that will include the majority of the outgassing moisture in the final analysis. RADC has proposed that the laboratories be required to adjust their data reduction routines so that 75% of the total moisture in the known standard be reported. This requirement should not affect the results for currently qualified vendor packages which do not contain absorbing species (i.e., epoxy, polyimides, and porous sealing glass). The new moisture standard will require a

change in the definition of internal moisture so that some of the desorbing moisture is included in the reported moisture. It is also RADC's intention to lower the moisture limit for all packages to 2000 ppm_v as a part of a progressive program to eliminate moisture from electronic packaging systems. As a preliminary requirement to lowering the moisture content, RADC will conduct further round robin correlation studies at 1000, 2000, 5000 and 10,000 ppm_v. Concurrently with the correlation tests, RADC will request DESC (Defense Electronic Supply Center) to sample current data from JAN suppliers to insure that all of them can meet the new limit before it is imposed. Recent Data indicates that 95% of the JAN qualified packages can now meet a 2000 ppm_v requirement.

ON THE LIGHTER SIDE

On many occasions over the past eight years, RADC has been called upon to resolve disputes regarding questionable water vapor analysis. A summary of the reasons for why moisture analysis on identically produced parts is sometimes radically different is presented below.

The Government has determined that the following can affect the moisture content of identically sealed parts:

1. A blister decided to outgas
2. The glass- feed through had internal surface cracks
3. Some one slipped in a dessicated lid
4. Purge gas tank ran dry
5. Some parts missed bakeout
6. Bulk liquid N_2 tank was filled during sealing
7. Compressed gas solenoid valve leaked inside dry box
8. Operator couldn't get seal - so removed from dry box and blew it off with clean dry air

9. One package had twice the amount of epoxy
10. Gas supply lines were contaminated
11. Used Neoprene gloves on the dry box
12. CERDIP lids were tossed into a container for bakeout
13. KC-1M super dry was allowed to sit out on the bench
14. Inspectors didn't check the super dry packaging for leaks
15. QC opened the dessicated DC-1M super dry containers to inspec them
16. The sealing furnace was cracked
17. When the furnace was moved, there was a pool of water on the floor
18. After solder dipping, the packages were cooled down in a water bath
19. Lids were mixed from overseas operation
20. Mass spec had a hiccup
21. Operator misplaced the decimal point
22. The percent constituents added up to 80% by volume
23. There was little gas left in the package
24. Wet epoxy parts were baked out next to clean empty controls

SUMMARY

The moisture specification of 5000 parts per million was chosen to eliminate gross corrosion in ICs and hybrids. It was based on many years of moisture research at RADC and elsewhere seeking scientific answers to practical problems involving measurement techniques, the use of organic materials and dessicants, and the establishment of bakeout schedules. Military parts are unique in that they must be demonstrated reliable over wide temperature extremes. These conditions have proven to accelerate moisture related failure mechanisms. The cost of part failure in an operational military system can be enormous. Continued system reliability problems have created a constant pressure to control the moisture content of

military electronic parts. Prior to 1976, many JAN parts had moisture contents greater than 10,000 parts per million. This coupled with analytical facilities which were orders of magnitude apart in correlation prompted the Defense Department to prepare MIL-STD-1018 and specify, for JAN parts, a maximum moisture content of 5000 ppmv.

For the past eight years RADC has pursued a program of improving calibration procedures and correlation standards. As a positive effect of this program, the moisture content of both hybrids and integrated circuits has been steadily dropping as an awareness of moisture and the problems it causes becomes known more widely. This has increased system reliability and reduced the cost of logistic support resulting in the savings of untold millions of taxpapers dollars. Unfortunately, the task is not complete. The test method is still only applicable on a pass or fail basis to military IC packages that do not contain organic materials. For other package types or moisture limits, the use of this test method should be for general guidance only realizing that the results from the Mil-Qualified test labs will generally not give the same answer at lower moisture limits or if the parts contain organic die attach materials. It is expected that this situation will be corrected shortly with the distribution of 1000 ppmv moisture standards and the rewriting of the specification to include organic containing packages. In the interim, manufacturers should still be concerned about packages with high moisture content and efforts should continue on product improvements that will produce dry hermetic packages.

Our common goal is to eliminate moisture as a cause of failure. To do this, limits have been set consistent with the ability to measure accurately. Changes have been programmed several years ahead of time. This will solve basic problems before restricting component availability.

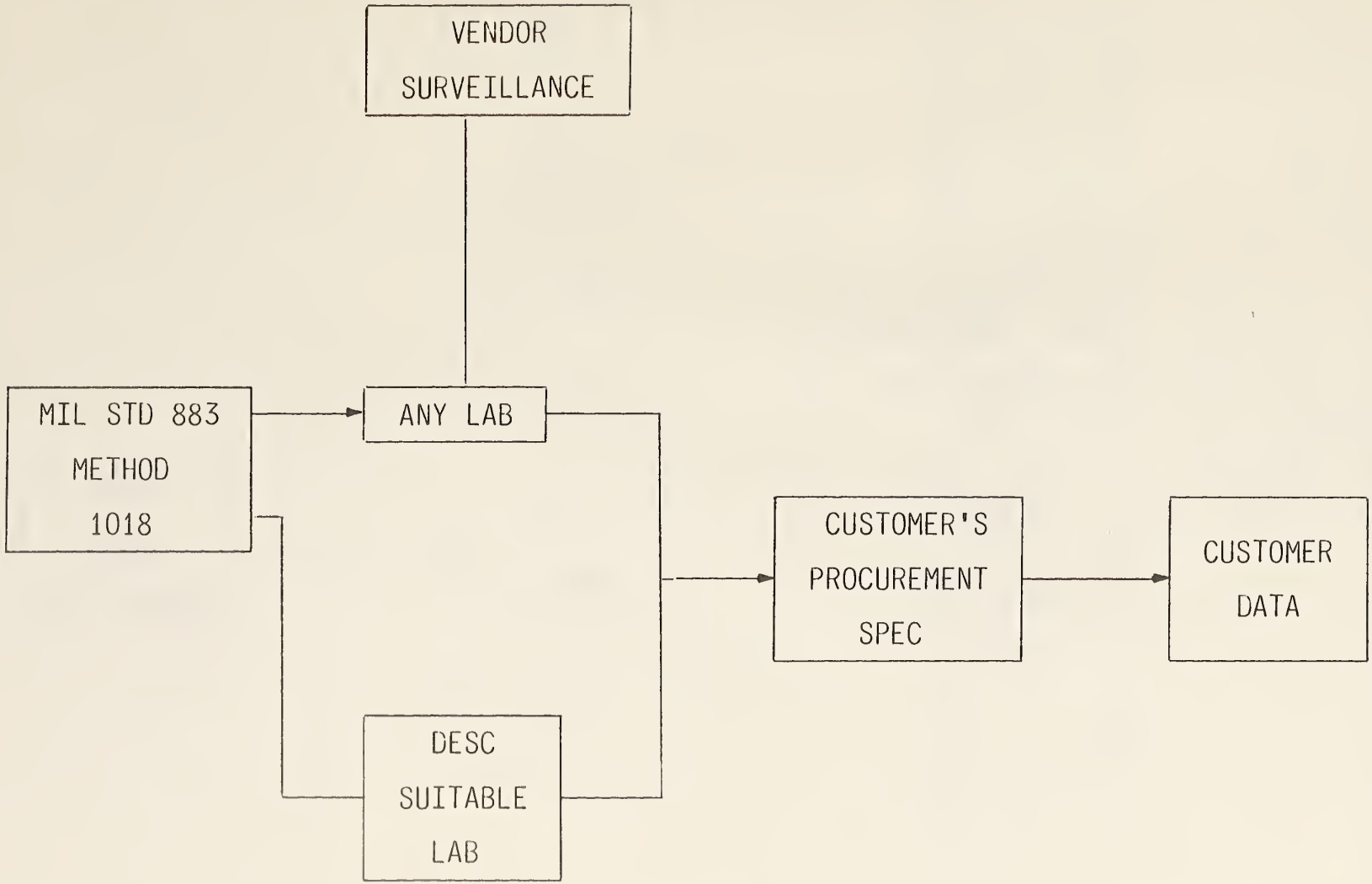
VENDOR
SURVEILLANCE
MIL STD 883
METHOD
1018
ANY LAB
CUSTOMER'S
PROCUREMENT
SPEC
CUSTOMER
DATA
DESC
SUITABLE
LAB

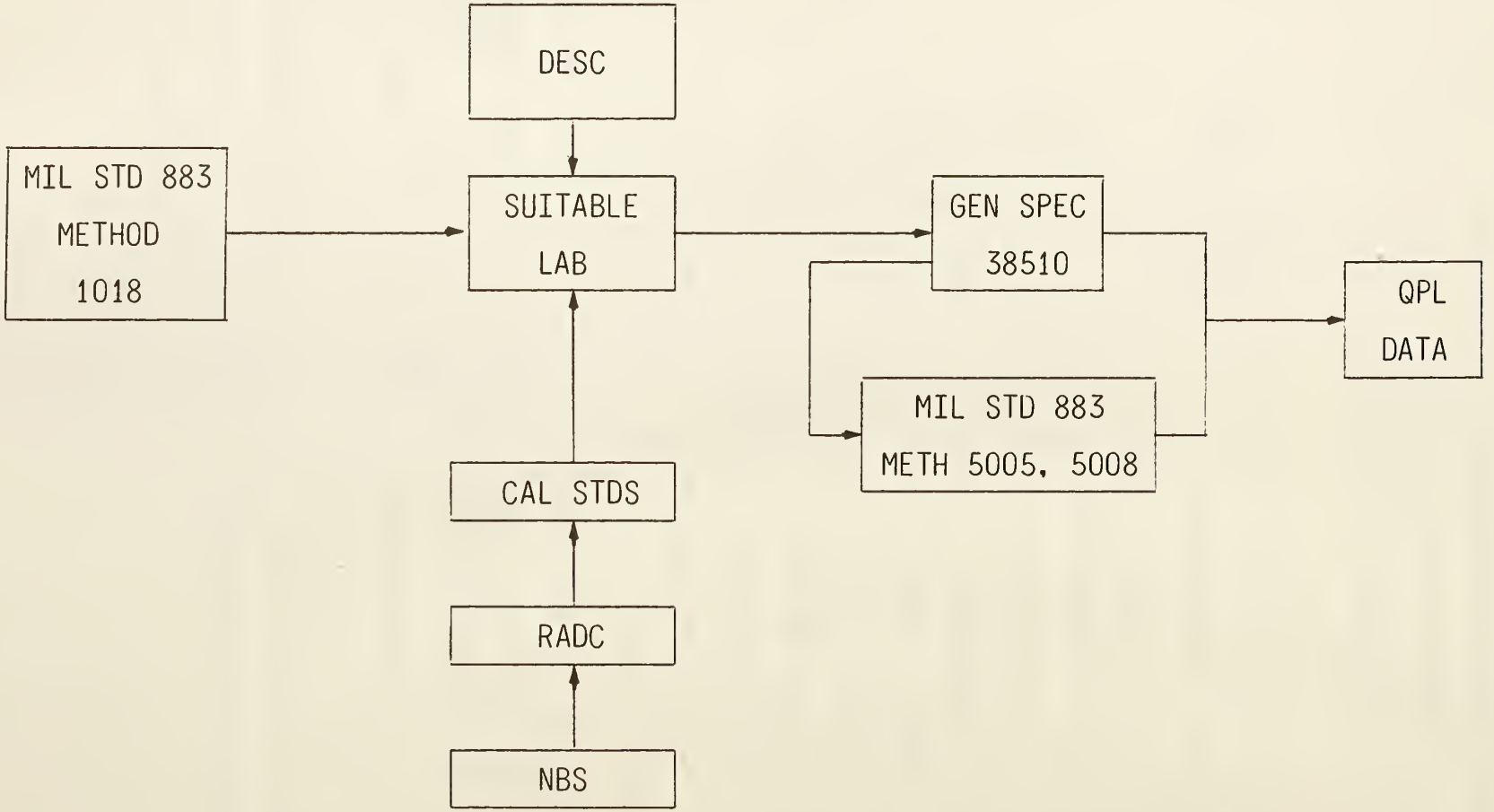

HOW THE MIL SPEC & STDS
WORK FOR JAN PARTS

3. SESSION II MOISTURE MEASUREMENT METHODS

3.1 SELECTING MOISTURE MEASUREMENT METHODS FOR SEMICONDUCTOR DEVICES

R. K. Lowry
Harris Semiconductor
P. O. Box 883
Melbourne, Fl. 32901-0101
305-724-7566

Package assembly and reliability engineers, failure analysts, and quality assurance personnel all struggle with various aspects of moisture control in IC packages. Choosing the best analytical method can be governed by a variety of factors, including cost, resources, point at which moisture information is needed, etc. The best testing method in one situation, e.g. screening incoming package lots for moisture content, may not be the best method for a different situation, e.g. analyzing a field failure. This paper will compare and contrast both developed methods and emerging (though not necessarily readily available) methods to assist in selecting package moisture measurement methods.

A COMPARISON OF PACKAGE MOISTURE MEASUREMENT METHODS

		METHODS DESTRUCTIVE TO THE SPECIMEN PACKAGE			METHODS NON-DESTRUCTIVE TO THE SPECIMEN PACKAGE		
		Mass Spectrometry	Derivative Infrared Spectroscopy	Chemical Ionization Mass Spectrometry	Surface Conductivity Sensor	Volume – Effect Sensor	Capacitance Ratio Test
A.	GENERAL AVAILABILITY OF THE METHOD	Wide	Limited	Limited	Wide	Wide	Wide
B.	OVERALL DIFFICULTY OF THE METHOD	Difficult	Moderately Easy	Difficult	Easy	Easy	Easy
C.	AVAILABILITY OF COMMERCIAL MEASURING SERVICES	4 Certified Laboratories	None	None	None	None	None
D.	COST OF COMMERCIAL SERVICES	$70-100 Per Specimen	—	—	—	—	—
E.	AVAILABILITY OF COMMERCIAL INSTRUMENTATION	Pemicka Corp., Many Others	None at this time	PCP, Inc.	Hams	Panametrics	Intended
F.	COST OF INSTRUMENTATION	Very High, >150K$	Moderately High, 25K$	High, 100K$	Low, <2K$	Moderate <5K$	Low <2K$
G.	COMPLEXITY OF INSTRUMENTATION	Complex	Moderately Complex	Complex	Simple	Simple	Simple
H.	PROVISION FOR TEST METHOD IN MIL-SPEC	Method 1018.2 Procedure 1	Candidate for Procedure 1	Method 1018.2 Procedure 1	Method 1018.2 Procedure 3	Method 1018.2 Procedure 3	Candidate for Procedure 3
I.	PHYSICAL STATE OF SPECIES DETECTED	Gas	Gas	Gas	Liquid	Gas	Liquid
J.	PARAMETER MEASURED	AMU 18, H_2O	Optical Absorbance at 6.05 μm	AMU 73, $H^+(H_2O)_4$	Leakage Current, $\sim 10^{-9}$ Amps	Impedance	Capacitance
K.	TEST VEHICLE REQUIRED IN SPECIMEN PACKAGE	No	No	No	Yes	Yes	No
L.	CALIBRATION	Three Volume Calibration Valve in Conjunction with NBS Dewpoint Hygrometer	Analyze Gas Mixture of Known Water Content at Various Pressures	Injection of Controlled Volume of Room Air of Known Relative Humidity	Correlate to Mass Spectrometer	Measure Response of Each Test Chip in Known Ambients	Measure Capacitance Ratio at 75% RH 22°C and Correct to -6°C.
M.	ACCURACY	Hardware for use as "Standard" packages, re-fillable in known moisture ambients and circulatable to participating measurement laboratories, is presently being developed					
N.	PRECISION	±20% at 5000 PPMV	±1% at 0.05 sec. Time Constant for 55μl Sample	Not Well Defined	Total Condensate Obtained Within ±2°C of Dewpoint	±8.5% at 1000 PPMV	Standard Deviations ~ ±30%
O.	ANALYSIS CONDITIONS	10^{-6} Torr 105°C	10^{-3} Torr 25°C	1 ATM 25°C	Cooling Profile of Specimen, 25°C to -35°C	Specimen at 25°C	Specimen at 0 to -6°C
P.	ANALYSIS TIME	15-45 Mins.	10 Mins.	15 Mins.	10 Mins.	10 Mins.	5 Mins.
Q.	SENSITIVITY	100-1000 PPMV	100-10,000 PPMV in 50μl Specimens	200 PPMV	500 PPMV	10 PPMV	~4000 PPMV, or 45% RH at 0°C
R.	SKILL LEVEL OF THOSE PERFORMING ANALYSES	Skilled Vacuum Technologist	Degreed Chemist	Degreed Chemist	Technician	Technician	Technician
S.	INFORMATION ON SPECIES BESIDES MOISTURE	All Volatiles	No	All Volatiles	No	No	No
T.	APPLICABILITY TO PACKAGE TECHNOLOGY DEVELOPMENT	Excellent	Good	Excellent	Excellent	Excellent	Good
U.	APPLICABILITY TO PACKAGING QUALITY CONTROL	Good, with Limited Sample Size	Good	Poor	Excellent	Excellent	Good
V.	APPLICABILITY TO QUALITY CONTROL OF INCOMING PARTS	Good, with Limited Sample Size	Good	Poor	Only if Sensors are in Subject Parts	Only if Sensors are in Subject Parts	Excellent
W.	APPLICABILITY FOR FAILURE ANALYSIS	Excellent	Good	Good	None	None	Good for Relatively Wet Specimens
X.	REFERENCES	1,2,3	4	5	6	7,8	9,10

REFERENCES

1. "Mass Spectrometer Moisture Measurements," Session I, Proceedings of ARPA/NBS Workshop on Moisture Measurement Technology for Hermetic Semiconductor Devices, March 22-23, 1978, Gaithersburg, MD, pp. 3-68.

2. Thomas, R.W., and Meyer, D.E., "Moisture in Semiconductor Packages," Solid State Technology, Vol. 17, No. 9, September, 1974.

3. Pernicka, J.C., and Raby, B.A., "The Paradox of Moisture Measurement: A Modern Tetralogy," in Proceedings of NBS/RADC Workshop on Moisture Measurement Technology for Hermetic Semiconductor Devices, II, November 5-7, 1980, Gaithersburg, MD, pp. 3-7.

4. Bossard, P.R., and Mucha, J.A., "Dynamic Measurement of the Water Vapor Content of Integrated Circuit Packages Using Derivative Infrared Diode Laser Spectroscopy," in Proceedings of the 19th Annual Reliability Physics Symposium, April 7-9, 1981, Orlando, FL, pp. 60-64.

5. Stimac, R.M., Cohen, M.J., and Wernlund, R.F., "Water Vapor Measurements in Small Volumes Using Atmospheric Pressure Chemical Ionization-Mass Spectrometry," in Proceedings of the 20th Annual Reliability Physics Symposium, March 30 - April 1, 1982, San Diego, CA, pp. 260-263.

6. Lowry, R.K., Miller, L.A., Jonas, A.W., and Bird, J.M., "Characteristics of a Surface Conductivity Moisture Monitor for Hermetic Integrated Circuit Packages," in Proceedings of the 17th Annual Reliability Physics Symposium, April 24-26, 1979, San Francisco, CA, pp. 97-102.

7. Kovac, M.G., Chleck, D., and Goodman, P., "A New Moisture Sensor for 'In-Situ' Monitoring of Sealed Packages," in Proceedings of the 15th Annual Reliability Physics Symposium, April 13-15, 1977, Las Vegas, NV.

8. Finn, J.B., and Fong, V., "Recent Advances in Al_2O_3 'In-Situ' Moisture Monitoring Chips for Cerdip Package Applications," in Proceedings of the 18th Annual Reliability Physics Symposium, April 8-10, 1980, Las Vegas, NV, pp. 10-16.

9. Merrett, R.P., Sim, S.P., and Bryant, J.P., "Using the Die of an Integrated Circuit to Measure the Relative Humidity Inside Its Encapsulation," in Proceedings of the 18th Annual Reliability Physics Symposium, April 8-10, 1980, Las Vegas, NV, pp. 17-25.

10. Bakker, N., "In-Line Measurement of Moisture in Sealed IC Packages," Philips Telecommunication Review, Vol. 37, No. 1, March, 1979, pp. 11-19.

3.2 THE INFLUENCE OF FILLING GAS OF HERMETICALLY SEALED PACKAGES ON DEVICE RELIABILITY: A DEMAND FOR A COMPLETE RESIDUAL GAS ANALYSIS

Luc J. Van Beek and Hendrik A. Loos
Bell Telephone Mfg. Co.
Gasmeterlaan 106
9000 Gent
Belgium
91/35 12 25

Abstract: A large number of reliability studies have proved that corrosion phenomena and device instabilities are merely caused by residual moisture and ionic species. Life testing (125°C, no bias, 1000 h) on different types of packages showed also a stringent relationship between the nature of the filling gas, composition of the chip metallisation and the rate of corrosion. Devices hermetically sealed in air are more sensitive to corrosion, not only by a general higher moisture content but also by the catalytic effect of the oxygen in air. Aluminum chip metallisation with 1% of silicon showed a higher degree of corrosion compared with pure aluminium.

In order to further quantify the observed phenomena, corrosion simulation tests are being performed. A broad range of surface sensitive analytical techniques, together with RGA-mass spectrometry, are being used in order to obtain a clear insight in the corrosion process.

Although these experiments are not in final state yet, preliminary results confirm the tendency of the earlier observed data: the presence of air (oxygen) in an hermetic package, together with moisture and ionic species, will give rise to corrosion artifacts much faster and more severe than a 100% nitrogen fill does.

Therefore, not only moisture-measurement, but a complete analysis of the package atmosphere should be an essential part of quality control in a high reliability manufacturing.

1. INTRODUCTION

In the past few years, various investigations (1,2,3) and failure analyses of microelectronic circuit packages have identified moisture, together with ionic species, trapped within the hermetically sealed packages, as a major reliability problem, throughout the industry. Consequently, research centers and manufacturers of hermetically sealed IC's have developed a number of techniques to accurately measure the moisture content (4,5) of these components.

Mass Spectroscopy has proved to be very successful in this manner, though for small partial pressures the technique still incorporates a number of difficulties. An important benefit of this technique is the information that can be obtained from the residual gas as a whole (its components), rather than just the result of an internal water vapor content to which the other techniques are limited.

The composition of a sealing gas can be very different: analyses of a large number of various packages revealed a great variety of residual gases. The main abundant appeared to be nitrogen or air, though various mixtures of both were also frequently encountered; in certain ceramic packaging techniques, oxygen or air is added to the furnace gas in order to get a better adhesion of the different parts (6).

Inertness of the encapsulated gas is a demand for reliable working conditions of the assembled product. Consequently, one should assess the possibility of an adverse effect in using an oxygen rich (air) atmosphere compared to a nitrogen one. This paper describes the status of a research work in this topic, which is being carried out at Bell Telephone Mfg. Cy., Gent, Belgium. The work is focussed specifically on Al - 1% Si metallization and wire bond material.

2. EXPERIMENTAL TECHNIQUES

2.1 RESIDUAL GAS ANALYSIS BY MASS SPECTROMETRY (RGA-MS)

The apparatus used to measure the internal water vapor content and the other gaseous components present in hermetically sealed packages is a modified Micromass 601 system of V. G. Gas Analysis Ltd. This type of mass spectrometer is equipped with a 6 cm radius electromagnet which is able to scan from amu 1 to 500. An adjustable expansion chamber and leak valve ensure that a molecular flow is produced to the ionisation chamber.

An electron current of 40 μA was used to generate the ions. The background pressure before puncturing a package was typically 2.10^{-6} mbar. Detection of mass spectra is done by an ion multiplier coupled to a 3 decades fast U.V. recorder. Spectra were taken in automatic scan mode from mass 12 to 22 with a 10 sec. scan time. One overall spectrum from mass 1 to 50 was taken after 1.5 minutes measurement time. The complete system was operated at elevated temperature being 100°C for the sample holder and 150°C for the expansion chamber and analyzer. A degassing and heating time of the charged system of one hour was applied. A calibration for moisture measurement was done for a baked 0.04 CC stainless steel calibration volume using a PANAMETRICS MG 101 moisture generator.

2.2 SURFACE - AND MICROANALYTICAL TECHNIQUES

- Electron spectroscopy
  Auger Electron Spectroscopy (AES-SAM) measurements were performed with a Physical Electronics Industries - 590 Scanning Auger electron spectrometer.
  The X-ray Photoelectron Spectroscopy (XPS-ESCA) apparatus is part of the same PHY 590 system.

- Electron microscopy
  The electron probe micro-analysis (EPMA) is a JEOL 733 superprobe, TRACOR 114-2000 automated.
  The Scanning Electron Microscope (SEM) is a JEOL 35 microscope.

- Mass Spectrometry
  A Leybold-Heraeus Laser Microprobe Mass Analyser (LAMMA), type 5000 was used for analysis of small particles.
  Secondary Ion Mass Spectrometry (SIMS) was performed with the CAMECA IMS - 300 ion analyser/ion microscope.

3. EXPERIMENTAL RESULTS

3.1 REAL DEVICES

3.1.1 R.G.A. - M.S.

A number of metal can transistors were life tested for 1000 hours at 125°C, without bias. The samples were electrically tested, before residual gas analysis was performed, according to the upper described methodology. The results for moisture and oxygen content at given in table 1 for 5 manufacturers. The composition is clearly different for each process.

It is shown by this table that the lower moisture contents are generally found for nitrogen sealed devices. This phenomenon has been reported earlier, at the Reliability Physics Symposium 1982 (7), to be the effect of oxidation of free silicon by competition of oxygen and water.

After decapsulation the corrosion phenomena were observed. Samples of manufacturers D and E with electrical catastrophic failure revealed wire bond interruption. Most of the corrosion was found on the wire bonds.

3.1.2 Study of Corroded Bond Wire

The material of the bond wires was Al - 1% Si, the same alloy as the metallisation of the chip. The Si dispersion in the wire was homogeneous, which is shown by a SEM backscattered electron image of an etched wire (figure 1).

Electron microscopy showed that the corrosion products are amorphous with a layered structure and are loosely bound to the wire (figure 2).

LAMMA analyses of about 40 corrosion particles originating from the foot-feedthrough area, with a diameter of 1 to 10 µm were performed. The identification of the species of which these patterns are indicative was done by comparison with spectra of pure reference compounds. Figure 3 gives an example of a corrosion particle which corresponds with $Al_2(SO_4)_3$ aq. Five different compound-groups were found: Al(Si) oxides, Al(Si) hydroxides and oxyhydroxides, Al - sulphates, Al(Si) chlorides and alkali (Na,K) and earth alkali (Mg,Ca) rich particles. These contaminants are coming from the glass bead of the bottom lid.

3.2 CORROSION SIMULATION EXPERIMENTS

In order to derive a proper understanding of the observed phenomena, and to assess the different parameters responsible for the corrosion process, short term direct corrosion simulation tests (8) were performed, in rigorously controlled laboratory conditions.

First, planar metallisation structures were chosed to fulfill the dimensional criteria of the analytical instruments.

Secondly, wire bonds were used in the simulation experiments.

The simulation tests selected were chosen according to the experience with the life testing experiments on the metal can transistors.

3.2.1 Planar Structures

The material used was silicon wafer on which a 1 µm thick Al - 1% Si or Al 99.99% layer was vacuum deposited. In all the experiments the temperature was kept at 95 ± 1% and the relative humidity at 100%. NaCl was added in the test desiccators as a corrosion stimulator and activator. Its concentration at the surface of the samples was adjusted to 0.8, 8 and 80 µg $NaCl/cm^2$. Tests were performed in either environmental air or under nitrogen gas. Exposure periods ranged between 5 and 200 hours.

It was hoped to derive more information about the corrosion mechanism, especially the influence of the environmental gas. A broad range of analytical techniques was employed for this subject; their respective results will be discussed in turn.

- Al - 1% Si
  Figure 4 shows an electron micrograph of two samples exposed to air and nitrogen, for 18 hours and 8 µg $NaCl/cm^2$. No attack of the surface was observed for the nitrogen exposed samples, but for the air exposed samples, pits are clearly visible.

  It was found that the number of pits formed after prolonged exposure is linearly related to the NaCl concentration (figure 5).

  XPS showed the presence of Al_2O_3, $Al(OH)_3$ or AlO(OH), for both atmosphere, though for nitrogen, under severe concentrations of NaCl, an Al-Si-Na-O ionic network was found. Scanning Auger Spectroscopy was used to determine the repartition of Al, Si and O on the corroded surfaces. Si enrichment - as oxide - was found at the first monolayer of the surface.

  Secondary Ion Mass Spectrometry in depth profiles confirmed the results of electron spectroscopy. Also Na enrichment was found at the oxide-metal interface.

- Al 99.99%
  Simulation experiments were carried out for Si-free Al to assess for its influence. Figure 6 shows the number of pits per unit area (arbitrary scale) in function of exposure time for 8 µg $NaCl/cm^2$ on Al and Al - 1% Si (reference) in air and nitrogen atmospheres. It is clearly shown that Si presence stimulates the corrosion phenomenon of Al. Its granules were too small to be visualized by SEM (< 200 Å).

  Electron Spectroscopy showed for all samples a pure Al_2O_3 layer on Al, for the air exposed samples reaching a thickness of 0.7 µm after 100 hours.

3.2.2 Al - 1% Si Bond Wire

Bond wire of Al - 1% Si metallisation underwent the same contamination and aging procedure as the planar structures did, the atmosphere being air. Figure 7 shows an electron micrograph of a 1.000 X magnified piece of wire bond after 25 hours exposure time. Small deformations of the surface are visible (diameter 0.1 µm 0 1 µm). These flatted spheres appeared to have grown out of the wire. Since the background of the wire contains a Si signal, it was not straightforward to geographically correlate these points with Si abundance. Therefore Al - 1% Si wire bonds were heat-treated for 12 hours at 500 ± 20°C. This treatment concentrates Si into larger volumes. It was shown by SEM (after etching in 2% HF) that these heat-treated wires contained Si particles with a diameter of 2 to 6 µm. A number of these wires were exposed to the described corrosive atmosphere for some hours. The early phase of the corrosion phenomenon could be visualized by SEM. It is believed that the observed phenomena were due to grain boundary corrosion.

4. CONCLUSIONS

The internal water vapor content of hermetically packaged devices decreases with lower oxygen contents. This phenomenon has been reported earlier by Bell Labs. to be the effect of the chemical reaction of moisture - in competition with oxygen - with free silicon of the chip.

Silicon presence in aluminum accelerates strongly the corrosion rate of the alloy.

Corrosion of aluminum and aluminum - 1% silicon in moist atmospheres is stimulated by the presence of oxygen. Therefore, one may consider being less tolerant to moisture content for oxygen containing or air sealed devices.

REFERENCES

1. P. Courtney-Saunders, Reliability Physics Brief, 7, 01 (1978).
2. R. W. Thomas, Proc. of the 26th Electronic Components Conference, edited by the Institute of Electrical and Electronics Engineers Inc., San Francisco, CA., April 26-28, 272 (1976).
3. B. Drotman, 19th Ann. Proc. Reliab. Phys., 19, 188 (1981).
4. R. Schubert, J. Vac. Sci. Technol. 14, 227, (1977).
5. R. K. Lowry et al., 17th Ann. Proc. Reliab. Phys., 17, 97 (1979).
6. C. A. Harper, Handbook of Electronic Packaging, Edited by C. A. Harper, McGraw Hill Inc., New York (1969).
7. M. L. White et al., 20th Ann. Proc. Reliab. Phys., 20, 253 (1982).
8. K. Barton, "Protection Against Atmospheric Environment, Theories and Methods", edited by John Wiley & Sons, chapter 6, New York (1976).

ACKNOWLEDGMENT

The authors wish to thank Prof. Dr. F. Adams, Prof. Dr. R. Gijbels of the University of Antwerp (U.I.A.) and Dr. M. Van Craen, as well as Mr. R. Vlaeminck and Dr. R. Vanden Berghe of Bell Telephone Mfg. Cy., for allowing the use of analytical infrastructure and fruitful cooperation.

Manufacturer	Moisture content	Oxygen content
A	< 500 ppmV	< 1 % in N_2
B	500 - 1.000 ppmV	5 % in N_2
C	1.500 - 3.000 ppmV	5 % in N_2
D	3.000 - 8.000 ppmV	21 % (AIR)
E	2.000 - 4.000 ppmV	21 % (AIR)

Tabel 1 : moisture and oxygen content for 5 different manufacturers.

Figure 1 : backscattered electron image of an etched (2 % HF 2 min.) Al - 1 % Si wire.

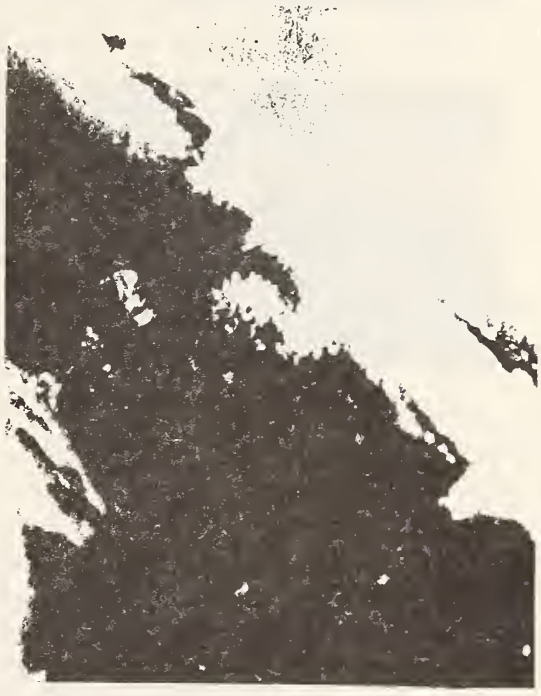

Figure 2 : backscattered electron image of a corroded bond wire.

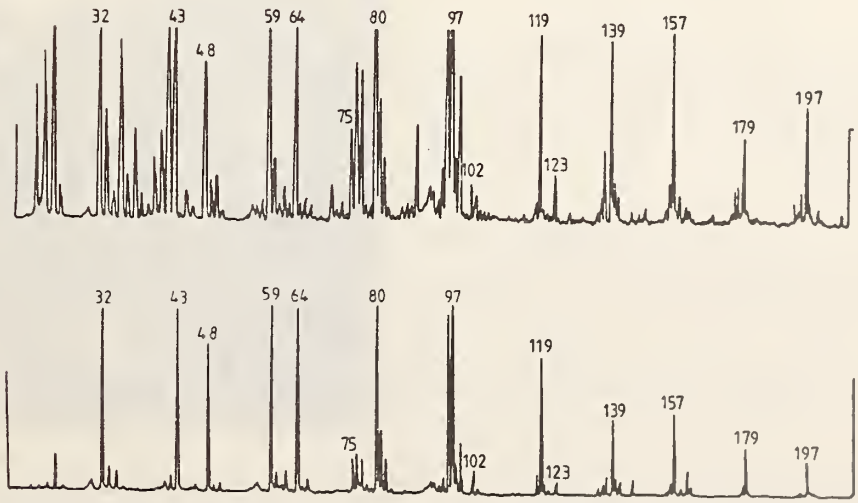

Figure 3 (Top) : LAMMA negative massspectrum of a 2 - 4 µm diameter corrosion particle, identified as aluminium sulphate by comparison with the pure $Al_2(SO_4)_3$ .aq Spectrum (below).

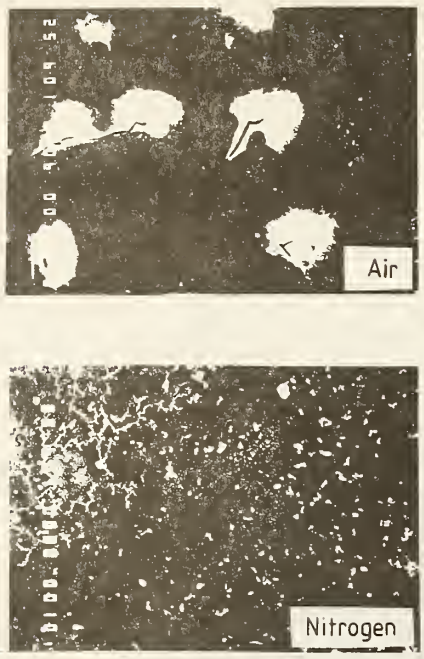

Figure 4 : backscattered electron image of two samples, respectively exposed to air and nitrogen, for 18 hours and 8 µg $NaCl/cm^2$.

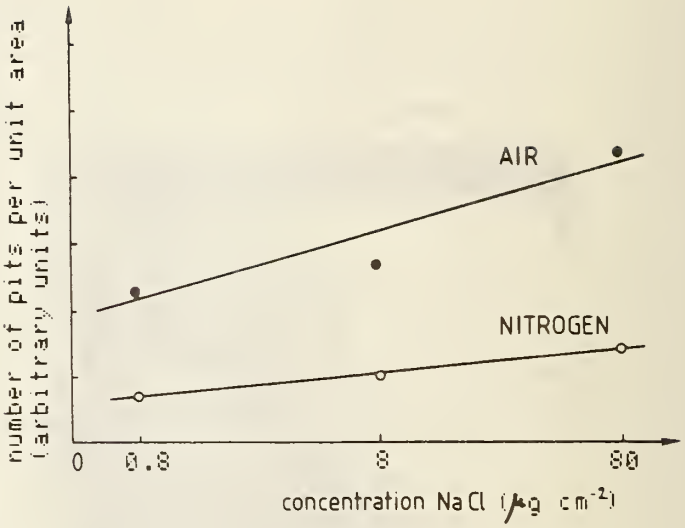

Figure 5 : the number of pits per unit area in function of NaCl concentration for 100 hours exposure.

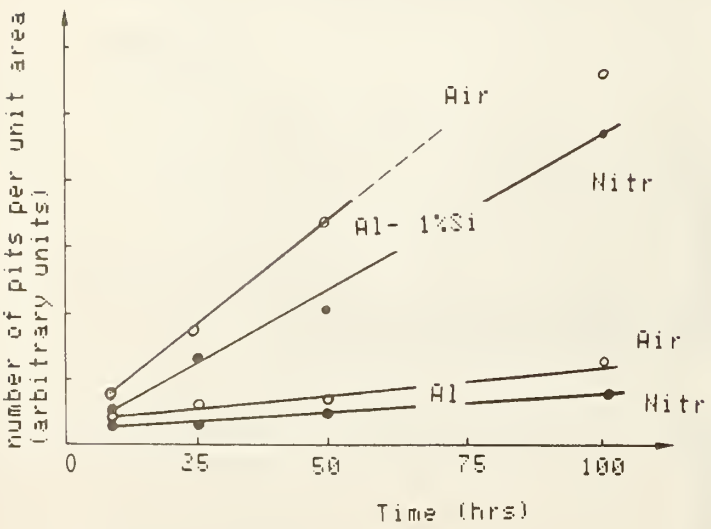

Figure 6 : the number of pits per unit area in function of exposure TIME FOR 8 µg $NaCl/cm^2$.

Figure 7 : backscattered electron image of a 1.000 X magnified piece of wire bond after 25 hours exposure time.

3.3 EXTENDED COMPUTER CONTROL AND DATA PROCESSING FOR THE MASS SPECTROMETRIC ANALYSIS OF PACKAGE ATMOSPHERES

Leslie J. Rigby
Standard Telecommunication Laboratories,
London Road, Harlow, UK CM17 9NA

In the comparative analysis of small gas volumes, the precision achieved by microprocessor controlled data acquisition can be significantly improved by an automated system for sample transfer. This objective has been partially realised with a Pernicka gas analyser with automated solenoid valves, which facilitates routine system equilibration to moisture by a pre-exposure and pump down cycle, and also guarantees a completely synchronous analysis procedure for all samples. Software has been developed which allows multiple ion data acquisition of all relevant ion currents for mass 2 to 50 and an early mass scan to cover the range from 51 to 97. Maximum sensitivity has been maintained by the automatic selection of the most appropriate isotopes for the major constituents, and possible interferences are taken into account by the use of previously determined ion current ratios. Helium pre-bombing at elevated temperatures exposes real and potential leaks to below 10^{-10} atm.ml/sec during the subsequent gas analysis.
Calibration curves for water will be presented and typical results with package volumes of from 5 to 0.001 ml will be used to illustrate the limits of detection that have been achieved.

INTRODUCTION

The mass spectrometric method of package analysis attempts to compare sample gas with suitable standards under carefully chosen and hopefully reproducible conditions. The sequence of the analysis and the subsequent data manipulation depends on the capabilities of the instrumentation and the availability of software. The choice of parameters used during data acquisition are usually the result of a fairly pragmatic approach to the difficulties associated with the transport of water vapour through the system and may have a considerable influence on the final result particularly when low water levels are being measured.

System Design

A Pernicka gas analysis system has now been in semi-continuous operation for over 18 months. The use of computer controlled solenoid valves closely defines the cycle time of the analysis and a sequence of rapid data acquisition and signal averaging improves data reliability. The following objectives define the computer software:

1. Complete gas analysis without prior knowledge of the major gaseous components
2. A sensitive test for hermeticity to below 10^{-10} atm. ml/sec
3. Fail safe and reproducible.

Gas transfer to a mass spectrometer is unfortunately a destructive process but is the only method which affords a complete assessment of the gas ambient in an encapsulated device and provides a high degree of accuracy for water measurement.
Computer control and measurement becomes essential for reliable measurement. The software can be designed to make rapid decisions regarding system failure and choice of ion currents to maximise sensitivity without multiplier saturation. Vacuum valves can be precisely switched and repetitive measurements made in an exact timing sequence so that reliable comparisons can

be made between sample and standard gases. Area computations for all the measured ion currents can include corrections for overrange data. Delay in sample puncture, and slow sample transfer caused by either incomplete puncture or absorptive materials within the package are potential errors which can be minimised by area measurement.

Fig. 1 shows a schematic of the system, in which valves V1-V4 are controlled by a dedicated Midas IV microprocessor. V2 is a needle valve which is preset according to an estimate of the package volume. The Balzers Q311 quadrupole mass spectrometer has very good mass stability and the resolution is adjusted to provide broad peaks with high sensitivity and consistent ion current sensitivity. Pressure and ion current data are read by Midas at 1 ms intervals and subsequently transferred to an HP 9825T computer which uses a millisecond clock to record time increments.

Table 1 shows the transfer parameters which were measured for values of V2 which were chosen to keep the initial pressure in the mass spectrometer to below 2×10^{-5} torr. For gas volumes below 0.2 atm. ml, V2 is at its widest setting and total transfer of the sample gas through the mass spectrometer ion source is achieved in about 3 minutes. During that time, five data readings are taken of sample chamber pressure and each of 32 ion currents in one cycle of an operation which is repeated 20 times. The 32 ions routinely monitored (Table 2) includes all the ions of interest up to mass 50. A single mass scan from mass 51 to mass 97 covers the remaining ions available for analysis. The analysis time is readily extended for smaller values of V2 by increasing the number of repeat readings of each ion current from 5 to a maximum of 80.

Experimental Procedure

All packages are prebombed in 2 atm. of helium (or krypton) for a minimum period of 16 hours at 150°C. Subsequent detection of 10 ppm of this tracer gas in a gas content of 0.1 atm. ml. yields an estimated leak rate of 5×10^{-11} atm. ml/sec. Up to 12 similar packages are then loaded into the heated carousel and evacuated for a period of 16 hours. The value of V2 is then chosen to suit the package volume and the following sequence of analysis is carried out using standard gas with a similar volume to that of the sample volume.

1. Dry nitrogen (for water background)
2. Moist air (for water calibration)
3. Samples
4. Repeat moist air
5. Calibration for other gases as required
6. Correct sensitivity and interference factors
7. Print out final report

Interference factors are calculated from standard gases for the list of major interferences given in Table 8.

Tables 3-5 show similar sequences of software procedures for nitrogen, air and sample gases respectively; the relevant differences are underlined. Ion currents of the naturally occurring isotopes of the major gases which can be selected to avoid saturation are shown in Table 6. Helium is the only gas which creates a difficulty and helium filled devices usually require a by difference estimate of the true helium content. Table 7 details the multiple ion detection (MID) sequence common to all standards and samples.

RESULTS

Standard water samples were obtained by either mixing laboratory air with dry nitrogen or by the use of a pressurised humidifier. The resultant gas stream of about 500 ml/min was sampled by a 3 volume control valve and monitored by a recording dew point hygrometer (Fig. 1). Typical water calibration curves for

this system (Fig. 2) indicate good reproducibility at the 1000 ppm level (0.1%). The decay curves for TO5 packages (Fig. 3) indicate how quickly the water transmission curves approach the background curve as the water content was reduced towards zero. At a level of 100 ppm the area under the water curve was about twice the area obtained in dry nitrogen.
The latter curve has a small positive slope which results from the slow release of water molecules pre-adsorbed on the surfaces of the sample chamber during the initial preconditioning by air exposure. Area measurements for all curves are terminated at the last measured point in an admittedly arbitrary fashion. However the alternative is to extrapolate to a suitably chosen baseline and may introduce errors, particularly when non-ideal curves are encountered. The present method does readily discriminate between different levels of moisture even though accuracy may become more difficult at concentrations below say 500 ppm.
Table 8 summarizes the estimated sensitivities and detection limits for the common gases. These values represent a best case situation and may be adversly influenced by the listed interferences.
Examples of final reports are reproduced in Tables 9-11. In these reports, the percent compositions of the usual components are obtained from the selected ion currents and their relative sensitivity factors listed in Table 8 after taking into account possible interferences from other species as discussed above. A list of detected other masses is produced by assuming unit sensitivity of all of these with respect to nitrogen. Table 1 indicates that some of these could result from the isotopes of major impurities (e.g. HDO^+ at mass 19, $^{15}N_2$ at mass 30), spill over of large peaks (e.g. an apparent mass 31 from a very large mass 32 ion current), or doubly charged ions (CO_2^{++} at mass 22) and these effects are usually denoted by a <notation.
The remaining ions of significance usually indicate the presence of other species which are normally organic in origin.
Table 4 shows comparative results from two TO5 packages. The present U.S. 883B Military Specification for water in encapsulated devices is 5000 ppm. The top set of data in Table 4 show a comfortably lower water content of 1150 ppm, low oxygen and carbon dioxide. The absence of helium indicates that hermeticity is better than 1.1×10^{-11} atm.ml/s. A helium content of 0.68% in the lower data correspond to a fine leak of 6.6×10^{-9} atm.ml/s. This is confirmed by higher levels of oxygen, water, argon and carbon dioxide which may all be attributed to air ingress.
Table 5 shows similar sets of data from very small diodes of less than 0.002 atm.ml. All detection limits are higher than those quoted in Table 8 but leak rates down to 7×10^{-10} atm.ml/s are still measurable. These devices had been subjected to a damp heat test so it is not surprising that 9% water had accumulated in a non-hermetic device.
Table 6 shows data which were obtained for two larger packages containing epoxide adhesive. Large quantities of water with detectable amounts of ammonia and several organic species can be attributed to a poorly cured adhesive. These results illustrate the need for a careful choice of a high quality resin and prolonged post baking procedures to minimise a potential source of harmful vapours in hybrid packages.

CONCLUSIONS

1. Rapid analysis system with high reliability
2. Good reproducibility at 1000 ppm water for sample volumes of 0.1 atm. cc
3. Minimum operator intervention
4. Automatic data presentation including simple hermeticity calculation.

ACKNOWLEDGEMENTS

The author thanks STL Ltd for permission to publish this paper.

Table 1 - Gaseous transfer parameters for quantities up to 30 atm.ml

Maximum quantity (atm.ml)	Initial chamber pressure	Vernier setting of V2	Initial quadrupole pressure in torr x 10^{-5}	Time to consume 50% of gas sample in seconds	Effusion rate in ml.s	Analysis time in minutes	% consumed in the allotted time
0.2	0.84	160	1.5	17	1.53	3.1	100
0.5	2.1	100	1.8	22	0.84	3.6	99.8
1.0	4.2	50	1.6	88	0.30	6.2	99.3
2.0	8.4	25	1.6	185	0.14	9.0	82
8.0	34	10	1.5	482	0.05	9.0	52
30	130	0	1.7	2390	0.011	16.4	21

Table 2 - list of 32 ions routinely monitored to the possible sources of each ion:

2 or 3	H_2^+ or HD^+ from hydrogen
4	He^+ from helium
7	N^+ ion from nitrogen
12	C^+ from carbon monoxide and carbon dioxide
15	$^{15}N^+$ (nitrogen), NH^+ (amines), CH_3^+ (hydrocarbons)
16 or 8	O^+ or O^{++} (oxygen), O^+ (water), NH_2^+ (amines), CH_4^+ methane
17	OH^+ (water), NH_3^+ (ammonia)
18	H_2O^+ (water)
19	HOD^+ (water), F^+ (fluorocarbons and HF)
20	Ne^+ (neon), Ar^{++} (argon), HF^+ (hydrogen fluoride)
22	Ne^+ (neon), CO_2^{++} (carbon dioxide)
26	$C_2H_2^+$ (hydrocarbons)
29	$C_2H_5^+$ (hydrocarbons), $^{14}N^{15}N^+$ (nitrogen)
30	$C_2H_6^+$ (ethane), $^{15}N^{15}N^+$ (nitrogen), CH_3NH (amines)
31	CH_3O^+ (alcohols), CF^+ (fluoro compounds)
32 or 34	O_2^+ (oxygen), S^+ (sulphur compounds)
35	Cl^+ (chlorine compounds)
36	$^{36}A^+$ (argon), HCl^+ (hydrogen chloride)
37	Cl^+ (chlorine compounds)
38	HCl^+ (hydrogen chloride), $C_3H_2^+$ (Unsaturated hydrocarbons)
39	$C_3H_3^+$ (aromatics and unsaturated aliphatics)
40	A^+ (argon)
41	$C_3H_5^+$ (hydrocarbons), CH_3CN^+ (nitrides)
42	CH_2CO^+ (lactones, furans, ketones, aldehydes)
43	$C_3H_7^+$ (hydrocarbons), CH_3CO^+ (ketones)
44	CO_2^+ (carbon dioxide), $C_2H_4NH_2^+$ (amines)
45	$C_2H_5O^+$ (alcohols, diols, ethers)
46	NO_2^+ (nitrogen dioxide, organic nitrates)
47	CCl^+ (chloro compounds), COF^+, $C_2H_4F^+$ (fluoro compounds)
48	SO^+ (sulphur compounds)
49	CCl^+ (chloro compounds)
50	CF_2^+ (fluoro compounds), C_4H_2 (aromatics)

Table 3 - First analysis, water background from dry nitrogen

1. Record pressure p and close V1 ($p \cong 2 \times 10^{-8}$ torr, ion source pressure $< 1 \times 10^{-9}$ torr).
2. Ask for moist air sample, test MS sensitivity
   Extend air exposure, test for mass accuracy and resolution
3. Pump for 5 minutes. Store pressure $p_1 \times 10^{-8}$ torr
4. Close V1 and open V2; measure residuals
5. Open V1 and evacuate to $p_1 \times 10^{-8}$ torr
6. Close V1 and ask for sample (admit sample from dry nitrogen stream) - close V4
7. Start clock, initial brief mass scan to test for viability and to determine working isotopes
8. Sample measurement
9. Store water areas as minimum values

Table 4 - Second analysis, water calibration

1. When p $(p_1 + 1) \times 10^{-8}$ torr, or t 10 min, close V1
2. Ask for moist air sample, test MS sensitivity - Read Dew Point meter and calculate ppm of water in air sample
3. Pump until p $(p_1 + 0.5) \times 10^{-8}$ torr or t 10 mins
4. Close V1 and open V2; measure residuals
5. Open V1 and evacuate to $p_1 \times 10^{-8}$ torr or t 10 mins
6. Close V1 and ask for sample (admit sample from air stream) - close V4
7. Start clock, initial brief mass scan to test for viability and to determine working isotopes
8. Sample measurement
9. Print out initial data including sensitivity to water

Table 5 - Third analysis, package puncture

1. When $p > (p_1 + 1) \times 10^{-8}$ torr, close V1
2. Ask for moist air sample, test MS sensitivity
3. Pump until $p < (p_1 + 0.5) \times 10^{-8}$ torr or $t > 10$ mins
4. Close V1 and open V2; measure residuals
5. Open V1 and evacuate to $p_1 \times 10^{-8}$ torr or $t > 10$ mins
6. Close V1 and V4 - ask for sample (puncture device and withdraw needle)
7. Start clock, initial brief mass scan to test for viability and to determine working isotopes
8. Sample measurement
9. Print out initial data

(Similar procedure for external mounted packages - rapid cycle mode).

Table 6 - Isotopes of major gases

	START	IF OVERRANGE	IF UNDERRANGE
HYDROGEN	2	3	
HELIUM	4	4	
NITROGEN	29	7	28
OXYGEN	34		32
ARGON	36		40
CO2	44	22	
WATER	18	17 and 19	

Table 7 - Sample measurement

1. Rapid MID cycles 1 and 2: Read time in mS, then 5 readings of Baratron and each of 32 ions. Store average of last 4 readings.
2. Single scan, of masses 51-97
3. Rapid MID cycles 3 - 5
4. Slower MID cycles 6 to 20, extend from 5 to over 20 readings depending on V2 setting
5. Evacuate remaining sample, open V2 and restart clock
6. Ratio up all overrange ion currents
7. Determine minima as true residuals
8. Subtract residuals, measure areas

Table 8 - Typical sensitivity factors and detection limits in a 0.1 atm.ml gas sample

Gas	Mass	Relative sensitivity	Detection limit in ppm	Interference
Hydrogen	2	45	10	Water
Helium	4	19	10	None
Carbon monoxide	12	15	50	CO_2
Methane	16	95	5	O_2, N_2
Ammonia	17	40	200	Water
Water	18	58	500	O_2
Nitrogen	28	100	5	CO, CO_2, Organics
	29	0.74		Organics
Oxygen	32	87	5	None
Argon	40	84	5	None
Carbon Dioxide	44	190	5	O_2

****

GAS ANALYSIS BY MASS SPECTROMETRY MODE: Batch

SAMPLE IDENTIFICATION: TO5 encapsulated transistor

MS file no = 12 DATE = 06:10:82 TIME= 11:45
RESULTS : TOTAL GAS CONTENT = 0.23 atm.ml Needle valve set to 100

COMPONENT	% COMPOSITION	OTHER MASSES	% REL.COMP.
Water	0.149	30	<0.0034
Hydrogen	0.062	19	<0.0031
Helium	< 0.0040	26	0.0017
Nitrogen	99.	31	0.0011
Oxygen	0.0012	42	0.0011
Argon	0.0008	43	0.0014
Methane	< 0.0009		
Carbon monoxide	< 0.0060		
Carbon dioxide	0.0197		

NOTES Helium content is equivalent to a leak rate of 1.1E-11 atm.ml/sec.

****

GAS ANALYSIS BY MASS SPECTROMETRY MODE: Batch

SAMPLE IDENTIFICATION: TO5 encapsulated transistor

MS file no = 13 DATE = 06:10:82 TIME= 11:58
RESULTS : TOTAL GAS CONTENT = 0.22 atm.ml Needle valve set to 100

COMPONENT	% COMPOSITION	OTHER MASSES	% REL.COMP.
Water	1.16	22	<0.0019
Hydrogen	0.040	30	<0.0046
Helium	0.68	19	<0.0035
Nitrogen	96.	20	<0.0115
Oxygen	0.98	26	0.0018
Argon	0.061	31	<0.0095
Methane	0.0032	35	0.0011
Carbon monoxide	< 0.0040	39	0.0015
Carbon dioxide	0.070	41	0.0009
		42	0.0011
		43	0.0022
		45	0.0015
		91	0.0016

NOTES Helium content is equivalent to a leak rate of 6.6E-09 atm.ml/sec.

Table: 9 Tabulated Data for 0.2 ml Packages

GAS ANALYSIS BY MASS SPECTROMETRY MODE: Batch

SAMPLE IDENTIFICATION: YY diode/38

MS file no = 21 DATE = 19:05:32 TIME= 09:31

RESULTS : TOTAL GAS VOLUME= 0.0019 atm.ml Needle valve set to 100

COMPONENT	% COMPOSITION	OTHER MASSES	% REL.COMP.
Water	1.82	19	< 0.024
Hydrogen	1.67	26	0.029
Helium	< 0.0300	39	0.0172
Nitrogen	96.	43	0.0160
Oxygen	0.031	50	0.022
Argon	< 0.0060	51	0.037
Methane	< 0.0050	78	0.070
Carbon monoxide	< 0.0300		
Carbon dioxide	0.58		

NOTES Helium content is equivalent to a leak rate of 6.3E-10 atm.ml/sec.

****

GAS ANALYSIS BY MASS SPECTROMETRY MODE: Batch

SAMPLE IDENTIFICATION: YY diode/68

MS file no = 22 DATE = 19:05:82 TIME= 09:52

RESULTS : TOTAL GAS VOLUME= 0.0013 atm.ml Needle valve set to 100

COMPONENT	% COMPOSITION	OTHER MASSES	% REL.COMP.
Water	9.0	22	< 0.0099
Hydrogen	1.85	19	< 0.030
Helium	0.35	20	< 0.058
Nitrogen	83.	26	0.021
Oxygen	4.6	39	0.037
Argon	0.47	43	0.032
Methane	< 0.0030	45	0.0170
Carbon monoxide	< 0.0200	50	0.026
Carbon dioxide	1.31	78	0.071

NOTES Helium content is equivalent to a leak rate of 1.8E-08 atm.ml/sec.

Table: 10 Tabulated Data for 0.002 ml Packages

GAS ANALYSIS BY MASS SPECTROMETRY MODE: Cyclic

SAMPLE IDENTIFICATIONTest Package with cured epoxide adhesive

MS file no = 25 DATE = 22/10/82 TIME= 13 34
RESULTS : TOTAL GAS CONTENT = 1.72 atm.ml Needle valve set to 25

COMPONENT	% COMPOSITION	OTHER MASSES	% REL.COMP.
Ammonia	0.0096	22	< 0.0007
Water	0.56	30	< 0.0044
Hydrogen	< 0.0007	19	< 0.0056
Helium	< 0.0020	20	0.0018
Nitrogen	99.	26	0.0179
Oxygen	0.0023	31	0.0066
Argon	0.0079	35	0.0015
Methane	0.0070	36	0.0008
Carbon monoxide	0.0130	37	0.0013
Carbon dioxide	0.032	38	0.0015
		39	0.0041
		41	0.0060
		42	0.0050
		43	0.0112
		45	0.0022
		46	0.0008
		47	0.0017
		48	0.0011
		49	0.0054
		50	0.0013
		64	0.0190
		66	0.0059

GAS ANALYSIS BY MASS SPECTROMETRY MODE: Cyclic

SAMPLE IDENTIFICATIONTest Package with cured epoxide adhesive

MS file no = 27 DATE = 22/10/82 TIME= 14 39
RESULTS : TOTAL GAS CONTENT = 1.75 atm.ml Needle valve set to 25

COMPONENT	% COMPOSITION	OTHER MASSES	% REL.COMP.
Ammonia	0.093	22	< 0.0057
Water	2.2	30	< 0.0074
Hydrogen	< 0.0010	19	0.0051
Helium	< 0.0030	20	0.0051
Nitrogen	97.	26	0.0155
Oxygen	0.0024	31	0.0183
Argon	0.0185	37	0.0034
Methane	0.0200	38	0.0053
Carbon monoxide	0.043	39	0.0193
Carbon dioxide	0.28	41	0.041
		42	0.041
		43	0.043
		45	0.0128
		46	0.0034
		49	0.0009
		50	0.0036
		55	0.0123

Table: 11 Tabulated Data for 2 ml Packages

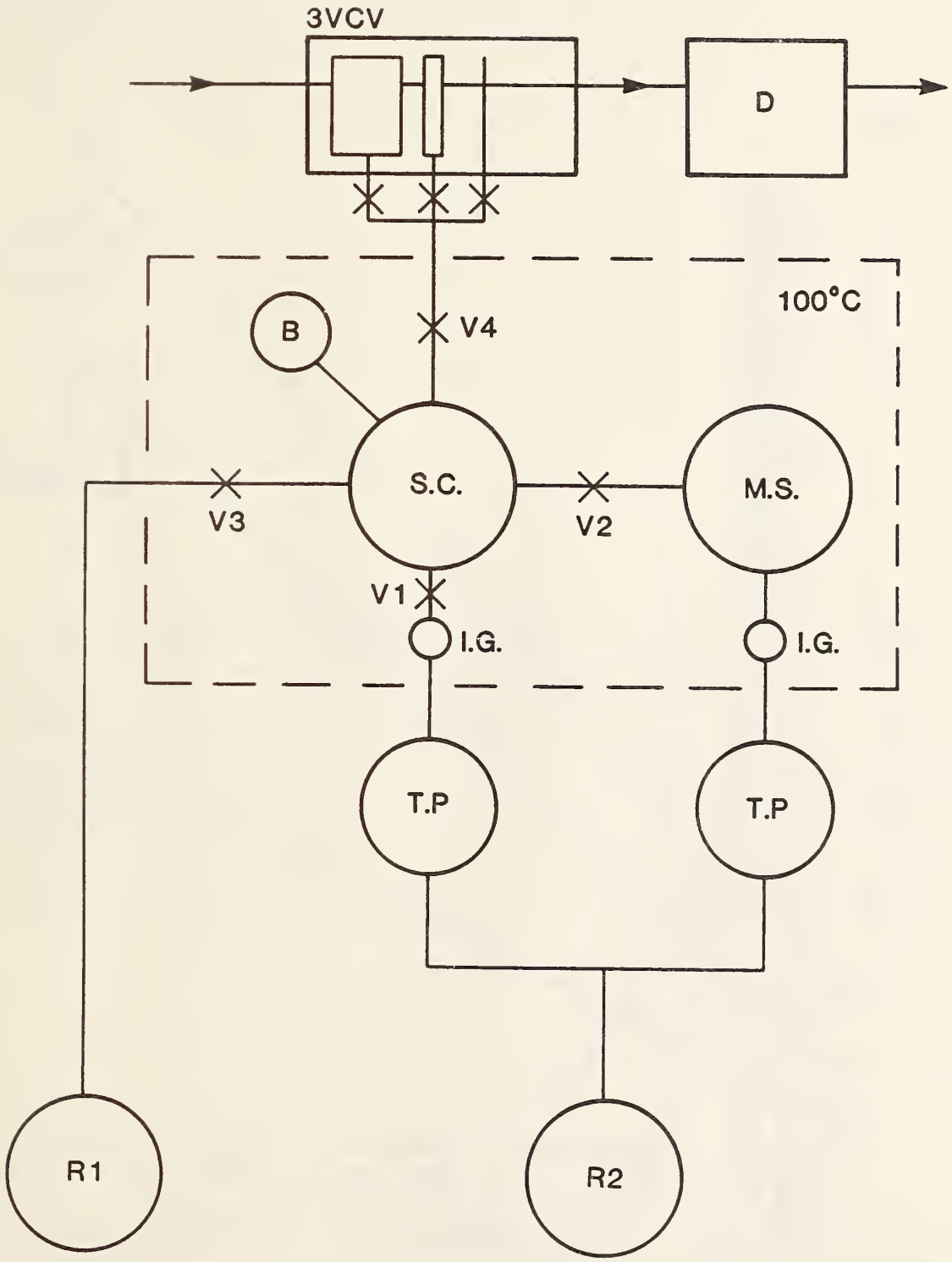

Figure 1 - Schematic diagram of sample chamber (SC) and Baratron gauge (B) with gas supply from a 3 volume calibration valve (3VCV). The quadrupole mass spectrometer (MS) and the sample chamber are maintained at 100°C and are pumped by two turbomolecular pumps (TP) monitored by ion gauges (IG) and backed by a common rotary pump (R2). R1 is used to initially pump SC via V3. D is a direct reading mirror hygrometer.

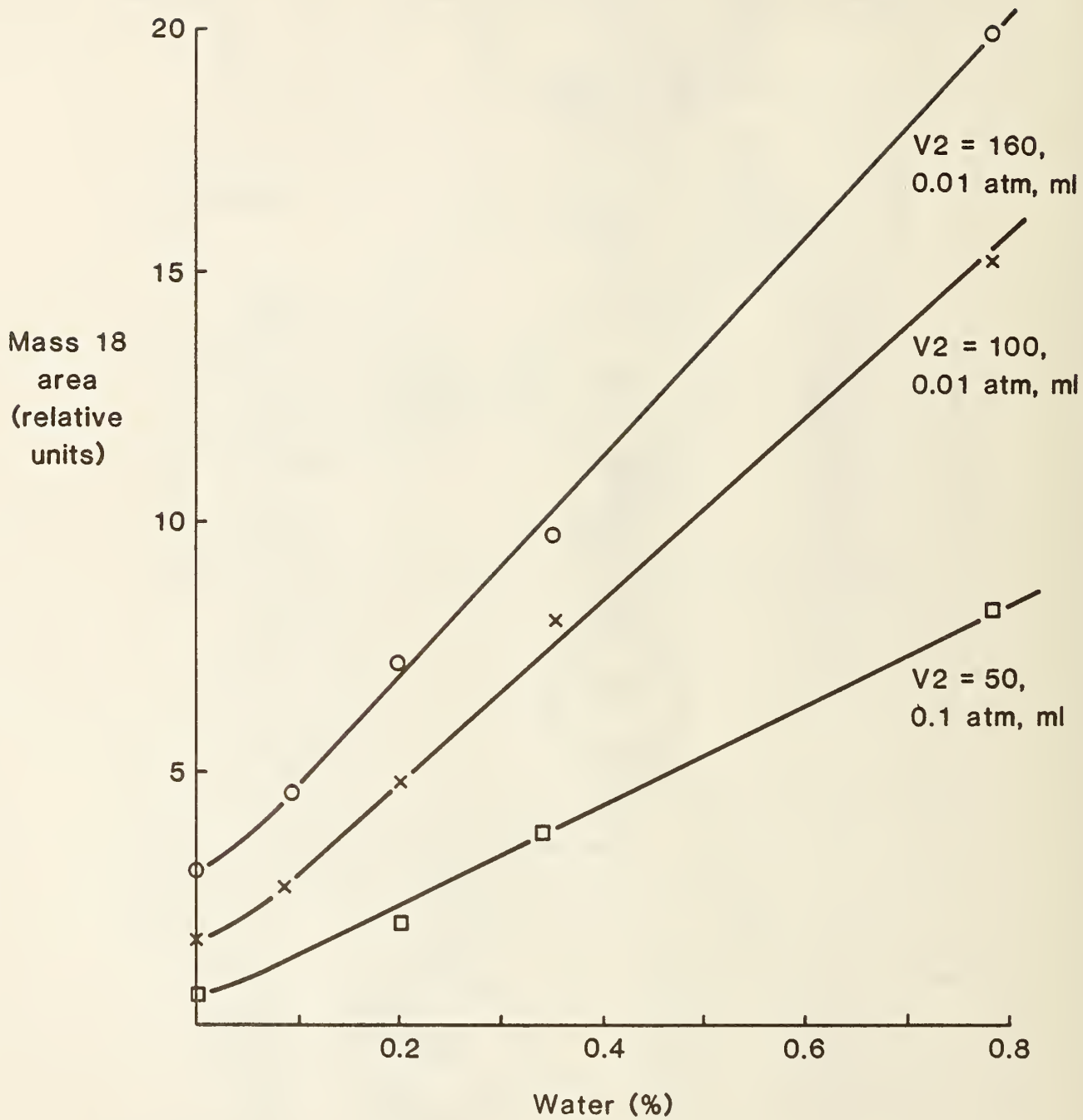

Fig. 2 Water calibration for gas volumes of 0.1 and 0.01 atm.ml and needle valve settings of 50, 100 and 160.

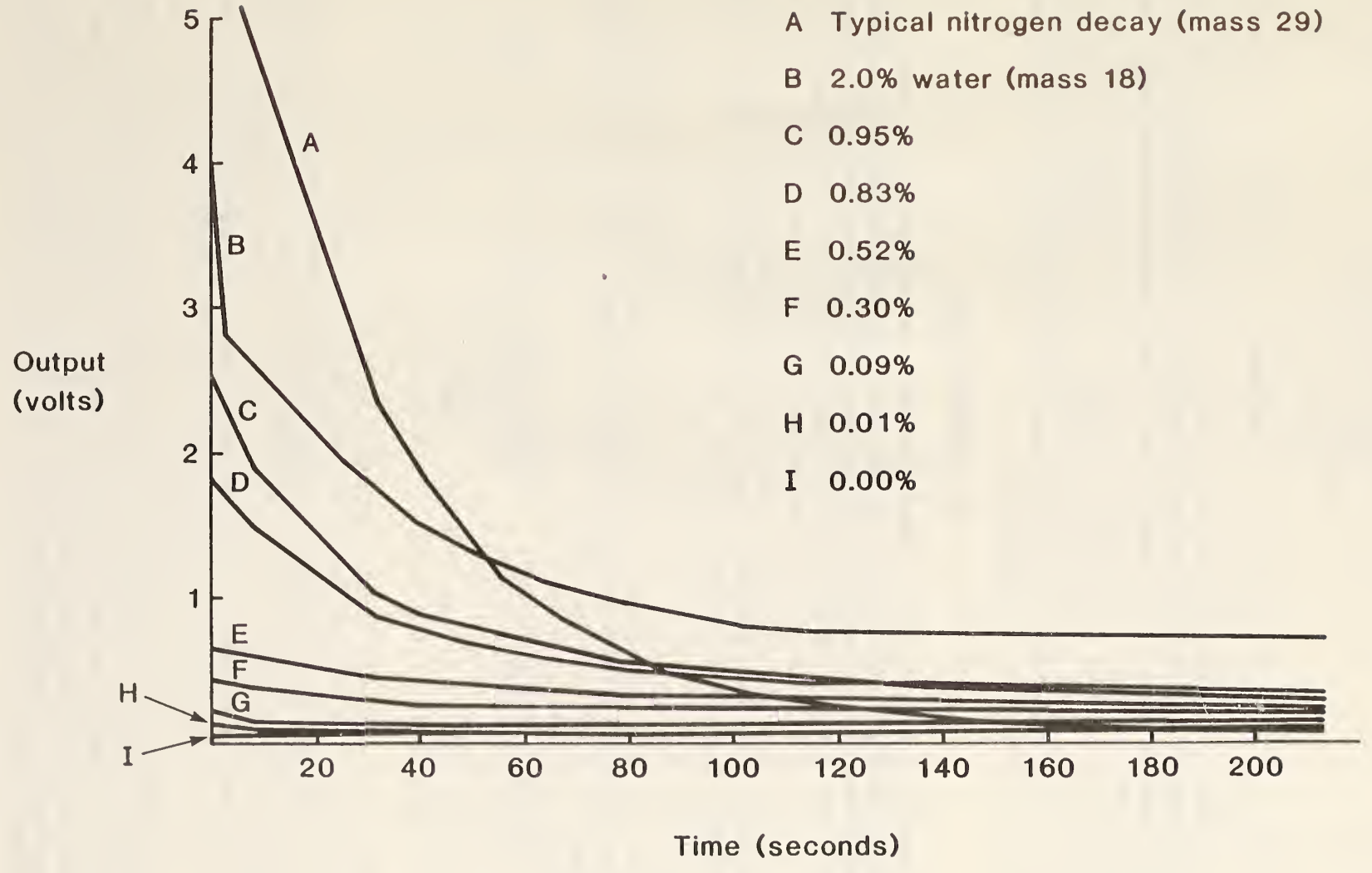

Fig. 3 Water transmission from TO5 packages with V2 = 100

3.4 GASEOUS COMPOSITIONS OF HERMETIC PACKAGE CAVITY AMBIENTS, II

R. K. Lowry
Harris Semiconductor
P. O. Box 883
Melbourne, FL 32901
305-724-7566

ABSTRACT

Mass spectrometric measurement of internal water vapor content also yields data on other volatiles in the package cavity. Identity and concentration of all species present can supply useful information for packaging technology improvements to produce cleaner and drier parts. In an extension of the discussion presented at the 1980 Workshop, and utilizing data from more than 1300 packages, this paper describes some of the relationships found between levels of moisture and associated levels of N_2, O_2, H_2, CO_2, and Ar in several different package styles.

INTRODUCTION

Mass spectrometry provides a measure of all volatile species within a hermetic package enclosure. Knowing the interrelationships between various volatiles in particular package styles gives clues to hermetic package ambient chemistry. This has proved important not only for moisture control [1], but also for other aspects of hermetic packaging problems [2]. In particular, effects of hydrogen on device electrical stability [3] and on metallization integrity [4-5] have been reported. Deleterious effects of ammonia in hybrid parts have also been described [6].

In the previous Workshop paper [1], some relationships between package moisture content and certain other volatiles were discussed for three different package styles. Trends identified were as follows, where n indicates the number of specimens:

Cerdip, n = 146	Braze Seal, n = 56	TO, n = 36
$H_2O \propto O_2$	$H_2O \propto H_2$	$H_2O \not\propto H_2$
$H_2O \propto Ar$	$H_2O \not\propto CO_2$	$H_2O \propto CO_2$
$H_2O \not\propto CO_2$		

$\propto$ means exhibits dependency. $\not\propto$ means no apparent dependency.

Some species in some packages were present only in the fractional volume percent range. But with the ever-diminishing limits on moisture content (2000ppmv by June 1984 plus initial work on a 500ppmv standard)[7] combined with the profound effects of hydrogen on device physics, the relationships discussed are technically important for advanced packaging technology.

In the time elapsed since the previous paper, many more parts have been analyzed. The above trends are re-examined here using data from over 1300 specimens analyzed since 1979. Data comes from assembly engineering studies as well as product qualifications. It is thus indicative of broad trends to be expected in a package type but is not entirely representative of typical delivered product.

DISCUSSION

Cerdip

Ceramic dual-in-line packages are composed of an alumina base and cap. The IC chip is attached to the base, and the lid is sealed to the base using a solder glass to enclose the chip in a hermetic cavity. Sealing is done in a temperature profiled furnace. Seal ambient is either natural or synthetic air. Where natural air is the sealing ambient, the trend of cavity constituents is typically

$$N_2 > O_2 > Ar \gtrless CO_2 > H_2O > H_2^* \text{ and other species}^*$$

Where synthetic air is the sealing ambient, the trend is typically

$$N_2 >> O_2 \lessgtr CO_2 > H_2O > Ar^*, H_2^*, \text{ and other species}^*$$

In these sequences items indicated by * are often not detected.

Table I summarizes relationships found between H_2O, O_2, Ar, and CO_2 within 694 Cerdip specimens. The data here is, first of all, a testimony to the ability to build dry Cerdips. Only 19 of 694 parts were > 5000ppmv. Thirteen of these 19 represented non-standard processing. It should be further noted that 2 of every 3 Cerdip packages contained < 1000ppmv moisture.

Oxygen. Ref. [1] alluded to the ability to control package moisture by controlling O_2 in the seal ambient. From Table 1 and Fig. 2 this is clearly established. An N_2 : O_2 ratio of about 18:1 is optimum for producing parts containing < 1000ppmv moisture.

Carbon Dioxide. Carbon dioxide within Cerdips is derived from organic binders and vehicles used in glazing the alumina piece parts. Variability in burn-out of these organics prior to and during seal causes substantial variation in the CO_2 content of individual Cerdip packages. Concentrations usually range from 2,000 to 20,000ppmv. A few specimens may contain significantly more or less than these amounts. From Fig. 1 there is a trend towards declining amounts of CO_2 with increasing H_2O above 5000ppmv. This may reflect the greater amounts of O_2 available to help pyrolyze the organics from the glass during the seal process as one progresses down Table 1.

Argon. Ref. [1] reported an apparent relationship between Ar and H_2O. An examination of the data from the 694 specimens reveals three distinct categories of Ar content. Parts contain either:

a. No detectable Ar
b. 100-1000ppmv Ar
c. > 8000ppmv Ar

Category (a) is made up of parts sealed in synthetic air. Category (c) is parts sealed in natural air, which itself contains 9340ppmv Ar. Category (b) is presumably an extension of (a) in which minor quantities of Ar were derived from the glass binders during seal, there is a small leakage of ambient air into the seal furnace being fed from N_2 and O_2 cylinders, or the packages at some time in their history were fine leakers and let in atmospheric Ar. Note that the tendency for parts to contain amounts of Ar inherent from air increases with their moisture content.

There is another interesting observation not reflected in Table 1. Parts sealed in synthetic air contain just as much CO_2 as those sealed in natural air. CO_2 derived from the sealing glass overwhelms the 330ppmv naturally available from air (Table 4).

Hydrogen A new relationship identified is that of H_2 in Cerdips. Between 100 and 5000ppmv, about 1 of every 5 Cerdips contain H_2, in the 0.1-0.2v% range with no apparent dependency on the H_2O content. Very dry and very wet (>5000ppmv) Cerdips do not contain H_2.

Variabilities in H_2 are, like CO_2, presumably due to variabilities in behavior of the glass during seal. H_2 content is observed to be glass lot oriented.

Presence of H_2 in the 0.2v% range in Cerdips is not trivial in light of Ref. [3]. Such quantities may be of no consequence to metallization integrity [4-5], however.

Braze Seal

These packages consisted of a ceramic body with a cavity for the chip onto which a gold-plated lid is brazed at low temperature to form a seal. The parts studied here were sealed in an N_2 atmosphere. The concentration of cavity species are typically:

$N_2 >> H_2 > H_2O > CO_2 >$ other species *

*"other species" seldom detected

Hydrogen Ref. [1] reported a definite trend of moisture with H_2. That trend is clearly evident in Fig. 4 , with significant quantities of H_2 increasing from 1 to 7v% with H_2O up to 7500ppmv H_2O.

The greater availability of H_2 increases H_2O content within the cavity. This may be due to internal chemical reactions where H_2 reactant yields H_2O as a product. Excessive H_2 atoms may occupy sorption sites on the gold surfaces within the cavity where H_2O might otherwise have been tied up. Out-diffusion of H_2 incorporated within the gold plating may be accompanied by desorption of H_2O as well. It is clear, though, that by correct choice of gold plating and pre-package sealing parameters both moisture and H_2 content in braze seal parts can be controlled.

CO_2 Previous studies on a limited number of specimens indicated no relationship between package moisture and CO_2. From Fig. 4, however, there is a weak dependency, with CO_2 rising slightly as H_2O increases. This is unlike the trend in Cerdip, where CO_2 tends to fall as H_2O increases. There is chronological importance to the data in Table 2 . In total, 10% of the samples analyzed contained >5000ppmv H_2O. A check of sample date code records reveals that only 4 of these were sealed after December 1980, corresponding to a <2% incidence of excessive moisture in braze seal over the past 34 months.

TO

These are the "can" style packages having the chip mounted on a gold-plated header and encapsulated inside a cylindrical lid welded to the header. The TO package lids in this study are nickel. Weld sealing is done in an N_2 atmosphere near room temperature. The concentration of species in the cavity is typically:

$N_2 >> H_2O > CO_2 > H_2 \lesssim O_2 >$ other species*

* often not detected.

Table 3 and Fig. 6 summarize data for 369 TO specimens.

CO_2 The tendency for CO_2 to increase with H_2O is clearly evident, similar to the trend for side braze (though amounts of CO_2 are greater) and opposite to that of Cerdip.

H_2 There are two categories of TO cans with regard to H_2, those which contain a few hundred parts per million H_2 and those which contain no detectable H_2. Incidence of H_2 appears to be lot-oriented, perhaps reflecting the manufacturing process treatments of the plated headers and/or the nickel caps. High-magnification examination of the caps reveals the nickel to be extremely porous.

Where parts do contain H_2, there is no particular trend with H_2O content if the 100-500ppmv H_2O data point is ignored. This agrees with that previously reported in Ref. [1].

H_2O Distribution A disturbing proportion of TO cans contain >5000ppmv H_2O; see histogram. It is important to understand a subset of the data not reflected in the histogram. Three-fourths of those >5000ppmv, as well as many of those in the 2500-5000ppmv category, were engineering test parts at an offshore assembly facility. Perfect moisture control was not anticipated in those particular parts.

CONCLUSION

Mass spectrometry yields useful information about all gaseous components within a hermetic package, in addition to its H_2O content. This paper has identified significant related trends in Cerdip between H_2O - O_2 and H_2O - CO_2, in braze seal between H_2O - H_2, and in TO between H_2O - CO_2. Knowing levels of species other than moisture will continue to be important, not only in the drive to lower moisture levels, but also in efforts to control hermetic cavity gas compositions for overall device reliability.

REFERENCES

1. Lowry, R. K., "Gaseous Compositions of Hermetic Package Cavity Ambients", NBS Special Publication 400-72, Workshop on Moisture Measurement Technology for Hermetic Semiconductor Devices II, November 5-7, 1980, pp. 15-18.

2. Ebel, G. H., "Application of 1018.2 to Hybrid and VLSI Devices", Proc. 21st Intl. Rel. Phys. Symp., Phoenix, AZ., April 5-7, 1983, pp. 274-281.

3. Sun, R. C., Clemens, J. T., and Nelson, J. T., "Effects of Silicon Nitride Encapsulation on MOS Device Stability", Proc. 18th Intl. Rel. Phys. Symp., Las Vegas, NV., April 8-10, 1980, pp. 244-251.

4. Shih, D., and Ficalora, P. J., "The Reduction of Au-Al Intermetallic, Proc. 16th Intl. Rel. Phys. Symp., San Diego, CA., April 18-20, 1978, pp. 268-272.

5. Murthi, A. K., and Shewchun, J., "The Effect of Hydrogen Ambients on Failure Mechanisms in CMOS Metallization", Proc. 20th Intl. Rel. Phys. Symp., San Diego, CA., March 30 - April 1, 1982, pp. 55-65.

6. Ebel, G. H., Minnowbrook Coordination Meeting on Hybrid Packaging, Sept. 18-21, 1983.

7. Moore, B. A., "Mass Spectrometric Measurement of Moisture Workshop", Proc. 21st Intl. Rel. Phys. Symp., Phoenix, AZ., April 5-7, 1983, p. 261.

TABLE I

CERDIP DATA SUMMARY

Moisture level, ppmv	n	Mean V% O_2	Mean V% CO_2	Hydrogen n[a]	Hydrogen Mean v% H_2[b]	Not Detected	Argon[c] <.04v% range	Argon[c] >0.7v% range
<100	24	1.86	1.91	1	0.01	16	8	0
100- 500	140	6.62	1.27	10	0.14	58	66	16
500- 1000	293	14.30	0.99	20	0.17	31	79	183
1000- 2500	186	14.52	0.97	27	0.21	25	53	108
2500- 5000	32	15.54	1.12	10	0.10	2	8	22
5000- 7500	2	17.90	0.47	0	-	0	0	2
7500-10000	2	19.70	0.21	0	-	0	0	2
>10000	15	19.45	0.11	0	-	0	0	15

a. n = number of specimens in which H_2 was detected.
b. mean value of H_2 for the n specimens.
c. n = number of specimens containing Ar in each indicated range.

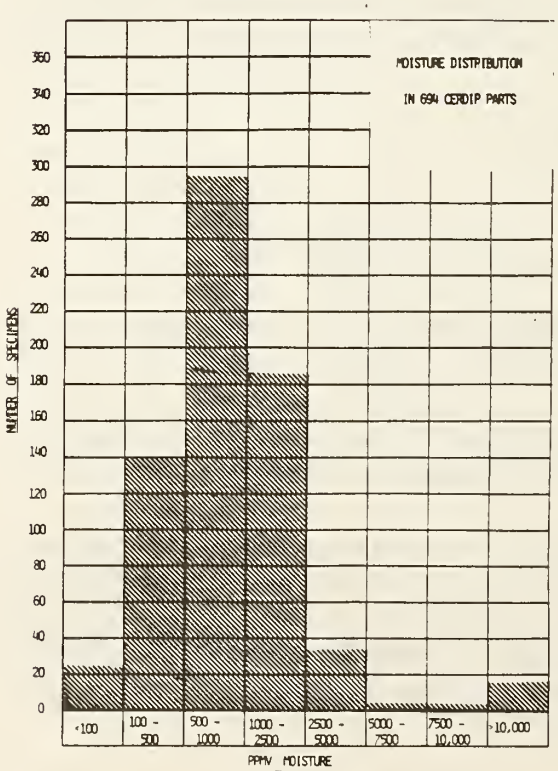

Figure 1

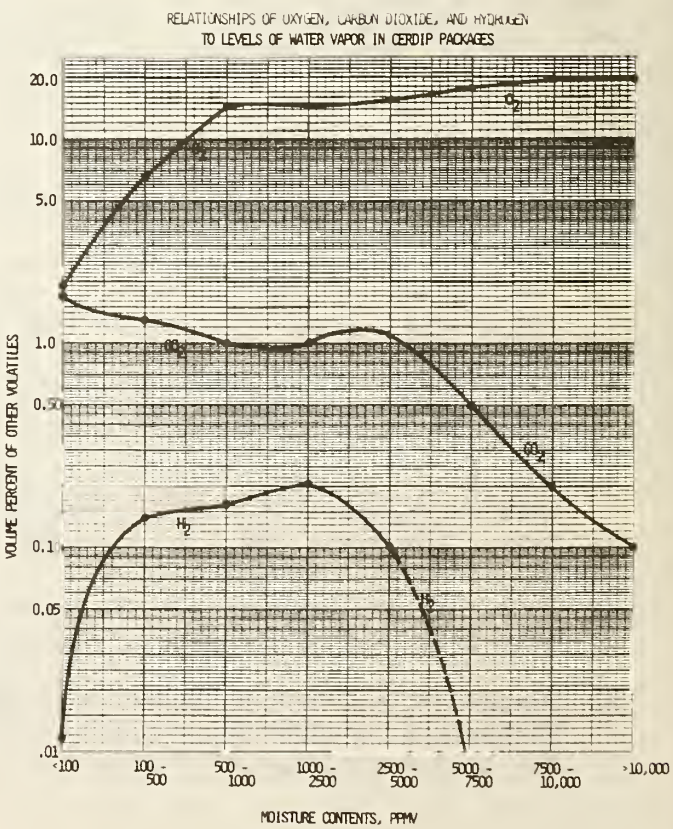

Figure 2

TABLE 2

BRAZE SEAL DATA SUMMARY

Moisture Range ppmv	n	Mean v%H_2	Mean v%CO_2
<100	16	1.08	0.023
100- 500	46	1.16	0.049
500- 1000	39	2.52	0.047
1000- 2500	66	2.89	0.062
2500- 5000	46	3.72	0.079
5000- 7500	15	6.24	0.077
7500-10,000	2	1.91	0.083
>10,000	8	0.86	1.51

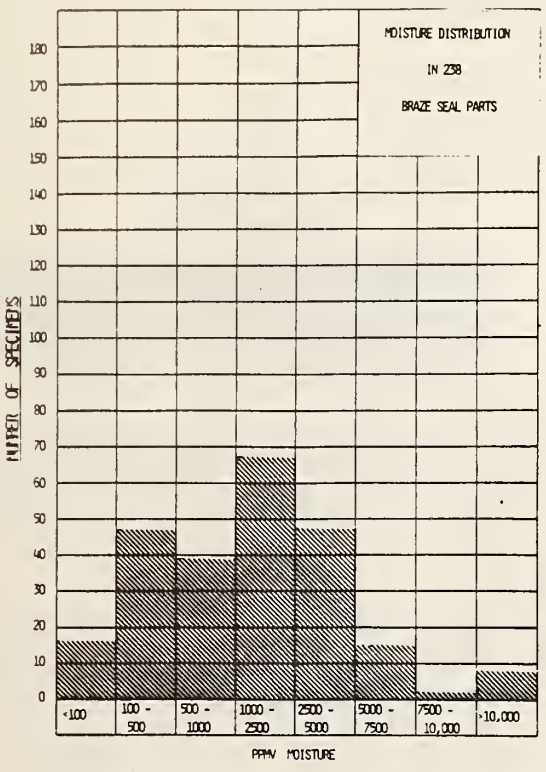

Figure 3

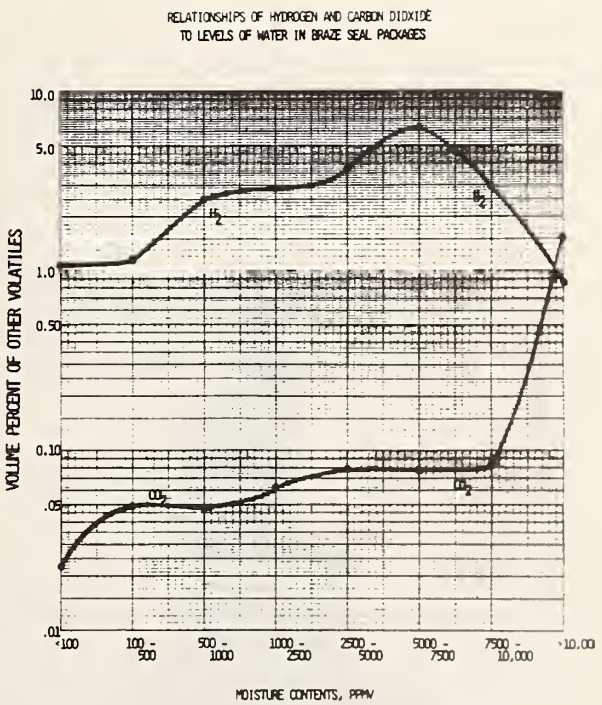

Figure 4

TABLE 3

TO DATA SUMMARY

Moisture Range ppmv	n	Hydrogen n[a]	Hydrogen Mean v% H_2	Mean v% CO_2
<100	10	0	-	0.063
100- 500	22	1	0.025	0.070
500- 1000	62	13	0.147	0.070
1000- 2500	135	60	0.041	0.104
2500- 5000	99	41	0.044	0.211
5000- 7500	27	13	0.021	0.250
7500-10000	6	3	0.017	0 467
>10000	8	2	0.022	0.450

a. n = number of specimens observed to contain H_2.
b. mean value of H_2 for the n specimens.

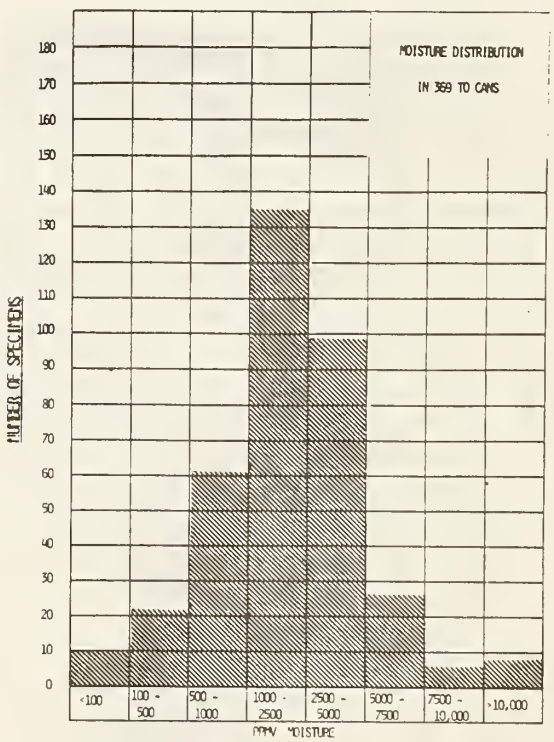

Figure 5

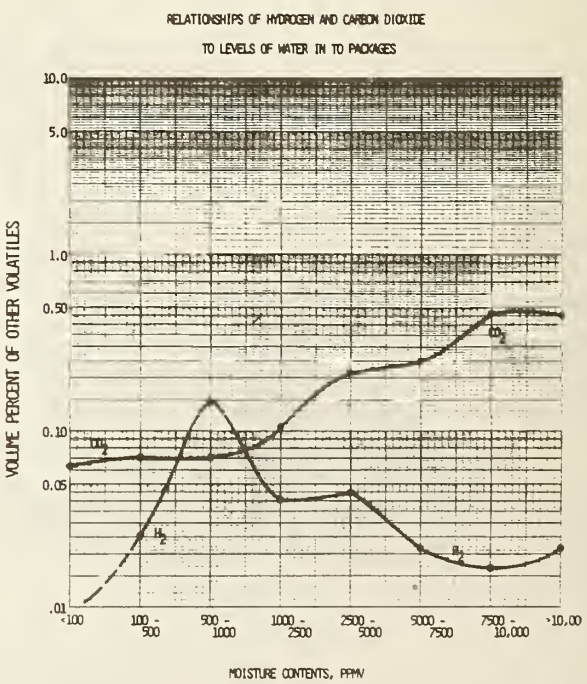

Figure 6

TABLE 4

NATURAL COMPONENTS OF ATMOSPHERIC AIR EXCEEDING 0.1 PPMV
(exclusive of water vapor)

N_2	78.084 ± 0.004	v%
O_2	20.946 ± 0.002	v%
Ar	0.943 ± 0.001	v%
CO_2	0.033 ± 0.001	v%
Ne	18.18 ± 0.04	ppmv
He	5.24 ± 0.004	ppmv
CH_4	2	ppmv
Kr	1.14 ± 0.01	ppmv
H_2	0.5	ppmv

from CRC Handbook of Chemistry and Physics, 53rd edition.

3.5 IMPROVEMENTS IN THE CAPACITANCE-RATIO METHOD OF USING AN IC DIE AS A MOISTURE SENSOR

R P Merrett
British Telecom Research Laboratories
Martlesham Heath
IPSWICH
IP5 7RE
United Kingdom
Tel 0473 642309

ABSTRACT Changes have been made to the method of using the frequency dependence of pin-to-pin capacitance to assess the water content of an IC encapsulation. The modified test is easier to perform and the results obtained can be directly compared with those of mass spectrometry.

1. INTRODUCTION

The assessment of the water content of hermetic semiconductor packages by mass spectrometry (1) is now an accepted method for product evaluation and failure analysis. However, despite considerable improvements in the operating procedures and precision of this test method, it seems unlikely that it will become simple enough for manufacturers to adopt for quality monitoring. Thus although it is difficult to control all of the factors which determine water content, manufacturers still lack a means of obtaining a rapid assessment of this aspect of their encapsulation process. In an attempt to fill this gap, the capacitance-ratio test was developed (2). Based on the use of an IC die to assess the relative humidity (RH) inside its package, the capacitance-ratio test is a rapid go/no-go procedure which is sensitive enough to detect 5000 ppm_v moisture contents.

If the internal atmosphere of an hermetic encapsulation contains moisture, there will be a conducting film of water adsorbed on the surface of the IC die, and this film introduces fringing fields which increase the pin-to-pin capacitances of the IC (2). The moisture induced capacitance is highly frequency dependent and can thus be measured by comparing the capacitance between a pair of pins of an IC at two test frequencies (100 Hz and 1 kHz). From these measurements it is possible to derive a parameter, called the capacitance-ratio, which is directly related to the moisture induced surface conductivity of the die.

In the capacitance-ratio test a measurement of the moisture induced capacitance is made when the die is cooled to a temperature at which the maximum permitted water content would cause a RH of 75% to exist at the die surface, and the package is rejected if the capacitance-ratio exceeds that corresponding to such a condition. The failure criterion is derived from a calibration procedure which involves opening a representative sample of the packages under investigation and subjecting them to a RH of 75%.

Since the test was first described it has been used for product evaluation and failure analysis of a wide variety of MSI and LSI circuits in both CERDIP and sidebrazed packages. From the experienced gained, several modifications have been made to the operating procedures. Specifically, the test method has been restructured in order to simplify the equipment required, and to make the results easier to compare with those obtained by mass spectrometry. Also, methods have been developed to minimise the contributions that both the package and circuit elements make to the measured frequency dependence. In addition, studies have been performed which show how outgassing of water from package materials can affect correlation between the results of the capacitance-ratio test and those from mass spectrometry. After these factors have been discussed, it will be shown that there may be an additional use for the information obtained when the calibration procedure is used to assess the sensitivity of an IC to moisture.

2. CHANGES IN THE METHOD OF MEASURING CAPACITANCE

Water adsorbed on the surface of an IC die forms a conducting film which provides additional capacitance coupling between the metallisation and the substrate (2). Although many ICs lack a direct connection to the substrate it is always possible to observe the influence of moisture, because the capacitance between any two pins includes the series combination of the metallisation to substrate capacitances associated with each pin. In order to maximise the response to moisture, one of the pins chosen should have a large capacitance to the substrate, ie be connected to an extensive area of metallisation. A pin connected to a supply rail satisfies this criterion and, subject to a reservation to be discussed, any input or output pin will be suitable for the other connection. (Although the response to moisture depends on the amount of metallisation connected to the second pin (3), the response for a 100 x 100 μm bond pad leading to 300 μm of 10 μm wide track is only twice as great as that for the same size bond pad connected directly to a diffusion.) Finally, because a pin-to-pin capacitance can be less than 1 pF, it is convenient to increase the capacitance presented to the test equipment, and thereby improve the resolution, by measuring the capacitance between a supply rail pin and a pair of other pins.

In order to separate the moisture measurement term from the intrinsic capacitance, the frequency dependence of the pin-to-pin capacitance is assessed by making measurements at 100 Hz and 1 kHz. The difference, d, between these two values of capacitance can be expressed as:-

$$d = \text{100 Hz capacitance} - \text{1 kHz capacitance} \qquad \ldots\ldots\ldots (1)$$

$$d = d_m + d_c + d_p \qquad \ldots\ldots\ldots (2)$$

where d_m is the contribution due to moisture.

d_c is the contribution due to circuit elements linking the tracks connected to the chosen pins. This term can be minimised by using a low amplitude measurement signal (20 mV rms).

d_p is a package contribution which is primarily due to water forming a conducting film on the internal surface of the package and thereby providing resistive coupling to adjacent pins.

For the capacitance-ratio test it is necessary to find a combination of pins for which d_m is the dominant term. In order to make the selection procedure as simple as possible, and to increase the probability of success, capacitance measurement equipment has been developed which enables the unwanted terms to be minimised. The two main units in this equipment are a 20 mV rms oscillator and a virtual earth amplifier having a reference capacitor as its feedback element. These are connected to the chosen pins of the IC under test as shown in Figure 1. Because most of the applied voltage appears across the IC, the capacitive component of the current flowing into the amplifier is directly related to the pin-to-pin capacitance of the IC, and thus the latter can be measured by using a phase sensitive amplifier to monitor the in-phase component of the output voltage of the amplifier. The contribution of the package to the frequency dependence of this capacitance is eliminated by earthing the pins either side of those connected to the amplifier. These 'guard pins' prevent currents flowing on the internal surface of the package from reaching the amplifier.

A substantial reduction in the contribution due to circuit elements can often be obtained by superimposing a DC bias voltage on the sinewave and thereby reverse biasing active elements connected to the chosen pins. This bias voltage is added, via a 4.3MΩ resistor, at the input to the amplifier and is prevented from reaching the latter by an 0.1μF blocking capacitor. The success of this technique can be assessed by measuring d when an exposed die is held at the test temperature and exposed to dry nitrogen. If the value thus measured is greater than the failure criterion derived from the 75% RH calibration, then the IC is suitable for the capacitance-ratio test.

3. AMENDED CALIBRATION PROCEDURE

A RH value of 75% was chosen for the calibration because it is high enough to produce a detectable moisture induced capacitance, while also being low enough to be within the range which will be found when packages having an unacceptable water content are cooled during the capacitance-ratio test.

Ideally, the calibration should be performed at the low temperatures (typically 0°C) needed to produce a 75% RH inside a package having a barely acceptable water content. However, because the temperature dependence of the moisture induced capacitance can be predicted, it is possible to simplify the equipment required by performing the calibration at room temperature.

Moisture enhances the pin-to-pin capacitance by an amount which is given by the equation (2):-

$$\text{Moisture induced capacitance} \propto \sqrt{\frac{\sigma}{f}} \qquad \ldots\ldots\ldots (2)$$

where f is the frequency of the measuring signal and σ is the surface conductivity. The temperature dependence of σ has been studied experimentally

(4) and, for RH values of greater than 70%, it has been found that the dependence can be described by an activation energy of 0.4 eV. Thus by using this value, and equation 2, it is possible to derive the relationship between (i) the value of d_m measured for a calibration condition of 75% RH at room temperature, and (ii) the value corresponding to 75% RH at the lower temperature specified for the capacitance-ratio test. However, although this extrapolation technique is suitable for most ICs, it should not be used when the sensitivity to moisture is such that surface conductivity becomes large enough to make the 100 Hz value of the parameter (σ/f) fall outside the range of validity of equation 2 (2). For this reason, it is now recommended that, instead of measuring d_m at the calibration condition, the response to this condition should be characterised by determining the amount, D, by which the 1 kHz capacitance increases when the RH is raised from $\leqslant$5% (a dry gas) to 75%. Using equation 2, and 0.4 eV activation energy for surface conductivity, it can be shown that the value of d_m at the test temperature is given by:-

$$d_m)_{T_t} = 2.16\ D \exp\left(2321\left(\frac{1}{T_c} - \frac{1}{T_t}\right)\right) \qquad \ldots\ldots\ldots (3)$$

where T_c°K is the calibration temperature and T_t°K is the temperature specified for the capacitance-ratio test.

When the calibration is performed on specimens bearing the same date code, die-to-die variations in the value of d_m are observed. These variations are presumably due to differing amounts of ionic surface contamination, since the latter is known to have a strong influence on surface conductivity. Thus, the failure criterion for the capacitance-ratio test must be based on the average value of d_m for several specimens: A sample size of 5 should normally be sufficient, because the die-to-die variations are usually less than 2:1.

From studies performed on different production batches from a given manufacturer, it is apparent that the batch-to-batch variations in the average value of d_m are usually much less than the die-to-die variations for a single batch. Thus, it may be possible to dispense with the need to perform regular calibrations once confidence in the stability of the manufacturing process has been established.

A minority of the CERDIP encapsulated components subjected to the calibration procedure had abnormally high values of d_m. In order to compare these calibration results with those obtained for other types of IC in CERDIPs, it is convenient to normalise the value of d_m by dividing it by the value of the 1 kHz capacitance. The normalised parameter, Φ, is called the capacitance-ratio and it can be related to the surface conductivity by the equation:-

$$\Phi = k\sqrt{\sigma} \qquad \ldots\ldots\ldots (4)$$

where the value of k depends on the thickness of the dielectric layers, and on the dimensions of the metallisation tracks. For a typical IC (3), k will be approximately equal to 2.5×10^{5} $(\text{mhos}/\square)^{-\frac{1}{2}}$. The values of Φ for two types of

LSI components having abnormally high sensitivities to moisture are listed in Table 1, where they are compared with results (for UVEPROMs) which are representative of the majority of components in CERDIPs.

Although the cause of the abnormally high values of Φ of some components has not yet been identified, the fact that such behaviour is confined to CERDIPs is an indication that it may be a consequence of the surface conductivity being enhanced by ionic contamination released by sealing glasses during the high temperature sealing operation associated with this type of package. Because the rate of moisture induced degradation is related directly to surface conductivity, it seems reasonable to postulate that components having abnormally high values of Φ are more likely to fail in service. The results of a failure analysis study which gives some credence to this hypotheses will be presented after discussing the changes made to the test temperature specified for the capacitance-ratio test.

TABLE 1

SUMMARY OF THE CALIBRATION RESULTS OBTAINED FOR VARIOUS TYPES OF IC IN 24 PIN CERDIPS

Type of IC	Value of Φ for a 75% RH at 0°C	
	Range	Average
Manf A	0.023 to 0.027	0.025
64k B	0.023 to 0.028	0.025
UVEPROM C	0.039 to 0.067	0.051
Custom D	0.030 to 0.150	0.085
LSI E	0.050 to 0.145	0.100

4. REVISION OF THE TEST TEMPERATURE

All of the moisture induced failure mechanisms of ICs depend on the moisture induced surface conductivity of the die. From the functional dependence of this conductivity on both temperature and RH, it can be shown that the risk of failure from a given amount of water is greatest at low operating temperatures (2). Thus, it follows that the maximum permitted water content can be specified in terms of the largest RH which can be tolerated at the lowest expected operating temperature. The value of this RH can be quantified by extrapolating experimentally derived surface conductivity data and, for the case of a requirement of a 20 year life at a lowest expected operating temperature of 0°C, it has been shown that the maximum permitted water content would produce a 45% RH at 0°C (2). Although this RH is too low for detection by a measurement of the moisture induced capacitance, such a measurement can be used to assess the

water content if localised cooling of the die is used: The package is held at 0°C and the temperature of the die is reduced to the value (-6.5°C) at which the maximum permitted water content would produce a RH of 75% at the die surface.

The advantages of this test procedure is that, because the RH inside the package is assessed at the worst case operating temperature, the criterion against which the package is judged is unaffected by the way in which the total water content of the internal cavity is shared between (i) the gas phase and (ii) physical adsorption on the walls of the cavity. The influence of adsorption is greatest at low temperatures and, for a given water content, the RH inside a package having highly adsorbent walls will be much less than that inside one which does not (eg a CERDIP and a metal package respectively). Thus, it can be argued that methods, such as mass spectrometry, which give the total water content of a package do not provide a fair indication of the risk of moisture induced failure. Nevertheless, because mass spectrometry has been adopted as the standard against which the accuracy of alternative techniques are judged, the test temperatures specified for the capacitance-ratio test have been changed in order to make the results comparable with those of mass spectrometry.

The generally accepted method of reporting the total water content measured by mass spectrometry, namely ppm_v, does not uniquely define the partial pressure of water, although the latter determines the rate of moisture induced degradation. For a given ppm_v value, the partial pressure depends on the total internal pressure of the package, and this quantity varies significantly between package types. For a CERDIP, where the total internal pressure is typically 0.5 bars, a water content of 5000 ppm_v corresponds to a partial pressure of 2.5 mbars, while for a welded metal package, where the total internal pressure is typically 1 bar, it corresponds to 5 mbars. Despite this discrimination against packages having a low internal pressure, the fact remains that the maximum water content requirement for general purpose components is usually expressed as 5000 ppm_v regardless of package type. Accordingly, the same procedure will be followed for the capacitance-ratio test.

In order to calculate the test temperature required to produce a 75% RH inside a package containing 5000 ppm_v, it is necessary to estimate the amount of water adsorbed by the walls of the internal cavity at the test condition. Thus it is desirable to minimise adsorption by keeping most of the package hot ($\geqslant$15°C), whilst using probe cooling to hold the die at the required temperature. The equipment needed to establish these conditions is thus similar to that (5) used for the 'dew-point' tests which involve plotting a moisture sensitive parameter (such as leakage current or capacitance) against die temperature.

The test temperatures corresponding to a 5000 ppm_v failure criterion are listed in the first column of Table 2. For completeness, the last two columns of this Table give the temperatures appropriate to a maximum permitted water content expressed in terms of (i) a partial pressure of 5 mbars (ii) a RH of 45% at 0°C.

TABLE 2

DIE TEMPERATURES SPECIFIED FOR THE CAPACITANCE-RATIO TEST ON THE BASIS THAT THE PACKAGE LID IS MAINTAINED AT ⩾15°C

Package Type	Test Temperature (°C) for a Maximum Permitted Water Content of:-		
	5000 ppm_v	5 mbars	45% RH at 0°C
Metal	0	0	-5
Side-Brazed	-5	-2	0
CERDIP	-13		

The accuracy of the revised test is primarily dependent on that of the estimate of the value of the physical adsorption term in the package model which is described in the Appendix. In order to check the predictions based on this model it is necessary to compare the results of the capacitance-ratio test with those obtained from mass spectrometry. A limited exercise of this type has been conducted on CERDIPs, and the capacitance-ratio test has been shown to be able to distinguish between packages having large (>8000 ppm_v) and those having small (<2000 ppm_v) water contents. However, the results presented in the next Section have shown that it can be difficult to make a fair comparison of the two tests when the water content is near the barely acceptable level.

The equipment needed to perform the revised test is simpler than that originally described (2) and, because it is not necessary to wait for the whole package to cool down, the test can be completed within 2 minutes.

5. LIBERATION OF TIGHTLY HELD WATER DURING MASS SPECTROMETRY

As part of the exercise to assess the accuracy of the revised capacitance-ratio test, an examination was made of CERDIPs having devitrifying glass seals. These packages, which had been in store for 7 years, were thus from an era when most such packages had unacceptable water contents (6).

From these studies it was evident that, in addition to the water in the gas phase and that physically adsorbed (ie 'loosely held') on the walls of the internal cavity, it is necessary to consider water which is 'tightly held' (eg chemisorbed) by packaging materials. The characteristic features of these two types of adsorption is that, whereas equilibrium between the gaseous state and physical adsorption is achieved in only a fraction of a second, it can take many

months for the amount of tightly held water to reach a steady state at room temperature (7).

The tests on the CERDIP packages showed that the elevated temperatures associated with mass spectrometry (1) were able to drive tightly held water out of packaging materials, and into the internal cavity. An example of this behaviour is shown in Figure 2 which gives the plot of capacitance-ratio versus temperature for a CERDIP before and after this had been baked at 100°C for 1 hour - a condition which is comparable with that which will be experienced prior to mass spectrometry analysis. Before the bake, the capacitance-ratio was barely measurable over the range 10 to -20°C, and the value at the test temperature (-13°C) corresponding to a maximum permitted water content of 5000 ppm_v was well below the failure criterion indicated by the cross. However, after the bake the capacitance-ratio test indicated that the water content was unacceptable, and this was later confirmed by mass spectrometry.

From the vintage and type of construction of these packages there is no reason to doubt that a capacitance-ratio test and mass spectrometry would have both indicated an unacceptable water content had they been performed shortly after manufacture of the packages. It must, therefore, be concluded that the amount of tightly held water gradually increased during the period of room temperature storage, and thereby caused a reduction in the amount of water which was able to come into contact with the die (and be detected by the capacitance-ratio test). When the temperature was subsequently raised to 100°C, some of the tightly held water would have been desorbed and this would explain the increase in the indicated water content.

Clearly, it is essential to use standardised pre-treatments during any attempts to demonstrate correlation between mass spectrometry and the capacitance-ratio test, and it must be recognised that there will be circumstances where mass spectrometry will overestimate the amount of water which presents a long term hazard to the encapsulated semiconductor.

6. THE CAPACITANCE-RATIO TEST AS A FAILURE ANALYSIS TOOL

When the capacitance-ratio test is used for product evaluation, the calibration can be performed on specimens from a homogenous population, and it is thus possible to obtain a reasonably accurate estimate of the response to moisture of the specimens to be evaluated. This procedure cannot usually be followed during failure analysis studies which typically involve components from many production batches, but in such cases it is nevertheless possible to use the test to rapidly identify the packages having the largest water content. To illustrate this application, results will be given for a LSI circuit which had a metallisation corrosion failure rate of about 700 FITs within 2 years of being used in equipment having a very low power dissipation.

Figure 3 is a histogram of the values of Φ obtained when 190 of the in-service failures were subjected to a capacitance-ratio test based on a die temperature of -13°C. From this data it is evident that there are two distinct groups of specimens, namely those having a value of Φ less than 0.01 and those for which it is greater than 0.1. Because the lower of these values is typical of the contribution due to circuit elements, it was concluded that specimens in the

other group had the higher water content. This supposition was confirmed by showing that only 44/190 of the specimens had corroded metallisation and that, without exception, these came from the group having the high value of Φ. (The remaining specimens were either classified as having failed due to a persistent substrate bond problem or as 'wrongly removed from service').

A calibration at a 75% RH on a representative sample of these CERDIP encapsulated specimens revealed that the response to moisture was significantly greater than that usually observed for ICs in this type of packages: The average value of Φ for a 75% RH at 0°C was 0.09 whereas the corresponding value for a typical CERDIP encapsulated die will be in the range 0.02 to 0.05. However, Auger electron spectroscopy did not reveal abnormally high levels of ionic surface contamination which could explain the 75% RH calibration results, and there seemed to be no connection between the latter and the hermeticity problem which was the cause of the unacceptable water content.

From the square law relationship between Φ and surface conductivity it can be concluded that, for a given water content, the surface conductivity of the service failures would have been at least 4 times greater than that for ICs having a normal sensitivity to moisture. Because the rate of moisture induced degradation is directly linked to surface conductivity, such a difference could account for the fact that corrosion failures occurred within less than two years of the components entering service. It is, therefore, likely that future failure analysis exercises will confirm that the results of the 75% RH calibration procedure are an indicator of the susceptibility of a component to moisture induced failure mechanisms.

7. CONCLUSIONS

The capacitance-ratio test procedures have been improved, and the results can now be more readily compared with those of mass spectrometry. A comprehensive assessment of the accuracy of the capacitance-ratio test has yet to be performed, but the results of a limited study have demonstrated the potential of the test as a means of rapidly detecting unacceptable water contents. Although the capacitance-ratio test is unlikely to match the precision of mass spectrometry, there are applications such as in-line monitoring, failure analysis, and incoming goods inspection, where the regular application of the capacitance-test would provide greater protection than would the spasmodic use of mass spectrometry.

By comparing the results obtained from the capacitance-ratio test with those from mass spectrometry it has been shown that, because the latter can release water which is normally tightly held by packaging materials, it will not always give a true indication of the amount of water which presents a long term hazard to the encapsulated die.

The results a failure analysis exercise, and of an assessment of CERDIP packages, suggest that the 75% RH calibration procedure associated with the capacitance-ratio test may provide an indication of the susceptibility of an IC to moisture induced degradation.

8. ACKNOWLEDGEMENT

Acknowledgement is made to the Director of the British Telecom Research Laboratories for permission to publish this paper.

9. REFERENCES

1 R W Thomas and D E Meyer, 'Moisture in SC packages', Solid State Technology, 17, 1974.

2 R P Merrett, S P Sim and J P Bryant, 'A Simple Method of Using the Die of an IC to Measure the Relative Humidity Inside its Encapsulation', Reliability Physics Symposium Proceedings, 18, 17, 1980.

3 R P Merrett, J P Bryant and R Studd, 'An Appraisal of High Temperature Humidity Stress Tests for Assessing Plastic Encapsulated Semiconductor Components', Reliability Physics Symposium Proceedings, 21, 73, 1983.

4 R P Merrett, S P Sim, 'Assessment of the use of Surface Conductivity as a Means of Determining the Moisture Content of Hermetic Semiconductor Encapsulations', ARPA/NBS Workshop on Moisture Measurement Technology for Hermetic Semiconductor Devices, 1978; NBS Special Publication 400-69, 94.

5 N Bakker, 'In-Line Measurement of Moisture in Sealed IC Packages', Philips Technical Review, 37, 11, 1979.

6 R W Vasofsky and R K Lowry, 'Moisture Evolution from Sealing Glasses: Dry CERDIP Packages', Reliability Physics Symposium Proceedings, 18, 1, 1980.

7 C Hayashi, 1957 Vacuum Symposium Transactions, 13, Pergamon Press, New York 1958.

8 D M Young and A D Crowell, 'Physical Adsorption of Gases' Butterworths 1962.

APPENDIX

MODEL OF THE INTERNAL ATMOSPHERE OF AN HERMETIC PACKAGE

The fractional relative humidity (R) inside an internal cavity of volumn V and surface area A at a temperature T, is a solution of the equation:-

$$P_o = R\, P_s)_T + \frac{A}{V}\, m)_R \qquad \text{..... (A1)}$$

where P_o is the partial pressure of water when the temperature is high enough for all the physically adsorbed water to be in the gas phase, $P_s)_T$ is the saturation vapour pressure of water at the temperature T, and $m)_R$ is the amount of physically adsorbed water per unit area when the fractional relative humidity is R. The value of $m)_R$ can be calculated by fitting a BET isotherm (8) to measured adsorption data (4):-

$$m)_R = \frac{0.21\ R\ x}{(0.11 + 0.98R - 1.09R^2)} \qquad \ldots\ldots\ldots (A2)$$

where the 'roughness factor' x is the the quotient of (i) the true adsorbing surface area and (ii) the geometric surface area of the internal cavity. For ceramics x will depend on the degree of sintering and values in the range 10 to 100 are likely, whereas for pressed metals it will vary from 1 to 3 (8). On the basis that the metals and ceramics used in package construction have x equal to 2 and 10 respectively, it is estimated that the value of (Ax/V) for completely metal packages is 3 while for ceramic or partly ceramic packages it is 10.

In the capacitance-ratio test, the die is held at the temperature T_t required for a barely acceptable water content to cause a fraction relative humidity (R) of 0.75 at the die surface, while the rest of the package is maintained at a temperature which is high enough to minimise adsorption on the walls of the internal cavity. By combining equation A1 and A2 it can be shown that T_t can be calculated by using:-

$$P_{om} = 0.75\ P_s)_{T_t} + 0.68\ \frac{A\ B\ x}{V} \qquad \ldots\ldots\ldots (A3)$$

where P_{om} is the partial pressure of water corresponding to the maximum permitted water content, and B is a factor which makes allowances for the reduction in adsorption due to localised cooling of the die (B = 1 for the case of uniform cooling of the package and the die).

When calculating the value of P_{om} corresponding to a maximum permitted water content expresses in terms of ppm_v, the total internal pressure of the package must be taken into account. For metal packages, side-brazed packages and CERDIPs, the total internal pressures will typically be 1, 0.8 and 0.5 bars respectively.

The value of (BAx/V) will depend on the way in which localised cooling is achieved. If a heater is used to keep the top of the package at 15°C while a cold probe, having dimensions comparable with that of the die, is pressed against the underside of the package, most of the adsorption will be confined to the die which will have a roughness factor x of near unity. In such a case the value of (BAx/V) is estimated to be 0.7 for metal packages and 1.5 for side-brazed packages and CERDIPs. These values have given fair agreement between the results of mass spectrometry and the capacitance-ratio test.

A direct measurement of (BAx/V) can be made by plotting the capacitance parameter d versus die temperatures, and then using the 75% RH calibration data to determine the die temperature at which the RH inside the package passed through 75%. By substituting this temperature into equation A3 it is possible to express the water content in terms of (BAx/V). The latter can thus be calculated if the water content is subsequently measured by mass spectrometery. To date this technique has been performed on a five 14 pin CERDIP packages, and

an average values of (BAx/V) was found to be 2.3, ie a slightly higher figure than the 1.5 used to calculate the test temperatures listed in Table 2. If further studies confirm that the higher value is more appropriate, these test temperatures will need to be revised.

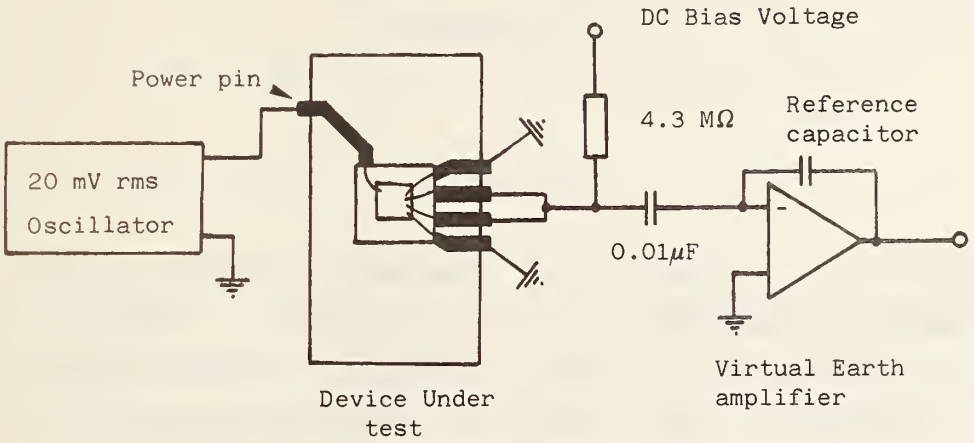

FIG 1 The general features of the equipment used to measure the pin-to-pin capacitance of an IC

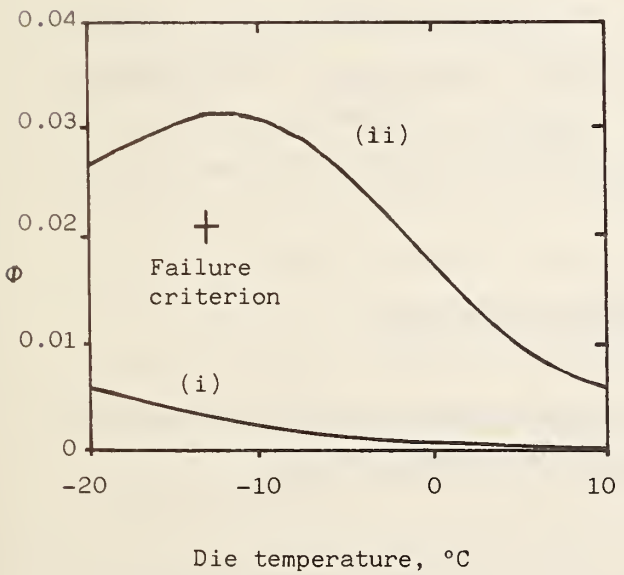

FIG 2 The temperature dependence of Φ for an IC in a CERDIP (i) after several years in storage at 20°C, and (ii) after baking for 1 hour at 100°C

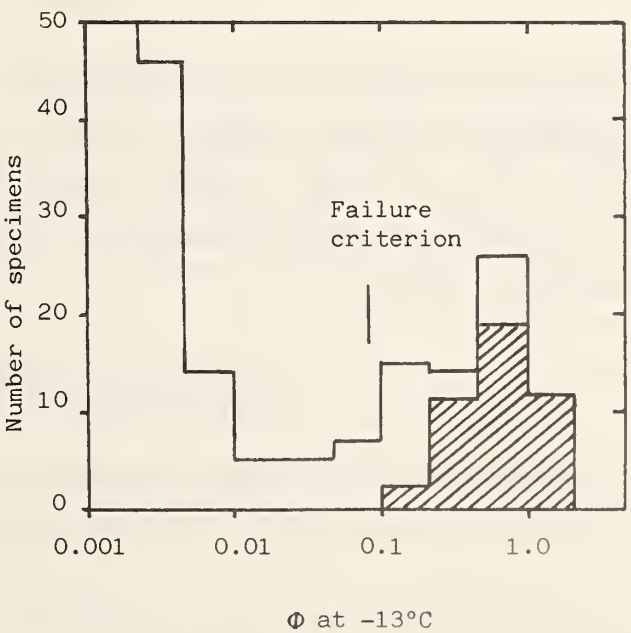

FIG 3 Histogram of the value of Φ for 190 in-service failures. The shaded area defines the specimens which had corroded metallisation

3.6 COMPARISON OF VARIOUS MOISTURE MEASUREMENT METHODS: TEST PROCEDURES AT RADC

N.K. Annamalai*
Rome Air Development Center (RBRE)
Griffiss AFB NY 13441
(315)330-4055

ABSTRACT

A description of test procedures being developed at RADC to compare various moisture measurement methods is given. The capacitance ratio test is suitable for go or no-go test while the Philips capacitance technique is suitable for use with the automatic test equipment. Other methods will be tested for sensitivity, convenience of use in view of the coming 2000 ppm_v requirement and the requirement for in-line testing for moisture.

INTRODUCTION

Mass spectrometry is an accepted method [1] to determine the moisture content in hermetically sealed packages, but this method is not simple or convenient for manufacturers to use in quality control. Mass spectrometry is destructive and requires skilled personnel, hence other simple methods suitable for in-line testing are being considered.

MOISTURE MEASUREMENT METHODS

A test facility to study and to compare the various moisture measurement methods is being developed at RADC. The various methods being considered are:

a. Philips Capacitance Technique
b. Capacitance Ratio Test

*Prof Annamalai is on a year sabbatical from Clarkson College of Technology, Postdam NY 13676

c. Harris Corporation Sensor Chips

d. Al_2O_3 Sensor Chips

Philips Capacitance Technique [2]

This is similar to the surface conductivity type. One advantage of this method is that it does not use extra pins. The capacitance between two leads - theoretically any two leads - of the IC chip is measured as a function of temperature.

Dry Package Circuit Model [3]

Let us consider a dry package, i.e., no moisture present in the package. Let us also consider any two pins of the IC chip that are connected to the metallization tracks. Between the metal track and substrate a capacitance Ct exists. The cross section of the IC die, when the package is dry, is shown in Figure 1a. The circuit model of the die when the package is dry is shown in Figure 1b. The measured capacitance is 2 Ct.

Wet Package Circuit Model [3]

Let us now consider a wet package, i.e., a certain amount of moisture present in the package. When the package is cooled, water will condense on top of the overglaze at a specified temperature depending upon the moisture content. This moisture introduces a capacitance CW_1 between the metal track and the water layer and another capacitance CW_2 between the water layer and the substrate (Figure 2a). The water layer has a resistance value of RW. The circuit model for a wet package is shown in Figure 2b. Comparing Figure 2b with Figure 1b one realizes that the water layer increases the capacitance meaured between the two pins. The water layer also introduces a resistance. Hence, as we decrease the temperature of the die, moisture condenses and shows up as an increase in capacitance. Dew point is a function of the moisture content.

Capacitance Plot

A capacitance plot as a function of temperature reported by N. Bakker [2] is reproduced in Figure 3. For a certain moisture content which corresponded to a dew point of $+12^{\circ}C$, the capacitance vs temperature plot is shown in Figure 3a. The

capacitance plot is shown for both cooling and heating. During cooling, at dew point, water condenses on the overglaze and capacitance increases. The capacitance remains high until water freezes. The water can remain in the liquid state (in the supercooled state) up to -20°C. The capacitance drops abruptly at the freezing point, due to the sudden freezing of the water film on the chip. Ice has a much lower conductivity than the water film. During heating capacitance increases since the ice melts. Upon further heating the water evaporates and the capacitance decreases. At above the dew point, all but a few monolayers of water has evaporated. Above the dew point, the heating curve coincides with the cooling curve. For an IC package with a moisture content too low to be detected, having a frost point below -25°C, the capacitance plot is shown in Figure 3b.

Moisture Determination Using Nomograph

A nomograph [4] for dew points and moisture content in ppm_v as a function of pressure is shown in Figure 4. The dew point for a package is determined from capacitance vs temperature plot. Knowing the package seal pressure and temperature, pressure at dew point could be obtained by using the relationship $p_1/T_1 = P_2/T_2$, where P_1 = pressure at time of seal, T_1 = absolute temperature at time of seal, P_2 = pressure at dew point, T_2 = Absolute temperature at dew point. Having determined the pressure at dew point, moisture content of the package in ppm_v can be obtained from the nomograph.

Capacitance Plot at Various Frequencies

The capacitance plot as a function of temperature is shown (Figure 5) at various frequencies [3]. The capacitance peak increases sharply at low frequencies. This can be understood by referring to Figure 2b.

Capacitance Ratio Test

The capacitance ratio test is an extension of Philips capacitance test. The fact that the capacitance of a wet package is frequency dependent is the concept used in this test. Measuring a difference in pin-to-pin capacitance at two frequencies while holding the die at constant temperature (dew point for a given moisture level) and comparing to a calibration value yields a pass/fail determination. This method is sensitive enough to determine 5000 ppm_v moisture level. This method may not be sensitive enough to determine low levels of moisture. This can be understood by

referring to Figure 2b and noting that low levels of moisture means a large RW. Large RW implies an open in that branch and the capacitance measured between pins is only 2 Ct (dry package capacitance). A detailed description of this method can be found elsewhere [3,5].

Harris Corporation Sensor Chips

Harris Corporation sensor chips are the surface conductivity type. These are in the form of chips fabricated in the integrated circuit production line by vacuum depositing aluminum over oxidized silicon followed by a photoresist step to delineate closely spaced interdigited metal strips. The chips are mounted inside the package to be tested, bonded for external electrical connection and the packages are then sealed by the applicable process to be investigated or monitored. When the temperature of the package is reduced, water condenses on the sensor chip and leakage current increases. Sensor chips are shown in Figure 6a and the corresponding leakage current as a function of temperature is shown in Figure 6b. Moisture content in ppm_v can be determined by using the nomograph if all the moisture can be condensed on the chip. A diode is also fabricated on the chip for use in temperature determinations. The chip uses up two extra pins not counting diode leads, but it is a non-destructive test.

Al_2O_3 Sensors

This is a volume effect sensor. The number of water molecules absorbed on the pore walls of Al_2O_3 determines the total complex impedance of the sensor. A detailed description of this device can be found in references 6 and 7. This sensor requires a calibration procedure. The sensor uses up two extra pins. A major concern is the aging problem associated with this sensor.

TEST PROCEDURES

A setup is being established at RADC to change the moisture content and test the device under various moisture conditions. This setup will be useful to test various methods and sensor chips. An environmental chamber made by Tenney Jr. equipped with wet a bulb and dry bulb thermometer controls is used for establishing a desired moisture content in the chamber. A small plexiglass box as shown in the photograph (Figure 7) is mounted inside this environmental chamber. The IC chip (1) with the top

lid removed will be mounted inside the small plexiglass box (2). The plexiglass box along with the bottom plate (3) is the simulated package. A small window (4), with the lid (5) open, keeps the small plexiglass box in equilibrium with the environmental chamber. During the test the window is closed to prevent any further moisture getting into this small box from environmental chamber. This small box is not hermetically sealed. To take care of this problem, testing has to be done at a sufficiently fast rate. An alternative design is to provide "O" ring seals at all openings. The coaxial connectors (6) are used for electrical connections. Temperature of the die is monitored by the diode on the chip. The die is cooled by a thermoelectic cooler (7). A heat sink (8) is provided for heat dissipation. The thermoelectric cooler is capable of cooling the die to $-30^{o}C$. The environmental chamber dry bulb is kept at $40^{o}F$ and the wet bulb is set at a temperature corresponding to a desired moisture level in ppm_{v}. Dew point sensors require cooling of the device and analyzing their response. The temperature and the response (capacitance or sensor current, etc) will be recorded by a Bascom Turner Instruments 8120R programmable plotter. The plexiglass box is quite large (infinite moisture source) compared to the IC package. Hence, the test does not represent a real life situation but is useful to compare the sensitivity of various moisture measurement methods. Another set of experiments planned are to seal CERDIP packages with known moistures and test them by various methods.

CONCLUSIONS

The two set of experiments planned will permit us to compare various moisture measurement methods and choose the appropriate one for in-line moisture measurement and also for use with automatic test equipment. The selection will be guided by the present 5000 ppm_{v} requirement and also by the future requirement of 2000 ppm_{v}.

REFERENCES

1. Benjamin A. Moore, "Mass Spectrometer Measurements at RADC," Proceedings of the ARPA/NBS Workshop V held at the National Bureau of Standards, Gaithersburg MD, March 22-23, 1978.

2. N. Bakker, "In-line Measurement of Moisture in Sealed IC Packages," Philips Telecommunication Review, Vol 37, No 1, March 1979.

3. R. P. Merrett, S.P. Sim, J. P. Bryant, "A Simple Method of Using the Die of an Integrated Circuit to Measure the Relative Humidity Inside its Encapsulation," Proceedings of the 18th Annual Relaibility Physics, Las Vegas NV, April 8-10, 1980.

4. Nomograph reproduced from Harris Corporation Moisture Sensor Chip Technical Bulletin.

5. R. P. Merrett, "Moisture Measurement by the Capacitance-Ratio Test," RADC-TM-82-2.

6. Kovac, M.G., Chleck, D., and Goodman P., "A New Moisture Sensor for In Situ Monitoring of Sealed Packages," Proceedings of the 15th Annual Reliability Physics Symposium, Las Vegas NV, April 13-15, 1977.

7. Finn, J.B. and Fong, V., "Recent Advnaces in Al_2O_3 In Situ Moisture Monitoring Chips for CERDIP Package Applications," Proceedings of the 18th Annual Reliability Physics Symposium, Las Vegas NV, April 8-10, 1980.

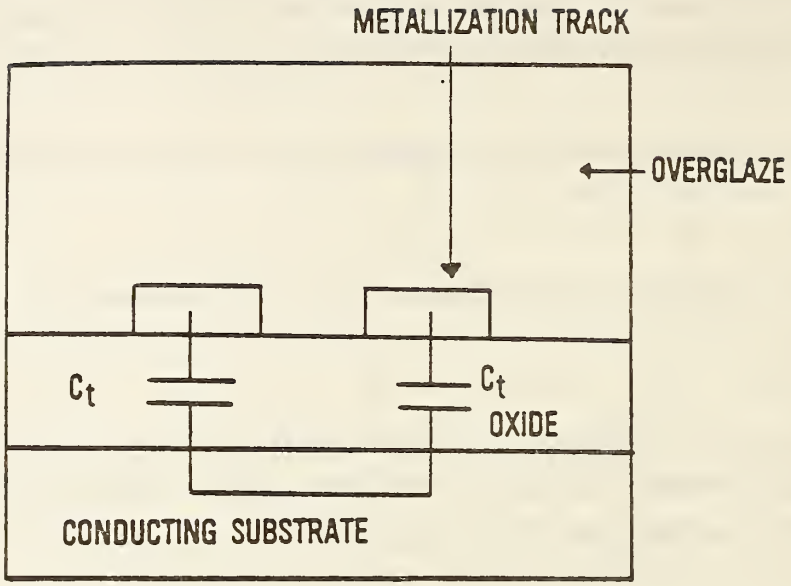

Figure 1a

CROSS SECTION OF AN IC DIE (NO WATER LAYER)

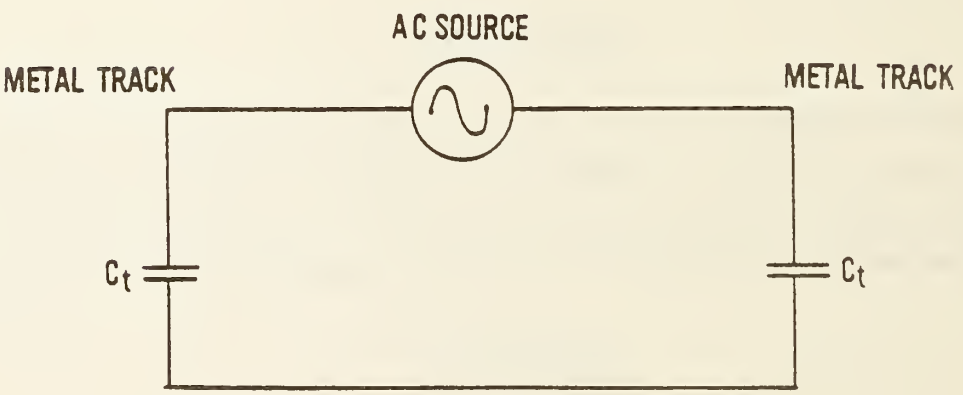

Figure 1b

CIRCUIT MODEL (NO WATER LAYER)

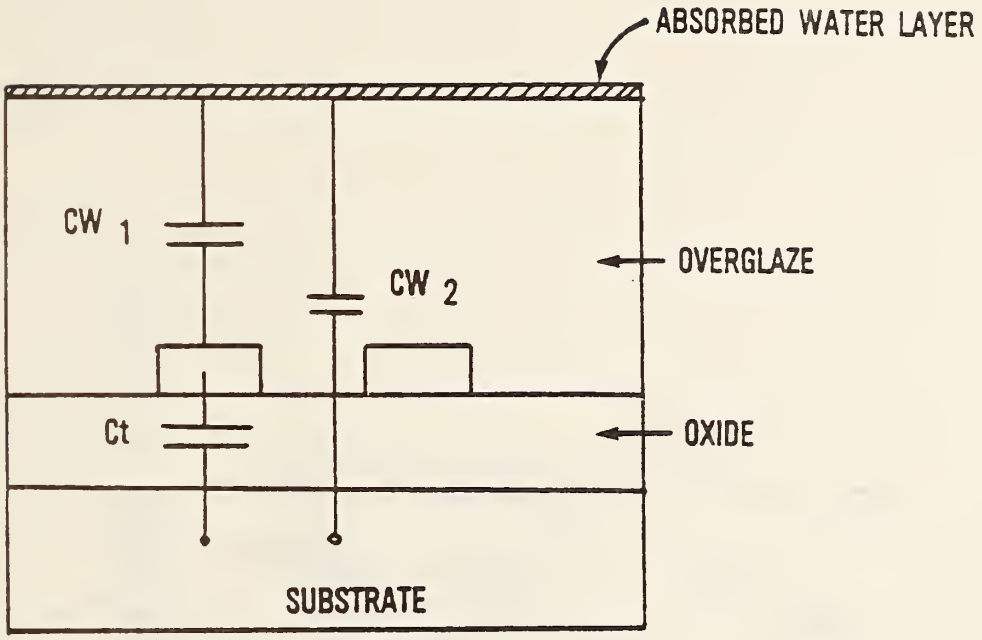

Figure 2a

CROSS SECTION OF AN IC DIE WITH ABSORBED WATER LAYER

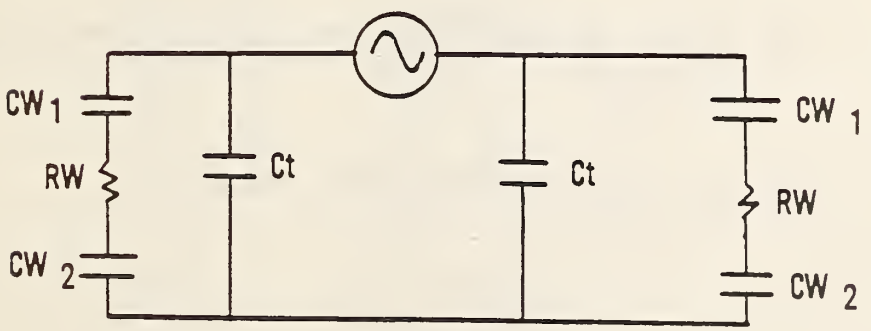

Figure 2b

CIRCUIT MODEL (WITH WATER LAYER)

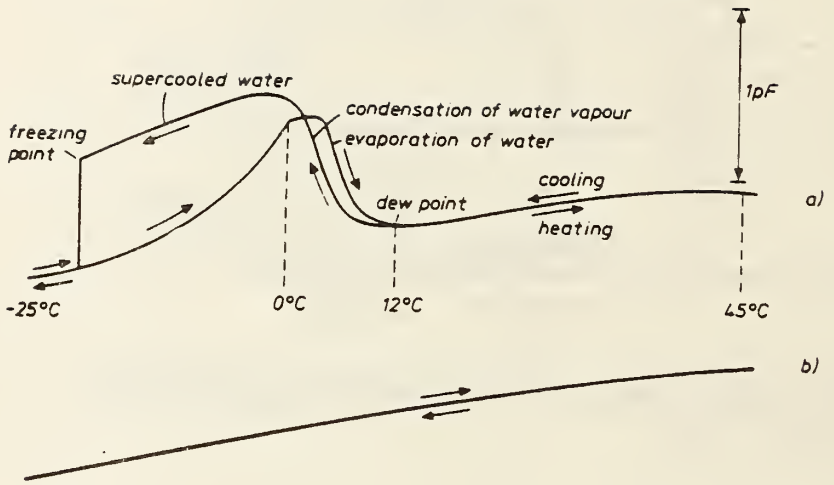

FIGURE 3 (A) CAPACITANCE PLOT AS A FUNCTION OF TEMPERATURE DEWPOINT AT +12C

(B) IC OF THE SAME TYPE WITH VERY LOW MOISTURE CONTENT

DEVICE TESTED: 14 PIN DIL PACKAGE

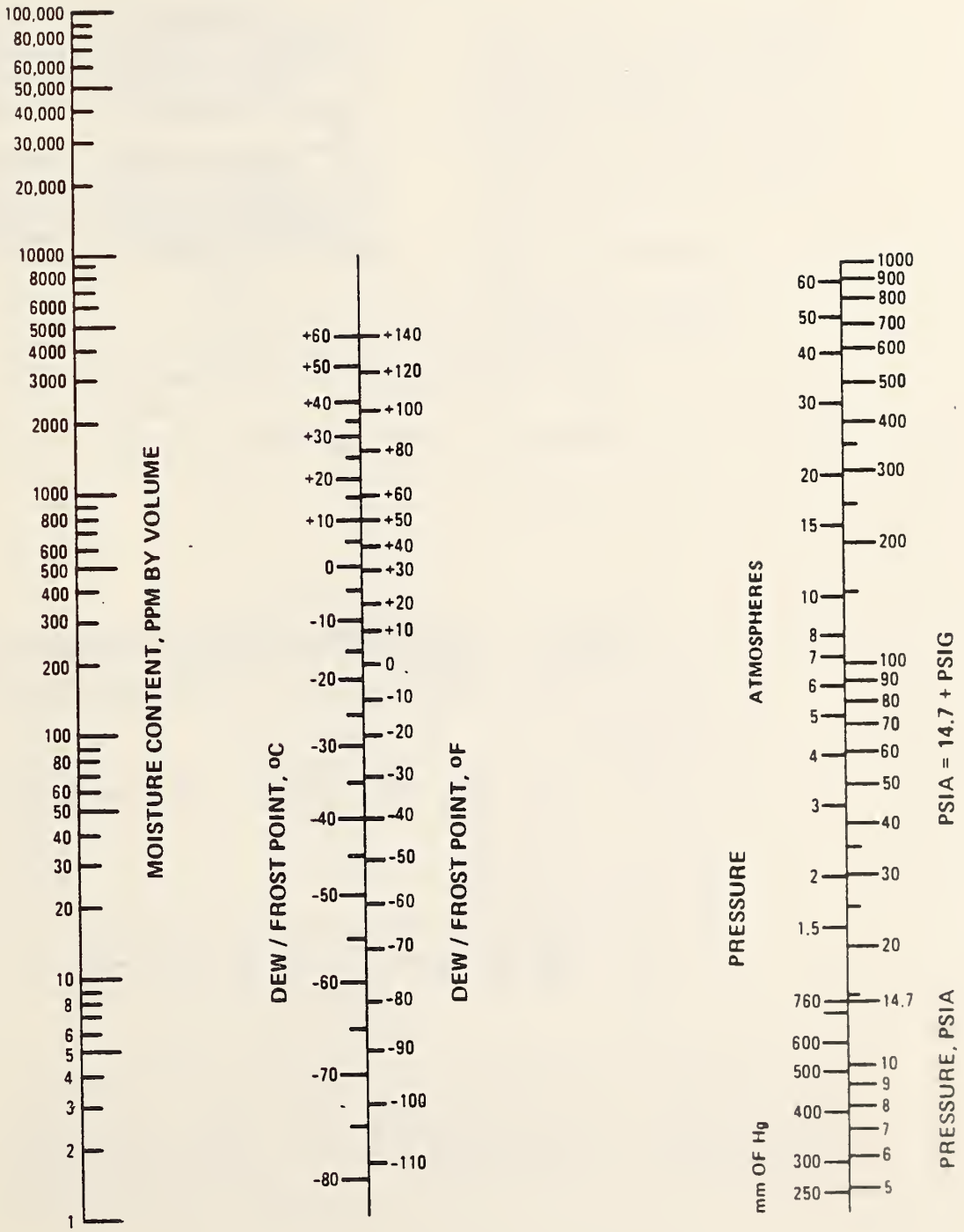

FIGURE 4 - NOMOGRAPH FOR DEWPOINTS & MOISTURE CONTENT IN PPM AS A FUNCTION OF PRESSURE

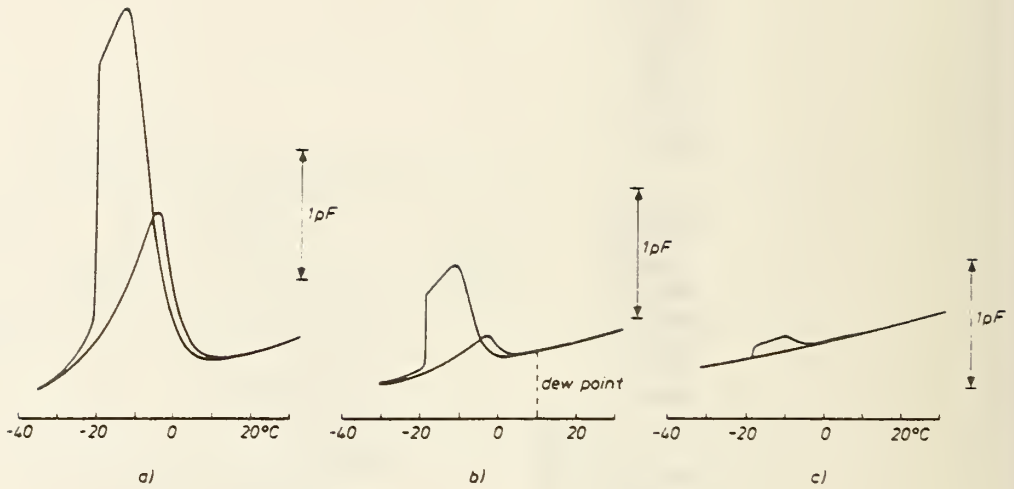

FIGURE 5 CAPACITANCE VERSUS TEMPERATURE CURVE OF AN IC AT (A) 1 KHZ (B) 10 KHZ AND (C) 100 KHZ

DEVICE TESTED: 14 PIN DIL PACKAGE

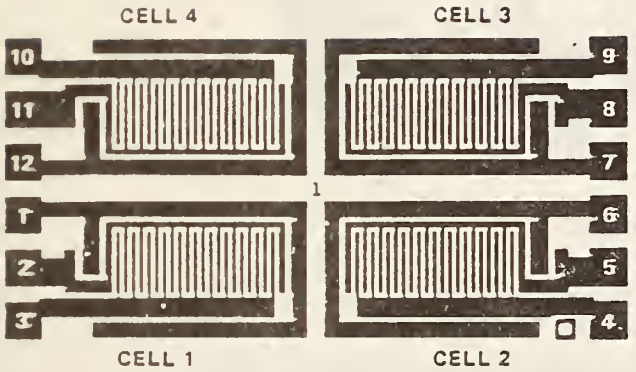

The HI-55001 has four electrically identical moisture sensing cells on chip. The user may apply any one cell or parallel combination of cells in a moisture measuring experiment. The individual cells are accessed as follows: Cell 1 – pads 2 & 3; Cell 2 – pads 4 & 5; Cell 3 – pads 8 & 9; Cell 4 – pads 10 & 11 respectively.

Chip Size: 95 mils by 50 mils.

FIGURE 6(A) - HARRIS CORPORATION SENSOR CHIP

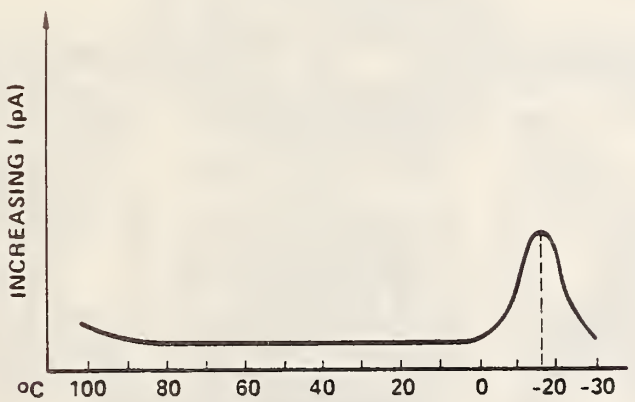

FIGURE 6(B) SENSOR CHIP CURRENT AS A FUNCTION OF TEMPERATURE. DEW POINT -18°C FOR A PACKAGE CAVITY PRESSURE OF 0.45 ATMOSPHERE. THIS TRANSLATES TO APPROXIMATELY 2800 PPM_U MOISTURE

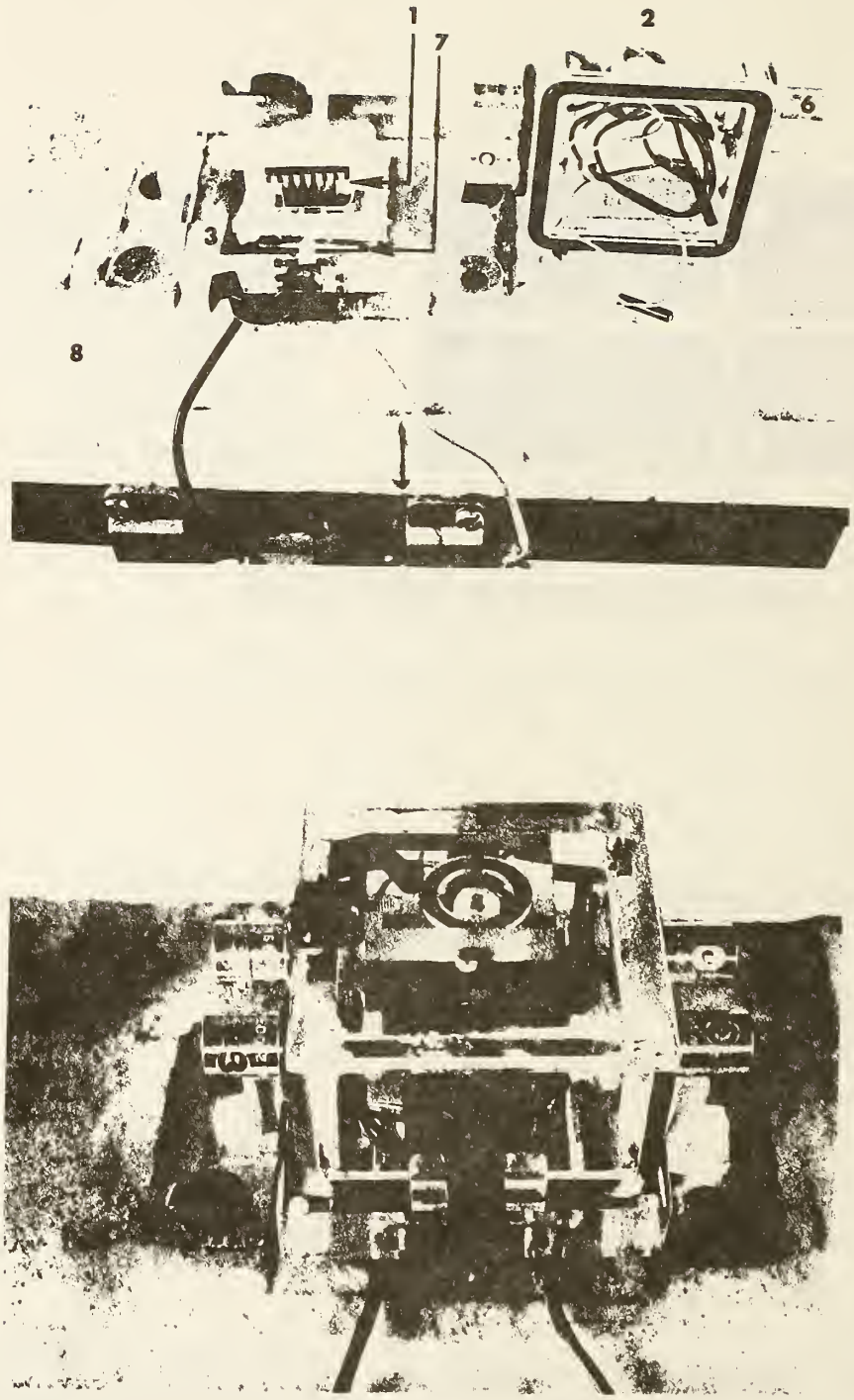

FIGURE 7 - SET UP FOR VARIOUS MOISTURE MEASUREMENT METHODS INSIDE THE ENVIRONMENTAL CHAMBER

3.7 LASER SPECTROMETRIC DETERMINATION OF MOISTURE

John A. Mucha

AT&T Bell Laboratories
Murray Hill, New Jersey 07974
(201) 582-3659

ABSTRACT

Derivative infrared diode laser spectrometry has been used for the rapid and precise ($\pm$ 50 ppm_v) determination of trace ($\geqslant$ 50 ppm_v) moisture in small (10-100 μL) samples of gas as they expand into an evacuated absorption cell. Adsorption/desorption of the analyte is the most serious potential source of error in the measurement; however, the application of time-resolved (resolution $\leqslant$ 10 msec) techniques permits accurate analyses in the presence of these dynamic processes. The experimental method and a simple model which accurately reproduces the concentration-time behavior observed during analysis are presented which permits the analyst to ensure the accuracy of any given measurement or detect and correct erroneous ones. The method has been applied to the determination of moisture in hermetically sealed integrated circuit (IC) packages and is shown to be capable of determining both gaseous and adsorbed moisture within the sample. Results for the packages sealed under controlled moisture conditions exhibit large discrepancies when compared to those obtained by mass spectrometry. Potential sources of the deviations are discussed along with advantages of this new method for IC moisture measurements.

INTRODUCTION

In this age of miniaturization, analysts are being pressed to develop new methods and tools with sufficient sensitivity to analyze smaller and smaller samples. Nowhere is this more true than in the microcircuit industry where the establishment of reasonable specifications for moisture in hermetic integrated circuit packages has been hampered by the inability to accurately and reliably make the measurement. For the past 10-15 years mass spectrometry has been the method most widely used [1]; however, its history has been checkered by lack of agreement and correlation between laboratories [2,3]. This is not so surprising when one considers that the volume enclosed within a memory device package typically contains between 0.01 $atm \cdot cm^3$ and 0.1 $atm \cdot cm^3$ of gas which at a typical moisture specification level (5000 ppm_v) contains an amount of moisture that would form monolayer coverage of a few (3-10) cm^2 of surface. Since the surface area of most laboratory apparatuses into which the sample is injected are generally an order of magnitude or more greater (i.e., several hundred cm^2), accuracy is limited by adsorption and desorption phenomena associated with the sampling process.

Here, we report a new method [4] for the determination of moisture in hermetically sealed integrated circuit packages using a derivative infrared diode laser spectrometer. Because of the high resolution ($\sim$0.001 cm^{-1}) and sensitivity of the instrumentation, trace analyses can be made on small volumes of gases with high selectivity. Furthermore, the time resolution ($\sim$0.01 sec) capabilities allow a complete history of the adsorption/desorption dynamics to be obtained in such a way that the analytical accuracy of results for each sample can be verified.

EXPERIMENTAL

A commercial Spectra Physics (Laser Analytics Division) semiconductor diode laser spectrometer was used for the studies presented here. Injection current modulation at 1 kHz was employed for derivative detection of water vapor spectra and the basic instrument has been modified for line locking. The modified spectrometer and a more detailed description of the gas handling and vacuum systems has been published elsewhere [5]. As before, the Pb $S_{1-x}Se_x$ diode laser was locked to the $2_{12} \leftarrow 1_{01}$ transition of water vapor at 1653.29 cm^{-1} and second harmonic detection was employed to detect the second derivative of sample absorption.

Additional modifications [4] were made to the spectrometer and sample cell in order to make the system suitable for the analysis of small volumes of gases. The time constant on the lock-in amplifier used for sample detection was

reduced to 3-10 msec in order to accurately monitor the time dependence of water vapor in the sample cell during analysis. The output of the lock-in amplifier indicating sample absorption was continuously monitored as a function of time using a chart recorder and microcomputer.

The most extensive modifications were those made to the 16 cm Pyrex sample cell in order to calibrate the instrument and open the integrated circuit (IC) packages for analysis. A diagram of the modified sample cell is shown in Figure 1. The calibration arm shown in the upper right portion of the figure contained a leak valve and small (55 μL) simulator volume for continuous and grab sampling, respectively, of a flowing standard water vapor mixture. The simulator volume, equilibrated with the standard (nominally 3000 ppm H_2O in N_2) under flow conditions, provided a convenient method for obtaining fresh (age < 100 msec) samples of known composition for elucidating the kinetics of the analytical method. In addition, the accuracy could be verified by direct comparison to results obtained using the leak valve to admit a continuous flow of standard at an identical pressure as that observed for the simulator.

The center arm of the sample cell contained a device for opening the IC packages and an MKS Baratron capacitance manometer for pressure measurements. The whole opener assembly was wrapped with heating wire and insulated. In this way the samples could be analyzed at any temperature while other parts of the system (cell, calibration arm, and pressure transducer) remained at room temperature.

The basic procedure consisted of evacuating the cell to the base pressure ($4 \times 10^{-6} - 1 \times 10^{-5}$ Torr), isolating the cell from the vacuum pumps and monitoring moisture as a function of time before and after the contents of the simulator volume or packages were released. The second-derivative signal which had been previously calibrated in units of absolute partial pressure of moisture (using continuous flows of standard at known pressures) along with total pressure measurements were sufficient to determine the moisture composition in the cell at any time.

MEASUREMENTS WITH THE SIMULATOR VOLUME

Because of the unique design of the calibration arm it is possible to make a direct comparison of measurements on the same gas as a small parcel in a closed system and as a continuous flow at steady state conditions in an open system. One such comparison is shown in Figure 2 for a moisture standard containing 3200 ppm_v H_2O at room temperature. The solid curve represents the experimental time dependence of the calibrated second derivative infrared signal when the contents of the simulator volume are released (t=0) into the sealed-off cell. In this instance the cell was isolated from the vacuum pumps 13 sec before the release and in the interim, a noticeable increase in the signal is observed due to desorption of residual moisture from the cell walls until a stable equilibrium is achieved. The amount of moisture desorbed depends, of course, on the previous history of cell with respect to previous exposures to moisture and the duration of evacuation between experiments. Usually, at room temperature it is relatively easy to obtain an insignificant amount of desorption by pumping the cell for several minutes between releases after an initial pump-down of several hours. However, as will be shown later, the presence of desorption in no way limits the experimental accuracy and pump down procedures do not have to be stringently controlled.

Opening the simulator volume (t=0) produces a dramatic, transient increase (T) in the moisture content of the cell which is followed by a rapid decay as moisture adsorbs to the surfaces of the system. After a period of time (40-50 sec) a new final equilibrium level is observed corresponding to (in this instance) ~75% of the moisture content of the simulator volume on the walls of the system at the end of the experiment.

One might be tempted to use the final equilibrium moisture content for analytical purposes; however, such an approach requires carefully prescribed evacuation cycles to ensure reproducible moisture sorption on the walls of the analytical system. This was judged to be too cumbersome for practical analyses.

The logical alternative then is to use the transient observed at opening for analyses. The accuracy of this approach can be determined using a continuous flow of standard at the same pressure as that noted for the parcel (0.229 Torr). Since we are dealing with trace analysis where the bulk of the sample gas (N_2 or air) is non-adsorbing, the final pressure is an accurate (usually ± 1%) indicator of the total amount of gas in the sample. The dashed line at the top of Figure 2 represents the experimentally observed steady-state signal amplitude when a continuous flow of standard is passed through the cell at 0.229 Torr. As can be seen the steady-state signal amplitude (CF) is identical to the transient signal (T). Thus, the transient is not only an accurate indicator of moisture content, but also is an exact replicate of the standard with no interference or error due to adsorption or desorption. Of course, this

condition is only present for a brief period of time and the ability to achieve this condition depends critically on the dynamics of the ongoing processes in the closed system.

KINETIC MODEL

The fact that the transient signal exactly matches the continuous flow signal is a very gratifying circumstance; however, such an observation places severe restrictions on the interplay of the dynamic processes which are an integral part of the analysis. To gain some insight into these restrictions and to establish guidelines for ensuring analytical accuracy, a simple model has been constructed based on a series of first-order processes. Consider the simple sequence of steps

$$A \xrightarrow{k_1} B \underset{k_{-2}}{\overset{k_2}{\rightleftarrows}} C \qquad (1)$$

as a representation of the microvolume sampling process. Here A represents gaseous moisture in a sample at atmospheric pressure; B is gas phase moisture in the cell at reduced pressure; and C is moisture on the walls of the cell. The rate constants k_1, k_2, and k_{-2} are first-order rate constants associated with sample opening and expansion into vacuum, adsorption, and desorption, respectively. As noted previously, the amount of moisture in a typical sample is sufficient for monolayer coverage of only a few cm^2 of the 625 cm^2 surface area of the system. Furthermore, in a cell evacuated to between 2×10^{-5} and 5×10^{-6} Torr a simple calculation based on the kinetic theory of gases [6] indicates the surface coverage due to physical adsorption is on the order of 2×10^{-3} to .04 monolayers prior to introduction of the sample. As a result, desorption and adsorption (the second step of eq. (1)) are likely to be nearly first-order processes since the surface coverage by analyte before and after sample introduction will remain small. The use of first-order kinetics to describe the first step is tenuous since the expansion of gas into the cell is a flow problem varying continuously from turbulent to transitional flow complicated by diffusion through connection tubes. Its justification rests solely on the simplicity of the resulting model and the ability to fit experimental data relatively accurately.

The general equations for the time dependence of the concentration of each species for the above kinetic model were given by Rakowski [7]. Here we are only interested in the temporal behavior of B, the analyte in the gas phase after opening, since it is the only measurable quantity. We desire to know under what conditions B_{max}, the maximum concentration detected (more specifically the difference between the observed maximum and moisture level immediately prior to opening, B_o), approaches A_o, the concentration of moisture in the original sample (i.e., $(B_{max}-B_o)/A_o \rightarrow 1$).

The simplest cases occur when the initial concentrations B_o and C_o are either zero or represent an equilibrium situation ($B_o/C_o = K^{-1}$, $K = k_2/k_{-2}$). For these cases the time dependence of B normalized to A_o is given by

$$\frac{B(t)-B_o}{A_o} = \left(\frac{k_2}{k_2+k_{-2}}\right)\left[1 + \frac{k_1(k_2+k_{-2})e^{-(k_2+k_{-2})t}}{k_2 + k_{-2} - k_1}\left\{\frac{(k_1-k_{-2})(k_2+k_{-2})}{k_1k_2}\, e^{-[k_1-(k_2+k_{-2})]t} - 1\right\}\right] \qquad (2)$$

Locating the maximum is simply a matter of differentiating eq. (2) with respect to time and leads to the time to reach a maximum concentration,

$$t_{max} = \frac{\ln[(k_1-k_{-2})/k_2]}{k_1-(k_2+k_{-2})} \qquad (3)$$

with that concentration given by

$$\frac{B_{max}-B_o}{A_o} = \left(\frac{1}{1+K}\right)\left[1 + K\, e^{-(k_2+k_{-2})t_{max}}\right] \tag{4}$$

Similarly, at long times eq. (2) yields the equilibrium concentration

$$\frac{B_{eq}-B_o}{A_o} = \frac{1}{1+K} \tag{5}$$

which by experimental observations permits the analyst to obtain the ratio k_2/k_{-2} (=K) directly. Examination of eq. (3) indicates that a maximum will always be observed when $k_1 > k_{-2}$.

Since most of the analyses of packages and simulator volumes exhibit a time dependence like that shown in Figure 2, eqs. (3) and (4) are most useful for assessing the analytical accuracy of using the transient signal. One can arbitrarily choose relative rate constants for the system dynamics and determine the effect on $(B_{max}-B_o)/A_o$. Figure 3 shows one appropriate representation of the results of such a procedure. Here the transient observed concentration $(B_{max}-B_o)$ relative to the true sample concentration (A_o) is presented as a function of the relative rate constants of opening and expansion to adsorption (k_1/k_2) for several different overall cell adsorption characteristics governed by the equilibrium constant, K. When K is small the cell is essentially non-adsorbing and large values of K refer to strongly adsorbing walls. Solid lines indicate conditions for which a concentration maximum is observed while dashed lines indicate no detectable maximum—only a rise in concentration to the equilibrium level (i.e., $k_1 < k_{-2}$). First one sees that when $k_1/k_2 \geq 100$, the transient signal and thereby the detected concentration is always within 5% of the true value regardless of the adsorption characteristics of the cell. Second, when a maximum is observed experimentally the determined concentration can never exceed the true value. Thus, the absolute accuracy of any given measurement can be determined by obtaining K and the relative rate constant k_1/k_2. In most cases, k_1/k_2 is sufficient. Since the time history has been recorded for both standard and sample such a determination can be made by computer simulations using eq. (2) and judicious choices of the three system rate constants.

The use of Figure 3 to assess and accurately correct errors in analysis rests on the validity of the model in describing the system dynamics and experimentally achieving the initial constraints ($B_o=C_o=0$ or $B_o/C_o=K^{-1}$) imposed previously. Since the analyst can monitor moisture prior to opening the sample or simulator volume to the system, he can easily determine that the latter does indeed apply. Actually, this constraint can be relaxed by modifying the model slightly to include desorption prior to opening the sample. This simply requires that one allows the second step in process (1) to proceed with $C_o \neq 0$ for the period of time from when the cell is isolated from the vacuum pumps until the sample is opened. For the case $C_o \neq 0$ and $B_o = 0$ (no gas phase moisture detectable during active evacuation) the return to equilibrium when pumping is terminated should be first order with an effective rate constant (k_2+k_{-2}). Thus, one can model the whole time dependence from the time the cell is sealed until equilibrium is established after the sample is introduced.

This provides a very important test for the validity of the model in describing the dynamics of the system. Based on the initial model presented one knows that since the transient signal is identical to the flow signal, $k_1 \gg k_2$. Furthermore, as observed in Figure 2 the cell is strongly adsorptive, $k_2 \gg k_{-2}$. This suggests that $k_1 \gg (k_2+k_{-2})$. Thus, desorption before introducing a sample and adsorption after should obey the same kinetics if the model is a reasonable representation of the dynamics of the system. The dots in Figure 2 are a theoretical fit to the data which confirms the validity of the model.

This fit was obtained using the rate constants $k_1=75\ s^{-1}$, $k_2=0.25\ s^{-1}$ and $k_{-2}=0.086\ s^{-1}$. The only other adjustable parameter was the relative amount of moisture on the walls $(C(t=-13s)/A_o)$ when the cell was sealed. This was determined in the fit to be $0.4\ A_o$. Since A_o is known for the simulator volume of standard it is a simple matter to compute the actual number of molecules of H_2O on the walls when the cell was sealed. This along with the geometric surface area of the system indicated an initial surface coverage of 0.03 which is in excellent agreement with the kinetic theory surface coverage noted earlier for a cell at 10^{-5} Torr.

A noticeable deviation between experiment and theory is present during the decay in Figure 2; however, this deviation is only 10%. Observations of numerous decays following the release of standard gases (concentrations from

1000 to 10,000 ppm_v) into the cell have indicated that the decay is actually bi-exponential with the two decay constants differing by approximately an order of magnitude. This is not surprising considering that metal and glass are present in the system and would likely exhibit different adsorption characteristics. The ability to obtain as good a fit as that shown is Figure 2 speaks well for the model chosen to represent the system. In addition, initial decay rates observed for the first 0.5 sec of the decay were accurately first order (±5%) for the above concentration range.

APPLICATIONS OF THE MODEL

In practice, we are more concerned with the few seconds in time before and after the sample is opened for establishing the accuracy of any given measurement. Extensive measurements on releases of the simulator volume over a year and a half have indicated that k_2=0.5 ± 0.1 s^{-1} and k_{-2}=0.05 ± .02 s^{-1} provide an excellent fit (±2%) to this critical portion of the analytical time dependence. It should be noted that these two rate constants represent properties of the cell and are relatively invariant for any analysis (so long as modifications to the system are not made). Since opening an IC package involves a mechanical device and an operator, it is likely to exhibit some variability. Therefore, one cannot arbitrarily assume that k_1 for a sample will be the same as k_1 (75 ± 15 s^{-1}) for releasing the simulator contents. Determining k_1 for a sample is simply a matter of measuring t_{max} using the high resolution time data stored in the microcomputer and eq. (3). From the ratio k_1/k_2 and Figure 3 (a more extensive grid for K values can be computed) corrections can be applied to samples which are not opened rapidly enough to satisfy the condition $k_1 >> k_2$. Rise times observed for typical samples using our opening procedure were typically 111 ± 22 msec compared to 66 ± 10 msec for releases from the simulator volume. This indicates that concentrations obtained for samples are likely to be lower than the true values. For the worst case t_{max} = 133 msec, k_1/k_2 = 60 indicating the maximum error to be less than 7%. The important conclusion here is that based on measurements of k_1 for the simulator volume, moisture detected in the cell is always within 3% of the true value established by continuous flow calibration and simulator volume releases can be used by themselves to calibrate the instrument. However, simulator volume releases *cannot* calibrate the kinetics of sample opening. Fortunately, the method of opening packages here is adequate for accuracy to within 5%. More importantly it is correctable.

Although the discussion of this type of error has relied heavily on real samples where the sample concentration is unknown, it is possible to conduct experiments using the simulator volume and continuous flow standards to test the ability of using the model to correct experimental results. For example, increasing the time constant of the detection electronics to 1 sec artificially changed k_1 and yielded a transient signal less than 50% of the continuous flow signal. From the observed t_{max}, k_1 was accurately determined to be the reciprocal of the lock-in time constant (12 dB roll-off) and data correction using Figure 3 retrieved the continuous flow signal value to within 2%. Similarly, by installing a wax plug with a 90 μm hole in the bore of the simulator volume an initial error of 17% (continuous flow *vs* transient) was observed; however, rate constants were easily extracted and results were correctable to better than 1%.

SENSITIVITY AND REPRODUCIBILITY

Figure 4 shows the time dependence for the analysis of a 0.066 atm·cm^3 sample of gas containing 325 ppm_v moisture. Based on the signal-to-noise ratio observed, the detection limit (S/N=1) corresponds to approximately 2 ppm_v per atm·cm^3 sample of gas. Noting that the detection limit scales linearly with the volume to path-length ratio (V_c/b) of the cell, a general detection limit of

$$\text{D.L. (ppm)} = 0.2\ (V_c/b)\ (P_sV_s)^{-1} \qquad (6)$$

should be applicable to any system when derivative diode laser spectroscopy is used for the determination of moisture in samples containing P_sV_s atm·cm^3 of gas. The apparent noise in Figure 4 is quite regular and is associated with optical interferences due to vibration (3 Hz) of the laser in the cold head of the closed cycle refrigerator used to control the temperature of the laser. Improved vibration isolation is available [8] which should virtually eliminate this problem and reduce detection limits correspondingly. This and incorporating an optimized cell (smaller V_c/b) are likely to increase sensitivity by at least two orders of magnitude.

Measurements on simulator volumes of standard are exceptionally reproducible. Over a typical 8 hr. period (see Figure 5) precision was found to be on the order of 1.5% (Rel. Std. Dev.) for a 3100 ppm_v standard.

COMPARISON WITH MASS SPECTROMETRY

Table I shows the results [9] for TO-18 packages tested as part of a recent Method 1018.2 recertification program. The mass spectrometric (MS) results (columns 2-5) are seen to exhibit generally good agreement with each other and the target values for the test packages. The infrared (IR) results at 25°C also agree well; however, IR analyses at 100°C (the ones that should agree) indicate much higher moisture contents — well above statistical variations. It is not surprising the 25°C IR analyses are in reasonable agreement with target values since the test packages were equilibrated and sealed at approximately this temperature. The higher results at 100°C are not surprising either since one would anticipate an equilibrium amount of moisture to be present on internal package surfaces. This moisture goes undetected at room temperature since desorption is a much slower process than expansion of the gas into the IR cell. At 100°C the equilibrium within the package shifts strongly to favor desorption of surface moisture and the IR analyses give the new total gaseous moisture (original surface & original gaseous).

On the other hand, internal correlation studies [10] on Western Electric production packages and controlled packages prepared by the methods of White and Sammons [11] have consistently exhibited agreement between the IR method and the MS spectrometric method employed at Bell Labs/Allentown [12]. These studies do indicate that the MS and IR methods can agree quantitatively and that the observed discrepancies in Table I are either due to an accelerated aging effect [9] that perturbs the moisture content of the package or a systematic error in the MS results.

The former interpretation [9] has merit since all analyses of these packages made nine or more months after the original certification study were in agreement with the 100°C IR data. These subsequent results included MS data from RADC which disagreed with the IR data originally and Bell Labs/Allentown which has always been in agreement with the IR data. Since the IR results were obtained on packages that were at temperature for more than an hour longer than those of the MS studies a thermally accelerated aging effect cannot be ruled out. However, the possibility of a systematic error in the MS data cannot be overlooked either. Simple calculations [6] of the moisture that might be anticipated on the internal surfaces ($\sim$0.4 cm^2) of the TO-18 packages indicates that multilayer adsorption is expected, even for packages sealed at the lowest concentration (1000 ppm). Furthermore, only five monolayers are required to explain the largest discrepancy observed. This quantity of moisture is not unlikely based on experimental studies [13] of physisorption of moisture on package materials. Thus, concentrations considerably higher than the target values are quite likely at an analysis temperature of 100°C. Model calculations on the MS method, similar to those presented earlier for the IR method, were carried out in order to gain some insight into systematic error as a possible origin of the observed discrepancies. Using such an approach, two possibilities were identified that could lead to errors in the MS data of the correct direction and magnitude. First, if the package opening procedure leads to a mass transport rate out of the package that is comparable to the transport rate into the ionization chamber, then burst mode calibration will fail to adequately "calibrate" the dynamics of the MS mass transport. This would certainly make MS results based on "peak" measurements systematically low; however, it should not effect integrated measurements unless background moisture levels are comparable to that detected for the package. Second, if mass transport between the antechamber and ionization chamber is rate limiting, there may be sufficient time for moisture to desorb from the walls of the 3-volume calibrator and be included in the calibration measurement. This additional moisture would have the net effect of reducing the apparent moisture content of a package for both "peak" and integrated MS determinations. Although, such modeling is by no means exact, it does suggest areas for closer scrutiny of the MS procedures.

CONCLUSIONS

A rapid and accurate analytical method utilizing derivative infrared diode laser spectrometry has been demonstrated for the determination of trace moisture in small volumes of gases which are opened to a larger, adsorbing analysis system. Since its inception time-resolved determinations of moisture using the diode laser spectrometer have never been in error by more than 5% based on a kinetic analysis of the data.

For the analysis of moisture in hermetic integrated circuit packages the infrared method offers a superior alternative to MIL-STD Method 1018.2 based on mass spectrometry. In addition to higher sensitivity and precision, the time-resolved method is highly insensitive to the moisture exposure history of the system walls and does not require cumbersome procedures for evacuating and conditioning that are inherent to the mass spectrometric determinations. The sample throughput of the laboratory instrument demonstrated here (50 packages per day) is almost a factor of two greater than that by the MIL-STD Method and should easily scale to a system capable of analyzing several hundred per day. Furthermore, since it is not necessary to heat the walls of the analytical system it is possible to study the effects of temperature on the sample package. By comparing results on representative samples at room temperature and 100°C one can estimate the amount of moisture on the internal surfaces of the package. This quantity is probably more important in assessing moisture effects on IC reliability. Since failure modes such as corrosion and current leakage are likely to involve ion mobility through a fluid surface medium (H_2O) the amount of moisture on surfaces is an extremely important piece of information.

REFERENCES

1. Thomas, R. W., IEEE Trans., Parts, Hybrids and Packaging, *1976*, PHP-12, 176.
2. Thomas, R. W. and Meyer, D. E., Solid State Tech., *1974*, 17 (9), 56.
3. Perkins, K. L., in "Semiconductor Measurement Technology: ARPA/NBS Workshop V, Moisture Measurement Technology For Hermetic Semiconductor Devices", H. A. Schafft, S. Ruthberg, and E. C. Cohen, eds. (NBS Spec Pub 400-69, 1981) p. 58.
4. Bossard, P. R. and Mucha, J. A., IEEE Proceedings of the 19th Annual International Reliability Physics Symposium, *1981*, p. 60.
5. Mucha, J. A., Appl. Spectrosc., *1982*, 36, 393.
6. Robinson, N. W., "The Physical Principles of Ultra-high Vacuum Systems and Equipment" Chapman and Hall Ltd: London, 1968; Chapter 7.
7. Rakowski, A., Zeit für Physik. Chemie *1907*, 57, 321.
8. Spectra Physics, Laser Analytics Division, Bedford, MA 01730.
9. Moore, B. A., IEEE Proceedings of the 21st Annual International Reliability Physics Symposium, *1983*.
10. White, M. L., Mucha, J. A. and Angst, D. L., unpublished results, 1981.
11. White, M. L. and Sammons, R. E., "NBS/RADC Workshop: Moisture Measurement Technology for Hermetic Semiconductor Devices, II", NBS Spec. Publ. 400-72, p. 49 (April, 1982).
12. Although most of the results are unpublished a general idea of the level of correlation can be gain by comparing refs 4, 11 and Gale, R. J., "NBS/RADC Workshop: Moisture Measurement Technology for Hermetic Semiconductor Devices, II", NBS Spec. Publ. 400-72, p. 19 (April, 1982).
13. Ammons, J. M., Hoff, G. R. and Kovac, M. G., "The Physisorption of Water onto Integrated Circuit Package Components," this monograph.

Table 1: Results* of R.A.D.C. TO-18 Round Robin (December, 1981)

	-MASS SPEC. AT 100 °C-				-INFRARED-	
TARGET	RADC	LAB 1	LAB 2	LAB 3	100°C	25°C
1000	2663	2800	1981	3067	5420	2639
3000	4535	5730	3317	8690	8630	3724
5200	5327	5670	5631	4453	10,250	4753
6000	6040	7800	5417	6676	12,257	5460
10,000	10,060	9900	8301	9170	14,220	8897

** All values in ppm by volume moisture*

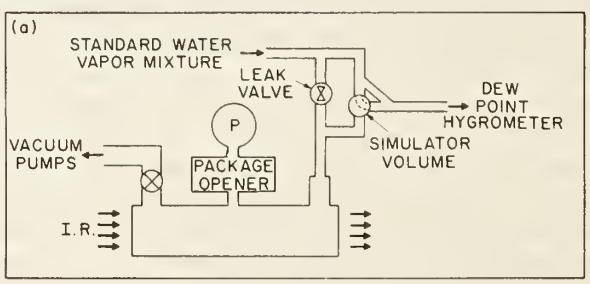

Figure 1: Infrared sample chamber.

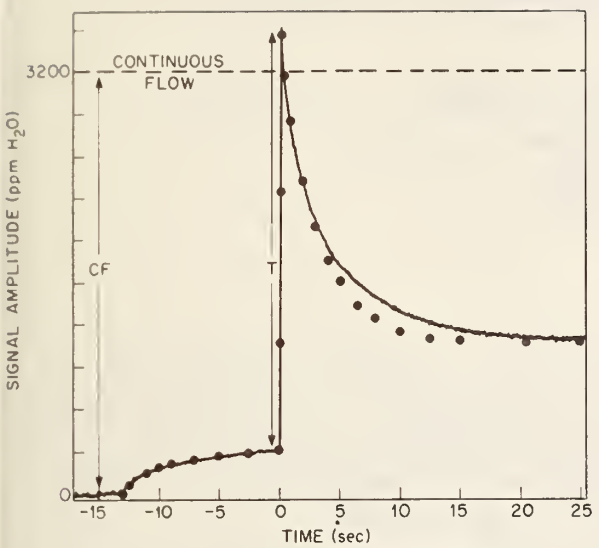

Figure 2: Time dependences for a simulator volume release (——) and continuous flow (– – –) of standard along with theoretical fit (•) to the data.

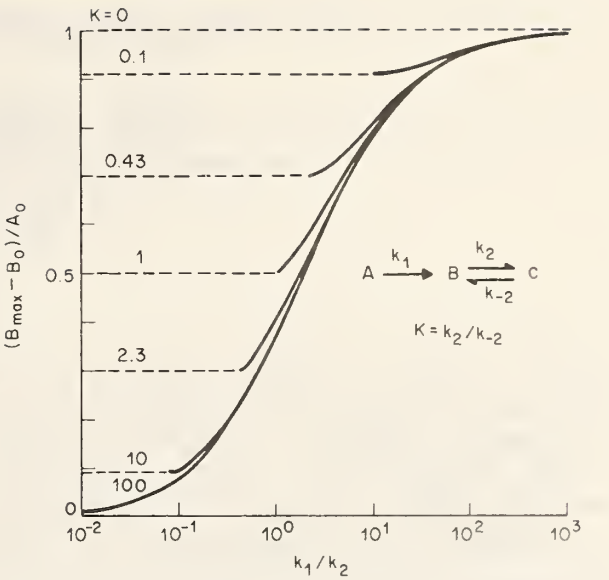

Figure 3: Relative kinetic parameters for assessing analytical accuracy.

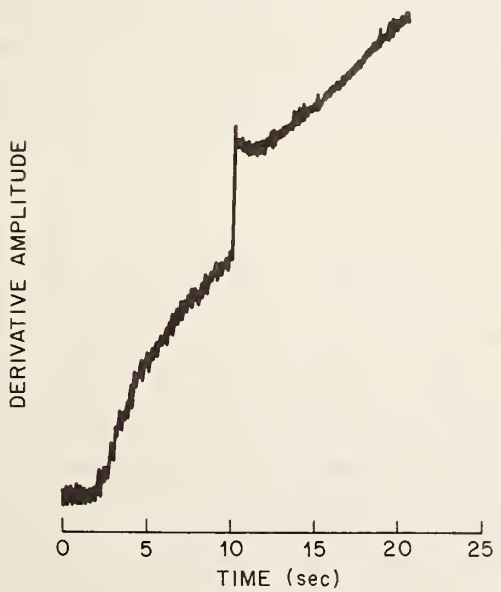

Figure 4: Time dependence for the analysis of an IC package containing 325 ppm moisture.

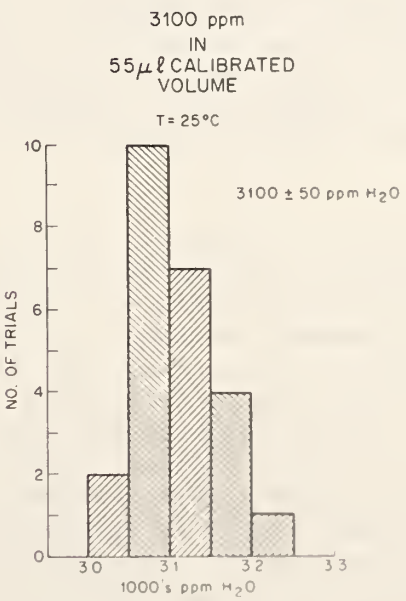

Figure 5: Typical reproducibility over an 8 hr period. Data includes variations in instrumental sensitivity due to laser retuning and variations in LiCl bubbler standard due to minor changes in room temperature.

3.8 TOTAL WATER MEASUREMENT EQUIPMENT AND PROCESS USING METHOD 1018, PROCEDURE 2

Craig Sloneker and Bruce Church
Medtronic, Inc.
6951 Central Avenue
Minneapolis, MN 55432
(612) 574-4761

ABSTRACT

Several systems are currently used for the determination of total water content of a hermetic package. Each has its advantages and disadvantages. The analysis sytem to be presented was originally designed and developed, observing Method 1018 of MIL-STD-883B, to provide a flexible, economical method of determining water content of implantable pulse generators (pacemakers) for process control.

Unique features of this water analyzer include its ability to accommodate various package sizes and perform an analysis with little technical attention.

Typical operational procedures for sample runs, calibration of the instrument, and equipment description with a descriptive layout will be presented. Both assets and drawbacks of this system will be discussed in an attempt to provide the audience with enough information to assess whether this would be a viable moisture measurement technique for their process applications.

4. SESSION III MOISTURE SENSORS

4.1 FUNDAMENTAL STUDIES OF THE AGING MECHANISM IN ALUMINUM OXIDE THIN FILMS

Chen-Hsi Lin and Stephen D. Senturia
Department of Electrical Engineering and Computer Science, and
Center for Materials Science and Engineering
Massachusetts Institute of Technology
Cambridge, MA 02139

ABSTRACT

This paper reports the results of electrical and infrared studies of aging mechanisms in hydrated aluminum oxide films of the type typically found in aluminum oxide moisture sensors. Three distinct components of the water of hydration are identified, referred to as "physisorbed", "chemisorbed", and "fixed". The physisorbed component adsorbs and desorbs reversibly at room temperature. Furthermore, presence of the physisorbed layer is found to enhance the aging rate at room temperature. The direction of aging is such as to indicate successively lower apparent moisture levels. Isotope exchange experiments show that the chemisorbed component is stable in dry room temperature ambients, but exchanges rapidly with the physisorbed layer in moist ambient. Annealing studies show that the fixed component is stable up to 250°C, above which a gradual phase transition of the hydrated oxide from pseudoboehmite to an α-alumina phase is observed. This result suggests that exposure of aluminum oxide moisture sensors to eutectic die attach and Cerdip sealing temperatures should be expected to produce an irreversible shift in moisture sensor characteristics.

INTRODUCTION

The use of thin porous hydrated aluminum oxide films for moisture measurement inside integrated circuit packages is well known [1]. Difficulties in maintaining device calibration during die attach and packaging operations [2] and long-term stability and hysteresis problems have been reported [3,4]. This paper reports results of a research program directed toward a fundamental understanding of the physical mechanisms that may be responsible for such phenomena as aging and hysteresis [5].

In typical aluminum oxide moisture sensors, the moisture-sensitive aluminum oxide (referred to as "AlOx" hereafter) is formed by aqueous anodization or hydration of a planar aluminum electrode, followed by the deposition of a porous gold upper electrode to make a parallel-plate capacitor structure. Moisture induced variation of the electrical conduction on the surfaces of the AlOx grains (and possibly in microcapillary-condensed water between the grains) gives rise to an effective interelectrode capacitance that increases with increasing ambient moisture. In order to eliminate any possible role of the gold upper electrode in our studies, all of the research reported here was done using characterization methods in which no upper electrode is required. These include measurement at low frequencies of the AC sheet resistance of the AlOx film using the charge-flow transistor [6], and infrared reflectance-transmission spectroscopy of the AlOx film in conjunction with D_2O–H_2O isotope exchange techniques. Film properties were studied as functions of time after preparation, and after a sequence of low- and high-temperature anneals.

EXPERIMENTAL METHODS

Sample Preparation

The AlOx films were formed by the standard technique of immersing an aluminum layer into boiling deionized water [7]. Substrates consisted of (1) silicon wafers, some with only a thermal oxide on them, others with complete charge-flow transistor devices fabricated in them. Pure aluminum (.99995) was deposited in a tungsten-filament evaporator, in thicknesses ranging from 50-150 nm for electrical studies to 1-1.5μm for infrared studies. The electrical samples were completely converted to AlOx, with an increase in thickness to 100-300nm, while the infrared samples were converted only part of the way, leaving some aluminum to serve as a reflector. Figure 1 illustrates the difference between (a) conventional samples, (b) our CFT samples, and (c) infrared samples. SEM, TEM, and X-ray diffraction studies revealed the structural and morphological characteristics of pseudoboehmite, which is similar to boehmite, AlO(OH), but with additional hydration, as reported by Sun, et. al. [8].

Electrical Measurements

The electrical properties were measured in the range 1-4000 Hz with charge-flow-transistor (CFT) devices, as described by Davidson and Senturia [9]. Using this technique, the AC sheet resistance of the film, R_S, can be determined with an accuracy of ±5% in the range 10^9-10^{17} ohms/square. During measurement, the device is kept at room temperature, typically 22-24°C, and in a chamber through which a dew-point-controlled air stream flows, as monitored by a General Eastern dew point hygrometer.

Infrared Measurements

A dispersive double-beam Beckman spectrometer was used for infrared measurements, with samples mounted on a 60° reflection accessory. Since the samples consist of AlOx on aluminum, the infrared beam passes through the AlOx film, is reflected by the aluminum, and passes again through the AlOx film, producing, in effect, a transmission spectrum. The sample was housed in a dew-point-controlled cell during measurement, nominally at room temperature, but actually at about 30°C due to infrared-beam heating.

Sample Aging and Annealing

Following preparation and between experiments, samples were generally stored in clean, closed wafer holders in normal lab ambient (22-24°C, and nominal 40% R.H.). Some samples were stored in nitrogen dry boxes. Room temperature "aging" refers to the results of periodic observations of electrical and infrared properties of samples stored either under lab ambient or dry nitrogen conditions. Annealing experiments of two types were performed. Low-temperature ($T \lesssim 250°C$) anneals were done by placing the samples in an air-ambient lab oven for intervals of 10 or 20 minutes, returning the sample to room temperature for characterization measurements. High-temperature anneals ($T \gtrsim 250°C$) were also done in an air-ambient oven, but for intervals as long as several hours.

RESULTS

Sheet Resistance Variation with Ambient Moisture

The room temperature sheet resistances of freshly prepared AlOx films vary by six orders of magnitude as the ambient dew point changes from −55 to +20°C, an agreement with earlier work [3]. An approximately linear relationship is observed between log R_S and dew point, both for aged and annealed samples. Typical data for two cases are shown in Figure 2. The major effect of aging and annealing (except for a few cases of annealing in a temperature-humidity chamber at high R.H.) is to shift the entire curve upward, which would correspond in a sensor to a shift of calibration toward lower apparent moisture level, consistent with reported results [2]. For purposes of following the aging and annealing processes, the measured R_S at a 10°C dewpoint at room temperature is used as a reference point.

Infrared Spectrum and Isotope Exchange

The infrared spectrum of a typical AlOx film (Fig. 3(a)) is characteristic of pseudoboehmite [7,10], which resembles boehmite (Fig. 3(b)), but with additional hydration. We choose to focus on the absorption peaks at 3300 and 3100 cm^{-1}, which correspond to the asymmetric ($_{as}$) and symmetric ($_{s}$b) stretching modes of the linear OH chains in boehmite [11]. Superimposed on these boehmite-like bands is a broad absorption attributable to H_2O [12]. These features can be revealed by isotope exchange with D_2O, as explained below.

By replacing the water in the dew point system with D_2O, isotope exchange reactions can be followed. The sequence of events is illustrated in Fig. 4. Immediately following preparation, the AlOx spectrum in moist ambient consists of the complete OH absorption [P(OH)+C(OH)+F(OH)] and no OD absorption. When exposed to dry ambient (dew point ≈ −45°C), the component labeled P(OH) disappears. This is the "physisorbed" component, which is fully reversible at room temperature. The C(OH) and F(OH) components (denoting "chemisorbed" and "fixed" OH, respectively), are stable at room temperature, even in dry ambients. However, when exposed to a moist D_2O ambient, the C(OH) component disappears, and the complete OD line [C(OD)+P(OD)] appears. That is, the physisorbed D_2O exchanges with the chemisorbed H_2O, producing both chemisorbed and physisorbed OD. Then, on re-exposure to dry ambient, the physisorbed OD component P(OD) disappears, but the chemisorbed OD component C(OD) remains. The cycle is reversible, in that exposure to moist H_2O ambient re-exchanges the OD spectrum back to the original total OH spectrum. The fixed component F(OH) is attributed to water of hydration within the pseudoboehmite grains.

Aging

The room temperature aging behavior of the AlOx film was monitored by periodic measurement of R_S at room temperature in a 10°C dew point (see Fig. 5). Following an incubation period of approximately 30 hours, R_S exhibited an approximately square-law increase with time, suggestive of the nucleation and growth of circular domains. Circular domains of diameter ≈5 μm were observed in many SEM photographs, but thus far, it has not been possible to demonstrate correlation between SEM observed domains and sheet resistance aging.

We observe a significant decrease in aging rate for samples stored in dry ambient, hence, samples not having the physisorbed water component (see Fig. 6). However, once exposed to a moist ambient, a very rapid increase in sheet resistance is observed. Note, in particular, the sharp increase in the solid dot data at 70

hours. This increase occurred within 30 minutes during the R_S measurement. Restoring the sample to the dry ambient did not decrease R_S; it simply restored the slower aging rate.

Annealing

Low temperature annealing ($T \leq 250°C$) consisted of a sequence of 20 minute exposures to each successively higher temperature in lab air, with the sample returned to room temperature between anneals for sheet resistance and infrared measurement. Based on the overall characteristics of the infrared spectrum, in conjunction with isotope exchange, we find that the film retains its pseudoboehmite structure during low-temperature anneals. The three water components behave differently with anneal. The physisorbed component decreases steadily with increasing annealing (Fig. 7). The chemisorbed component is stable until 120°C is reached, above which it decreases. The fixed component is stable at least to 250°C. The corresponding behavior of R_S is shown in Fig. 8. Note the increase in slope above about 120°C. The increase in R_S below 120°C is attributable to the loss of physisorbed moisture, and the additional rate of increase above 120°C suggests that the chemisorbed component does contribute somewhat to the overall moisture sensitivity of electrical properties. High temperature annealing ($T \geq 250°C$) produces a gradual loss of fixed water, and a gradual phase transformation to α-alumina, as evidenced by the infrared spectrum.

CONCLUSIONS AND DISCUSSION

There are three principal findings in this work. The first is that three distinct components of water of hydration can be observed with isotope exchange techniques, in conjunction with infrared spectroscopy. The second is that the aging rate of AlOx samples is dependent on the presence of the physisorbed component, which may actually be microcapillary condensed liquid water between the AlOx grains. The third is that the pseudoboehmite structure of the AlOx film is stable at temperatures below 250°C, but exposure to higher temperatures will produce a gradual phase transformation to α-alumina.

The primary implication of these results for the use of AlOx sensors for moisture measurement inside integrated circuit packages is in explaining the effect of high-temperature exposure that may result either from eutectic die-attach or typical Cerdip sealing processes. Such high temperature exposures can be expected to produce the irreversible shifts in device calibration during packaging that are typically observed.

ACKNOWLEDGEMENT

This work was supported in part by the Thermal Processes Division of the National Bureau of Standards under Grant NB80-DADA-1004 and by the National Science Foundation under Grant ECS-8114781. The authors wish to thank Dr. Kenneth G. Kreider and Dr. S. Hasegawa of the National Bureau of Standards, and Dr. David R. Day of MIT for their suggestions and assistance. Devices used in this work were fabricated in the MIT Microelectronics Laboratory, a Central Facility of the Center for Materials Science and Engineering, which is sponsored in part by the National Science Foundation under contract DMR-81-19295. Thanks are also due to Norman F. Sheppard for his device fabrication assistance. Some of the measurement instrumentation used in this work was purchased under NSF contract ENG-7717219 and under programs sponsored by the Office of Naval Research.

REFERENCES

1. M. G. Kovac, D. Chleck, and P. Goodman, A new moisture sensor for in-situ monitoring of sealed packages, Proc. IEEE 15th Reliability Physics Symposium, Las Vegas, April 1977, pp. 85-91.

2. M. Brizoux, J. Perdrigeat, D. Kane, and R. Gauthier, Recent evaluations of Al_2O_3 in situ moisture sensors for industrial electronic hermetic components application, Proc. Moisture Measurement and Control for Semiconductor Devices, III, Gaithersburg, MD, November, 1983, this volume.

3. S. Hasegawa, Performance characteristics of a thin-film aluminum oxide humidity sensor, Proc. 30th Electronic Components Conference, San Francisco, April, 1980, pp. 386-391.

4. M. Sze, an anodized aluminum humidity sensor, Sc.D. Thesis, Department of Chemical Engineering, Massachusetts Institute of Technology, 1970, unpublished.

5. See also C.-H. Lin and S. D. Senturia, The aging of hydrated aluminum oxide thin films, Proc. Solid State Transducers '83, Delft, June, 1983; Sensors and Actuators, in press.

6. S. L. Garverick and S. D. Senturia, An MOS device for AC measurement of surface impedance with application to moisture monitoring, IEEE Trans. Electron Devices, ED-29 (1982) 90-94.

7. W. Vedder and D. A. Vermilyea, Aluminum + water reaction, Trans. Faraday Society, 65 (1969) 561-584.

8. T. S. Sun, J. D. Venables, and J. M. Chen, Effects of surface morphology and chemical composition on the durability of adhesively bonded aluminum structure, Martin Marietta Laboratories Annual Technical Report MMR TR 80-34C, Baltimore, MD, p. 8.

9. T. M. Davidson and S. D. Senturia, The moisture dependence of the electrical sheet resistance of aluminum oxide thin films with application to integrated moisture sensors, Proc. IEEE 20th International Reliability Physics Symposium, San Diego, April, 1982, pp. 249-252.

10. R. S. Alwitt, The aluminum-water system, in Oxides and Oxide Films, Vol. 4, John W. Diggle and Ashok K. Vijh, Eds., Marcel Dekker, New York, p.169.

11. K. A. Wickersheim and G. K. Korpi, Interpretation of the infrared spectrum of boehmite, J. Chem. Physics, 42 (1965) 579-583.

12. D. Eisenberg and W. Kauzmann, The Structure and Properties of Water, Oxford, New York, 1969, p. 230.

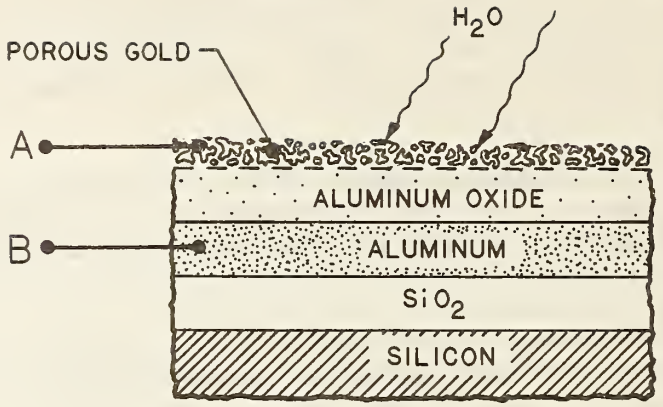

(a) CONVENTIONAL

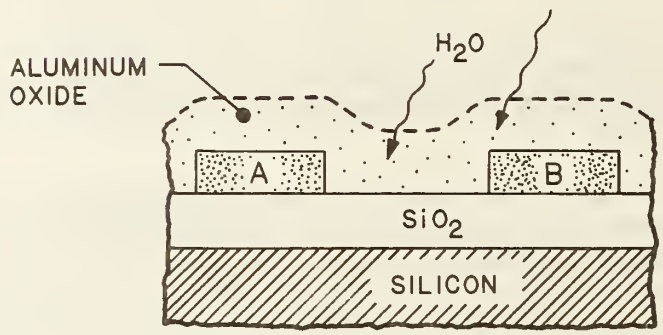

(b) CHARGE-FLOW TRANSISTOR

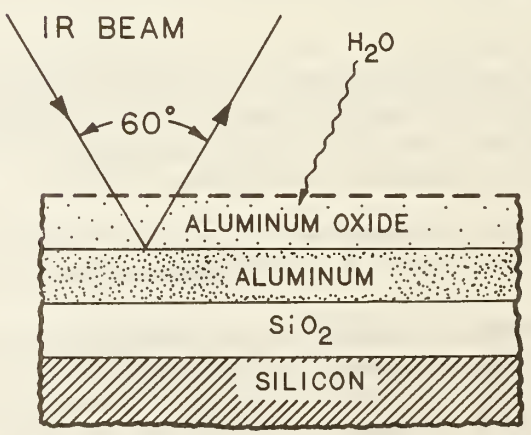

(c) INFRARED

Figure 1 Schematic illustration of the cross-sections of (a) conventional moisture sensors, (b) the CFT electrode structure, and (c) the infrared samples.

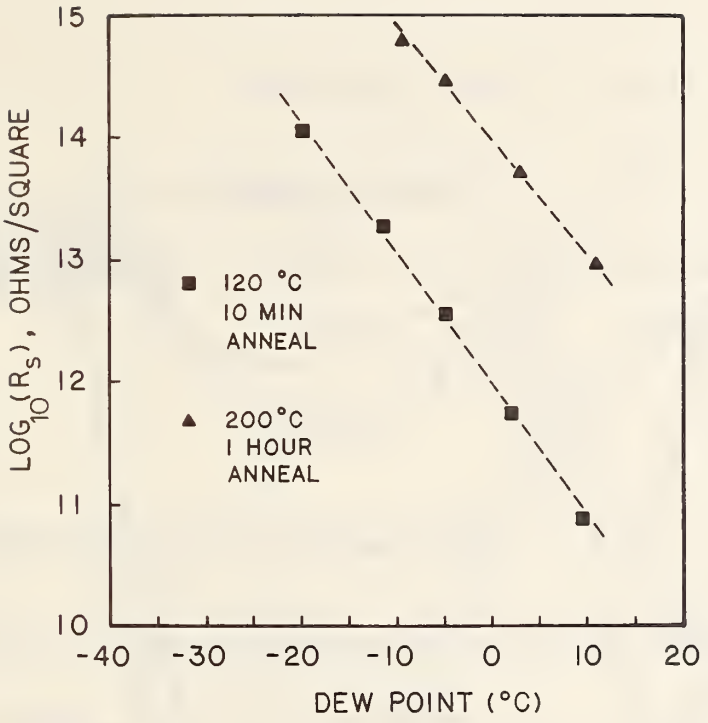

Figure 2 Sheet resistance of two annealed samples, showing the approximately linear relationship between log R_S and dew point.

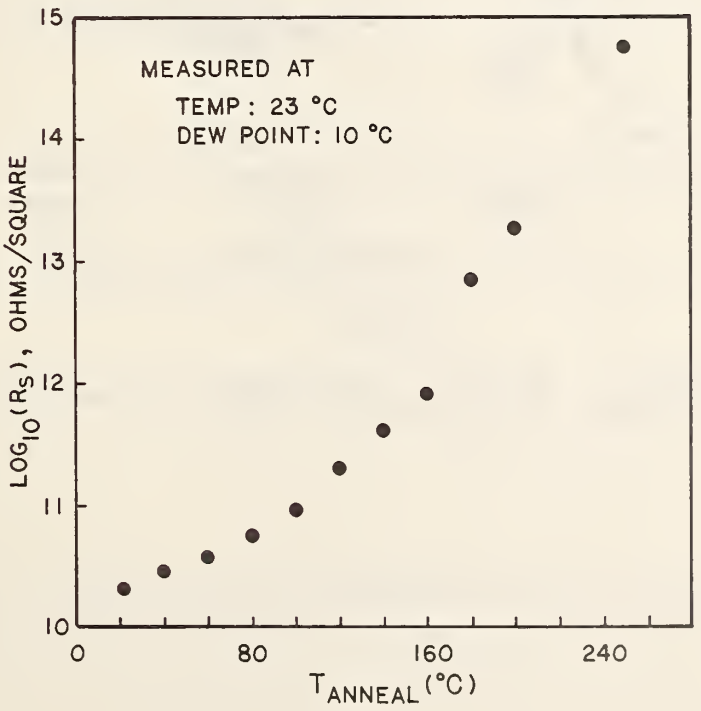

Figure 8 The low-temperature annealing effect of R_S.

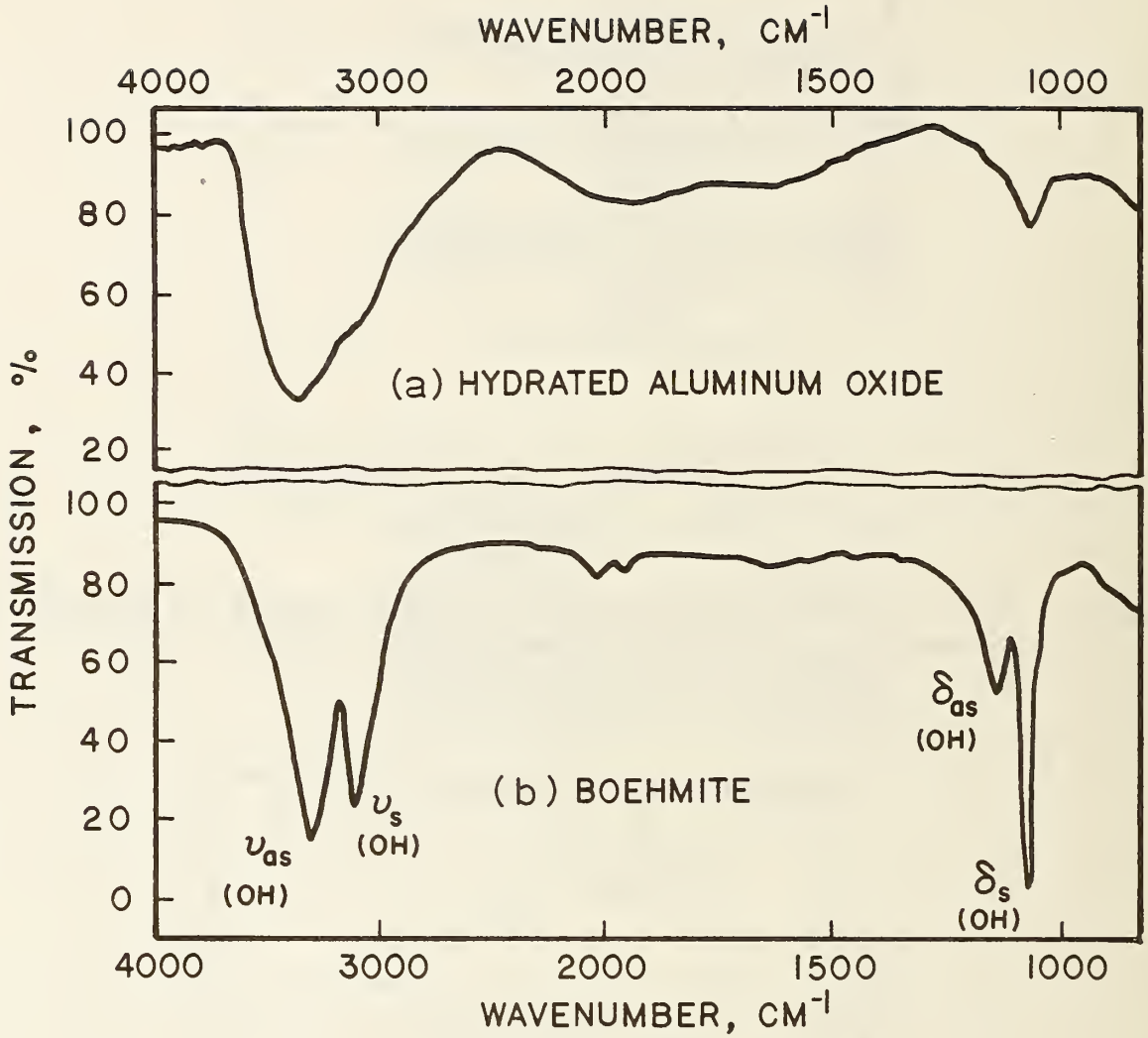

Figure 3 IR spectra of (a) AlOx film and (b) boehmite.

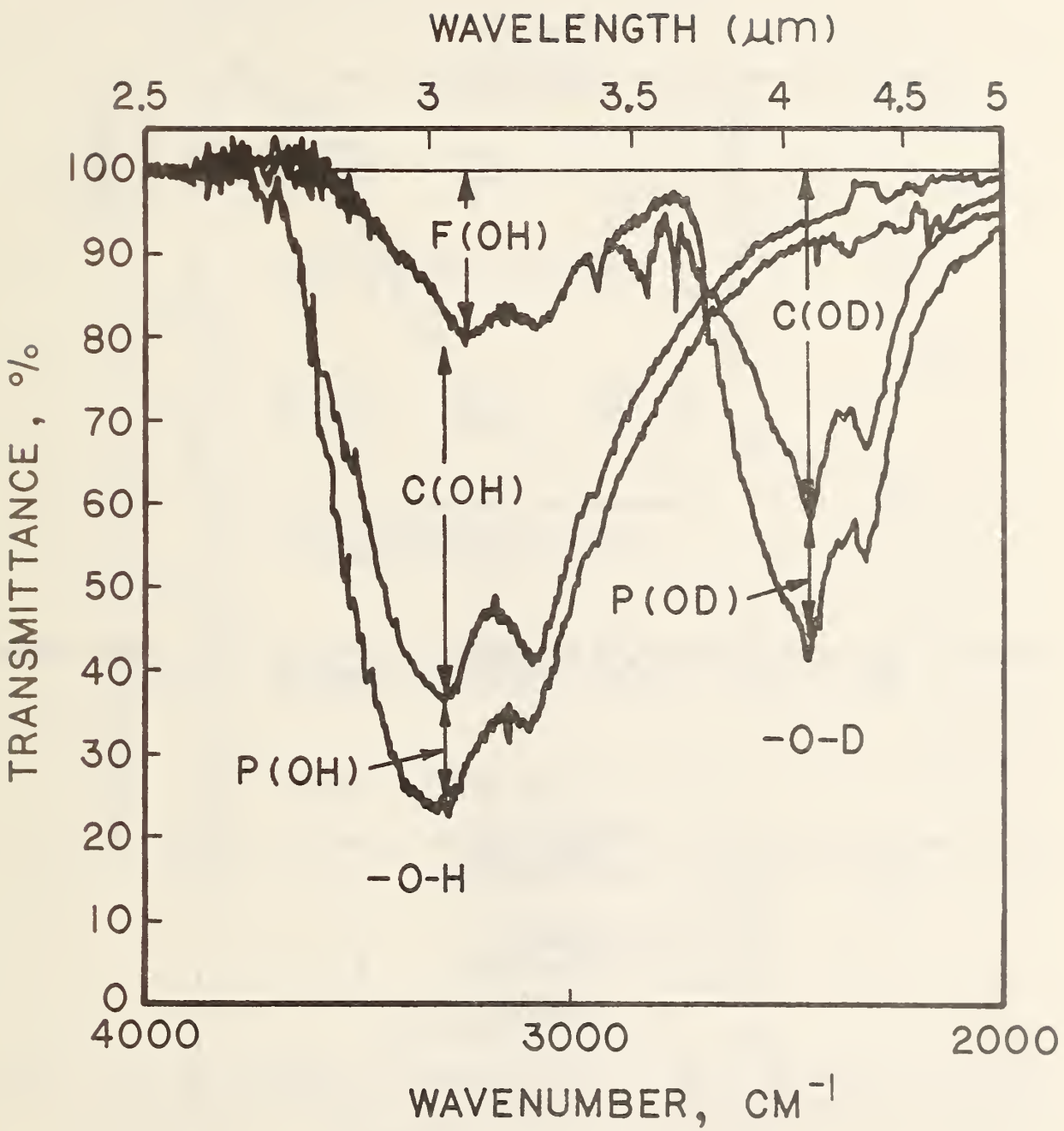

Figure 4 Three OH and OD components of the infrared spectrum.

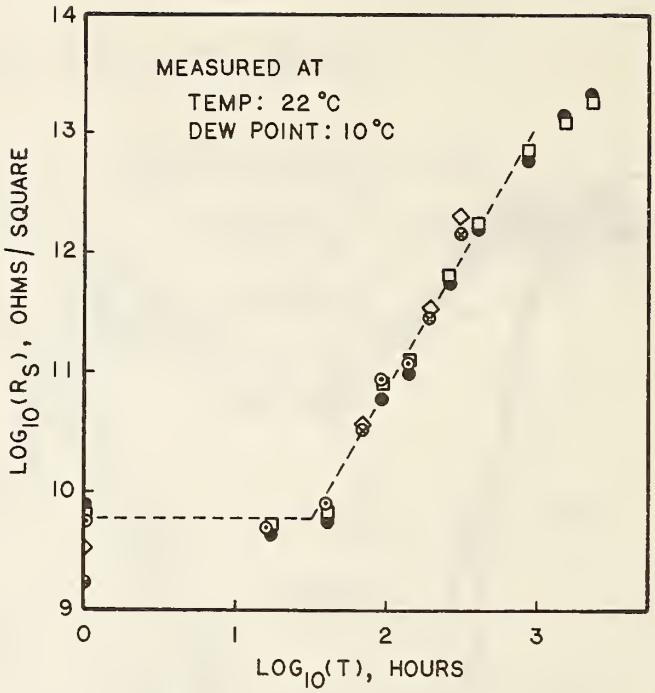

Figure 5 The time dependence of the sheet resistance of five samples prepared at two different times and aged in room ambient.

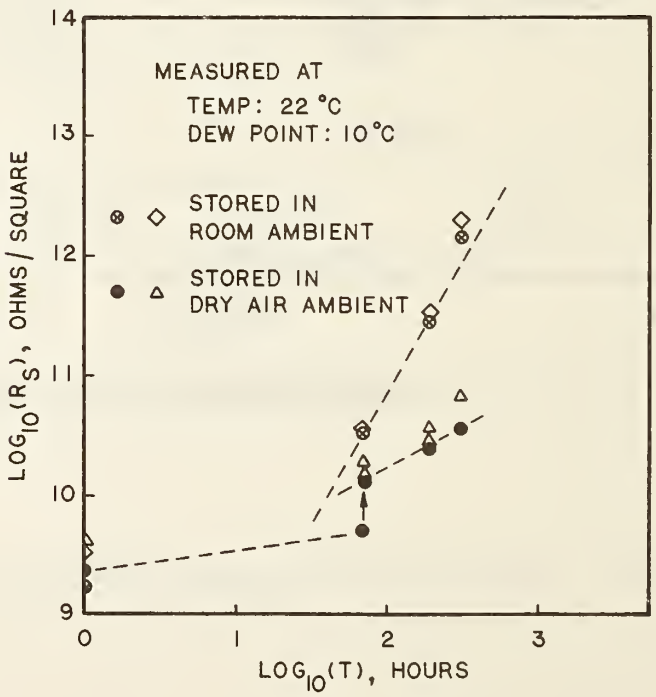

Figure 6 The time dependence of the sheet resistance of four samples prepared at the same time. Two were aged in room ambient, the others in dry air ambient.

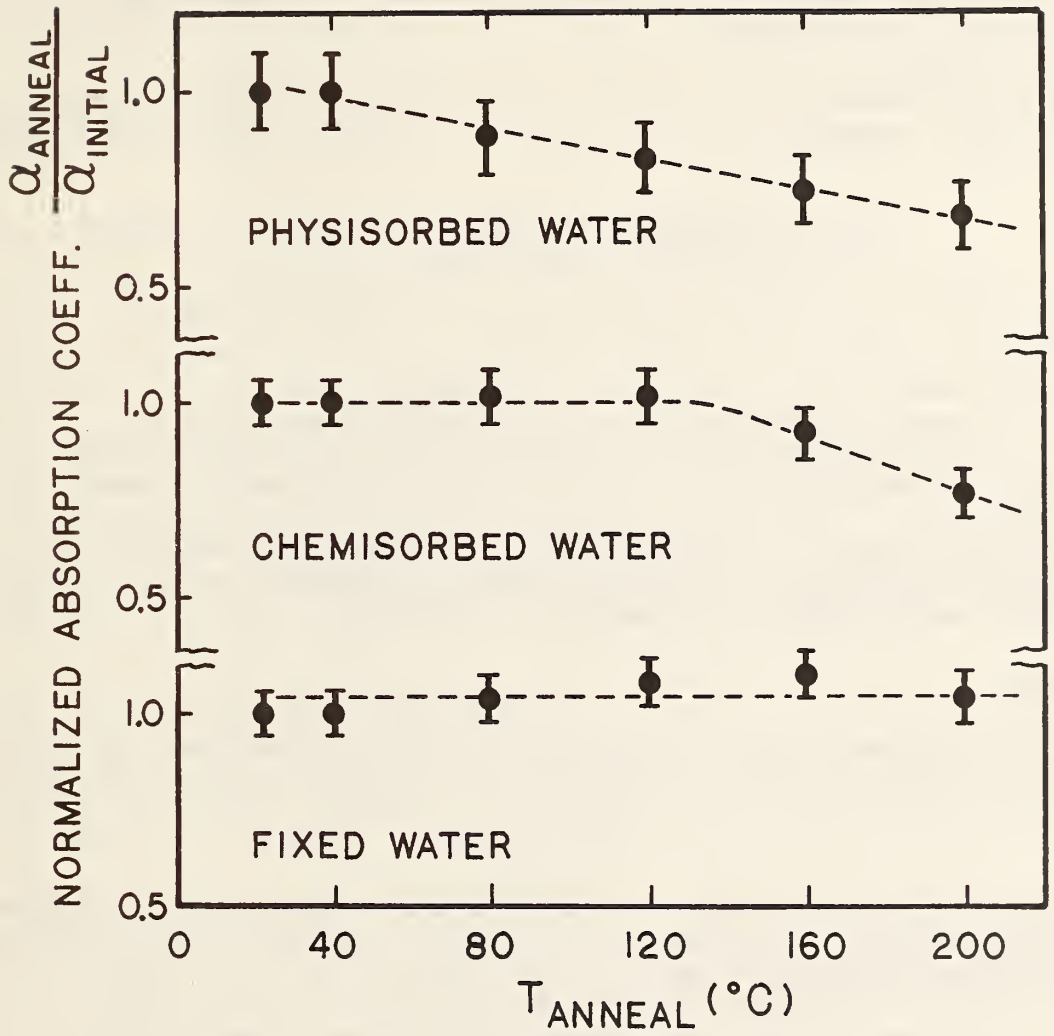

Figure 7 The low-temperature annealing effect on the IR normalized absorption intensities of the three components of the OH absorption spectrum.

III.2 RECENT EVALUATIONS OF AL_2O_3 IN SITU MOISTURE SENSORS FOR INDUSTRIAL ELECTRONIC HERMETIC COMPONENTS APPLICATION

M. Brizoux and J. Perdrigeat
Thomson - CSF/SCTF
Domaine de Corbeville
91401 - Orsay, France
(6) 019-70-00

D. Kane and R. Gauthier
I.N.S.A. Lyon
20, av. Albert Einstein
69621 - Villeurbanne, France
(7) 893-31-12

Presented by Judith Weiner
Thomson-CSF, White Plains, New York

ABSTRACT

The sensitiveness of Al_2O_3 sensors to the assembly procedures (used in the hybrid and semiconductor manufacturing) demands a recalibration of the sensor for each different process used. This operation is costly and time-consuming, and the precision is not acceptable for industrial standards.

A better knowledge of the assembly dispersion parameters (namely, temperature, and time) and the mathematical model of the sensor response will make their usage possible for industrial application.

KEY WORDS:

Accuracy, aluminum, assembly process, effect, mathematical model, moisture measurement, oxide sensor.

INTRODUCTION

It is now well documented that excessive moisture trapped within sealed electronic packages has become of major concern due to its ability to degrade the electrical performance with time.

Actually the specifications MIL-STD 883B and MIL-M 38510E require, in hermetic packages, a moisture level lower than 5000 ppmV for class B and 3000 ppmV for class S.

Among the several methods, the nondestructive electrical test of dew point sensors is really attractive; but in accordance with these standards, it is necessary to demonstrate the ability of these sensors for an industrial application goal.

Interest in this study was to provide an in situ sensor response mathematical model, taking into consideration housing die parameters. This mathematical model is intended to provide improvement in measurement accuracy, less expensive cost, and calibration time.

Al_2O_3 SENSOR SENSITIVITY TO ASSEMBLY PROCESS

Response Versus Assembly Process

The experimental setup for the sensor susceptibility to assembly process is the following.

Twenty-one sensors are assembled in 24 pins side-brazed packages by adhesive (H2OE) or eutectic perform (Au-Si) before and after sealing (for eutectic die attach).

Figure 1 shows the different magnitudes of sensor calibration curves, obtained from our test equipment (picture 1), as it could be expected[1,2,3].

Effect of Assembly Parameters Dispersion on Calibration Curve

The calibration curves reproducibility from one wafer run to another and the necessity of assembly parameters control present a great high interest in determining the opportunity of an industrial use in our semiconductor division.

To bring the sensors' sensitivity close to the above parameters:
- Many sensors (63 in all) from three wafer runs were assembled in 24 pins side-brazed packages with eutectic perform (Au-Si) die attach and U.S. Al bonding, and calibrated with our test equipment (results in figure 2).
- Keeping the same package and assembly process, we have just changed the eutectic time and the time control accuracy; calibrations made on 14 sensors are shown in figure 3.

The results presented above have shown:
- The great dispersion of sensors' response due to the assembly process[3].
- Necessity to calibrate each run of wafer.
- Accuracy of eutectic condition (acceptable results for eutectic time dispersion of 2 seconds).

We used many assembly processes (hybrid package, CERDIP, side-brazed, TO ...), and we found out that it is difficult to measure the humidity level that way because of the cost (high price of these sensors, minimum of five sensors for each calibration) and the delay (time-temperature effect on sensor response implies time recalibration, monosource manufacturer).

However, the fidelity of such sensors, measured at different times in the same condition, allows us to say that it can be used industrially, providing that a mathematical response model is possible (recalibration after the time-temperature effect would not be useful in this case).

MATHEMATICAL MODELISATION OF SENSOR RESPONSE

Test Program

An important test program has been established to validate the assumption advanced in the above paragraph. Experiments are made on the same wafer run of sensors in 24 pins side-brazed packages, die attach by ambient cure adhesive (araldite AV 138) and U.S. Al bonding (cold process). None of the packages was sealed.

A network taking into account time and temperature of sensor storage (commonly used in our different assembly divisions) was defined as follows (see Table 1).

Table 1: Test Program

Température	Time			
Ambient (référence)	t = 0			
150°C	24 h	168 h	500 h	1000h
350°C	10 s	30 s	2 mn	10 min
430°C	5 s	10 s	1 mn	10 min

5 sensors in each (σ, t) conditions

Calibration curves were obtained from humid gas generation at eight dew/frost point (-47°C, -43°C, -37°C, -°27C, -21°C, -13°C, -2°C, +8°C).

Note: Sensors baked at (150°C, 500 h and 500°C, 1000 h) failed. Visual inspection passed; the failure analysis has not yet shown the origin.

Results

Figures 4 and 5 are two examples of the weak dispersion of the 5 sensors in each couple (σ, t). After that only average curves will be considered.

All the results of this study are summarized in figure 6; at first glance it can be noticed that all the curve variations agree with time-temperature evolution.

MODELISATION

Calibration Curve Modelisation at Constant (σ, t)

We tried to identify a response curve by an exponential and polynomial function; an example is given in figure 7 (reference sensors). Third order polynomial function, in this example, is a good model (accuracy better than one dew/frost point). The same model has been applied on the couples σ, t (figures 8, 9, and 10) and pointed out that the polynomial function was acceptable for the different temperatures until 430°C, only if the polynomial was of fifth order (accuracy better than two dew/frost points).

$$V = A.T^5 + B.T^4 + C.T^3 + D.T^2 + F.T + F$$

V: sensor response
T: dew/frost point (see Table 2).

Table 2: Polynomial Curve Parameters

parameters (σ, t)	A	B	C
Reference	0	0	$9,2\ 10^{-8}$
150°C, 24 h	$2,9\ 10^{-8}$	$3,7\ 10^{-6}$	$1,7\ 10^{-4}$
150°C, 168h	$3,8\ 10^{-8}$	$4,5\ 10^{-6}$	$1,9\ 10^{-4}$
350°C, 10 s	$1,1\ 10^{-8}$	$1,2\ 10^{-6}$	$5,10^{-5}$
350°C, 30 s	$1,1\ 10^{-8}$	$1,5\ 10^{-6}$	$7,1\ 10^{-5}$
350°C, 2 mn	$1,4\ 10^{-8}$	$1,9\ 10^{-6}$	$9,1\ 10^{-5}$
350°C, 10mn	$8,2\ 10^{-9}$	$1,1\ 10^{-6}$	$5,1\ 10^{-5}$
430°C, 5s	$1,4\ 10^{-8}$	$1,9\ 10^{-6}$	$9,6\ 10^{-5}$
430°C, 10s	$6,5\ 10^{-9}$	$9\ 10^{-7}$	$4,8\ 10^{-5}$
430°C, 1mn	$7,3\ 10^{-9}$	$1\ 10^{-6}$	$5,4\ 10^{-5}$
430°C, 10mn	$3,7\ 10^{-10}$	$7\ 10^{-8}$	$4,9\ 10^{-6}$
Parameters (σ, t)	D	E	F
Référence	$1,2\ 10^{-3}$	$5,8\ 10^{-2}$	1,4
150°C, 24 h	$4,2\ 10^{-3}$	$7,5\ 10^{-2}$	1,3
150°C, 168h	$4,2\ 10^{-3}$	$7,5\ 10^{-2}$	1,3
350°C, 10s	$1,2\ 10^{-3}$	$2,7\ 10^{-2}$	$6,6\ 10^{-1}$
350°C, 30s	$1,7\ 10^{-3}$	$2,6\ 10^{-2}$	$5,4\ 10^{-1}$
350°C, 2mn	$2,1\ 10^{-3}$	$2,8\ 10^{-2}$	$4,7\ 10^{-1}$
350°C, 10mn	$1,1\ 10^{-3}$	$1,4\ 10^{-2}$	$3,3\ 10^{-1}$
430°C, 5 s	$2,4\ 10^{-3}$	$3,5\ 10^{-2}$	$5,9\ 10^{-1}$
430°C, 10s	$1,3\ 10^{-3}$	$2,3\ 10^{-2}$	$4,9\ 10^{-1}$
430°C, 1 mn	$1,4\ 10^{-3}$	$2\ 10^{-2}$	$4,1\ 10^{-1}$
430°C, 10 mn	1,7 10-4	$3,6\ 10^{-3}$	$2,3\ 10^{-1}$

Table 2 : polynomial curves parameters

Drift Calibration Curve Model Versus Time-Temperature Storage (σ, t) and Dew/Frost Point (T)

Time effect: the graphs for the equation shown in figures 11, 12, and 13 are plotted in log-log coordinates at constant T and σ.

$$\log V = -a \cdot \log t + b$$

or

$$V = \frac{K}{t^a} \text{ with } \begin{matrix} a = f(T) \\ k = g(T) \end{matrix}$$

Temperature effect: we propose an Arrhenius model, very often used in semiconductor field, such as:

$$V = c \cdot \exp \frac{-d}{k\sigma}$$

where k is the Boltzmann constant.

Consequently, a mathematical model of Al_2O_3 sensor response can be given as:

$$V = P(T) \cdot \frac{K}{t^a} \cdot c \exp\left(\frac{-d}{k\sigma}\right)$$

where P (T) is the fifth order polynomial function.

Remark: An industrial assembly process is characterized by several couples (σ, t). Frequently, σ values are very different, in this case, for close t values, we have to consider only the maximum temperature; and for close σ values ($\Delta\theta < 30°C$) we make a linear summation of time values.

HIGH TEMPERATURE STORAGE EFFECT

It is interesting to be able to follow the component's behavior (included a sensor) with respect to the humidity level and hermeticity[4,5] during electronic board and equipment functioning.

To approach this kind of behavior, we baked the sensors at 85°C and 125°C, which are assembled in 24 pins side-brazed packages with eutectic perform (Au-Si) die attach and U.S. Al bonding, during 168 h, 500 h, and 1000 h.

Results (figure 14) obtained for 125°C bake point out that the calibration curve's drift is stopped after 168 h (same results are obtained for the 85°C bake).

At present time, we have not seen any incompatibility between the use of the sensors and the knowledge of component's humidity level and hermeticity drift on equipment.

It should be necessary to confirm these first results by a temperature cycling test for 500 to 1000 cycles.

CONCLUSION

This study has proved the semiconductor and hybrid industrial application of Al_2O_3 sensors in moisture measurement.

This would be possible by tightening assembly process parameters and modelisation of calibration curve.

The high quality and reliability demand of the complex VLSI semiconductor will be satisfied by the control of several physical parameters, like humidity level.

ACKNOWLEDGMENTS

The authors wish to thank the internal working group "METAVAPEAU" for their help in the definition of the test program and Dominique Osselin and Michel Bordas for their contribution to these experiments. They also thank Alain Godefroy and Jean-Pierre Plantard for their technical advice. The authors are also grateful to Mr. Fong from Panametrics, Inc. for fruitful discussions.

REFERENCES

1. V. Fong, "The Effects for Assembly Techniques Upon the Performance Characteristics of Al_2O_3 In-Situ Moisture Sensors", NBS/RADC Moisture Workshop, March 22-23, 1978.

2. A. Koudounaris and E. E. Wargo, "Detection and Control of Moisture in Space Hybride", Technical Report, November, 1980.

3. M. L. White and R. E. Sammons, "A Procedure for Preparing Hermetic Packages with Known Moisture Levels", NBS/RADC Workshop, November 5-7, 1980.

4. D. R. Fancher and R. G. Horner, "Hybride Package Hermeticity and Moisture Level Monitoring", ISHM Proceedings, September, 1978.

5. J. B. Finn and V. Fong, "Recent Advances in Al_2O_3 In-Situ Moisture Monitoring Chips for Cerdip Package Applications", IEEE, 1980.

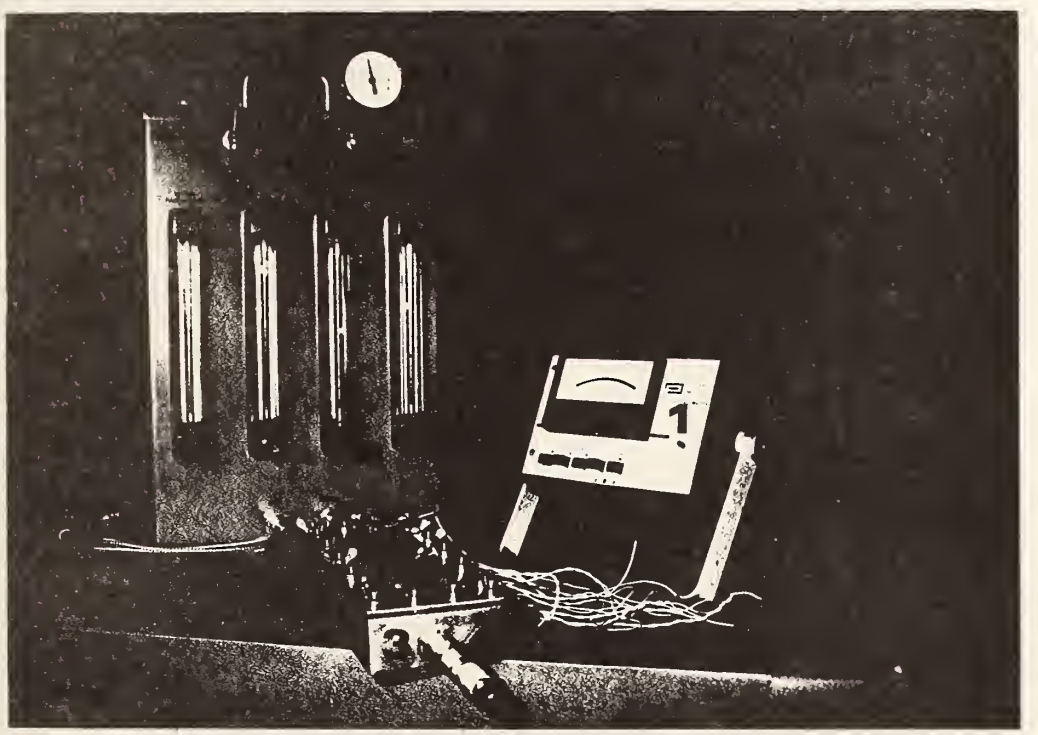

Picture 1. Test equipment description

1 - hygrometer model 771 for MINI-MOD HT sensors
2 - humidity generator MG 101
3 - calibration box

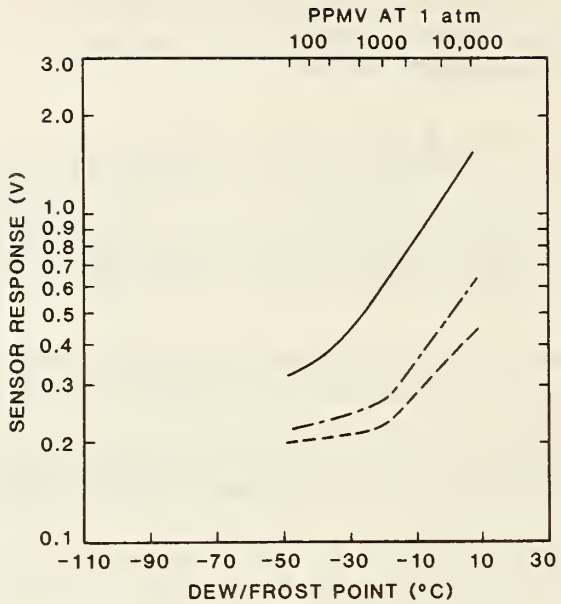

Figure 1. The assembly process effect on calibration. (-) an average calibration curve before sealing with adhesive die attach and curve cycles at 180°C for one hour. (-•-) calibration curve before sealing with Au/Si eutectic die attach at 420°C for 15 s. (---) calibration curve after sealing with Au/Si eutectic die attach and sealing at 370°C for 4 s in N_2/12% H_2.

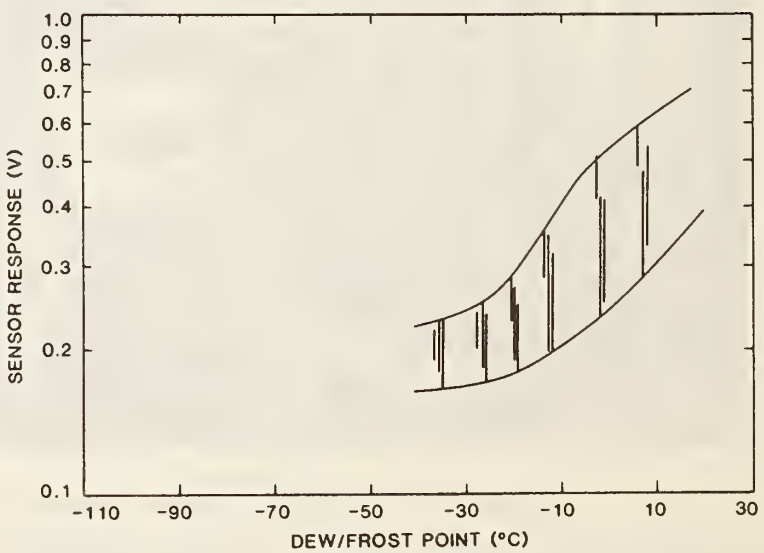

Figure 2. Dispersion in sensor response between 3 lots for side brazed packages with Au/Si eutectic die attach and ultrasonic Al wire bonding. Twenty-one sensors per run.

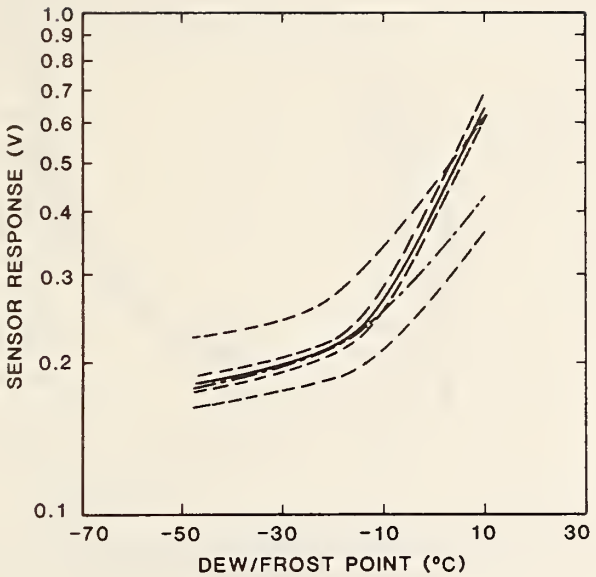

Figure 3. Dispersion in sensor response with eutectic attach heating time. (-) average values for 9 s. (-•-) average values for 15 s. Maximum and minimum values are also shown for each condition.

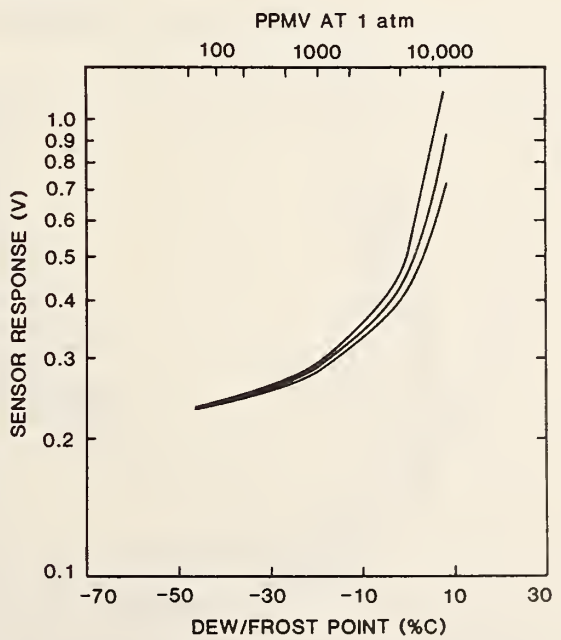

Figure 4. Sensor calibration after 350°C at 2 min with average, minimum, and maximum values indicated.

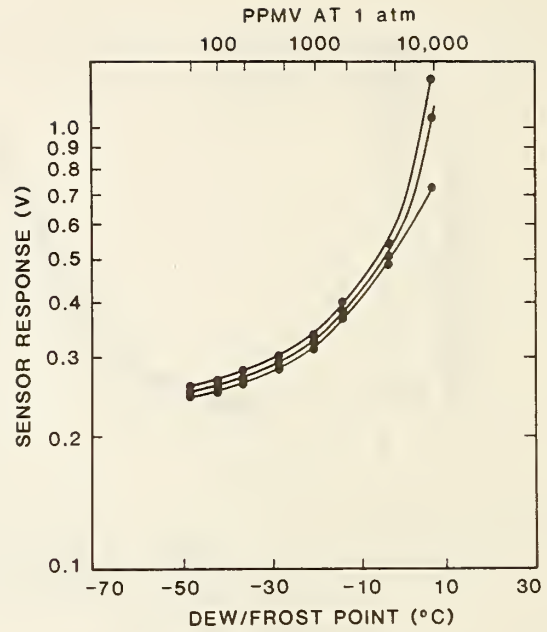

Figure 5. Sensor calibration after 450°C for 5 s with average, minimum, and maximum values indicated.

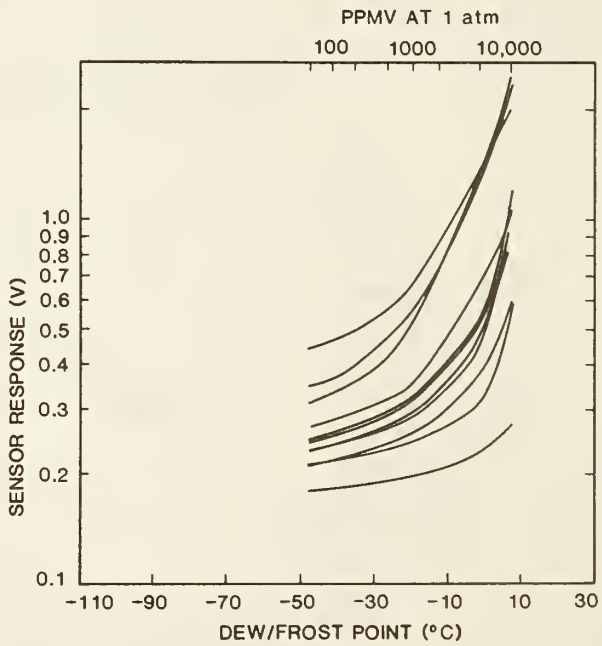

Figure 6. The effect of time and temperature on sensor calibration curves. The uppermost curve represents initial values. In descending order the curve represents the effect of 24 h at 150°C, 168 h at 150°C, 10 s at 350°C, 5 s at 430°C, 30 s at 350°C, 10 s at 430°C, 2 min at 350°C, 1 min at 430°C, 10 min at 350°C, and 10 min at 430°C.

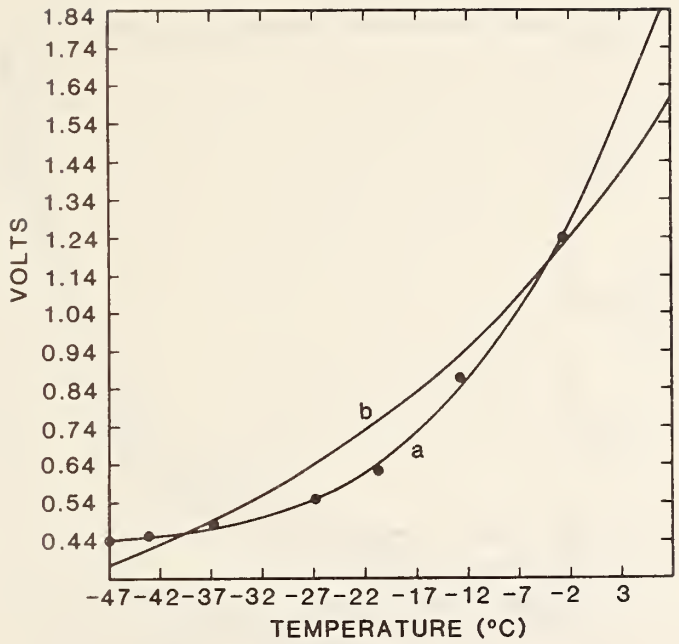

Figure 7. Response in reference sensors. a. exponential function, b. polynomial function (3rd order).

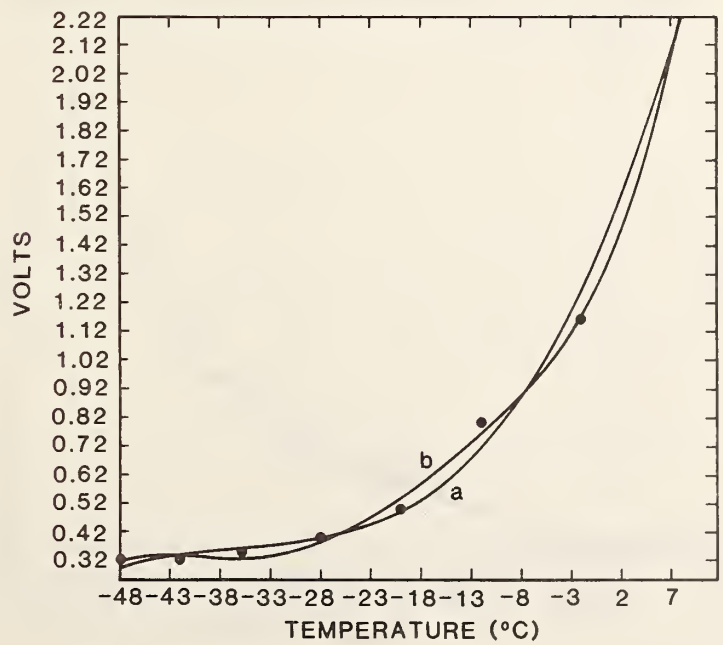

Figure 8. Response after 150°C, 168 h: a. 3rd order polynomial function, b. 5th order polynomial function.

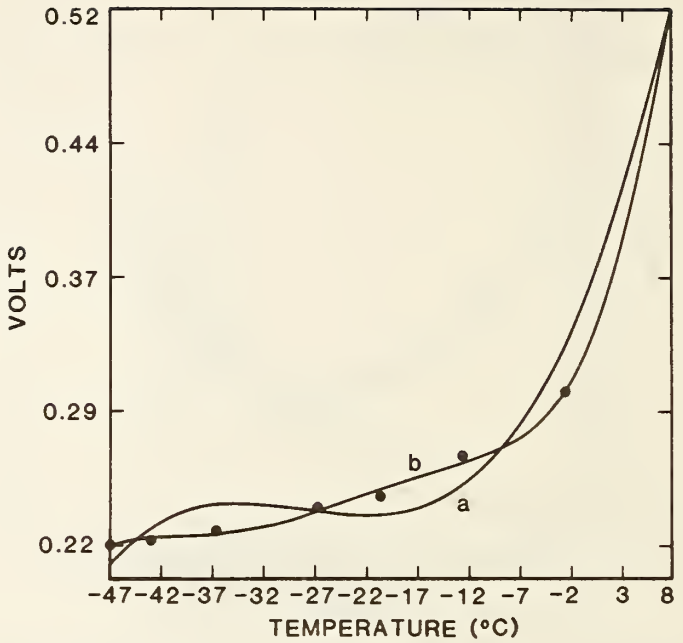

Figure 9. Response after 350°C, 10 min: a. 3rd order polynomial function, b. 5th order polynomial function.

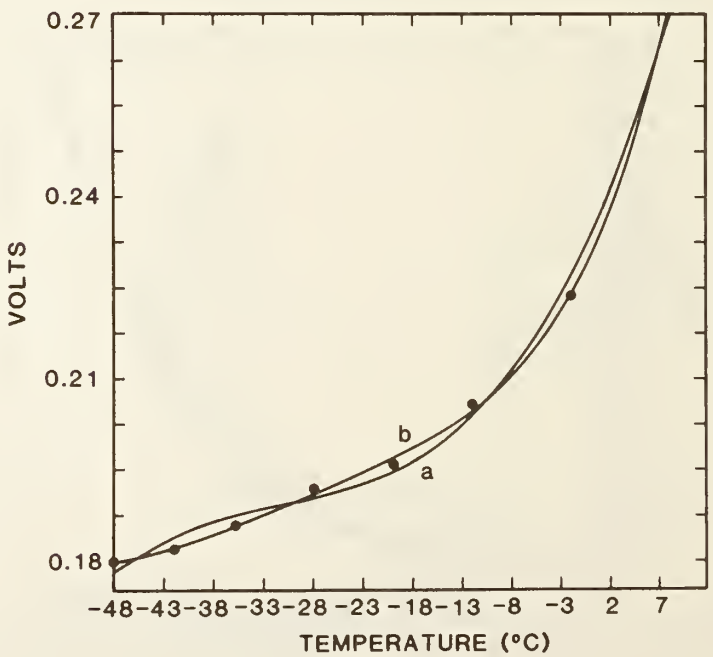

Figure 10. Response after 430°C, 10 min: a. 3rd order polynomial function, b. 5th order polynomial function.

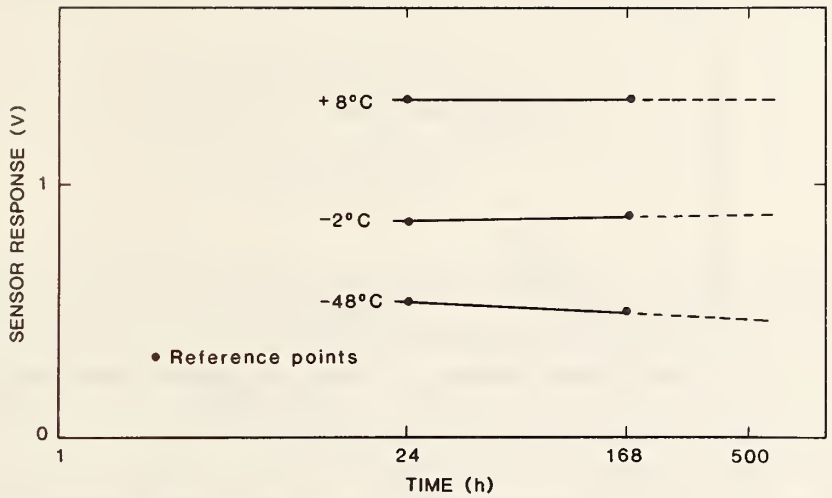

Figure 11. Drift in response for given dew/frost points (T) as a function of temperature-time storage (θ,t). θ = 150°C and T = -48, -2, +8 °C.

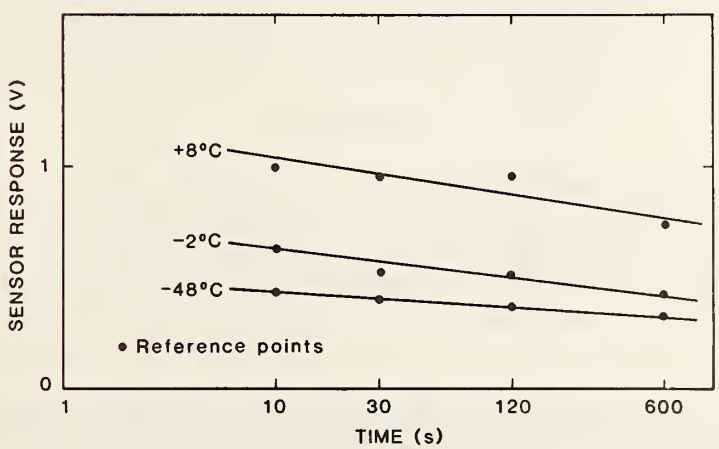

Figure 12. Drift in response for given dew/frost points (T) as a function of temperature-time storage (θ,t). θ = 350°C and T = -48, -2, +8 °C.

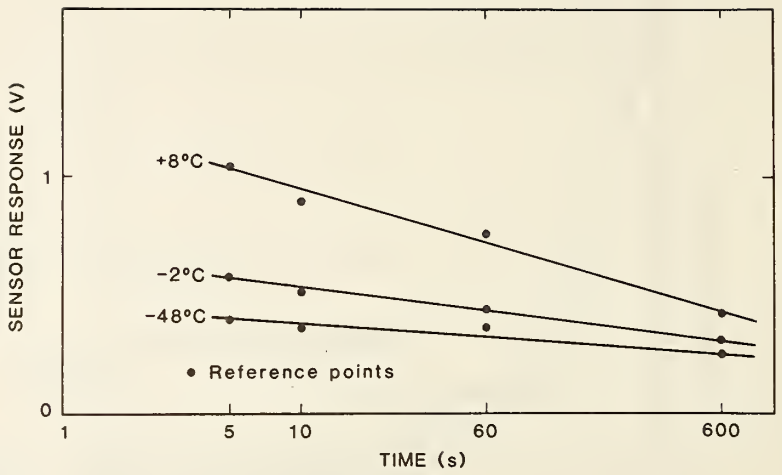

Figure 13. Drift in response for given dew/frost points (T) as a function of temperature-time storage (θ,t). θ = 430°C and T = -48, -2, +8 °C.

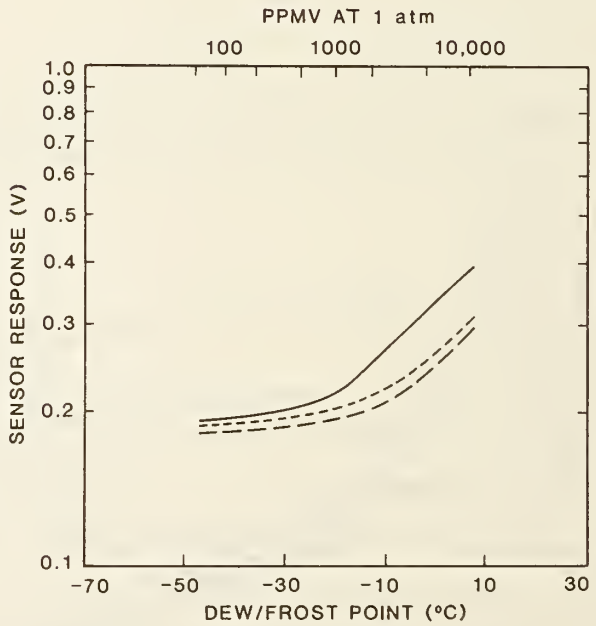

Figure 14. High temperature storage effect on calibration. (-) initial values. (-----) after 168 h at 125°C. (•---•) after 500 h at 125°C (— —) after 1000 h at 125°C.

4.3 MOISTURE SOURCES AND MEASUREMENT IN CERDIP PACKAGES WITH ALUMINA SENSORS

Harold Joss
Coors Porcelain Company
17750 W. 32nd Avenue
Golden, Colorado 80401
(303)277-4057

Abstract: This paper discusses the findings of work completed at the Coors Porcelain Company in the electronic package program. The alumina sensor, as manufactured by Panametrics, Inc. (Waltham, Mass.) is chosen from the several commercially available moisture test methods due to its ease of use and non-destructive character. The non-destructive nature allows not only moisture level determination, but also a monitoring system that can observe internal moisture levels as a function of time, adding insight to the effect of aging on package moisture levels. Experimental procedure and routine chip calibration is described, as is the method by which this device is correlated to mass spectrometry. An equation defining this relationship is offered.

Several CERDIP manufacturing processes and material variables are examined in general terms, and the alumina sensors are used to establish the fixed level contributions of each variable to total package moisture. Results indicate that each moisture source may not be dependent on the other sources. Throughout the test, a systematic decrease in package moisture with respect to time was noted in all samples. A hypothesis is proposed to explain this occurrence.

1. INTRODUCTION

When the low moisture program at Coors Porcelain Company was started, the first major objective defined was to establish a method by which the moisture inside a hermetically sealed package could be accurately measured. At that time several commercial test methods were available. Two of these were non-destructive techniques, both involving use of chips that could be placed inside of the package before sealing.

The first chip type was a surface conductivity moisture sensor, HIO-55001-6, purchased from Harris Corporation, Semiconductor Products Div., Melbourne, Florida. Initial testing with the Harris cell was unsuccessful, as no peak was clearly discernable. Later work with this method did yield some information, but it was decided that an easier to use technique would be desirable.

The next nondestructive technique investigated utilized an alumina moisture sensor chip, MM-HT, purchased from Panametrics, Inc., Waltham, Massachusetts. The first work done with this chip (and the Panametrics model 771 hygrometer which is used to read it) was generally successful. Some of the first readings were scattered, probably due to less than perfect assembly techniques.

Assembly is a sensitive operation, as the alumina portion of the sensor chip undergoes some physical changes in pore size, surface area, or density when heated during die attach, lead imbed, bakeouts, and seal[1]. The chip can be recalibrated after this thermal cycling, but the process must be constant for the recalibration to be meaningful. Then, when the alumina sensor test procedure is stabilized, the test values can be calibrated to mass spectrometry, the reference test procedure chosen for this program.

2. PROCEDURE

In order to minimize the effects of heat treatment, a standard CERDIP sample preparation and assembly procedure was developed. All CERDIP materials were processed on the same day under the same conditions (unless one was deliberately changed as a variable). Package assembly, including die attach, wire bond, and lead imbed were standardized. Since most vitreous sealing glasses on the market today seal at similar temperatures[2], all samples were glazed using the same temperature profile and atmosphere (air dried to -35°C dewpoint).

Some of the original packages containing the alumina sensors were sent to Panametrics for calibration. Briefly, their procedure involves de-lidding the packages and bringing them back to their original (dry) condition under flowing dry nitrogen. The samples are then placed in a humidity-controlled chamber and the sensor readings recorded at various dewpoints. From this data a calibration curve is constructed, an example of which is shown in figure 1.

To maintain the same calibration curve throughout the study, a series of steps were taken to insure that any replacement lots would be the same as the first lot. Initially the replacement chips were matched to the originals on a best fit basis by Panametrics. To verify this calibration at Coors, test samples were assembled. One chip from the new lot and one chip from the old lot were placed in each of six packages and sealed. In this way the two lots were evaluating exactly the same environments. If the readings for the two sets were the same, as was always the case, the replacement lot would be used.

The moisture sensor chips still needed to be correlated to mass spectrometry. Initially, equation (1), established by Finn and Fong[3] was used to convert sensor moisture levels to mass spectrometry values.

$$M = (6.42 * 10^6 * A)^{.397} \qquad (1)$$

where M = mass spectrometry value in ppm
A = alumina sensor value in ppm

For the first correlation test, 11 packages previously tested for moisture with alumina sensors were chosen to represent the entire spectrum of moisture values from below 500 ppm to 9000 ppm. Each 24 lead CERDIP was marked and delivered to Oneida Research Services, New Hartford, New York. Once the samples were returned, each of the two readings, representing the two test methods, were analyzed on a specimen by specimen basis.

3. RESULTS AND DISCUSSION

Sensor moisture values were compared to the mass spectrometer values using a standard correlation and linear regression analysis. However, it was found that the meter readings themselves provided a better correlation coefficient (0.96) than the predicted moisture values derived through use of equation (1). The results of this second analysis, listed in Table I, are shown graphically in figure 2. Using this information, a linear relationship between the alumina sensor meter reading and actual mass spectrometer moisture was derived. The result was equation (2).

$$M = (150890 * R) - 21629.5 \qquad (2)$$

where M = expected mass spectrometer value, ppm
R = Panametrics 771 hygrometer meter reading

Equation (2) will go negative at a very low meter reading. However, some packages tested in this range were also evaluated by mass spectrometry and found to have moisture levels below 750 ppm. Since this project was not concerned in particular with accurate measurement and correlation in this range, and since packages with those moisture levels are generally considered acceptable, it was not considered a problem.

During the course of this study, several interesting observations were made. First, all of the curves have a generally decreasing moisture level with time. Examples of this can be seen in figures 3 - 6. Although no mathematical study was made, the plots seem to fall on a straight line if moisture level is plotted against log time.

This moisture level reduction could have been caused by a drift in the response of the sensor itself. However, tests have been performed whereby samples 2 weeks to 2 months old have been measured by mass spectrometry and their readings verified. This not only supported the belief that the moisture decrease was real, but also that the 100°C preconditioning of the sample for mass spectrometry was not driving extraneous moisture into the cavity.

A better explanation for the moisture level reduction is that the package itself may take a long time to reach equilibrium after seal. This is not a new concept[4,5], and moisture may be reabsorbed onto lids, walls, and bases after thermal cycling. Since the chip surface is the most insulated area from the package exterior, it is probably the last to observe any condensation[6,7]. This is obviously the case with an alumina sensor chip, as condensation on it would raise the moisture readings, rather than decrease them.

Another interesting discovery in this work concerned changes in moisture level when variables in the CERDIP manufacturing process were altered. This in itself was not surprising, but by cross-checking variables, it seemed that moisture introduced (or removed) by each process variable was independent of the other variables. If this was the case, moisture sources are additive and more than a

few key factors require attention when low moisture levels are necessary. An example of one of these comparisons is illustrated in figure 3. In this figure, three different glazing atmospheres are investigated. The results illustrate that much lower moisture levels can result through use of atmospheres B and C during the CERDIP glazing cycle.

Although atmospheric moisture absorption by the raw materials can be a source of package moisture, humidity doesn't seem to be a problem once the CERDIP is properly glazed. As a test, six Coors low moisture CERDIP sets were stored at -40°C dewpoint and six other sets stored at +27°C dewpoint for 16 hours. When sealed, these parts had the same moisture levels (figure 4). The test was repeated with a different sealing glass and the results were essentially the same (figure 5).

A final characteristic noted was that sealing glasses have intrinsic moisture levels. This concept is well known in the industry and has been previously cited[8,9]. Results indicated that these moisture levels are independent of other moisture sources, like the process variables. The variation between glasses is consistent enough to classify them into three general categories (figure 6). Of the four glasses displayed here, LS 0113 is representative of a high moisture glass, KC 401 and SG 202 are moderate moisture level glasses, and LS 0803 is an example of a low moisture glass. Devitrifying type glasses were not included in this study, but would be expected to fall into the high category. It is worth noting that a dry process CERDIP has a moisture level that is a function of the glass specified by the customer, as processing can only remove processing moisture sources.

The moisture in sealing glasses is created, at least in part, by the starting materials and smelting (manufacture and refining) process. The raw materials used to manufacture glasses usually include nitrates, hydrates, sulfates, and carbonates. During the smelting process, these materials decompose to form the oxides that make up the glass itself. The gasses given off are mostly removed during the firing process, where the molten glass can bubble like any other liquid. However, some of these dissolved gasses are never removed and subsequently incorporate themselves into the glass structure. Once these materials have been chemically absorbed by the glass, quite a bit of heat may be required to drive them off[10]. It is therefore proposed that package sealing temperatures are high enough to drive some of these impurities out of the glass structure. These can then combine to form an atmosphere which includes H_2O, CO_2, N_2, and SO_2 within the CERDIP itself.

4. CONCLUSIONS

Several conclusions may be drawn as a result of this study.

1. The alumina moisture sensor chip does correlate to mass spectrometry.

2. The moisture levels seen by a chip sealed within a CERDIP package become systematically lower with time.

3. Moisture sources emanate from both processing parameters and the materials used, particularly the sealing glass. These sources are not interdependent.

REFERENCES

1. Kovac, Michael G., "Performance Characteristics of Al_2O_3 Moisture Sensors Inside Sealed Hybrid Packages", ISHM Symposium, Baltimore, Md., October 1977, pp. 249-252.

2. Pittman, J. D. and Joss, H. D., "Low Temperature Sealing Glass Strength Study for Type C Chip Carriers", Proceedings 32nd Electronic Components Conference, 1982, pp. 277-281.

3. Finn, J. B. and Fong, V., "Recent Advances in Al_2O_3 'In Situ' Moisture Monitoring Chips for CERDIP Package Applications", Proceedings 18th Annual International Reliability Physics Symposium, Las Vegas, Nevada, April 1980.

4. Kovac, Michael G., "Cross Correlation Experiments on Different Types of Sensors", Proceedings NBS/RADC Workshop, Moisture Measurement II, November, 1980, pp. 79-89.

5. Davy, J. Gordon, "Thermodynamic and Kinetic Considerations of Moisture Sorption Phenomena", Proceedings NBS/RADC Workshop, Moisture Measurement II, November, 1980, pp. 184-200.

6. Kovac, Michael G., "Microenvironments and Accelerated Testing", Proceedings NBS/RADC Workshop, Moisture Measurement II, November 1980, pp. 165-174.

7. Hale, John C. and Fong, Victor, "Moisture Sensors, Mass Spectroscopy, and Mil Standards", Proceedings NBS/RADC Workshop, Moisture Measurement II, November 1980, pp. 90-97.

8. Shukla, Rama K. et. al., "Moisture Content of Solder Glasses", Proceedings NBS/RADC Workshop, Moisture Measurement II, November 1980, pp. 213-219.

9. Lowry, Robert K., "Dry Sealing Glasses - A Summary of Research", Proceedings NBS/RADC Workshop Moisture Measurement II, November 1980, pp. 220-233.

10. "Vacuum Hot Gas Extraction Apparatus", P & P 9, pp. 28-29, Nippon Electric Glass Co., Ltd., Otsu City, Japan (1980).

MINI-MOD®

CALIBRATION CURVE

PANAMETRICS, INC.
Waltham, Ma. 02154
(617) 899-2719 x 227

DATE 12/9/80
TYPE/WAFER Coors
Customer Sealed Units

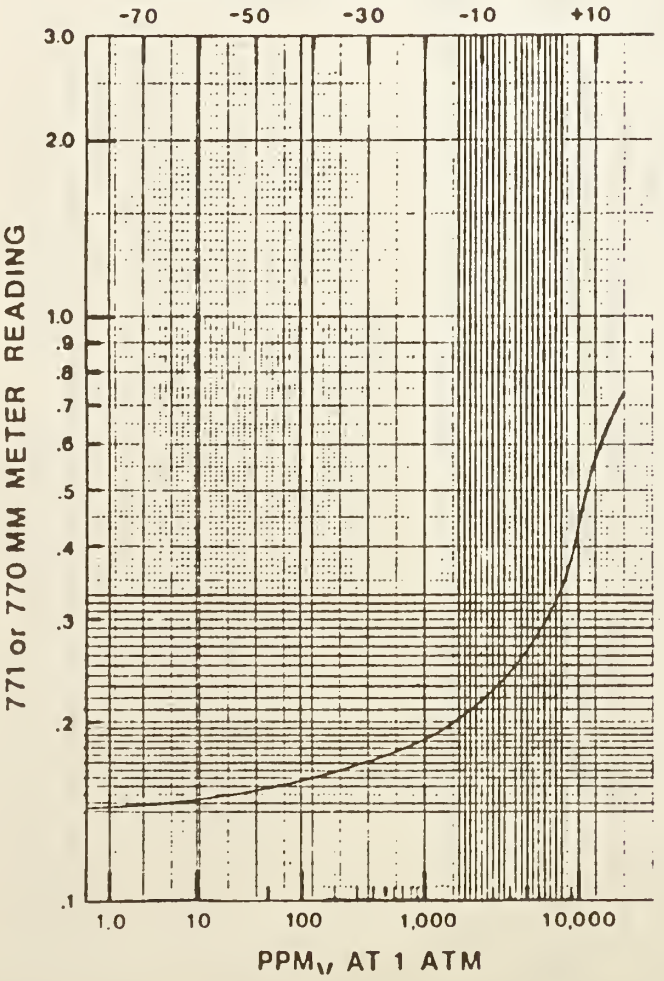

Figure 1: Factory Calibration Curve

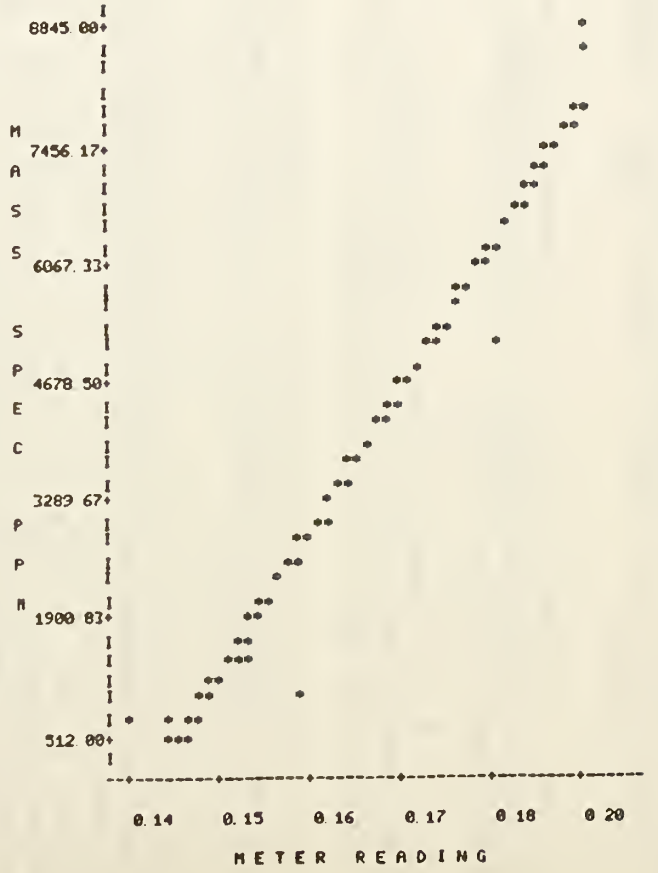

Figure 2: Correlation Between Panametrics 771 Reading and Mass Spec PPM

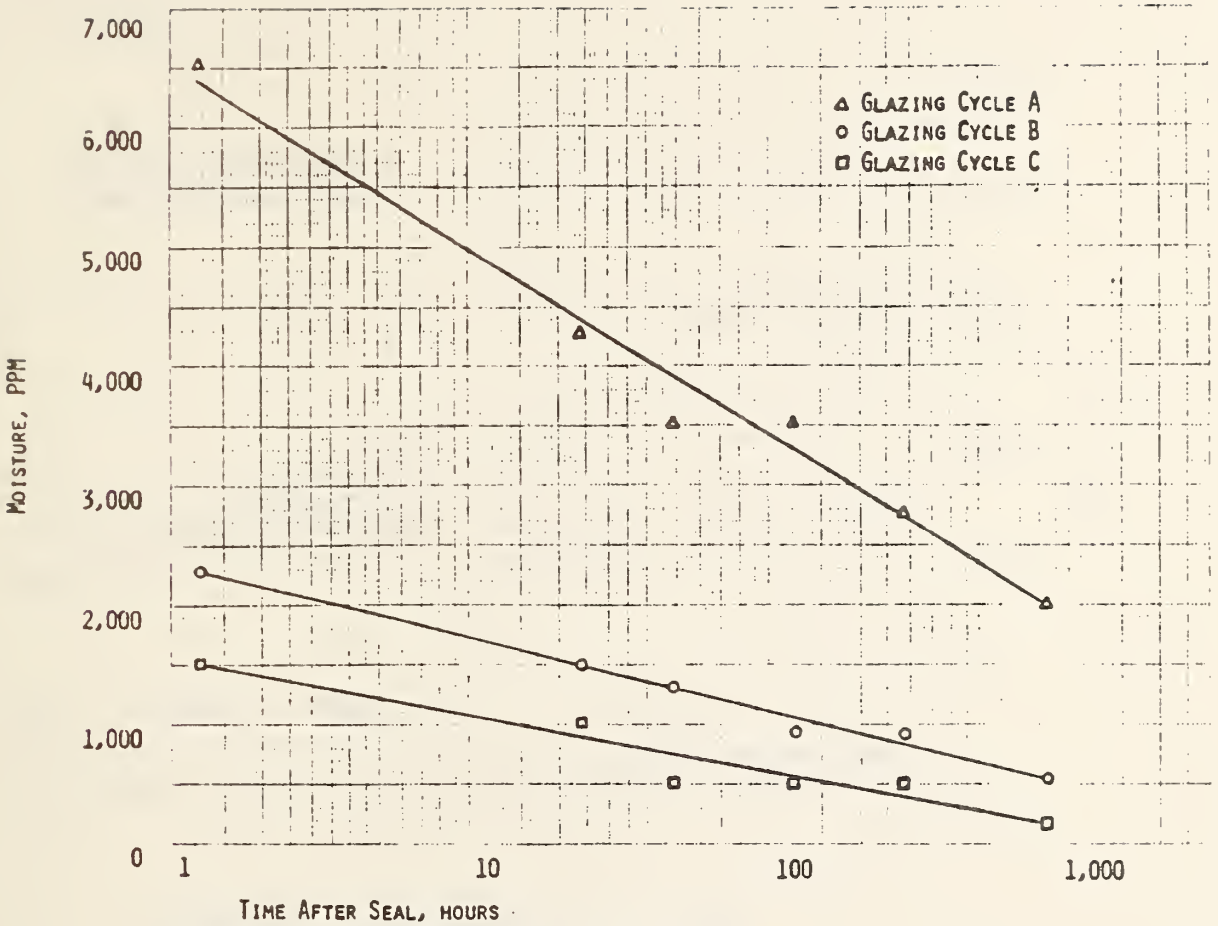

FIGURE 3: COMPARISON OF CERDIP GLAZING CYCLES

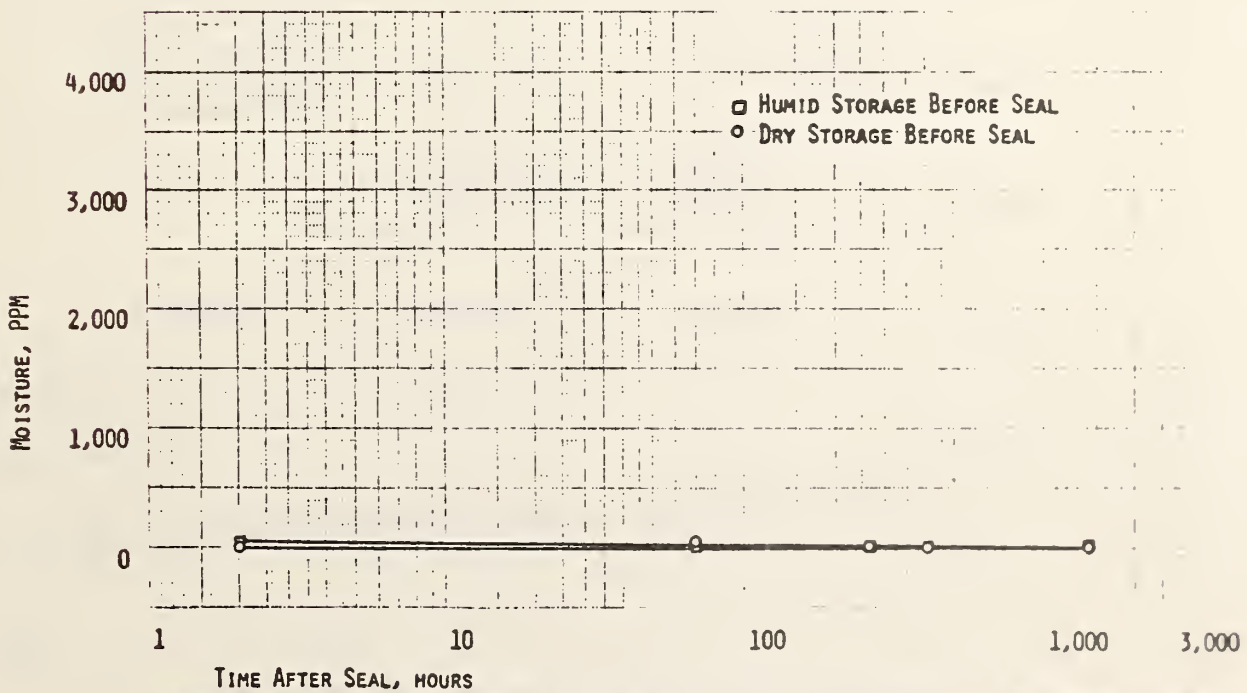

FIGURE 4: EFFECT OF GLAZED CERDIP STORAGE CONDITIONS ON SEALED PACKAGE MOISTURE - LS0803

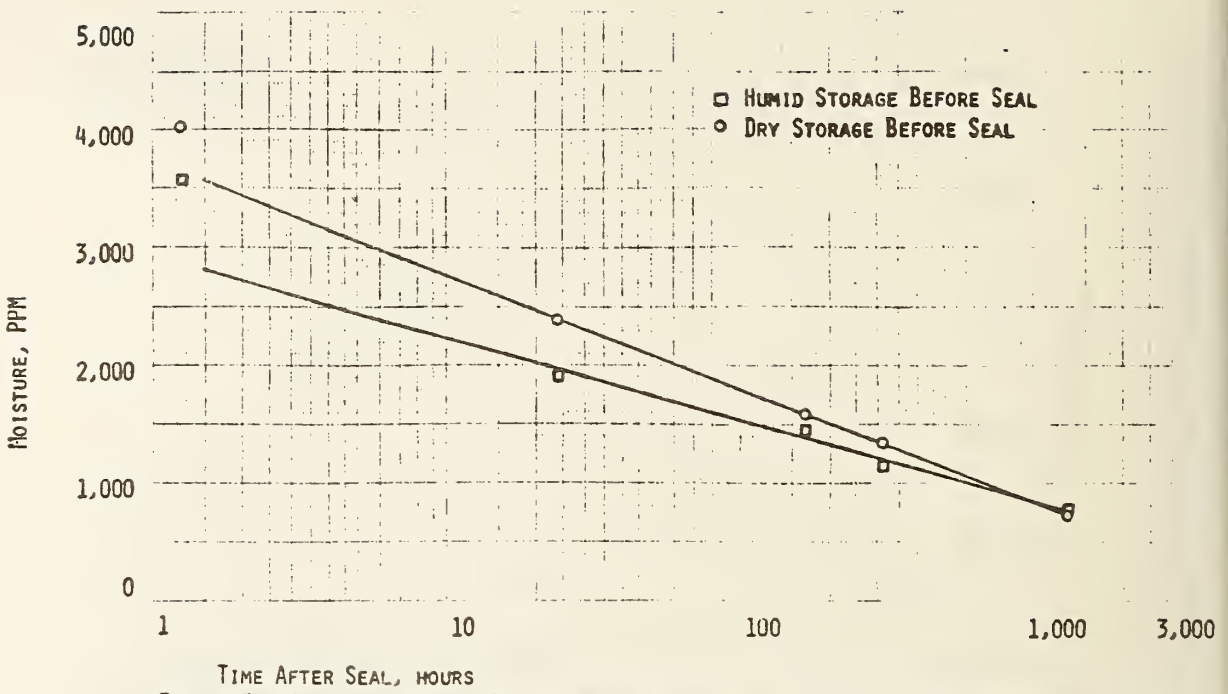

Figure 5: Effect of Glazed Cerdip Storage Conditions on Sealed Package Moisture - LS0113

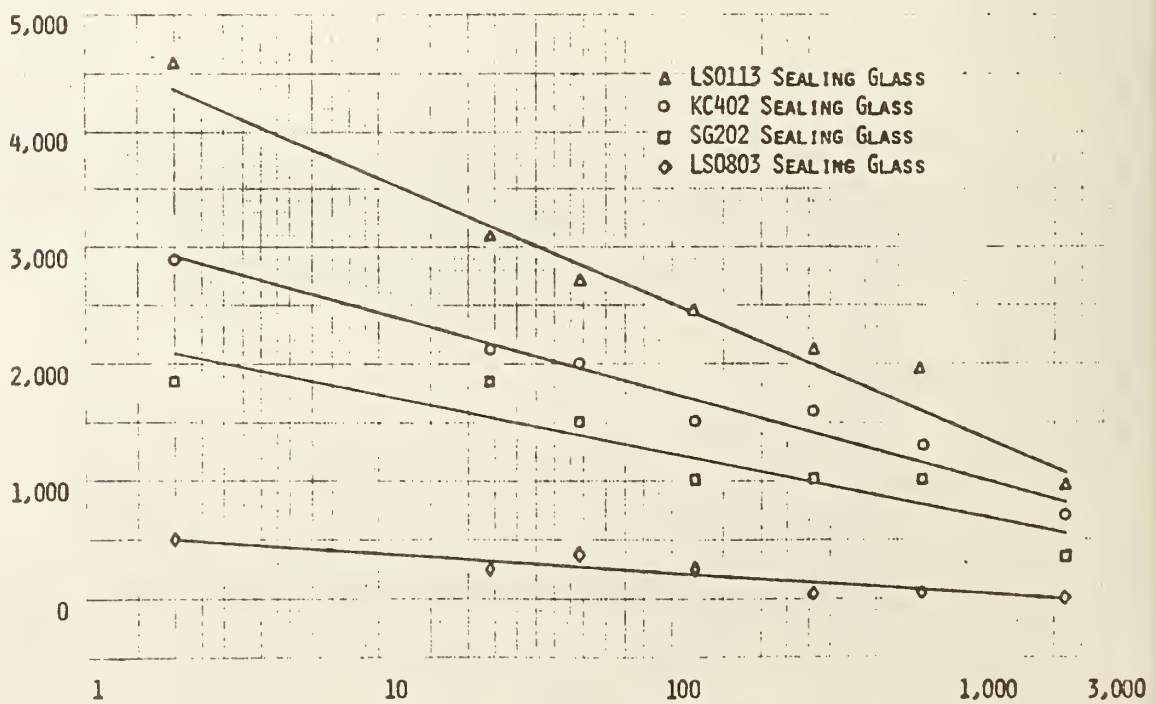

Figure 6: Effect of Different Sealing Glasses on Package Moisture.

C O R R E L A T I O N & L I N E A R R E G R E S S I O N

VARIABLE X: METER READING VARIABLE Y: MASS SPEC PPM

NUMBER OF PAIRS (N) = 11

CORRELATION COEFFICIENT (R) = 96

DEGREES OF FREEDOM (DF) = 9

SLOPE (M) OF REGRESSION LINE = 150890

Y INTERCEPT (B) FOR THE LINE = -21629.5

Table I: Correlation Between Panametrics 771 Hygrometer Reading and Mass Spec PPM

4.4 MOISTURE CONTENT CONTROL USING ALUMINA SENSOR

Carl M. Roberts, Jr.
Analog Devices
Semiconductor Division
804 Woburn Street
Wilmington, MA 01887
(617) 935-5565

ABSTRACT

Implementation and use of an aluminum oxide sensor to control header sealed package moisture content at the point of package seal in an integrated circuit assembly process is discussed. Correlation of moisture content readings between the aluminum oxide sensor and mass spectrometric determination of moisture is also addressed.

INTRODUCTION

MANUFACTURING SITUATION

At Analog Devices Semiconductor (ADS), volume assembly of hermetic header product (Figure 1) is typically done at assembly locations in Korea, Taiwan, and the Philippines. Once received at ADS, the finished product is sampled and inspected at Incoming Quality Control (IQC) for conformance to ADS assembly specifications. Samples from each received assembly lot are also sent to an outside lab for mass spectrometric analysis of internal moisture content. Product acceptable to 5000 PPM moisture content is released for electrical testing while product in excess of 5000 PPM is rejected, impounded, and typically dispositioned to scrap.

IQC data during the first half of 1981 indicated that too many header assembly lots were rejecting for high moisture content. The MASS SPEC data for moisture content was usually available for analysis and IQC decisions typically five to six weeks after the product was sealed at the assembly location. With such a time lag from the point of seal to the actual receipt of moisture data, reject lots created several difficult situations: first, the rejected product was impounded and typically dispositioned to scrap; second, rejected product severely disrupted product schedules; third, work-in-process might be similarly affected with high moisture content.

ADS AND MOISTURE

ADS' attention to moisture content is certainly in response to MIL SPEC requirements but, more specifically, is founded in the product ADS produces. Most ADS product includes thin film resistors (Figure 2) in addition to the normally used aluminum.

The presence of thin film resistors in any IC product tends to, in theory, increase the probability that device corrosion may occur under the right circumstances: as in the case of high moisture content in the sealed package. The thin film resistor itself has a possibly greater tendency to suffer from corrosion in the presence of high moisture simply because of its thinness of construction, approximately 100 Angstroms, versus the thickness of typically

deposited aluminum, approximately 15000 Angstroms. Aside from the thinness, interconnects between thin film resistors and aluminum are often sites of high voltage potential relative to adjacent device circuitry, which again coupled with high moisture increases the tendency of device corrosion. Additionally, wafer product fabricated at ADS is typically laser trimmed through the top layer glassivation to the thin film resistor to electrically modify certain resistors (Figure 3). The laser trim process has the potential to crack the top layer glassivation at the point of trim which, within limits, is visually acceptable to 883B MIL SPECS. The crack, if present, is a site of possible moisture ingression right to the thin film resistor and thus is another construction factor contributing to corrosion tendency.

The mere presence of thin film resistors, the interconnects from thin film resistors to aluminum, and the possible glassivation cracks at laser trim sites are not singularly or collectively reasons for device corrosion. They are conditions of construction that, when coupled with high moisture, would tend to make such constructed devices more susceptible to experience and exhibit corrosion. At ADS, the attention to moisture and control of such is therefore more specifically centered in product concerns rather than in conformance to MIL SPEC requirements. In fact, the 5000 PPM moisture control limit is applied to both military and commercial product at ADS.

CORRECTIVE CONTROL ACTION

The occurrence of moisture rejections at IQC in early 1981, the time delay between product seal and available MASS SPEC data, and ADS' attention to moisture because of product construction prompted a need to effect measurement and control of moisture during the assembly process at the point of actual package seal. The procedure selected to effect such measurement and control was the implementation and use of the Panametrics MINI-MOD-HT moisture sensor chip.

Discussed herein is the implementation procedure done at ADS to effect use of the moisture sensor chip, results from two years of such a control procedure, and, finally, a comparative examination of moisture PPM readings for identical units measuring moisture with the moisture chip and then as measured through MASS SPEC. The theory of operation of the Panametrics MINI-MOD-HT moisture sensor chip is well documented in many available papers and will not be addressed.

MOISTURE SENSOR CHIP: PRODUCTION USE

INITIAL EVALUATION

Effecting the use of the moisture chip as a control measurement in production is a relatively straightforward procedure that must carefully be tailored to the assembly process steps of the package to be controlled. The response of the moisture chip to indicate any particular moisture level is affected by the thermal exposures that the moisture chip experiences. In this regard, to effect control at a particular point in the assembly process, the moisture chip should be exposed only to the normal assembly thermal excursions that actual production product would experience up to the point in the process that the control measurement is effected for the package to be controlled.

In implementing the control procedure at the point of seal for ADS header product, the assembly thermal excursions are only two and include eutectic die attach and oven baking of product prior to seal (Figure 1).

Moisture sensor chips were acquired from Panametrics. A small quantity of approximately twenty units were eutectic die mounted, aluminum ultrasonic wire bonded, baked and sealed exactly as normal production assemblies. The units were serialized and then individually connected to a Panametrics Model 771 meter and the reading for each unit was recorded.

The meter reading at this point is essentially meaningless without a means to convert the reading to moisture PPM. This is done by generating a calibration curve at Panametrics (or some alternative source) with a moisture generator traceable to the National Bureau of Standards. Prior to sending units to Panametrics to generate the calibration curve, all twenty units were first sent to an outside lab for MASS SPEC readings of moisture content. The MASS SPEC moisture readings were recorded against the original serialized Panametrics meter readings with the intent of comparing the moisture PPM readings of the two measurement techniques once the Panametrics calibration curve was available.

Ten units were sent to Panametrics and all ten were used to develop the calibration curve. The procedure is relatively simple. Each unit is individually mounted to the moisture generator and different known levels of moisture are generated and exposed to the moisture chip (the header lid was punctured during MASS SPEC testing thus allowing a path for moisture access to the moisture chip). Each unit is simultaneously connected to a Panametrics Model 771 meter and as each known level of moisture is generated the corresponding meter reading is recorded. All the recorded meter readings are then averaged at each known moisture level. The averaged meter readings are then plotted against the known corresponding generated moisture level where the vertical axis is the meter reading and the horizontal axis is the known generated moisture level. A curve is then drawn on the graph fitting the plotted points. The drawn curve is the calibration curve. An example of a completed calibration curve is shown in Figure 4.

The twenty units that had originally been read on the Panametrics meter were now converted to moisture PPM using the calibration curve. Comparing the moisture data unit for unit with both measurement techniques did not show a one for one correlation. However, the comparison did indicate a sufficient enough relationship such that a maximum allowable moisture chip meter reading could be selected as a process measurement control point, while applying some factor of safety. The selected maximum reading, with the applied factor of safety, would allow the control process to be used to effect the desired intent while not tightening down too much so as to cause unnecessary production stoppages.

Having done the above process once, the entire set of actions was repeated again and again so as to examine the consistency of the moisture chip system as well as test the validity of the selected

moisture meter control point as compared to MASS SPEC moisture readings for the same units. The results of such evaluations confirmed the original findings: the moisture chip and the selected control point sufficiently related to the corresponding MASS SPEC readings to at least use the moisture chip as a tool for process control. Precise correlation studies at this early time in the use of the moisture chip was not appropriate as the initial intent was to control a seal process with a tool, specifically the moisture chip. More precise statistical correlation studies would be considered long after the moisture chip was well established as a production control tool and more data of comparative readings of moisture was available. It should be noted here that MASS SPEC is done at 100°C and looks at vapor phase, adsorbed and absorbed moisture while the moisture chip is operated or read at 25°C and measures only vapor phase moisture. Given a specific application of control for a specific package with unchanging process conditions, a statistical study might relate the two techniques. Again, this analysis was deferred until more data was available.

One additional evaluation was completed prior to production implementation. All of the samples generated for the above tests were done in the ADS Wilmington facility with a process defined as in control so none of the sealed units exceeded 5000 PPM as tested through MASS SPEC. Many groups of units were now processed through a variety of sealing conditions to generate: extraordinarily dry parts by multiple baking, normal parts by the normal specified process, and various increasingly wet groupings of parts by progressively reducing and finally eliminating the prebake step. All units were read on the Panametrics meter and segregated into acceptable and rejectable groupings. The units were all tested through MASS SPEC. Although the unit for unit readings did not directly correlate in PPM, the groupings did correlate---all the reject units were rejects, and all the acceptable units were acceptable. As a tool for control, the test data indicated the process was ready to be implemented.

PRODUCTION IMPLEMENTATION

Panametrics meters were purchased for each assembly location and a long term volume order for moisture chips was issued. Procedural specifications were written including a log book for recording the moisture chip meter readings. Serialized library parts were created in the ADS Wilmington facility. These parts were read on each meter to assure meter consistency. Some of the serialized library parts were also shipped with each meter to each assembly facility, but without any readings as taken in ADS Wilmington.

Each facility was first requested to report by telex their reading of the serialized parts. This identified that each meter was working correctly, and that each facility was also using the meter properly. The serialized library units have continued to be periodically read and reported back to ADS Wilmington to maintain a system check. Two years after implementing the procedure, virtually all of the serialized library units read exactly as when originally read.

Each facility then assembled several moisture chips per the documented procedures. Each was serialized, read and returned to ADS

Wilmington. These were then read in ADS Wilmington to assure the accuracy of the readings from each facility.

With user understanding in place and accuracy established, production control was implemented as follows. The using facility would assemble through wirebond an inventory of moisture chips and store these in a nitrogen dessicator. At the start of each shift of header seal, the first lot to be sealed would be baked with five moisture chips from the prepared inventory. Both the baked production parts and the five moisture chip assembled units are then moved into the sealing chamber. The moisture chips are then sealed and removed from the sealing chamber. Readings are then taken for moisture using the Panametrics meter. If the readings are acceptable, production sealing proceeds. If any one reading is rejectable, production sealing does not proceed until the process is corrected and another complete bake, seal and read sequence is acceptably completed. Used moisture chips are serialized, read, logged, and returned for ADS reading to assure facility use accuracy and possible MASS SPEC reading for correlation studies.

TWO YEARS LATER

The described control procedure has been in effect for header assemblies for slightly more than two years. Having used more than 17,000 moisture chips in the previous two-year period and, having also measured another 15,000 production units through MASS SPEC during the same period, several points are clear:

1. Production seal stoppages have occurred where moisture chip readings were high;

2. Rejections at IQC for moisture content as measured by MASS SPEC has been reduced significantly, almost to noise level, and the rejections that do occur are typically borderline or within a plus 20% of the 5000 PPM control point;

3. An enhanced moisture awareness has been effected at each assembly facility;

4. The moisture sensor chip has, as a process tool, assisted in accomplishing the desired goal of controlling moisture at the point of seal and reducing rejections at ADS IQC.

MOISTURE SENSOR CHIP VERSUS MASS SPEC

Having used approximately 17,000 moisture chips in the past two years, and having also measured moisture by MASS SPEC on another approximately 15,000 actual production units over the same time period, reading moisture by the moisture chip and then reading the same units by MASS SPEC seemed an appropriate analysis for assessing correlation between the two techniques. Figure 5 presents a graphic representation comparing the PPM moisture content of 108 moisture chip units as measured first by the Panametrics meter (horizontal axis), and then as measured by MASS SPEC (vertical axis). The small dots are actual MASS SPEC PPM readings for any individual unit at a particular moisture chip PPM reading. The large dots are averages of

the MASS SPEC PPM readings for the group of units at a particular moisture chip PPM reading. Some comments on the data follow:

1. The moisture chip readings are always lower than the corresponding MASS SPEC readings. This is generally attributed to the already discussed measurement differences of the two techniques: MASS SPEC is done at 100°C and examines vapor phase, adsorbed and absorbed moisture while the moisture chip reading is done at 25°C and examines only vapor phase moisture.

2. The wide range of MASS SPEC moisture readings at any one particular moisture chip reading could be argued to be affected: first, by MASS SPEC inaccuracies or tolerances; or second, by moisture chip inaccuracies or tolerances; or third, by variations in sorption and desorption characteristics within the sealed package that would affect the amount of vapor phase moisture available to be detected when read by the moisture chip. All probably contribute, but the variations in the process of eutectic die attach or mounting of the moisture chip probably contributes most to the variation. The moisture chip response is affected by heat exposure: for a given calibration curve in the ADS application, moisture chips deliberately exposed to twice the normal time at the die attach temperature as those used to establish the calibration curve will read a lower moisture level when baked and sealed simultaneously with those units used to establish the calibration curve. This is a point of possible further investigation.

3. In the ADS application, the die attach process is manual so operator variation is present with each assembled moisture chip. Looking at the situation from a broad perspective and assuming this is a relatively constant variation, as is typically the situation with most repetitive manual manufacturing operations, then this variation when examined over many months is probably no more significant then the reading accuracy of MASS SPEC or the accuracy of the moisture chip as affected by the Panametrics fabrication process. Assuming this to be generally appropriate, using both techniques to then measure the moisture of a group of moisture chips generated over a broad period of time would tend to average into any correlation study all the possible variations. Essentially, the affect of the variations would be minimized in their impact, positive or negative, on a correlation examination.

4. Using regression analysis, Figure 5 shows within the 50 to 1000 PPM moisture chip range, or the corresponding approximately 500 to 4500 PPM MASS SPEC range, that there is little correlation between the two techniques at this range as evidenced by the calculated 0.188 correlation coefficient.

5. Conversely, the same regression analysis within the 500 to 2000 PPM moisture chip range, or the corresponding 1500 to 7000 PPM MASS SPEC range, shows an excellent level of correlation between the two techniques at this range as evidenced by the calculated 0.871 correlation coefficient.

SUMMARY

In considering the use of the Panametrics MINI-MOD-HT moisture sensor chip as an in-line process control measurement tool, careful attention must be given to identifying the point at which control is to be effected for the specific application and the procedure through which the actual control process is established. Implemented properly, the MINI-MOD-HT is an excellent and repeatable process control tool.

As applied at ADS for the header package sealing process, the MINI-MOD-HT does demonstrate a promising correlation to MASS SPEC moisture readings. Additional study and evaluation may be necessary to understand the variations affecting the moisture chip response with the intent of further improving the accuracy and correlation to MASS SPEC particularly as relates to an apparent pending MIL SPEC change to a 2000 PPM moisture control limit.

FIGURE 1

ADS use of moisture chip was for control of metal can or header type TO-99 and TO-100 packages. Assembly and sealing of the moisture chip exactly replicates normal production process.

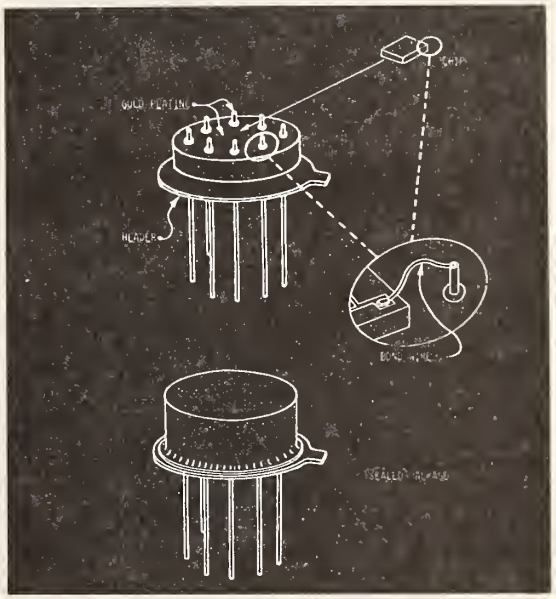

FIGURE 2

Portion of typical ADS device is shown. Bottom half of picture shows many thin film resistors connected to aluminum.

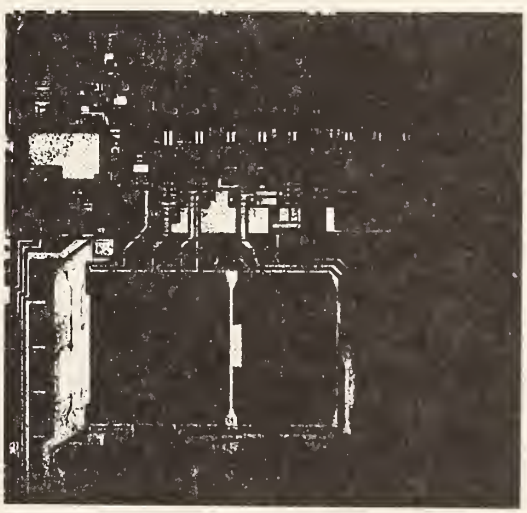

FIGURE 3

Close up of two thin film resistors is shown. Resistor on the left shows a small area of laser trim.

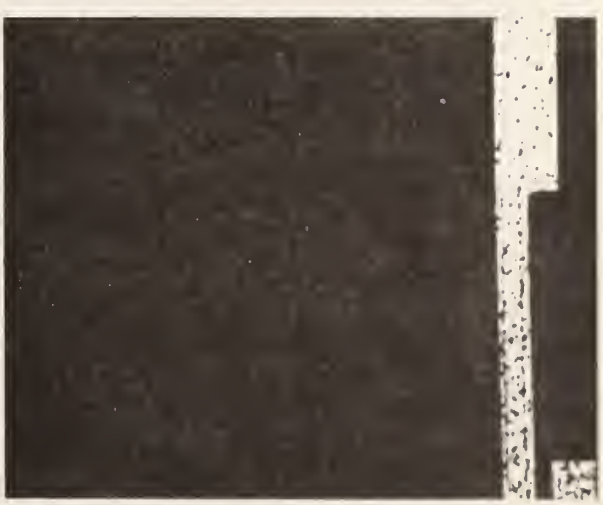

FIGURE 4

Typical calibration curve as generated by Panametrics. The reading of moisture as reported by the Panametrics meter is on the vertical axis and is converted to moisture via the generated calibration curve and down to the horizontal PPM axis.

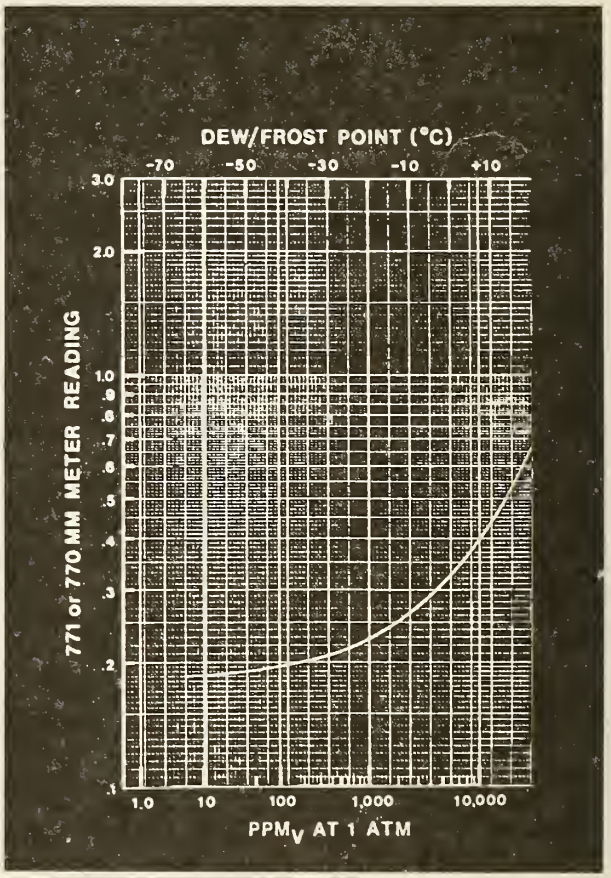

FIGURE 5

Graph of moisture content readings of units measured first with the moisture chip and then by MASS SPEC.

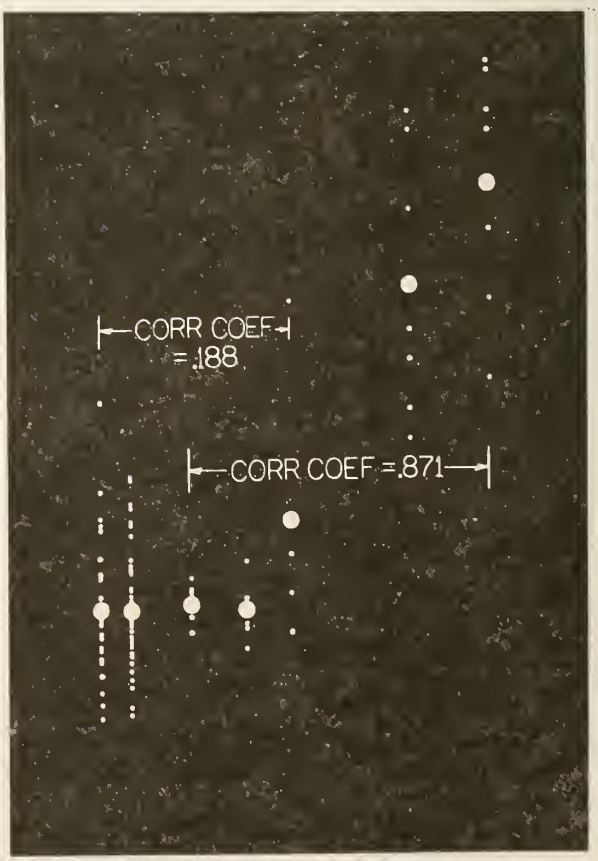

4.5 MONITORING OF MOISTURE IN CERDIP DEVICES USING A MOISTURE SENSOR CHIP

John Hunter
Advanced Micro Devices, Inc.
901 Thompson Place
P.O. Box 3453
Sunnyvale, CA 94088
(408) 749-3089

ABSTRACT

For effective process control over moisture levels in cerdip package assembly a method of measurement is needed which can (a) be readily set up within the manufacturing facility and (b) provide results in a time short compared with the assembly cycle time.

A moisture sensor which can be incorporated into an actual cerdip package satisfies these requirements. The paper will describe some practical aspects of implementing such a sensor (the Panametrics Mini-Mod HT) in a production situation. The aspects covered will be:

(a) calibration against mass spectroscopy (previous publications on this topic were found not to be applicable in all cases);

(b) effects of assembly processing variables on the sensor readings (in particular, sensor readings are not stabilized until some time after seal; also any high temperature operations after seal impact the readings obtained); and

(c) recommended method of use.

The conclusion is that this moisture sensor chip is an effective in-line monitor; moreover it can also be used as a powerful problem solving tool, in which respect it is superior to mass spectroscopy because it is (a) quick and (b) non-destructive. However, calibration against mass spectroscopy is not straightforward; and this calibration is affected by changes in assembly process flow and package configuration.

INTRODUCTION

There have been several publications about alumina moisture sensor chips, including References 1 and 2, which describe the principal of operation of the Panametrics Mini-Mod HT and how its electrical impedance can be calibrated against moisture levels inside cerdip packages. These references conclude that the Mini-Mod HT can be a reliable means of determining pass or fail to the limit of 5000 ppm_V as defined in Method 1018 of Mil-Std-883B. They also make the point that such a moisture sensor chip can provide a valuable means of in-line process control, since a measurement can be taken quickly and easily shortly after seal.

This facility for process control is especially useful in an offshore assembly operation remote from laboratories capable of performing moisture analysis by mass spectroscopy. Therefore it was decided to implement the Panametrics Mini-Mod HT as an in-line process control for cerdip assembly in AMD's offshore assembly plants. This paper will describe some of the difficulties which were encountered during this implementation, and how they were resolved. All of the measurements were carried out on 24 lead cerdip packages.

DESCRIPTION OF PREVIOUS CALIBRATION PROCEDURE

It is necessary to summarize some of the calibration data contained in References 1 and 2 in order to clarify the situation.

The first stage in calibration is to determine the relationship between chip impedance (as measured by a meter manufactured by Panametrics called the Model 770MM) and the amount of moisture per unit volume in the atmosphere adjacent to the chip's surface. This calibration is actually unique for each individual chip; however the variation from chip to chip within one batch is small enough that one calibration curve can accurately represent all chips within that batch. This calibration is performed as a service by Panametrics and Figure 1 shows an example of one such calibration, which is obtained by decapping a package containing a sensor chip and measuring its impedance as it is exposed to atmospheres of various known humidities.

Now there are two components to the moisture inside a sealed cerdip package. One component is the moisture present as vapor. This is the component which is detected by the sensor chip. The other component is the moisture which is adsorbed (more or less tightly) on the internal surfaces of the package. This component is not detectable by the sensor chip, but part of it will contribute to a mass spectroscopy measurement. This is because some of the adsorbed moisture will desorb from the internal surfaces under the high temperatures and lower pressures obtained during the measurement. So, in order to obtain a value which can be referred to as an "equivalent mass spectroscopy value", it is necessary to do a direct calibration of ppm_{VSC} (ambient vapor moisture level as directly detected by the chip) against ppm_{VMS} (moisture level obtained by actual mass spectroscopy). The experimental relationship obtained in Reference 1 was:

$$ppm_{VMS} = [6.42 \times 10^6 \ (ppm_{VSC})]^{0.397} \quad \ldots\ldots (1)$$

This relationship (which is shown graphically in Figure 2) is a best fit to a series of measurements on 14/16 lead cerdips sealed by various manufacturers using various sealing glasses. The relatively large amount of moisture desorbable from the internal surface can be seen from Figure 2. For example, the Mil-Std-883B limit of 5000 ppm_V as measured by mass spectroscopy (ppm_{VMS}) corresponds to only 300 ppm_V as detected by the sensor chip (ppm_{VSC}).

This completes the calibration procedure, enabling a meter reading to be converted to an equivalent mass spectroscopy value. It would seem relatively straightforward to implement this procedure directly; however, in practice, some difficulties appeared. One concerned calibration against mass spectroscopy; the second changes in meter reading after seal.

CALIBRATION AGAINST MASS SPECTROSCOPY

Initial measurements used equation (1) to calculate the equivalent mass spectroscopy values, and the results were suspiciously high. Therefore, it was decided to do an independent calibration against mass spectroscopy. Twenty-eight units sealed with sensor chips were sent to Oneida Research Services, Inc. for mass spectroscopy analysis. The crosses shown in Figure 3 are the actual calibration points; the continuous curve is calculated as a best fit to the experimental points; and for comparison, the dotted curve is a graphical representation of what would be obtained by applying equation (1). It is apparent that the value of ppm_{VMS} calculated from equation (1) is appreciably higher than that which was actually obtained.

[It should be noted that Figure 3 is a direct plot of meter reading against mass spectroscopy, whereas the procedure previously described involves two stages; first, meter reading to ppm_{VSC}; second, ppm_{VSC} to ppm_{VMS}. The reason for this two-stage method is that the relationship between meter reading and ppm_{VSC} varies from batch to batch, so a separate calibration curve should be used for each batch of sensor chips. However, the calibration curves for the first three batches received were so close that it was decided, in the interests of simplicity, to use a constant calibration curve, enabling a direct translation of meter reading to equivalent mass spectroscopy.]

It is assumed that the prime reason for the discrepancy between the two curves shown in Figure 3 is the fact that the experimental vehicles used were 24 lead devices, which have a much larger internal volume than the 14/16 lead devices used to generate equation (1). With 24 lead packages, the ratio of moisture adsorbed on the internatal surfaces should be smaller than for 14/16 lead packages, due to the lower surface area:volume ratio. This explanation is consistent with the results obtained. In any case, it is clear that the correlation to mass spectroscopy is a function of internal package configuration, and a separate calibration should be carried out for each new package configuration.

CHANGES IN MEASURED VALUE AFTER SEAL

It was observed that the meter reading of a given sensor chip fell significantly during the first few days after seal, simply during storage at room temperature. An actual example is shown in Figure 4, where the fall after 3 days corresponds to an apparent decrease of over 1000 ppm. The presumed explanation for this effect is that a few days are required for equilibrium to be reached in the process of adsorption of moisture on to the internal surfaces of the package. The problem introduced by this effect is that it is necessary to wait a few days after seal before a valid reading can be taken - this detracts somewhat from the immediacy of feedback necessary for effective process control.

This phenomenon was not the only type of change in meter reading after seal. All cerdip production lots are processed through the standard Mil-Std-883B screens, including High Temperature Storage (24 hours at 150°C). After this bake, the sensor chip meter readings were lower than before (see example shown in Figure 5). The fall in meter reading during this baking operation is typically greater than that which occurs simply by storage at room temperature.

To investigate this effect further, an experiment was done to see if similar results could be detected by mass spectroscopy. A random sample of 20 units was pulled from a production lot directly after seal. The lot was then processed through High Temperature Storage, after which a further random sample of 20 units was pulled. The samples were sent together to Oneida Research Services for moisture measurement by mass spectroscopy. Histograms of the results are shown in Figures 6 and 7, which show a fall in measured moisture which parallels that detected by the sensor chip. This shows that during the bake some of the moisture vapor is adsorbed "permanently" on some of the internal surfaces of the package - permanently enough, at any rate, to survive the temperature and pressure conditions of the mass spectroscopy measurement.

Permanent moisture reduction inside hermetic packages through chemical reactions has been described (Reference 3). It may be that such reactions occur during the High Temperature Storage process;

e.g. $Si + 2H_2O \rightarrow SiO_2 + 2H_2$

However, hydrogen was not detected consistently in all the packages analyzed, so this may not be the complete explanation, especially since the lowest temperature evaluated in Reference 3 was 250°C, and maybe 150°C would be too low a temperature for appreciable chemical reaction to occur. It could be that the adsorbed moisture is bound with various degrees of tightness from loose physical bonding to a full chemical reaction. This seems to be an area worthy of more investigation, for this reason:

Any baking operation done after seal, but before moisture measurement, can affect that measurement. The 150°C, 24 hour bake just described caused a reduction; on the other hand, a lower temperature or shorter bake might increase measured values by causing desorption of moisture from internal surfaces. Better understanding of the mechanisms involved would enable more meaningful measurements to be done.

Anyway, this particular investigation was limited to establishing a sensor chip measurement method that could be reliably related to mass spectroscopy. It was concluded that this could only be done by measuring the sensor chip after exposure to all high temperature post seal operations (which in this case included not only High Temperature Storage but also Temperature Cycling).

(Incidentally, all the data points in Figure 3 were obtained on units which had been processed through these high temperature operations.)

This means that a measurement cannot be taken until a few days after seal. As previously shown, such a delay is necessary anyway, even if no high temperature operations were carried out, due to the effect shown in Figure 4. However, even though this delay somewhat reduces the efficiency of feedback, the technique remains an effective process control, since it is still a lot more immediate than sending samples out to a mass spectroscopy laboratory.

CONCLUSIONS

The Panametrics Mini-Mod HT is a useful and reliable means of in-line moisture monitoring. However, the following precautions should be taken.

1) Calibrate each individual package configuration individually against mass spectroscopy.

2) Take a reading only after the level of moisture vapor has stabilized itself through all post-seal processes.

REFERENCES

1) "Recent Advances in Al_2O_3 "In-Situ" Moisture Monitoring Chips for Cerdip Package Applications" by J.B. Finn (Mostek) and V. Fong (Panametrics) - March 1980 IEEE.

2) "Moisture Sensors, Mass Spectroscopy and Mil Standards" by John C. Hale (Texas Instruments) and Victor Fong (Panametrics) - National Bureau of Standards, November 5, 1980.

3) "Attaining Low Moisture Levels in Hermetic Packages" by White, Striny and Sammons of Bell Telephone Laboratories - July 1982 IEEE/Proc. IRPS.

FIGURE 1

CALIBRATION OF METER READING TO PPM_V

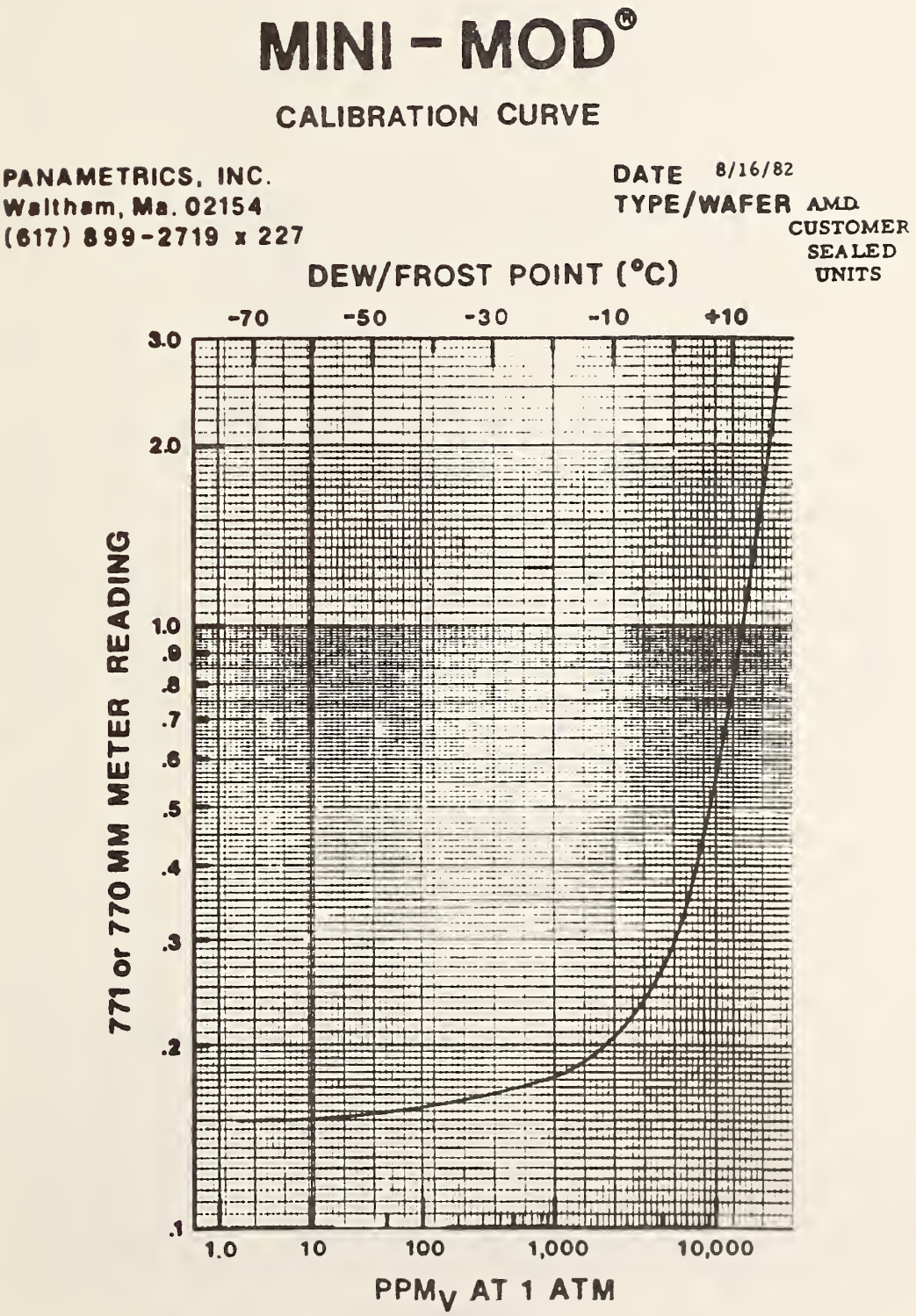

FIGURE 2

CHIP CALIBRATION VERSUS MASS SPECTROSCOPY

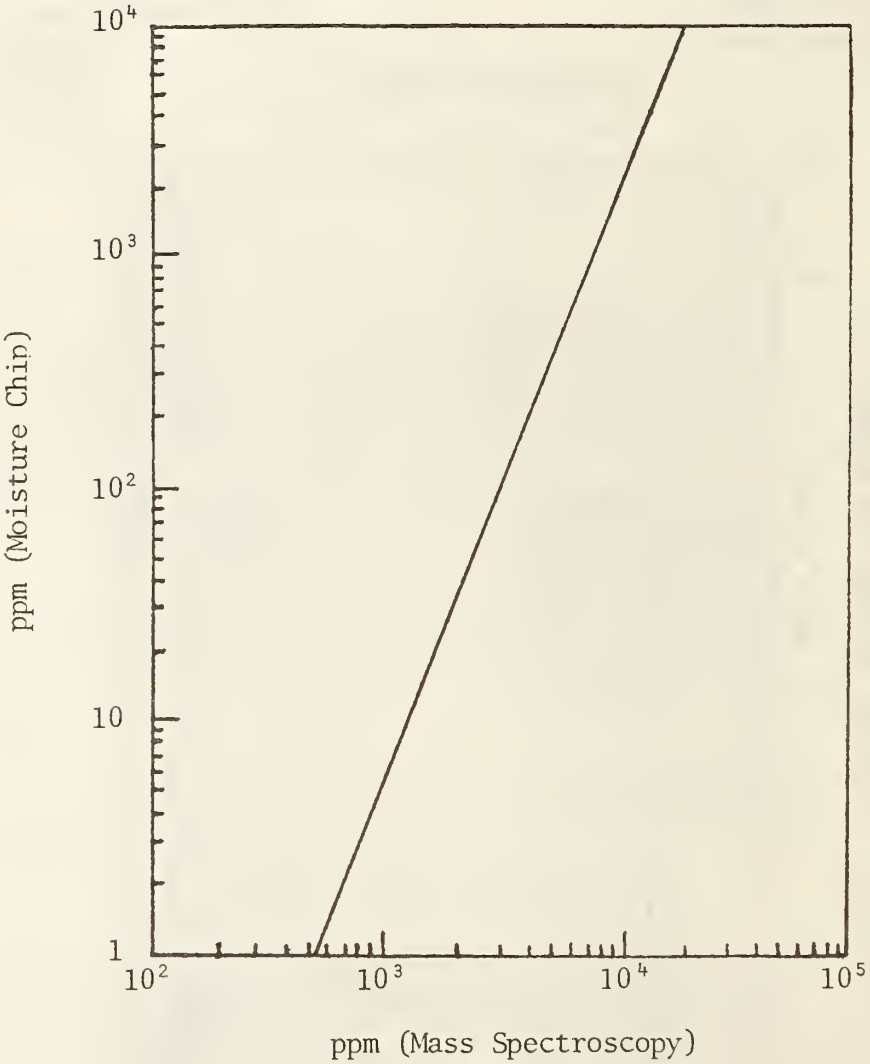

FIGURE 3

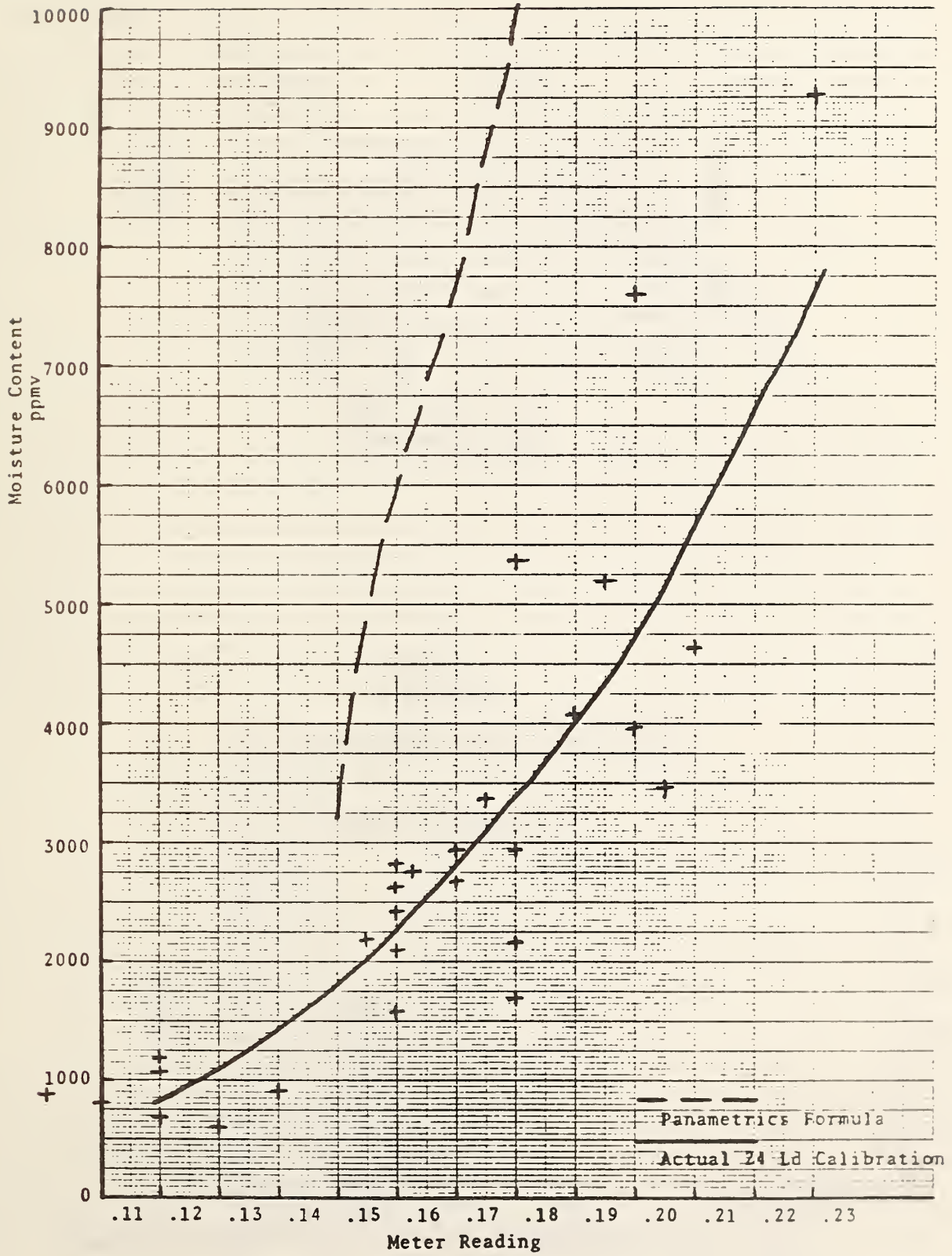
10000
9000
8000
7000
6000
5000
4000
3000
2000
1000
0
Moisture Content
ppmv
.11
.12
.13
.14
.15
.16
.17
.18
.19
.20
.21
.22
.23
Meter Reading
Panametrics Formula
Actual Z4 Ld Calibration

FIGURE 4

CHANGES IN MEASURED VALUE AFTER SEAL

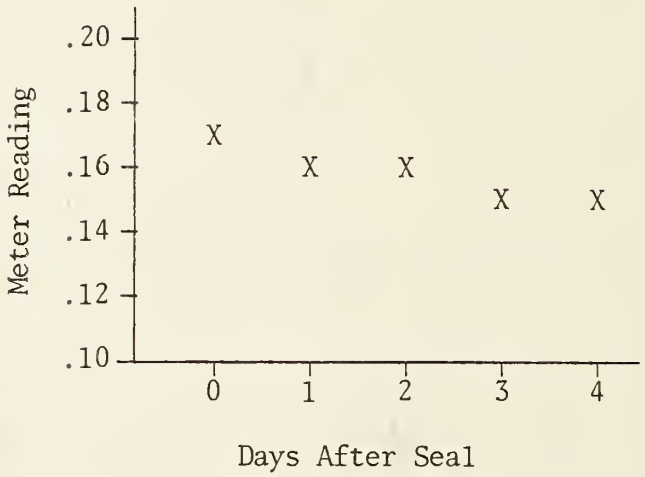

FIGURE 5

CHANGES IN MEASURED VALUE AFTER SEAL

(24 Hours at 150°C)

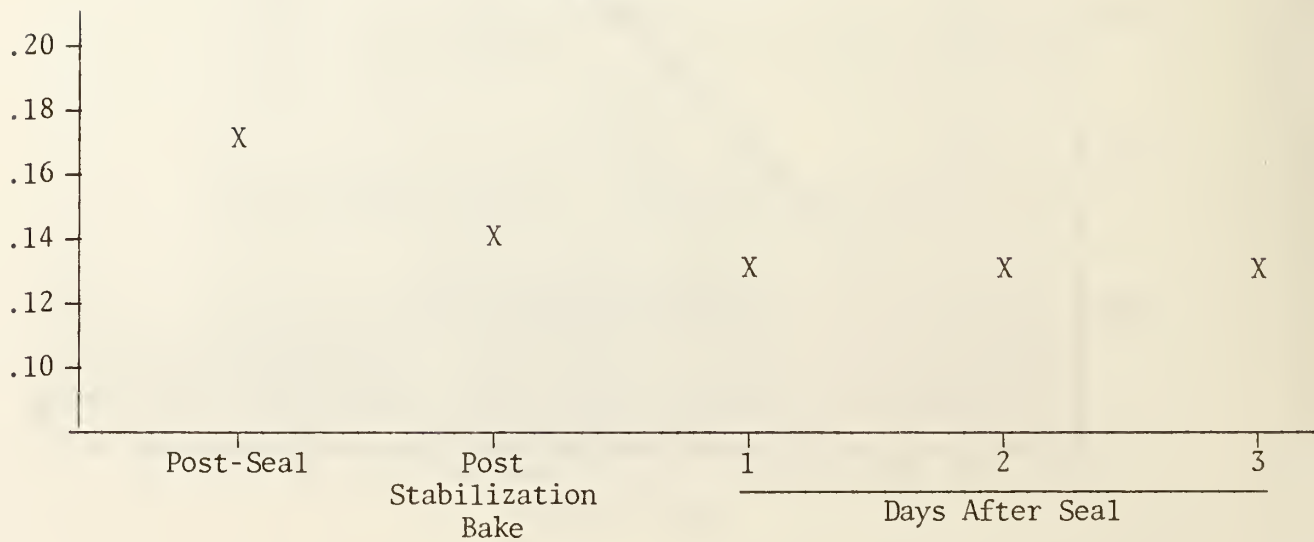

FIGURE 6

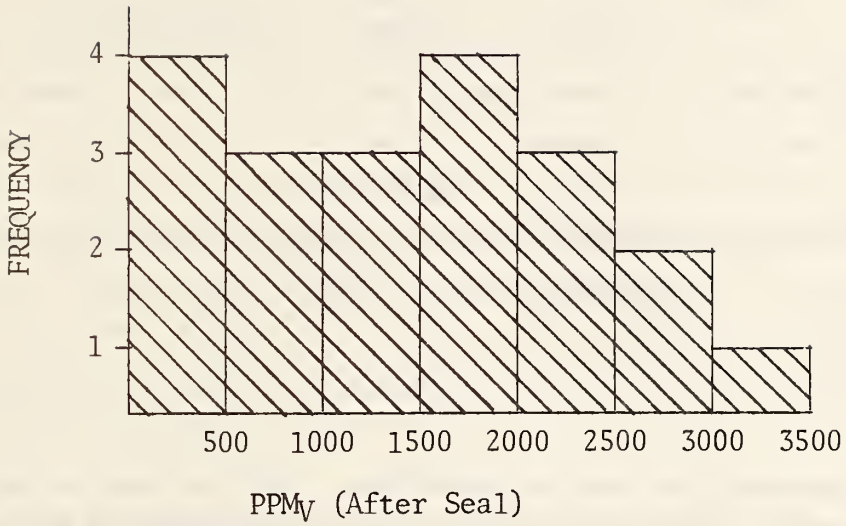

FIGURE 7

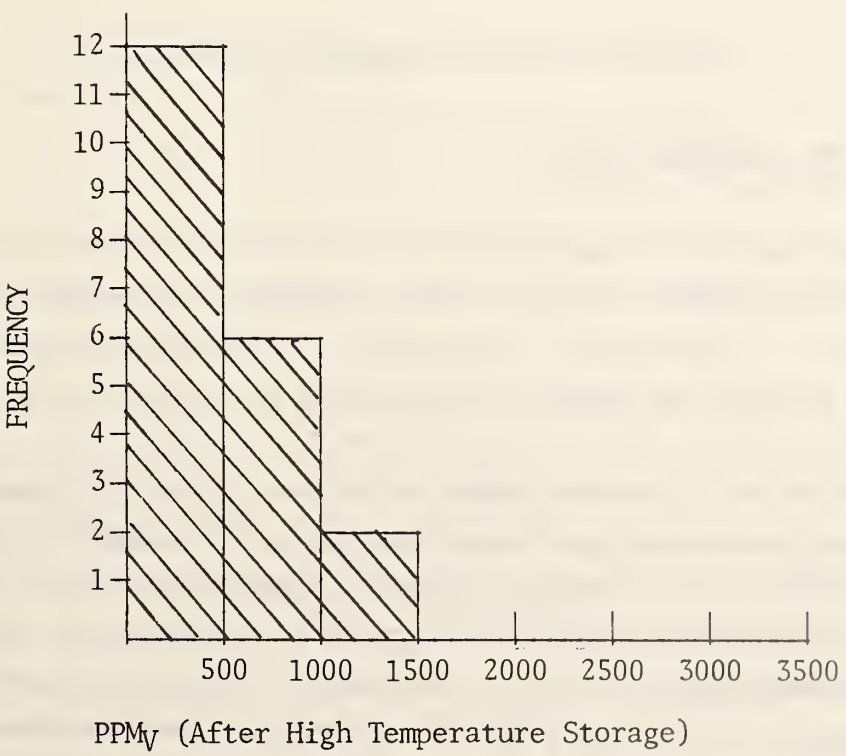

5. SESSION IV HERMETICITY AND MOISTURE

5.1 HOW TO RAISE THE PERMISSIBLE LEAK RATE BY FOUR ORDERS OF MAGNITUDE

J. Gordon Davy
Westinghouse Manufacturing Systems and Technology Center
9200 Berger Rd., Columbia, MD 21045

ABSTRACT

This paper presents bad news and good news. The bad news is that the maximum permissible leak rates specified in the military standards are too large by at least 3 orders of magnitude, and that for microelectronic packages the true values are too small to measure. The good news is that the true permissible leak rate can be raised by four orders of magnitude or more by the inclusion in the package of means to capture water as it enters through small leaks. Three different means are presented. Experimental studies are needed before any specification changes are made. Also, expressing moisture level in terms of dew point and ppmV is misleading and should be avoided.

WHAT IS THE TRUE PERMISSIBLE LEAK RATE?

Expressing the Moisture Level

The maximum permissible leak rate for semiconductor devices is determined by the maximum permissible increase in the internal moisture level. Since moisture level is expressed in many ways, it is desirable to begin by considering how best to express the level for this application.

Moisture levels based on measurement by an in-situ device (alumina capacitor, interdigitated structure) are often reported as a measured or calculated dew point. Dew point is an inappropriate measure because it neglects the primary role of adsorption during the cooling process. In fact, the behavior of water in small sealed packages cannot be understood or explained apart from an understanding of adsorption. For such packages, a dew point may not even exist [1].

Moisture levels based on measurement by a gas analysis system are often reported in parts per million by volume (ppmV). The unit ppmV is appropriately used as a measure of relative abundance of the gas of interest (water in this case) to the total of all gases. It is the ratio of the partial pressure of water vapor to the total pressure, or the ratio of the number of water molecules per unit volume to the number of all gas molecules per unit volume. Relative abundance is what is determined by a mass spectrometer, but it does not indicate how wet a package is. For example, in most vacuum systems the background pressure is due primarily to water vapor. The relative abundance of water in such systems is well above 500,000 ppmV, but that does not mean they are wet.

Sometimes the relative abundance is multiplied by the total internal pressure, to correct to one atm, but the resulting number is still reported as ppmV. This is actually a misleading way of referring to the partial pressure of water vapor in millionths of an atmosphere or microbars. As an example, 5000 ppmV (referred to 1 atm) equals 5000 microbars, alternately expressed as 5 millibars or 5×10^{-3} atm. (The partial pressure of a gas in a mixture of gases is the pressure that would be measured for that gas if it were the only gas present.)

Since it is the partial pressure and not the relative abundance of water vapor that indicates the wetness of the package, partial pressure is what should be used. Conversion is simple. The partial pressure in microbars is numerically equal to the relative abundance in ppmV, multiplied by the internal pressure. If the internal pressure is unknown, it can be calculated by dividing the gas content found during gas analysis (in pressure-volume units such as atm cm^3) by the gas volume of the package.

Another useful way of referring to moisture level is the relative humidity. RH is the ratio of the partial pressure of water vapor at a given temperature to the saturation vapor pressure (maximum possible partial pressure) at that temperature. The saturation vapor pressure of water increases exponentially with temperature. Its value is well established for all temperatures and can be found in reference handbooks. The alumina capacitor responds (with a temperature coefficient) to the relative humidity [1].

The moisture level can also be expressed as a vapor density in units of grams or moles per unit volume of vapor space. The mass of water vapor per unit volume, m/V, corresponding to a partial pressure of 5×10^{-3} atm can be calculated by assuming ideal gas behavior, which is reasonable for pressures less than the saturation vapor pressure (i.e. for relative humidity less than 100%): $m/V = PM_w/RT$, where R, the gas constant, is expressed as 82.06 atm $cm^3 mole^{-1} K^{-1}$ and M_w is the molar mass of water, 18 g $mole^{-1}$. Taking T = 298K for room temperature, m/V is 3.7 μg cm^{-3}.

Dividing the mass of water vapor present in the package by the internal surface area gives a measure of susceptibility to surface leakage currents if it were to condense or be adsorbed: one monolayer is approximately 30 ng cm^{-2}.

It is also important to distinguish which moisture level in the package is being referred to [1]. Total moisture includes not only water vapor, but also adsorbed and absorbed water. Total moisture is determined by those gas analysis techniques which integrate the moisture signal over time after package puncture. It includes water which until puncture was not water vapor and thus was unavailable for adsorption or condensation upon cooling. The appropriate way to measure the moisture level by gas analysis is to soak the package at the maximum anticipated storage temperature long enough for equilibrium to be established (this sets the maximum level of water vapor), and then measure the moisture level based on the peak value as quickly as possible after puncture.

The reason for this method is that puncturing upsets the equilibrium; it is important to minimize the contribution due to water which enters the vapor phase after puncture. The time to reach equilibrium depends on materials present in a package. The time constant for physisorption (metal surfaces) is less than a second; for chemisorption (ceramics) and absorption (organic materials such as adhesives) it may be days. If such latter materials are present, in significant quantities, the required time should be determined by experiment.

Calculating the Permissible Leak Rate

The maximum permissible leak rate is calculated by calculating the rate at which water vapor can be permitted to enter the package. It involves:

1. The package internal cavity (gas) volume V cm^3.

2. The required lifetime (including storage) of the package, t_ℓ years.

3. The maximum permissible moisture level. Though generally taken as 5×10^{-3} atm (5000 ppmV) at 100°C, the actual physical requirement is that there not be a layer of surface water thick enough to allow enough current flow for dendritic growth or corrosion. The surface water need not be condensed (in fact the RH can be as low as about 35% at room temperature); adsorbed water a few molecular layers thick has been found sufficient [2], even down to temperatures of -20°C. (At lower temperatures, ion mobility is slow enough to not be a problem.)

   It should be understood that if the water vapor is at the maximum permissible level, then no further increase in moisture level is acceptable, and the permissible leak rate is zero. This of course cannot be measured. In other words, <u>the moisture level at the time the package is sealed should be low enough to give a safety margin for water vapor which enters through the maximum permissible small leak during the lifetime of the package.</u>

   For the calculation which follows, it is assumed that the room-temperature moisture level in the package can be allowed to increase during the package lifetime by an amount Δp_w of 5×10^{-3} atm. It should be remembered that microelectronic packages have a large ratio of internal surface area to internal volume, so that the level of water vapor drops sharply as the package is cooled. Thus the tolerable partial pressure of water vapor in the package at room temperature (for example) is higher than at 0°C.

4. The average ambient moisture level p_{wa}, which varies with the intended application of the device. To bracket the range, two values are considered:

   a. p_{wa} = 0.043 atm, corresponding to 100% RH at 30°C or 75% RH at 35°C. This applies to the tropics.

   b. p_{wa} = 0.011 atm, corresponding to an air-conditioned office. For this case, an unacceptable rise in the RH and amount of adsorbed water would be a possibility if the package were taken outdoors on a cold day.

The maximum rate at which water vapor can be allowed to enter a package is given by

$$R_{wmax} = \Delta p_w V / t_\ell \qquad (1)$$

This rate, which is not directly measurable, needs to be converted to an air-equivalent standard leak rate L - the rate at which air at 1 atm pressure (absolute) on one side of the leak would escape into vacuum on the other. The relationship between rates under different conditions depends on the type of gas flow that exists. For this calculation, it will be assumed that the transport mechanism for gas molecules through a leak is molecular flow. This means that the leak rate for any gas is proportional to the difference in partial pressure for that gas between inside and outside the package, and to the inverse square root of the molecular mass of the tracer gas.

The maximum permissible air-equivalent standard leak rate is given by

$$L_{max} = R_{wmax}(1 \text{ atm}/p_{wa})(M_w/M_a)^{1/2} \qquad (2)$$

where M_w and M_a are the molecular masses of water (18) and air (28.7). Use of the values discussed for Δp_w and p_{wa} leads to

$$L_{max}(\text{tropics}) = 2.9 \times 10^{-9} V/t_{\ell} \qquad (3a)$$

$$L_{max}(\text{office}) = 1.1 \times 10^{-8} V/t_{\ell} \qquad (3b)$$

It is sometimes felt that the entry of water vapor could be reduced if the package were pressurized. The intuitive impression is that the gas inside would prevent the entry of air by blowing it back. However, for small leaks, the principal flow mechanism is molecular flow, in which encounter between gas molecules along the leak path is rare. Note that the equations above do not depend on the initial pressure in the package. Thus, pressurization does not reduce the rate of entry of water molecules.

Comparison with Military Standards

Figure 1 compares the permissible leak rate based on maximum allowable internal moisture level (tropics and office) for an assumed 10-year lifetime with the rates specified in the military standards. The conclusions to be drawn from this figure are:

1. There are no specifications directly applicable to large packages.
2. The existing specifications are somewhat inconsistent.
3. The existing specified leak rates do not increase linearly (as they should) with package volume.
4. The existing specifications exceed the limits calculated by the techniques presented here by three to four orders of magnitude. In other words, the existing specifications can only guarantee protection from moisture for lifetimes of days or weeks, not years.

It is important to note that measuring leak rates smaller than 10^{-8} atm cm^3 sec^{-1} presents formidable difficulties. Also, very small leaks tend to plug by themselves from ordinary handling. The plug may prevent tracer-gas flow during leak testing but be permeable to water. If leak test results are to be reliable, packages must be handled carefully to prevent this plugging until after the final test. One way around the problem of needing to measure small leak rates is to look for increases in the internal moisture level, using an in-situ moisture sensor or a bare integrated circuit chip [2].

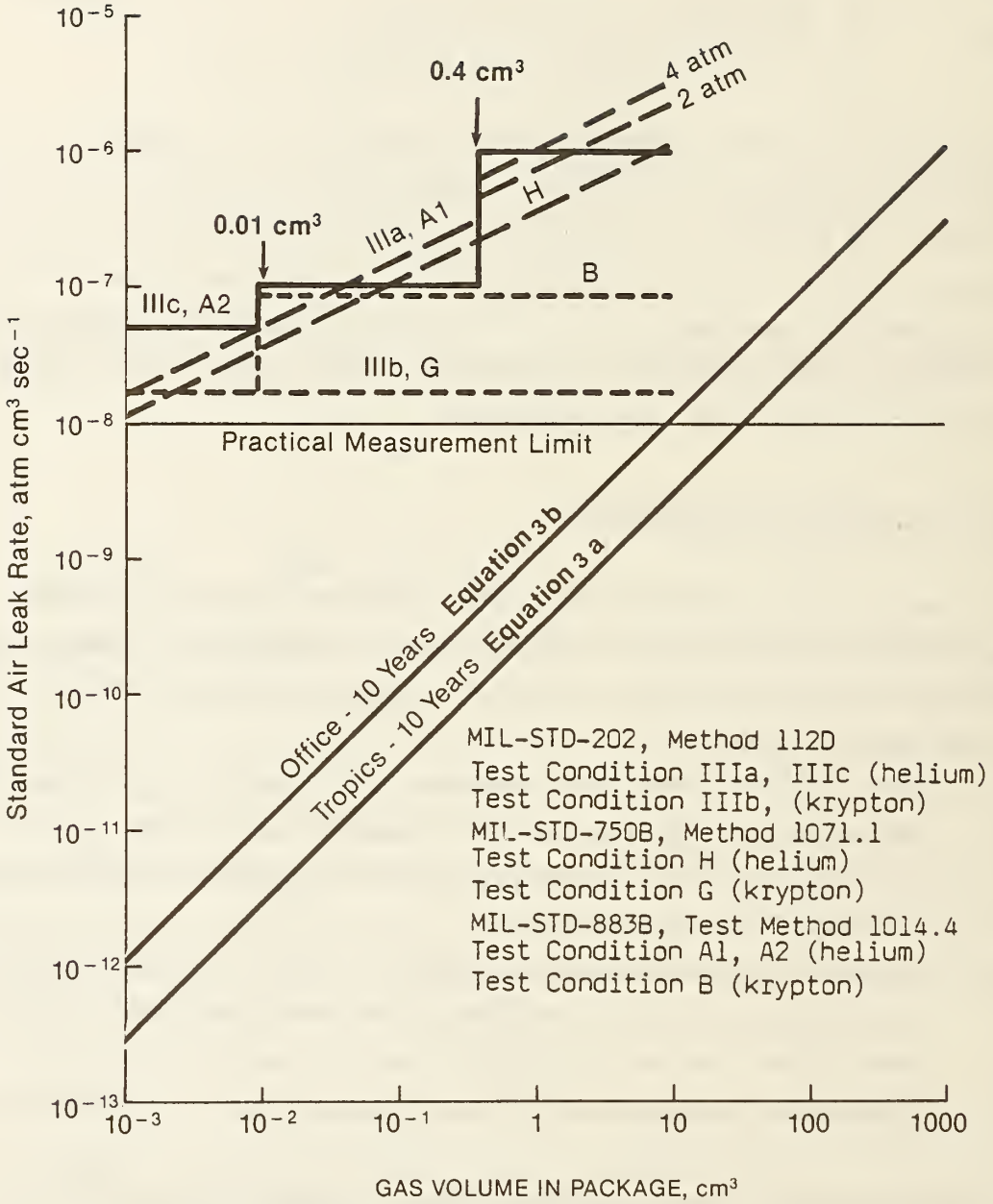

Figure 1 Calculated Maximum Permissible Leak Rates Compared with Military Specifications Rates by Various Methods

A reasonable question to raise is why, with such difficult-to-meet requirements, aren't there more moisture-related failures? There are several possible answers.

1. Many packages are truly hermetic - they don't leak at all.
2. Many packages live in environments where chilling never occurs(e.g., an office).
3. Water condenses, but not where it can cause problems, because the vulnerable areas run hotter than the ambient.
4. Water gets used up as fast as it gets in by reacting chemically with the materials of construction of less-critical parts (e.g., rusting of package walls).
5. There are no vulnerable areas (chip passivation is defect-free, surfaces are conformally coated, etc.).
6. The failure is not recognized by service personnel as moisture-related and thus is not reported.

There have been many published reports of attempts to establish a statistical correlation between moisture level or leak rate and failure rate of microelectronic devices. Unfortunately none has been successful, in spite of the fact that the role of water in causing failures is well established.

HOW CAN THE PERMISSIBLE LEAK RATE BE INCREASED?

The strategy for increasing the permissible leak rate is to capture the water as it leaks in, so it does not become available as water vapor. This can be done by the use of a suitable dessicant, or by decomposing the water in a chemical or electrochemical reaction.

Molecular Sieve Dessicant

Molecular sieve is the term used to refer to a class of synthetically produced crystalline alumino-silicates that have been "activated" for absorption by removing their water of hydration. This dehydration does not cause a change in structure. Instead, it leaves pores approximately the size of water

molecules. The name derives from its property of being open to small molecules while excluding large ones. While dessicants are often said to adsorb water, in the case of molecular sieve it is actually a bulk rather than a surface process, and thus the term absorption is more appropriate. Molecular sieves can be purchased inexpensively from chemical supply houses in the form of small pellets or spheres.

Molecular sieve dessicant allows the permissible leak rate to be increased, because a far greater mass of water can exist in the package for a given relative humidity. Figure 2A shows for four temperatures how the relative humidity varies with the weight percent of water which type 4A molecular sieve has absorbed [3]. The curves for types 3A and 5A sieve are similar.

As a package containing the sieve is heated, a very small fraction of the absorbed water desorbs, causing the relative humidity to increase somewhat. The results can be predicted adequately by assuming that the weight percent of absorbed water does not change. It can be seen that if the dessicant contains 10 weight percent water and is at equilibrium with the ambient in the package, the relative humidity is very low - not only at 0° and 25°C, but even when heated to 100°C or 125°C. In fact, the partial pressure at these latter temperatures is 6×10^{-3} and 12×10^{-3} atm respectively. When the hot package is allowed to cool, re-absorption reduces the partial pressure again, although it may take some time to return to complete equilibrium. The superiority of molecular sieve to other dessicants in retaining water when heated is shown in Figure 2B.

The specific gravity of the sieve is about 0.75. If 50% of the gas volume in the package is occupied by molecular sieve, and this sieve is allowed to absorb 10% of its weight in water, the mass of water per unit volume is $m/V = 0.75 \times 0.5 \times 0.1 = 37$ mg cm^{-3}.

In the assumptions upon which equations 3a and 3b are based, the pressure was allowed to increase by 5×10^{-3} atm. The mass of water causing this pressure increase was calculated above as 3.7 μg cm^{-3}. The ratio of m/V (50% sieve) to this figure is 10^4, which means that the use of molecular sieve in the package increases the permissible leak rate by this factor. This increased rate is large enough to measure even for small packages (see Figure 3).

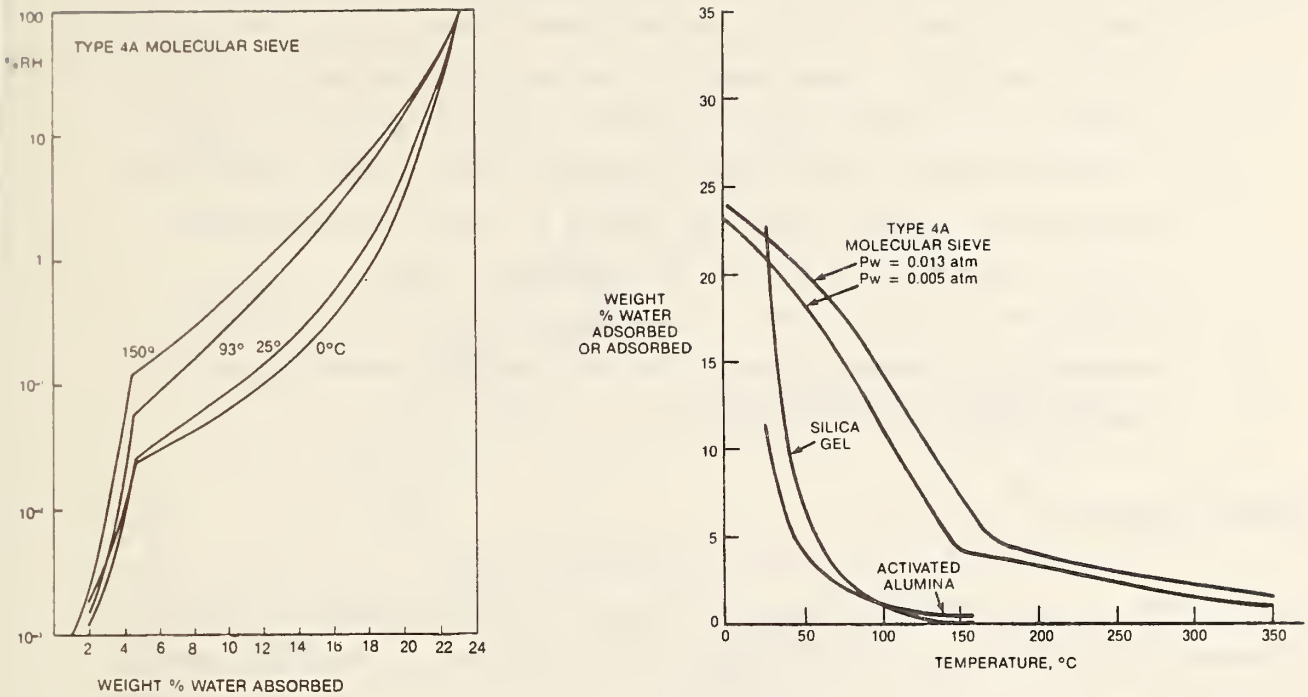

Figure 2. A. Isotherms for Type 4A Molecular Sieve; B. Isobars for Three Dessicants: Silica Gel and Alumina (p_{wa} = 0.013 atm) and Type 4A Molecular Seive (p_{wa} = 0.005,0.013 atm).

WITH DESSICANT

$$L_{max}(\text{tropics}) = 2.9 \times 10^{-5} V/t_l \qquad (4a)$$

$$L_{max}(\text{office}) = 1.1 \times 10^{-4} V/t_l \qquad (4b)$$

The results are proportional, of course, so that if 25% of the gas volume is occupied by molecular sieve, the permissible leak rate is increased by 5,000 instead of 10,000.

The dessicant could be in a paper bag, or held in place as a covering on the underside of the cover with an adhesive which was permeable to water vapor. Unfortunately, the use of dessicants in microcircuit packages is prohibited (without express approval) by MIL-STD-454G, Requirement 64 and MIL-M-38510E.

There are two reasons for the military's reluctance to accept dessicants [4]:

1. There have been some bad incidents when another type (not molecular sieve) was used. Upon heating, the dessicant released a significant amount of water which upon chilling condensed before it could be re-adsorbed (see Figure 2B). Molecular sieve differs from other desiccants in that is must be heated far above normal maximum storage temperatures before it releases its water.
2. Every new material added to a package has to be evaluated for unexpected secondary effects, and may require screening by the manufacturer or user for purity.

Chemical Reaction

Another way of capturing the water that leaks into the package is by an irreversible chemical reaction, referred to as gettering. Here are several possibilities:

1. Reaction with an unplated area on the underside of the Kovar lid of a hybrid package, burnished just before sealing to expose fresh metal, to form rust and hydrogen gas. This reaction may be partially reversible and thus not as reliable as the other possibilities [5].
2. Reaction with silicon in gold-silicon eutectic, melted in a dry environment to expose fresh silicon, to form silicon oxide and hydrogen [6].
3. Reaction with a suitable metal such as barium that is evaporated after the package is sealed - a method that has been widely used for vacuum tubes, to form metal oxide and hydrogen.
4. Reaction with suitably packaged calcium carbide to form calcium hydroxide and acetylene gas [7].

The carbide reaction is

$$\underset{\text{calcium carbide}}{CaC_2} + 2\,H_2O \longrightarrow \underset{\text{calcium hydroxide}}{Ca(OH)_2} + \underset{\text{acetylene}}{C_2H_2}$$
(water)

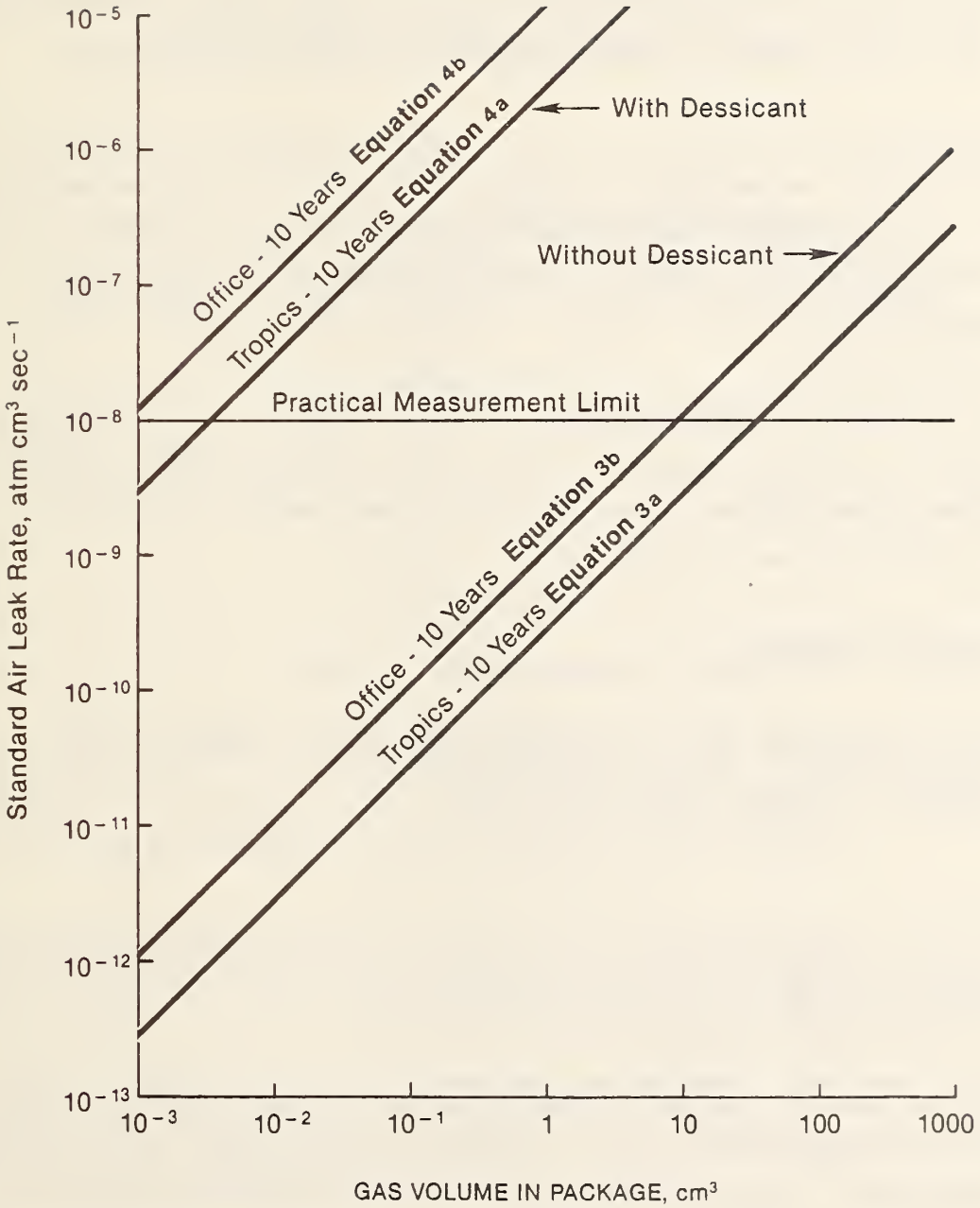

Figure 3 Maximum Permissible Leak Rate for Packages Containing 50% Molecular Sieve Dessicant Compared to Rates Without Dessicant

The equation above shows that one mole of carbide reacts with two moles of water. Assuming (as for molecular sieve) a 50% filling of the package and given a specific gravity of 2.22 and molecular mass of 64.1 for calcium carbide this means that 623 mg of water per cm^3 of gas volume can be allowed to leak in. This is about 17 times greater than for molecular sieve.

The acetylene partial pressure rises only until a steady-state condition develops, at which one molecule of acetylene escapes for every two molecules of water entering. Using a method similar to that shown in the next section, the corresponding partial pressure is calculated to be 0.62 p_{wa}, a few hundredths of an atm.

An example of suitable packaging might be a paper bag or a thin coating of an adhesive which would be permeable to water vapor and acetylene. Since calcium carbide is not really a dessicant, it is not clear whether there is any military restriction on its use.

Electrochemical Reaction

Water can be decomposed into its elements hydrogen and oxygen by the electrochemical reaction called electrolysis:

$$2\ H_2O \longrightarrow 2\ H_2 + O_2$$

Required is a suitable medium for carrying water molecules to the electrodes, and a potential difference of at least two volts.

This could be done in a sealed package by use of a special material referred to as a solid polymer electrolyte, a sulfonated fluorocarbon with the DuPont trade name Nafion. This material has been used for moisture analysis in gas streams [8], using it in the form of a thin-wall tube with platinum wire spirals inside and out for electrodes.

A sheet of Nafion could have an electrode grid applied to each side, say by evaporation (see Figure 4). A piece could be mounted in a sealed electronic package with the electrodes attached to two feedthrough pins. Most electronic packages are connected to a DC power supply of at least 3 volts anyway, so no additional external wiring would be involved.

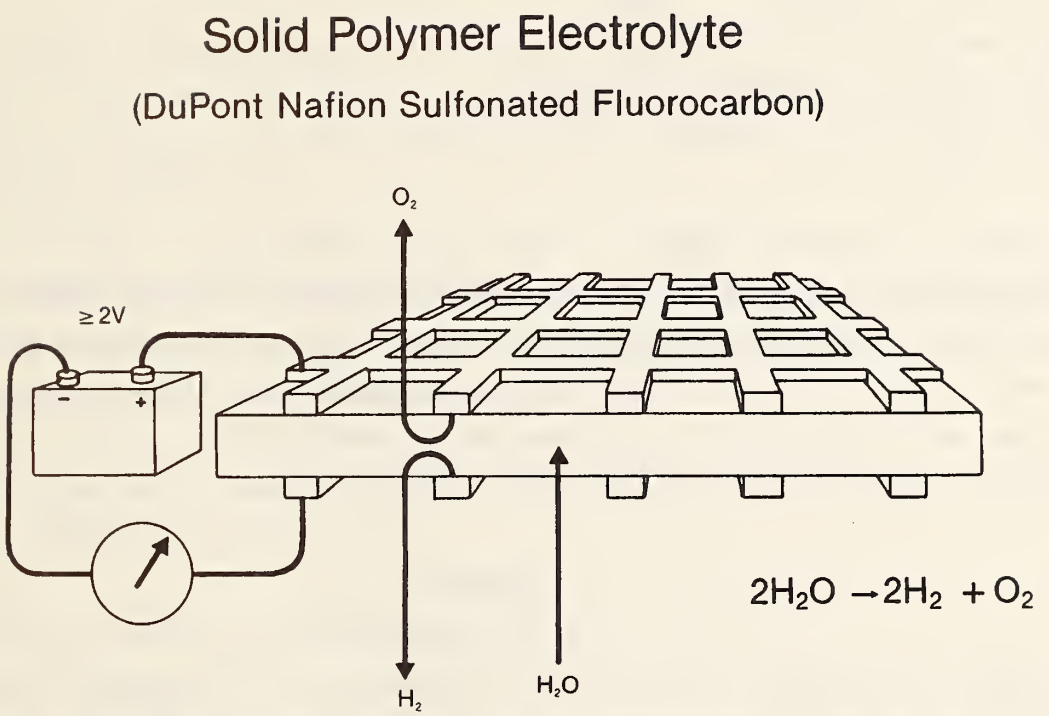

Figure 4 Electrolysis of Water

For diagnostic purposes an electrometer could be used. This would allow determination of moisture content, using the Faraday constant of 96,500 coulombs per gram-equivalent (10,700 coul per gram of water).

With voltage applied to the electrodes, water molecules diffuse into the polymer and hydrogen and oxygen molecules diffuse out. With continuous power, a slight overpressure will develop, since two molecules of reactant (water) yield three molecules of product (hydrogen and oxygen). The partial pressure of hydrogen and oxygen inside will increase until at steady state, the escape rate equals the production rate.

This can be expressed

$$R_w = R_{H_2} = 2R_{O_2}$$

Expressing the rates in terms of the various partial pressures, molar masses, and the air-equivalent standard leak rate, the steady-state partial pressures can be expressed in terms of the ambient moisture level p_{wa}.

$$P_{H_2} = P_{wa} \, (M_{H_2}/M_w)^{1/2} = P_{wa}/3$$

$$\Delta P_{O_2} = \frac{1}{2} P_{wa} \, (M_{O_2}/M_w)^{1/2} = 2P_{wa}/3$$

$$P_{H_2} + \Delta P_{O_2} = P_{wa}$$

The partial pressure of oxygen in the package rises until it exceeds that of air (0.21 atm) by Δp_{O_2}. During this time the partial pressure of fill gas drops. These results are independent of the size of the leak over the range for which molecular flow is a suitable assumption. For larger leaks, the limit is set by the rate at which the Nafion could support electrolysis of the water.

SUMMARY

This paper has presented the case for allowing the use in hermetic packages of materials which can capture water vapor and thus prevent it from increasing to a level which could cause damage to the devices inside. Without the use of such materials, the true maximum permissible leak rate is too small to measure.

Three such materials have been presented: molecular sieve, which absorbs water, calcium carbide, which reacts with water, and Nafion polymer electrolyte, which support the electrolysis of water. Since new materials added to a package may cause unanticipated effects, the ideas presented here should be studied experimentally before any specification changes are made.

The case has also been presented for abandoning the expression of moisture level in terms of dew point and relative abundance (ppmV) in favor of expressions in terms of partial pressure (atm, millibars, etc.), relative humidity, and mass per unit volume and area.

REFERENCES

1. J. G. Davy, "Thermodynamic and Kinetic Considerations of Moisture Sorption Phenomena", pgs. 184-200, Moisture Measurement Technology for Hermetic Semiconductor Devices, II, NBS/RADC Workshop, November 5-7, 1980, NBS Special Publication 400-72.

2. R. P. Merrett et al, "A Simple Method of Using the Die of an Integrated Circuit to Measure the Relative Humidity Inside Its Encapsulation", Proc. International Reliability Physics Symposium, 1980, 17-25.

3. "Molecular Sieve Type 4A Pellets, Water Adsorption Isotherms", Union Carbide Data Sheet F-43A-1.

4. Robert W. Thomas, private communication

5. W. E. Swartz et al, "The Adsorption of Water on Metallic Packages", Proc. International Reliability Physics Symposium, 1983, 52-59.

6. M. W. White et al, "Attaining Low Moisture Levels in Hermetic Packages", Proc. International Reliability Physics Symposium, 1982, 253-259.

7. W. M. Hickam and W. R. Morgan, "Mass Spectrometric Moisture Analysis of Hermetic Semiconductor Devices by Acetylene Conversion", pgs. 153-158 in Moisture Measurement Technology for Hermetic Semiconductor Devices, ARPA/NBS Workshop V, March 22-23, 1978, NBS Special Publication 400-69.

8. D. D. Lawson, "Long-Lasting Solid-Polymer Electrolytic Hygrometer", Technical Support Package for NASA Tech Brief, Vol. III, No.1, Item 52, June 1978.

5.2 HERMETICITY AND MOISTURE INGRESS

A. DerMarderosian
Raytheon Company
Sudbury, MA 01776
(617) 443-9521, x2791

Abstract

This discussion will deal with the basic concepts of hermeticity testing and current practices and procedures in the electronics industry. The talk will also include work related to moisture ingress rate as a function of air leak rate and offer a rationale which can be used as a guideline for hermeticity specifications.

Summary

Hermeticity testing has a long and somewhat tarnished history in the electronics industry. When electronic components were large and somewhat simply structured, the bubble tests and crude helium leak tests of yesteryear seemed reasonable and "comfortable." With the increasing use, however, of smaller semiconductors and finally integrated circuits, the value of those test techniques became questionable and several new ones were quickly developed and adopted by the industry. For a time, everyone had his favorite test procedure, including some of the older ones. The basic principle of each of these types of tests will be discussed, highlighting their advantages and disadvantages. In addition, specifications will be discussed, particularly the maximum allowable leak rates and how they affect our own industry. Moisture ingress rates as a function of air leak rate will be examined from an experimental and theoretical viewpoint. Finally, these data will be examined with particular attention on the maximum allowable moisture content of packages as specified in Method 1018 of MIL-STD-883.

OUTLINE

- HERMETICITY TESTING
- MOISTURE INGRESS
- LEAK RATE GUIDELINES

DEFINITION OF HERMETICITY

"THE STATE OR CONDITION OF BEING AIRTIGHT"

NEED FOR HERMETICITY

TO CONTAIN THE MATERIAL IN A PACKAGE AND EXCLUDE ALL OTHERS OUTSIDE OF THE PACKAGE I.E., GENERALLY LIQUIDS AND GASES IN THE HOPE OF OBTAINING A MORE RELIABLE PART

STANDARD LEAK RATE IN THIS DISCUSSION IS DEFINED AS THE QUANTITY OF DRY AIR @ 25°C PER UNIT TIME WHICH PASSES THROUGH A LEAK WITH A PRESSURE OF 14.7 PSIA ON ONE SIDE OF THE LEAK AND A PRESSURE OF LESS THAN 1 TORR ON THE OTHER SIDE. UNITS ARE GIVEN AS FOLLOWS:

ATMOSPHERIC CUBIC CENTIMETERS/sec, AIR

OR

ATM cc/sec, AIR

STANDARD CONDITIONS FOR LEAK RATE DETERMINATION

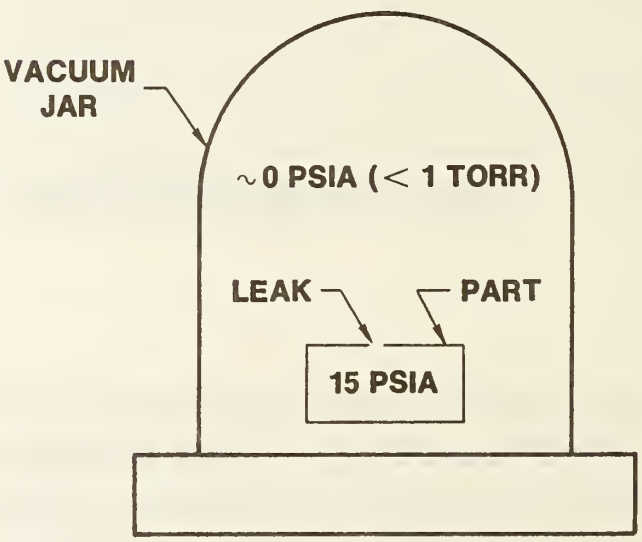

TYPICAL RANGE OF LEAKAGE

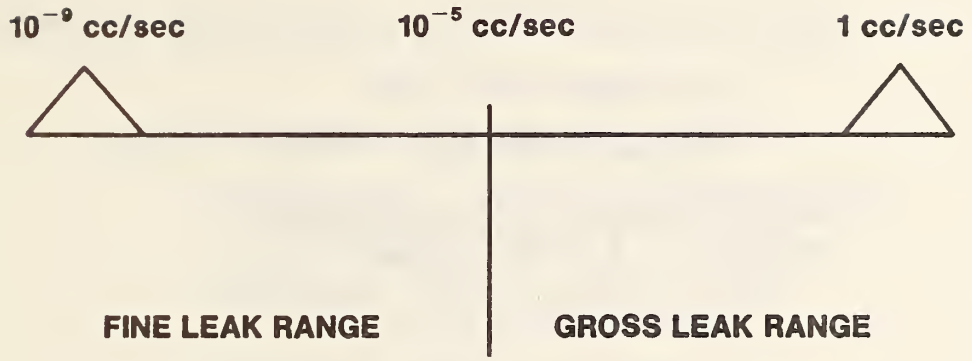

G.W.N.

L.R.	WGT (AIR)	WGT (H_2O)	# OF MOLECULES
1×10^{-9} cc/sec	1.3×10^{-12} gms	8×10^{-13} gms	2.7×10^{10}
1×10^{-7}	1.3×10^{-10}	8×10^{-11}	2.7×10^{12}
1×10^{-5}	1.3×10^{-8}	8×10^{-9}	2.7×10^{14}
1×10^{-3}	1.3×10^{-6}	8×10^{-7}	2.7×10^{16}
	1 cc = 1.3×10^{-3} gms	1 cc = 8×10^{-4} gms	

M.G.W.N.

L.R.	TIME TO LEAK ONE (1) cc
1×10^{-1} cc/sec	10 SECONDS
1×10^{-3}	1000 SECONDS
1×10^{-5}	1.2 DAYS
1×10^{-7}	4 MONTHS
1×10^{-9}	33 YEARS

HISTORY OF LEAK TESTING

FIRST MILITARY SPEC CALLED OUT (MIL-S-19500)

- JOY BOMB TEST (1956)
- HELIUM LEAK TEST ($\sim$ 1960)

MAX. ALLOWABLE LEAK RATE ALL PARTS = 1×10^{-8} cc/sec

FOLLOWED SHORTLY THEREAFTER BY IMPROVEMENTS IN GROSS LEAK TEST (EARLY 1960's)

BUBBLE

- HOT WATER, OIL, ETHYLENE GLYCOL, GLYCERINE (GENERALLY 90-150°C)
- VACUUM ($\Delta P \sim$ 10-14 PSI)
- BACKFILL (PRESSURIZED IN FLUID, THEN HOT BATH)

OTHER

- WEIGHT TEST, OMNI-SEAL, FREON L.D.

FINE LEAK TEST WAS FURTHER REFINED IN MIL-STD-883 (1968)

- TEST CONDITION WAS MORE CAREFULLY DEFINED WITH ADDITION OF TERRIFYING EQUATION WHICH ACCOUNTED FOR PERTINENT PARAMETERS

PRESENT POPULAR TEST METHODS

GROSS LEAK (MIL-STD-883, 750, 202)

- BUBBLE TEST — OPERATOR OBSERVES FOR BUBBLES ESCAPING FROM THE PART

  PRINCIPLE: ΔP IN PACKAGE FORCES GAS OUT INTO FLUID

  METHOD: HEAT/Δ PRESSURE

BUBBLE TEST (CONT'D)

PERTINENT FACTORS:

- SURFACE TENSION OF FLUID
- TEMPERATURE OF FLUID
- LEAK SIZE/DIMENSION
- PRESSURE DIFFERENTIAL

BUBBLE FORMATION

$$P = \frac{4\theta}{d}$$

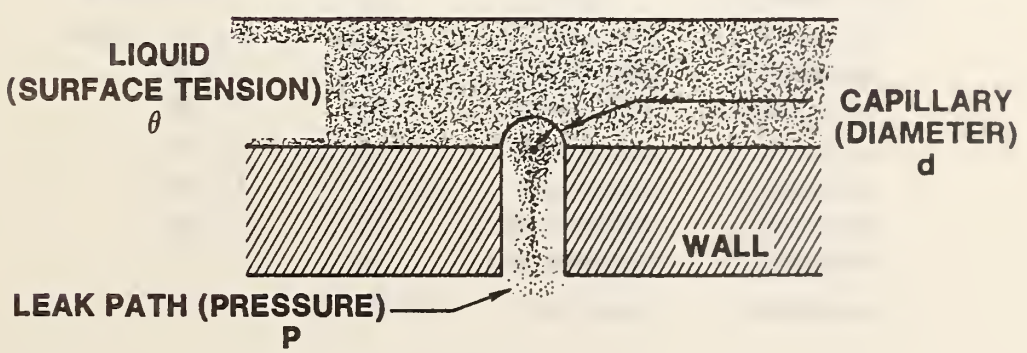

INCREASE IN PACKAGE PRESSURE AS A FUNCTION OF TEMPERATURE OF FLUID

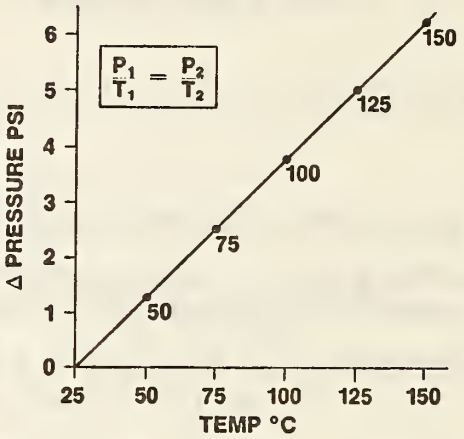

DIFFERENTIAL PRESSURE REQUIRED TO INITIATE BUBBLING VS LEAK RATE IN VARIOUS FLUIDS (CAPILLARY LEAK)

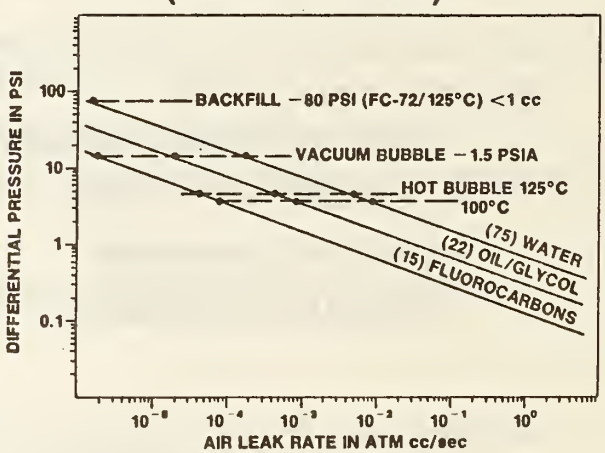

BUBBLE TEST CHART

MIL-STD PROC./CONDITION	TYPE	ΔP	SENSITIVITY
202/COND. A	(HOT MIN. OIL)	4.9	5×10^{-4} cc/sec
202/COND. B	(SIL. VACUUM)	13	2×10^{-5}
202/COND. D	(HOT FC-40)	4.9	3×10^{-5}
750/COND. C_1	(HOT FC-43)	4.9	3×10^{-5}
750/COND. C_2	(BACKFILL)	UP TO ~ 80	1×10^{-6}
750/COND. D	(HOT ETH. GLY)	3.7	8×10^{-4}
750/COND. F	(HOT MIN. OIL)	4.9	5×10^{-4}
883/COND. C	(BACKFILL)	UP TO ~ 80	1×10^{-6}

NON-BUBBLE GROSS LEAK TESTS

- WEIGHT TEST (MIL-STD-883, COND. E. DEV. AT RAYTHEON DURING APOLLO PROGRAM)
- OMNI-SEAL HERMETICITY (WESTINGHOUSE MID 1960'S)
- FREON LEAK DETECTOR (G.E.)

ALL TESTS USE THE BACKFILLING TECHNIQUE WHICH FORCES A LIQUID INTO A LEAKING DEVICE UNDER HIGH PRESSURE (>30 PSIG)

WEIGHT TEST

- WEIGH THE PART
- PRESSURIZE UNDER FC-77
- RE-WEIGH
- WEIGHT INCREASE > 0.5 Mg IS REJECT

COMMENTS:

1. MOST RELIABLE OF ALL GROSS LEAK TESTS
   RANGE: $5 \times 10^{-6} \Rightarrow > 10^{1}$ cc/sec
2. NOT POPULAR; MAIN COMMENT IS LOST

OMNI-SEAL HERMETICITY TEST

- PRESSURIZE UNDER ALCOHOL
- MEASURE ELECTRICAL LEAKAGE BETWEEN COVER AND LEADS, ETC.
- REJECT IF LEAKAGE IS EXCESSIVE (<200 MEGOHM)

COMMENTS

- NOT A MIL-SPEC; NOT IN COMMON USE
- POTENTIAL HAZARD IF OPERATOR/EQUIPMENT MISSES LEAKER, i.e., IONICS IN PACKAGE
- MAY ONLY PARTIALLY FILL AND CAUSE POSSIBLE LONG TERM RELIABILITY PROBLEM

FREON LEAK DETECTOR

- PRESSURIZE UNDER FREON T.F.
- "SNIFF" PACKAGE WITH LEAK DETECTOR
- REJECT IF SIGNAL EXCEEDS BACKGROUND LEVEL

COMMENTS

- NOT A MIL-SPEC; NOT IN COMMON USE
- HAS HIGH "OVERKILL" RATE
- QUESTION RELIABILITY OF PART IF MISSED

FINE LEAK TESTING

HELIUM LEAK TEST

- THE HELIUM LEAK TEST IS PERFORMED BY ALLOWING THE LEAKING GASES OF THE TEST ITEM TO PASS THRU A SPECIAL MASS SPECTROMETER WHICH IS DESIGNED TO BE SENSITIVE TO HELIUM GAS
- PART MUST HAVE HELIUM GAS PRESENT INTERNALLY, i.e., INITIAL FILL OR BACK PRESSURE TECHNIQUE ("BOMBING")

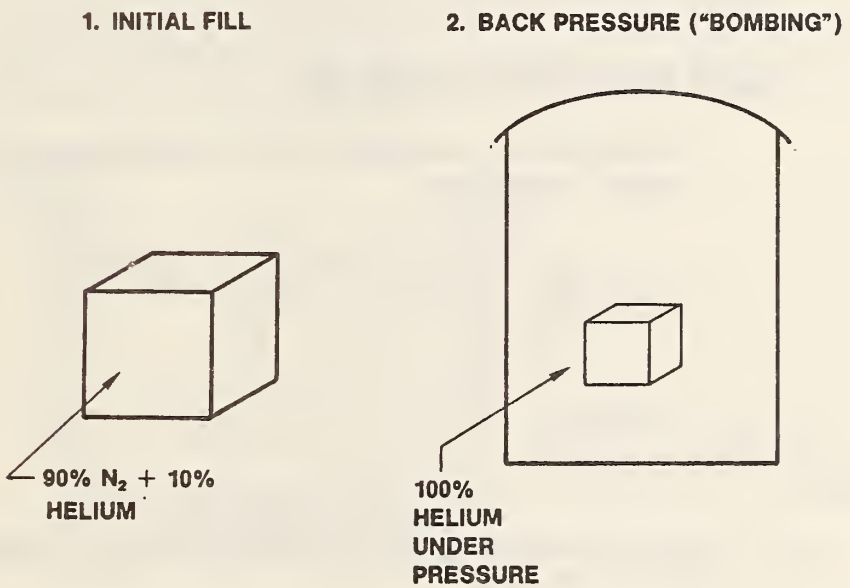

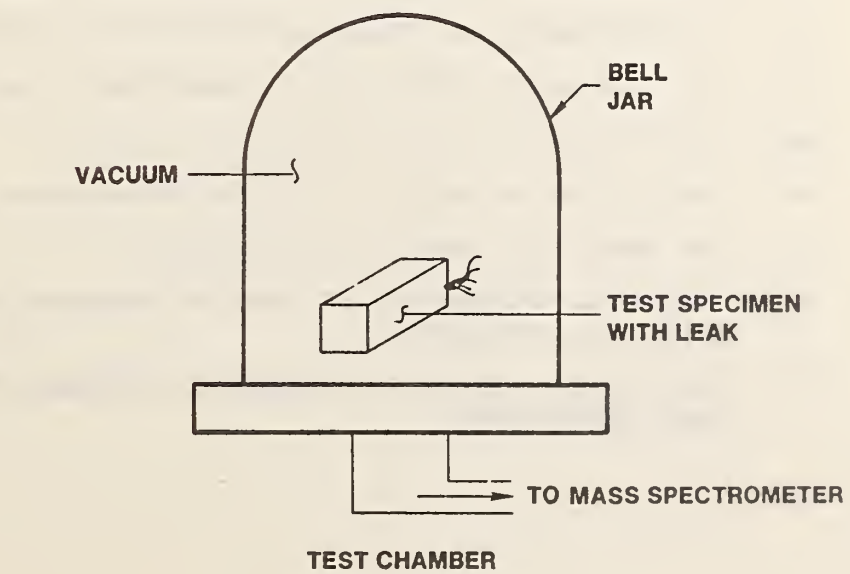

HELIUM LEAK TEST (CONT'D)

- 90/10 MIXTURE IS SIMPLEST. READING ON METER IS MULTIPLIED BY 10 TO OBTAIN STANDARD HELIUM LEAK RATE. THE VALUE IS THEN DIVIDED BY 2.7 TO OBTAIN THE STANDARD AIR LEAK RATE

EXAMPLE:

METER READING $= 1 \times 10^{-7}$ cc/sec

HELIUM L.R. $= 1 \times 10^{-6}$ cc/sec He

AIR L.R. $= 3.7 \times 10^{-7}$ cc/sec AIR

LEAK RATE DETERMINATION

- BACK PRESSURE ("BOMBING")

1. REQUIRES CALCULATION OF THE TRUE LEAK RATE USING SCARY EQUATION:

$$R_1 = \frac{LP_E}{P_O}\left(\frac{M_A}{M}\right)^{1/2}\left\{1-e^{-\left[\frac{Lt_1}{VP_O}\left(\frac{M_A}{M}\right)^{1/2}\right]}\right\}\left\{e^{-\left[\frac{Lt_2}{VP_O}\left(\frac{M_A}{M}\right)^{1/2}\right]}\right\}$$

WHERE

R_1 = THE MEASURED LEAK RATE OF TRACER GAS (He) THROUGH THE LEAK IN ATM cc/s

L = THE EQUIVALENT STANDARD LEAK RATE IN ATM cc/s

P_E = THE PRESSURE OF EXPOSURE IN ATMOSPHERES ABSOLUTE

P_o = THE ATMOSPHERIC PRESSURE IN ATMOSPHERES ABSOLUTE (1)

M_A = THE MOLECULAR WEIGHT OF AIR IN GRAMS (28.7)

M = THE MOLECULAR WEIGHT OF THE TRACER GAS (He) IN GRAMS (4)

t_1 = THE TIME OF EXPOSURE TO P_E, IN SECONDS

t_2 = THE DWELL TIME BETWEEN RELEASE OF PRESSURE AND LEAK DETECTION, IN SECONDS

V = THE INTERNAL VOLUME OF THE DEVICE PACKAGE CAVITY IN CUBIC CENTIMETERS

RADIOISOTOPE TESTING

- AN ALTERNATE METHOD OF FINE LEAK TESTING WHICH UTILIZES Kr^{85} GAS AS A TRACER INSTEAD OF HELIUM
- THIS TECHNIQUE USES THE BACK PRESSURE METHOD ONLY AND HAS ESSENTIALLY THE SAME EFFECTIVE RANGE AS HELIUM
- DETECTION OF GAS PENETRATION INTO LEAKY PACKAGES IS ACCOMPLISHED BY MEASURING THE COUNT RATE OF EMITTED GAMMA RAYS THRU THE WALLS OF THE PACKAGE

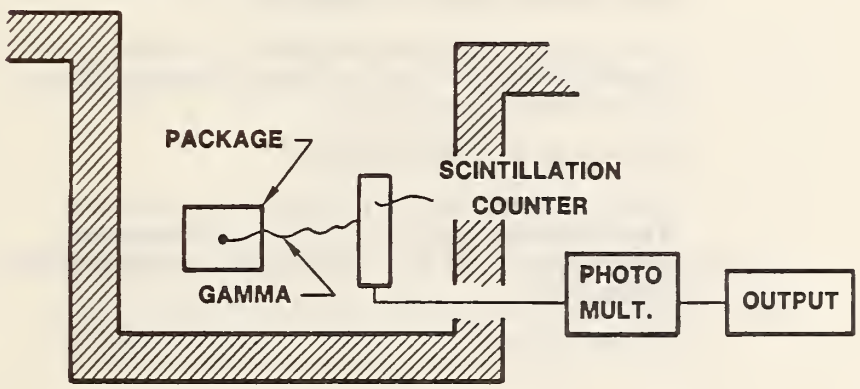

RADIOISOTOPE TESTING (CONT'D)

- AS WITH THE HELIUM TEST, THIS METHOD ALSO HAS A METHOD OF CALCULATING LEAK RATE AS SHOWN BELOW

$$Q_s = \frac{R}{SKT\bar{P}t}$$

Q_s = THE MAXIMUM CALCULATED LEAK RATE ALLOWABLE, IN ATM cc/secKr.

R = COUNTS PER MINUTE ABOVE THE AMBIENT BACKGROUND.

s = THE SPECIFIC ACTIVITY, IN MICROCURIES PER ATMOSPHERE CUBIC CENTIMETER.

k = THE OVERALL COUNTING EFFICIENCY OF THE SCINTILLATION CRYSTAL IN COUNTS PER MINUTE PER MICROCURIE OF KRYPTON-85.

T = SOAK TIME, IN HOURS.

P = P_e^2-P_i^2, WHERE P_e IS THE ACTIVATION PRESSURE IN ATMOSPHERES ABSOLUTE AND P_i IS THE ORIGINAL INTERNAL PRESSURE OF THE DEVICES IN ATMOSPHERES ABSOLUTE.

t = 3600 SEC/HOUR

ANOMALOUS BEHAVIOR OF LEAKS

- MAJORITY OF LEAKS ARE NOT CAPILLARY HOLES; CRACKS WHICH MEANDER
- PHYSICAL NATURE TENDS TO MAKE THEM
  - PRESSURE SENSITIVE
  - TEMPERATURE SENSITIVE
  - PRONE TO CAPILLARY ABSORPTION AND PLUGGING i.e. FLUIDS AND HUMIDITY

GEOMETRY OF REAL LEAKS

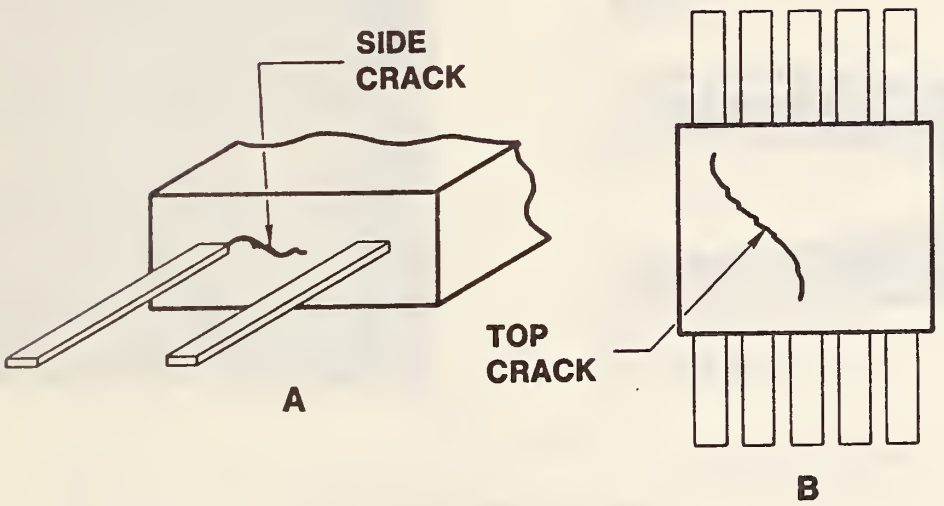

PURPOSE

- TO DETERMINE THE RATE OF WATER VAPOR PENETRATION INTO PACKAGES WITH KNOWN LEAK RATES.
- TO PROVIDE DATA WHICH MAY BE USED AS A GUIDELINE IN ESTABLISHING MAXIMUM ALLOWABLE LEAK RATES FOR SEMICONDUCTOR PARTS.
- TO ESTABLISH AN ANALYTICAL METHOD FOR USE IN CALCULATING WATER VAPOR PENETRATION RATES FOR ANY DEVICE TYPE WITH A KNOWN LEAK RATE.

CALIBRATED GROSS LEAKER
CONSTRUCTED FROM 1 MM CAPILLARY

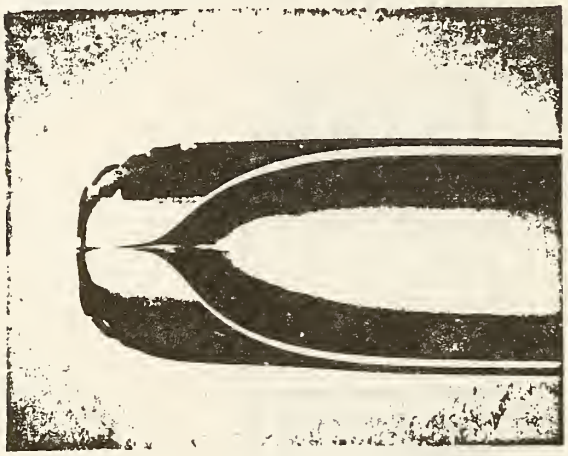

COMPLETED ASSEMBLY OF CALIBRATED
GROSS LEAKER AND TO-5 CAN

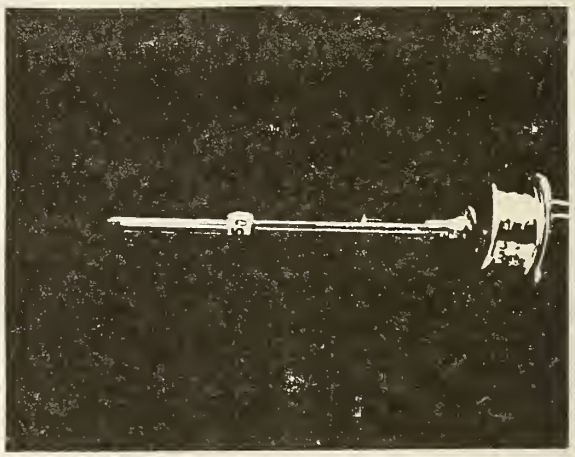

SURFACE CONDUCTIVITY
MOISTURE SENSOR

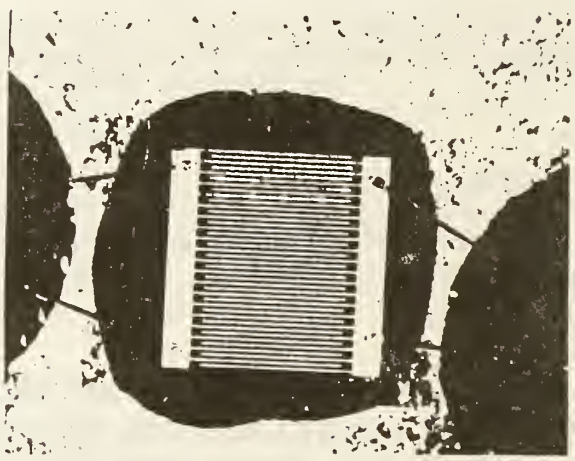

MOLECULAR FLOW

MOLECULAR FLOW OCCURS WHEN THE MEAN FREE PATH OF THE GAS IS GREATER THAN THE LONGEST CROSS–SECTION DIMENSION OF THE PHYSICAL LEAK.

$$Q = \frac{30.48\ r^3}{\ell}\sqrt{\frac{T}{M}}\ (P_1 - P_2)$$

AIR LEAK RATE VS WATER VAPOR LEAK RATE

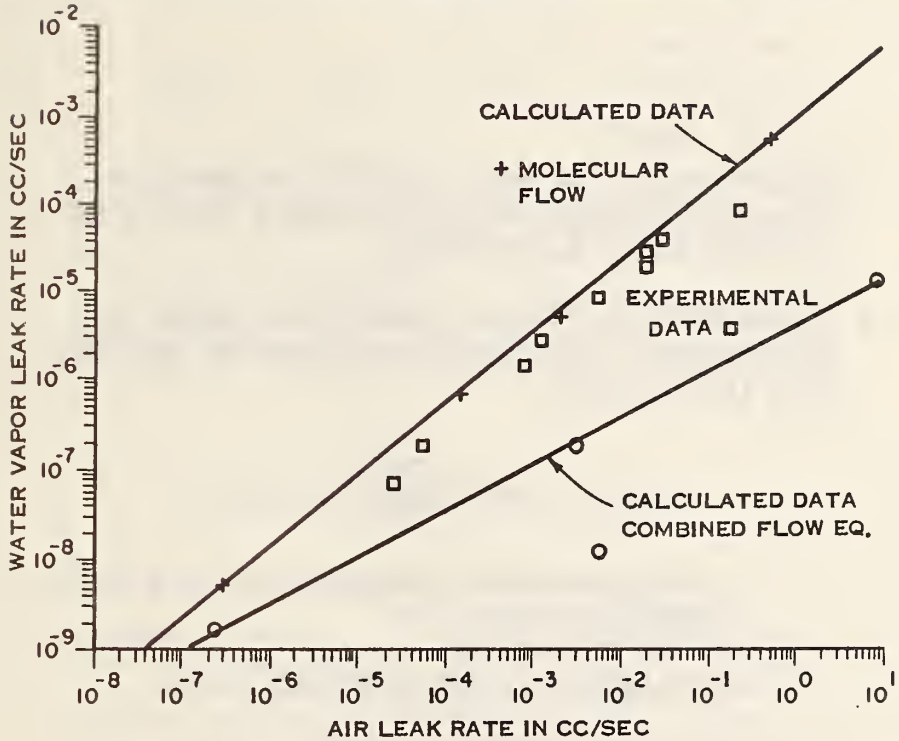

AIR LEAK RATE VS WATER VAPOR LEAK RATE FOR 1/4 X 1/4 FLATPAK

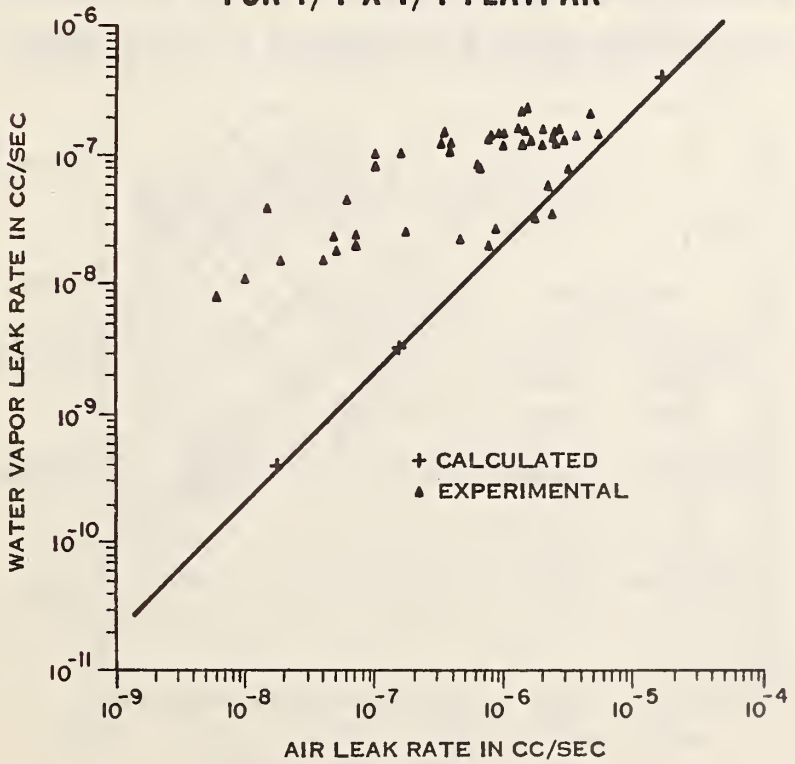

LEAK RATE SPECIFICATION

- THE INGRESS OF MOISTURE IS THE MAJOR CONCERN FOR SEMICONDUCTORS. PROCESS LIQUIDS ALSO A CONCERN
- MAXIMUM ALLOWABLE MOISTURE LEVEL IN PACKAGES AT PRESENT IS 5000 PPM. 500 PPM FOR THE FUTURE

$$\tau = \frac{.011V}{Q_A}$$

τ = TIME CONSTANT IN HOURS FOR H_2O VAPOR INGRESS (63%)

V = INTERNAL VOLUME OF DEVICE IN CC

Q_A = AIR LEAK RATE IN CC/SEC

WATER VAPOR PENETRATION TIME AS A FUNCTION OF AIR LEAK RATE FOR VARIOUS TYPE PACKAGES

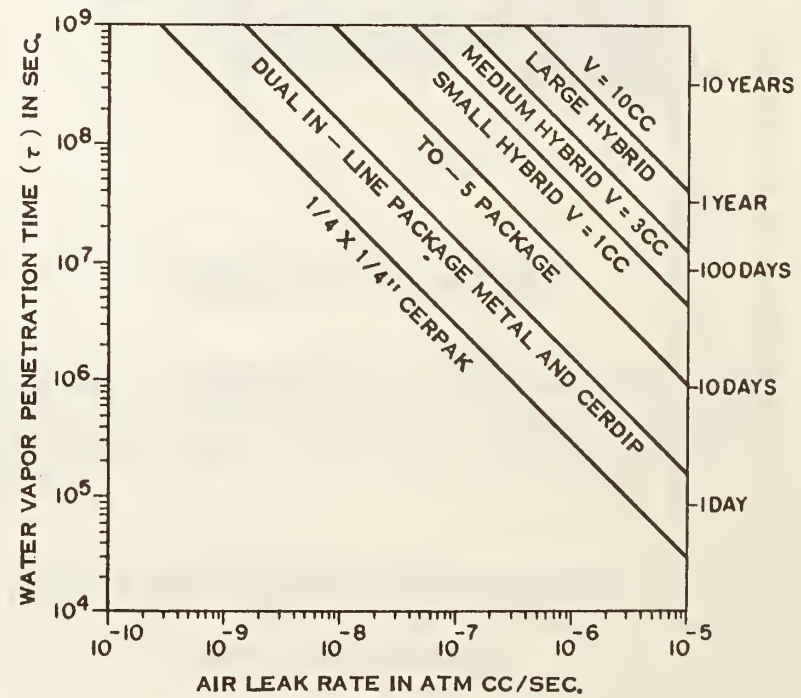

MOISTURE PENETRATION TIMES

VOLUME	METHOD	MAX. ALLOW. L.R. (L)	TIME TO EXCEED (1018) AVG. AMB. = 10,000 PPM	
			5000 PPM	500 PPM
< 0.4 CC $R = (5 \times 10^{-6}$ CC/SEC)	FIXED He (.01 CC)	4.5×10^{-6} CC/SEC	71 DAYS	5 DAYS
< 0.4 CC $R = (5 \times 10^{-6}$ CC/SEC)	FIXED He (.39 CC)	2.8×10^{-7} CC/SEC	1.2 YEARS	32 DAYS
≥ 0.4 CC $R = (2 \times 10^{-7}$ CC/SEC)	FIXED He (.4 CC)	6×10^{-7} CC/SEC	214 DAYS	15 DAYS
≥ 0.4 CC $R = (2 \times 10^{-7}$ CC/SEC)	FIXED He (5 CC)	2×10^{-6} CC/SEC	2.2 YEARS	57 DAYS

MOISTURE PENETRATION TIMES

VOLUME	METHOD	MAX. ALLOW. L.R. (L)	TIME TO EXCEED (1018) AVG. AMB. = 10,000 PPM	
			5000 PPM	500 PPM
< 0.01 CC	FLEXIBLE (He) (.009 CC)	5×10^{-6} CC/SEC	58 DAYS	4.1 DAYS
.01-.4 CC	FLEXIBLE (He) (.01 CC)	1×10^{-7} CC/SEC	32 DAYS	2.3 DAYS
	(.4 CC)	1×10^{-7} CC/SEC	3.5 YEARS	92 DAYS
> 0.4 CC	.41 CC	1×10^{-6} CC/SEC	132 DAYS	9.4 DAYS
	5 CC	1×10^{-6} CC/SEC	4.4 YEARS	114 DAYS

MOISTURE PENETRATION TIMES

VOLUME	METHOD	MAX. ALLOW. L.R. (L)	TIME TO EXCEED (1018) AVG. AMB. = 10,000 PPM	
			5000 PPM	500 PPM
< 0.01 CC	FIXED (K_r^{85}) (.009 CC)	1×10^{-6} CC/SEC	.79 YEARS	21 DAYS
≥ 0.01	FIXED (K_r^{85}) (0.01 CC)	5×10^{-6} CC/SEC	64 DAYS	4.6 DAYS
	(0.4 CC)	5×10^{-6} CC/SEC	7.0 YEARS	.5 YEAR
	(5 CC)	5×10^{-6} CC/SEC	88 YEARS	6.3 YEARS

EFFECTS OF PACKAGE VOLUME

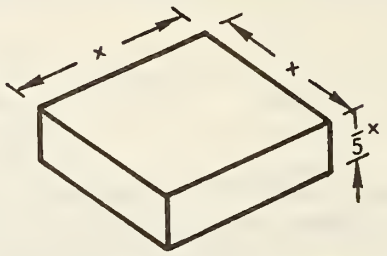

MODEL FOR CALCULATIONS

X CM	INTERNAL AREA CM^2	INTERNAL VOLUME CM^3	RATIO $\frac{\text{AREA}}{\text{VOL.}}$
.17	.08	.001	80
.37	.38	.01	38
.79	1.7	.1	17
1.7	8.2	1	8.2
3.7	38	10	3.8
7.9	175	100	1.75

MAXIMUM ALLOWABLE PACKAGE MOISTURE CONTENT

VOLUME CM^3	MOISTURE CONTENT PPM_v	MOISTURE CONTENT GRAMS	APPARANT SURFACE AREA CM^2	WATER THICKNESS CM	NUMBER OF MONLAYERS —
.001	13,000	9.6×10^{-9}	.08	1.2×10^{-7}	3
.01	6,200	4.6×10^{-8}	.38	1.2×10^{-7}	3
0.1	2,700	2×10^{-7}	1.7	1.2×10^{-7}	3
1.0	1,300	9.8×10^{-7}	8.2	1.2×10^{-7}	3
10	600	4.6×10^{-6}	38	1.2×10^{-7}	3
100	280	2.1×10^{-5}	175	1.2×10^{-7}	3

MAXIMUM ALLOWABLE MOISTURE CONTENT AS A FUNCTION OF INTERNAL PACKAGE VOLUME

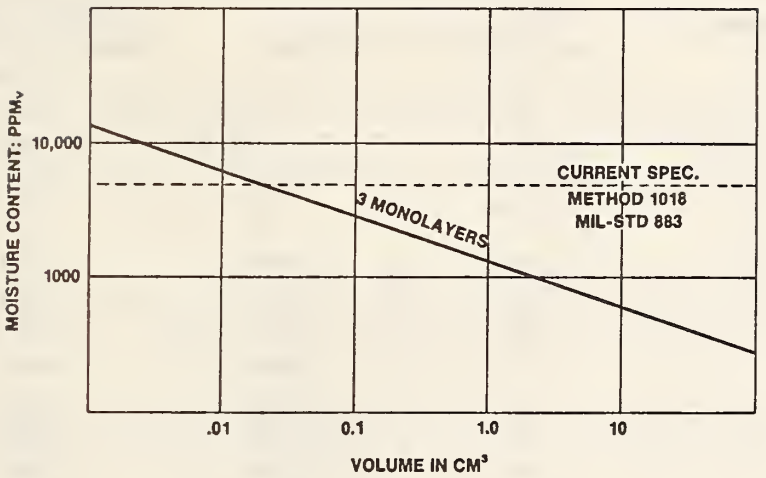

MOISTURE INGRESS TIME

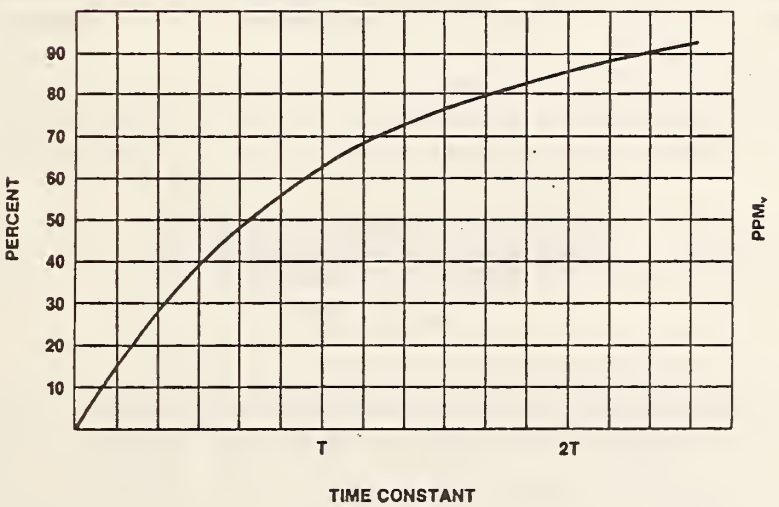

TIME TO REACH ONE(1) T AND 3 MONOLAYERS OF H_2O

VOLUME C.C.	L.R. ATM CC/SEC	T HOURS	TIME TO REACH 3 MONOLAYERS HOURS (AVG AMB 13K PPM_V)
.001	1×10^{-6}	11	55
.001	1×10^{-7}	110	550
.001	1×10^{-8}	1,100	5,500
.01	1×10^{-6}	110	66
.01	1×10^{-7}	1,100	660
.01	10^{-8}	11,000	6,600
.1	10^{-6}	1,100	257
.1	10^{-7}	11,000	2,570
.1	10^{-8}	110,000	25,700
1	10^{-6}	11,000	1,283
1	10^{-7}	110,000	12,830
1	10^{-8}	1,100,000	128,300
10	10^{-6}	110,000	5,500
10	10^{-7}	1,100,000	55,000
10	10^{-8}	11,000,000	550,000
100	10^{-6}	1,100,000	27,500
100	10^{-7}	11,000,000	275,000
100	10^{-8}	110,000,000	2,750,000

TIME TO REACH 3 MONOLAYERS OF H_2O AS A FUNCTION OF PACKAGE INTERNAL VOLUME AND AIR LEAK RATE.

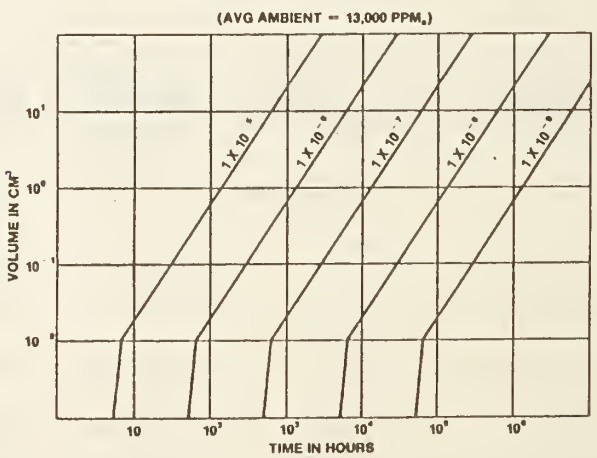

5.3 LEAK DETECTION, GROSS AND FINE, USING HELIUM AS A TRACE GAS

Paul R. Forant
Varian/Lexington Vacuum Division
121 Hartwell Avenue
Lexington, MA 02173
(617) 861-7200

In this moisture measurement workshop you have been discussing various methods of determining moisture content in electronic devices and the means of controlling moisture. A key ingredient in the prevention of moisture contamination is proving the hermeticity of the devices.

MIL-STD-883B, Method 1014.2, details the test of semiconductor devices to determine the effectiveness of the seal. Two fine leak methods using helium or a radioisotope trace gas are prescribed. Three gross leak test methods using a fluorocarbon immersion test or weight gain and a dye penetrant test are also prescribed.

These gross leak tests must be made after fine leak testing as the liquids used would plug small leaks and make them impossible to find in the fine leak methods.

It is desirable to test for gross leaks first and remove those from the lot being tested. Current experience indicates that gross leaks represent over 50% of the leakers present in production lots. It is probable that the fine leak method rejects many gross leaks, particularly if the internal volume is large. The best solution would be to develop a test method that would create the maximum overlap and extend the range of useful testing in the gross leak mode to find as many leakers as possible.

The first illustration is the equation for relating the leak rate indicated to the actual leak rate when using the bombing technique. Figure 2 is derived by solving the equation for the parameters in the fixed conditions for test, i.e., 60 psig for 2 hours and testing within 1 hour.

The vertical line is drawn at 5×10^{-8} atm. cc/sec. which is the fine leak reject limit for devices with a volume of less than .4 cc. If the volume exceeds .4 cc the reject limit is 2×10^{-7} std. cc/sec.

If we assume that the gross leak test will find leaks as small as 5×10^{-6} atm. cc/sec., which appears to be an optimistic assumption, then there are leaks which will escape detection by either the fine or gross leak method if the component has an internal volume of .0001 cc or .001 cc. This is the problem we are addressing. At .01 cc, actual leaks between 3×10^{-7} and 1×10^{-6} atm. cc/sec. will be rejected. Larger leaks will have to be found by gross leak testing methods. As the internal free volume increases, the gross leaks that are as large as 1×10^{-4} atm. cc/sec. for .1 cc volumes and as large as 3×10^{-3} atm. cc/sec. for 1 cc volumes will be identified by the helium fine leak method.

It is the gap that exists on the smaller devices that are a problem for overall hermeticity testing. There is a solution to this situation, and it has been described in detail in a paper written by Stanley Ruthberg entitled, "A Rapid Cycle Method for Gross Leak Testing with the Helium Leak Detector". This was published in the IEEE Transaction on Components and Hybrids and Manufacturing Technology, Vol. CHMT3, No. 4, Dec. 1980. Mr. Ruthberg has built a rapid-cycle helium leak tester for testing devices over a range of 1×10^{-5} to more than 1 atm. cc/sec.

If we were to contemplate a test system that combined the gross and fine leak test

in close sequence, the gap currently existing between gross and fine leak testing would be eliminated, and furthermore, the signal from the leaks would be increased to assure that apparently marginal tests would become definitely defined.

The following conditions are proposed for gross and fine leak testing:

1. The parts are first to be pressurized to 60 psig for 2 hours and tested within 1 hour.

2. The rapid-cycle gross leak test calls for a booster pressurization at 30 psig for 6 seconds.

3. Transfer to the second chamber in 1 second.

4. Evacuating and testing the part in 5 seconds.

These parameters are readily achievable in current leak testing equipment when operated with the appropriate material handling, fixtures and microprocessor controls.

If the part is gross leak tested in this manner, the part can then be fine leak tested in the same test mode by transferring it to a third chamber for removal of surface helium, so that when transferred to a fourth chamber, the fine leak test at 5×10^{-8} std. cc/sec. can be conducted.

The leak test is made with the above parameters of a long-term "bombing" and a booster bombing just prior to test. For gross leak testing the reject limit of 5×10^{-6} std. cc/sec. can be achieved. We can now reject leaks in accordance with the following:

Volume cc	Leak Detection Range
.01	5×10^{-5} to .5 atm. cc/sec.
.10	2.5×10^{-6} to 10 atm. cc/sec.
1.0	1×10^{-6} to 10 atm. cc/sec.

The prebombing of the part to 60 psi for 2 hours plus the short-term booster bombing covers the marginal area as well as the gap on the smaller devices. The indicated signal is substantially greater than that available from the long-term bombing and dwell currently used.

Equipment to accomplish the test has been built and is described in detail in Stanley Ruthberg's paper referenced above. Varian has conducted surveys of the industry to see if such equipment would be saleable. The interest was high with the stipulation that the test method be added to the gross leak test methods permitted by MIL-STD-883.

Using the formulae for flow rates for filling the part with helium and the rate of loss of helium during the handling and test phases, a minicomputer could be programmed to adjust the bombing cycle for higher pressures or longer dwell, decreasing dwell time after bombing or decreasing pump down and test time. These variables are readily calculated and the test setup can be adjusted to assure rejection of defective parts.

The high-quality levels currently achieved by manufacturers indicate that several parts can be tested at once and the rejects can be handled in small lots or indi-

vidual screening. With multiple parts testing the problems of sorbed and residual helium would probably cause problems if a single chamber were used for both bombing and testing. Two chambers for gross leak testing and two for fine leak testing are indicated to achieve good correlation to standard control devices of known leak rate.

We will be actively pursuing a change to the MIL-STD so that we can go ahead with a development program that will make commercial hardware available for this test method.

$$S_t = P\,[1 - e^{-3600\,aT}]\,[e^{-at}]\,L$$

where:

S_t = indicated leak rate (standard cm^3/s),

P = bombing pressure of helium (atmospheric pressure, absolute),

T = bombing time (h),

t = waiting time (s) between bombing and testing,

L = actual leak rate (standard cm^3/s atmospheric pressure, absolute) (Note 1),

a = L/V where V = internal volume (cm^3), and

e = 2.71 (natural logarithm).

Illustration 1.

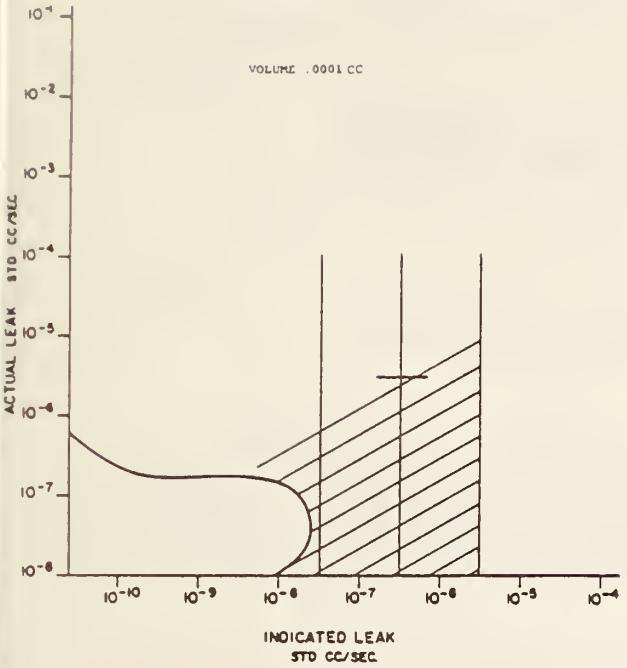

BOMB TIME - 2 HRS.
BOMB PRESSURE - 60 PSIA
DWELL - 3000 SEC.

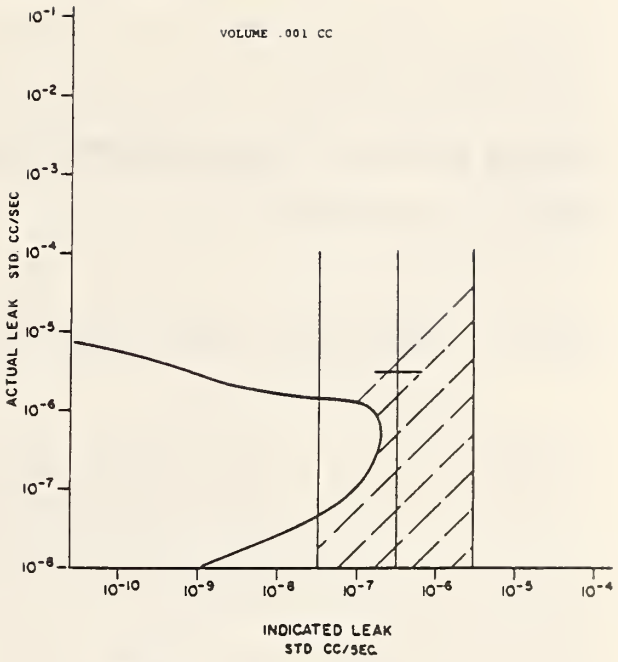

BOMB TIME - 2 HRS.
PRESSURE - 60 PSIA
DWELL - 3000 SEC.

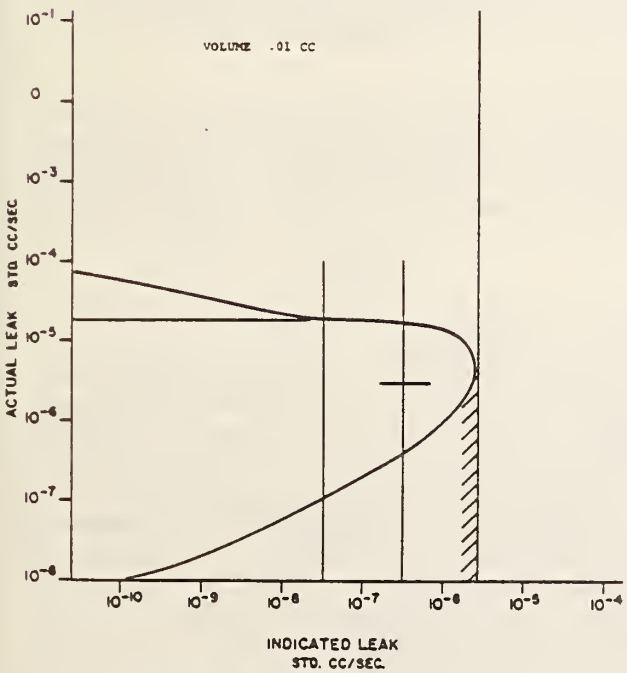

BOMB TIME - 2 HOURS
PRESSURE - 60 PSIA
DWELL - 3000 SEC.

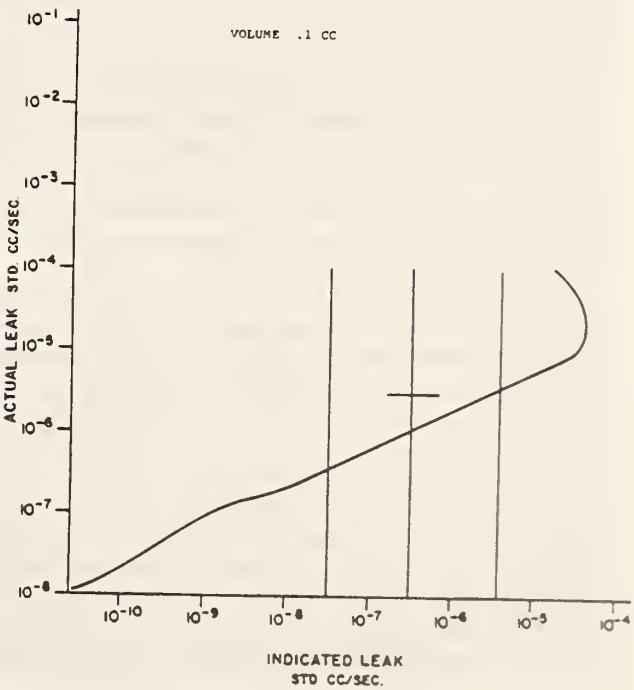

BOMB TIME - 2 HRS.
PRESSURE - 60 PSIA
DWELL - 3000 SEC

Illustration 2.

Reprinted from Applied Optics, Vol. 21, page 3702, October 15, 1982

SESSION IV, Paper 5.4

Using optical correlation to measure leak rates in sealed packages

James W. Wagner, Louis C. Phillips, Edward P. Mueller, and Robert E. Green, Jr.

An optical correlation technique has been shown to accurately measure leak conduction rates from 10^{-1} to 10^{-6} atm cc/sec. Using hybrid microcircuit packages with glass capillary leakers, dimensional changes were detected as the packages were exposed to a small increase in external pressure. The rate at which the package returns to its original dimensions is measured and used, along with the internal free volume, to compute the leak rate. Because of its several advantages, the technique has the potential to become a useful nondestructive quality-control technique.

I. Introduction

Of the several techniques available for detecting and measuring leak rates in sealed electronics packages, most quantitative techniques use a tracer gas which is either sealed into the package or forced in under pressure and then measured as it escapes through leaks in the package. Owing to the rapid loss of gas from packages with leak rates larger than $\sim 1 \times 10^{-5}$ atm cc/sec, these tracer-gas techniques suffer a loss in sensitivity in the gross-leak range unless special techniques are employed.[1] Unfortunately, present gross-leak test methods typically are nonquantitative, have limited ranges and detection efficiencies, may not detect very large leaks or porosities, and may contaminate and thereby accelerate failure of leaky devices not accurately screened by the test.[2]

A new optical technique, which measures minute displacements of the package walls as a result of applied external pressure, has been studied as a potential means for measuring leak rates in sealed packages. The technique has been shown to provide a high degree of accuracy in measuring leak rates over the entire test range from 10^{-1} to 10^{-6} atm cc/sec. Since no tracer gases or detection fluids are used, the optical technique offers several advantages over conventional leak test methods. The optical method is noncontaminating, directly measures the air leak rate (no conversion required), is immune to interferences from absorption of tracer gas by polymer components on or in the package, and is potentially faster since no back pressurization with tracer gases or fluids is required. In addition, it is virtually impossible for a very large leaker to be missed using the optical method. Although the data presented here were generated from tests on a series of hybrid microcircuit packages, the method may be applied to transistor and microcircuit packages, food containers, or even larger packages as long as the internal free volume of the package is known.

James Wagner and Edward Mueller are with U.S. Food & Drug Administration, Bureau of Medical Devices, Center for Medical Device Analysis, 8757 Georgia Avenue, Silver Spring, Maryland 20910; the other authors are with Johns Hopkins University, Department of Materials Science & Engineering, Baltimore, Maryland 21218.

Received 14 May 1982.

II. Theory

If a leaky package stored for some time at atmospheric pressure P_a is then subjected to a step increase in pressure to some pressure P_e on equilibration, the change in standard volume within the package will be

$$\Delta V = V_f \left(\frac{P_e}{P_a} - 1 \right),$$

where V_f = internal free volume, and ΔV = difference between final standard gas volume and V_f.

The time dependence of the internal-pressure increase is described for the various modes of flow through the leak as a function of leak size, geometry, and pressure difference.[3] For the case of purely molecular flow, the volume of gas which passes through the leak, $V_1(t)$, can be expressed as a simple exponential relationship $V_1(t) = \Delta V[1 - \exp(-t/\tau)]$, where τ is a function of temperature, leak geometry, molecular weight of air, and the internal free volume of the package. The leak rate for a fixed pressure difference, $P_e - P_a$, is simply the slope of this curve at $t = 0$:

$$\text{leak rate}_{P_e} = \frac{d}{dt} V_1(t)\Big|_{t=0} = \frac{\Delta V}{\tau} = \frac{V_f}{\tau} \left(\frac{P_e}{P_a} - 1 \right).$$

Therefore, given P_e and V_f, the leak rate can be computed exactly for the molecular flow case and approximated for viscous laminar flow.

The optical method discussed here measures τ by detecting displacement and subsequent relaxation of

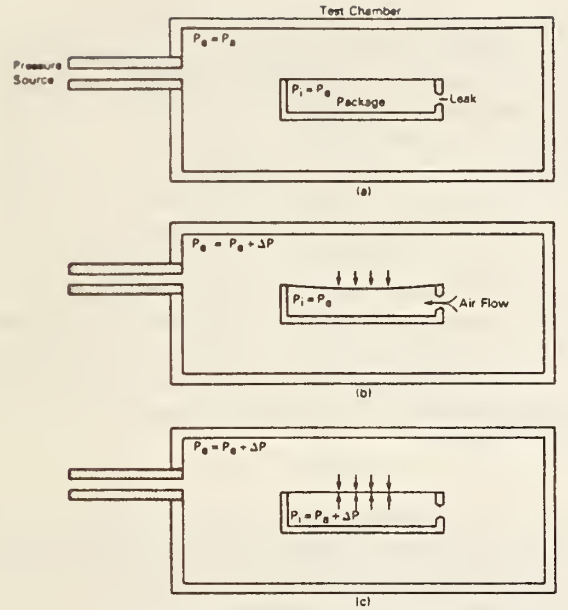

Fig. 1. Package-lid displacement resulting from increased chamber pressure.

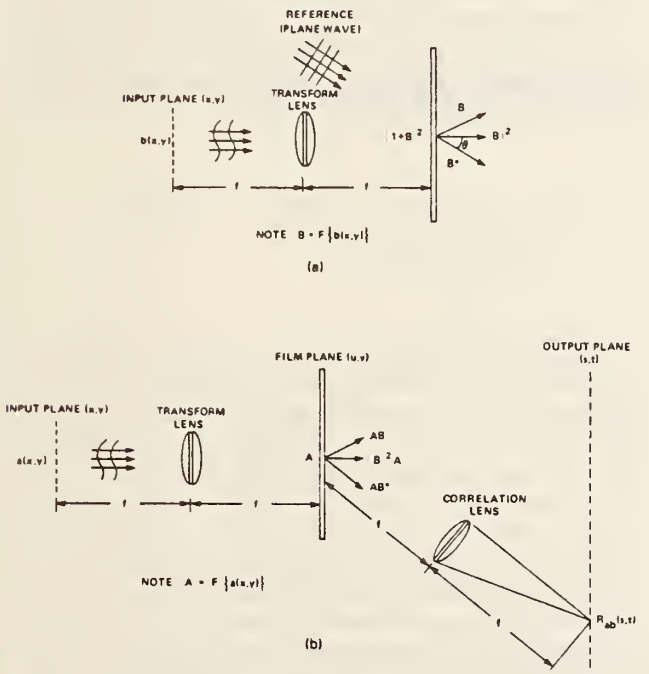

Fig. 2. (a) Constructing the matched filter; (b) generating the correlation signal.

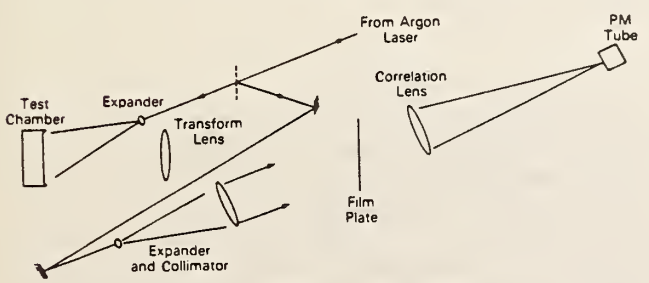

Fig. 3. Optical setup used to measure leak rate.

the package surface as a result of an applied external-pressure change. Figure 1 illustrates the displacement/relaxation phenomenon showing a package placed in a sealed chamber whose pressure may be controlled. Initially, the air within the chamber and the package are both at atmospheric pressure [Fig. 1(a)]. At some time, t_0, the chamber pressure is increased to some value above atmospheric pressure. Figure 1(b) shows that, at this time, the package lid is immediately displaced and air begins flowing into the package through the leak. As time passes, the pressure within the package equilibrates with that in the chamber, allowing the package lid to return to its original position [Fig. 1(c)].

To detect package-lid displacement, a coherent optical-processing technique known as optical correlation or matched filtering[4] is used. Before the chamber pressure is increased, a Fourier transform hologram[5] is made of the package lid viewed through a window in the front of the test chamber. This hologram, once developed, has an amplitude transmittance proportional to the complex conjugate of the Fourier transform of the object surface [see Fig. 2(a)]. To detect displacement of the package surface, this hologram can now be used as a matched filter as shown in [Fig. 2(b)]. The output of the correlator system is a symmetric pattern of light whose amplitude is proportional to the cross-correlation of the object surface at the time the hologram was exposed and the object surface in real time after the hologram is developed. If the object surface remains unchanged ($P_e = P_i$), the output of the system is the autocorrelation of the surface with a very high peak intensity in the center (0,0). As correlation of the surface with its original state decreases, this (0,0) intensity will also decrease. By using a pinhole to select only this (0,0) value, a photomultiplier tube can be used to detect and record the degree of correlation.

The actual system configuration as shown in Fig. 3 does not project an accurate cross-correlation signal in the output plane. This results from the fact that to improve the efficiency of the system, neither the object nor the film plate are located as they should be in the front focal planes of the transform or correlation lenses, respectively. Fortunately, it has been shown that the (0,0) value of the output signal remains unchanged by this configuration.[6]

When pressure is applied to the package, the surface deflects inward and the correlation signal drops to a minimum value. Once the pressure within the package equilibrates with that of the chamber, the correlation signal will return to its original value. The time required for the signal to return to its original value is used to compute the time constant, τ, for the package leak.

III. Procedure

To test the application of optical correlation to leak testing, twelve hybrid microcircuit packages were fitted with glass capillaries of known leak rate. The packages measure 33 × 18 × 4 mm, are made of Kovar, and have a measured internal free volume of 1.11 mliter (see Fig. 4). The sidewalls and bottom are 1 mm thick and the

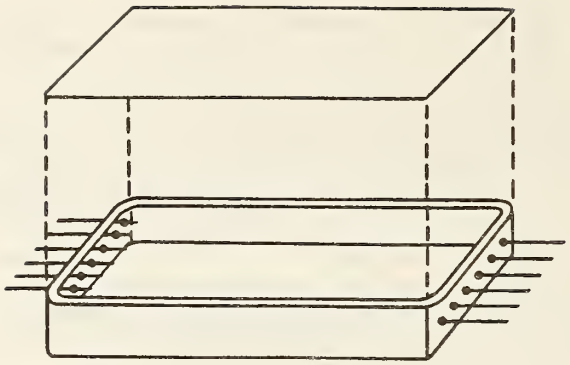

Fig. 4. Package construction.

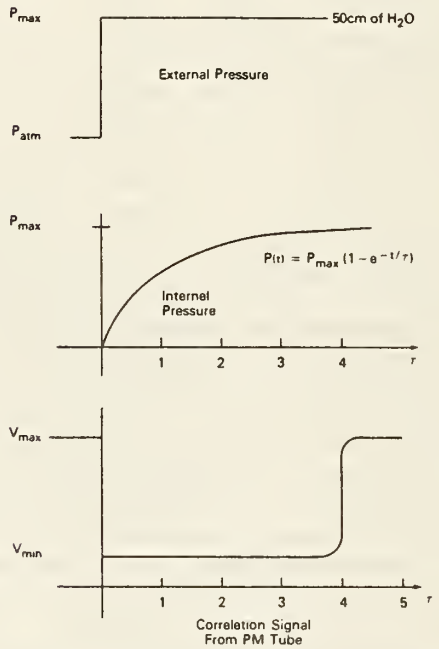

Fig. 5. Dependence of correlation signal on chamber and package pressure.

lid, which is either welded or soldered in place, is 0.4 mm thick.

The package is placed in the test chamber located in the object plane of the optical correlator (refer to Fig. 2). A film plate (Agfa 10E56) is exposed using equal object and reference beam intensities. To ensure precise alignment of the developed hologram, the film plate is placed in a liquid-cell holder throughout the exposure, development, and playback. During playback, the reference beam is blocked and the photomultiplier (PMT) and pinhole are aligned in the back focal plane of the correlation lens for maximum signal. A strip-chart recorder is used to record the output of the PMT. When the pressure in the test chamber is increased by 50 cm H_2O (4.9 kPa), the correlation signal drops to a minimum value. As the pressure within the package equilibrates with that of the chamber, the recorder correlation signal returns to its autocorrelation value (see Fig. 5).

Using a nonleaker, the relationship between the leak-rate time constant, τ, and the recovery time for the correlation signal was established. By precisely controlling the pressure within the chamber, it was discovered that the knee at the point where recovery of the correlation signal begins corresponds to a pressure difference of ~0.8 cm H_2O across the package lid. This is 1.6% of the initial applied-pressure difference. Therefore, the time between the drop in the correlation signal and the knee at the beginning of recovery corresponds to the time required for the interior-package pressure to come within 98.4% of its final equilibrium value. This means that the recovery time corresponds to approximately four time constants since $1 - \exp(-4) = 0.982$ or 98.2%.

The recovery time for a test 10^{-1} atm cc/sec leak is ~2 sec. However, the recovery time for the test packages with leaks finer than 7×10^{-4} atm cc/sec is >5 min. For these packages a slightly different procedure is used. Instead of waiting for the recovery time, the pressure within the chamber is slowly backed off after some known dwell time, typically 5 min. The pressure within the chamber when the correlation signal returns indicates the package pressure after the dwell time at the increased chamber pressure. Using these data, the time constant may be computed as follows:

$$\tau = -\frac{T_d}{\ln\left(1 - \frac{Pi - Pa}{Pe - Pa}\right)}, \text{ where } T_d = \text{dwell time.}$$

To verify the accuracy of the experimental results using the optical technique, each package leak was directly tested using a water manometer method shown schematically in (Fig. 6). A hole was drilled through the lid of each test package over which a glass burette was secured using a cyanoacrylic cement. The burette constitute one arm of a U-tube water manometer in which a 50-cm difference in water height was established. As air leaked into the package, the column-height difference was reduced. The time required for the column heights to change indicating that 0.1 cc of air had passed through the leaker was recorded. The leak rate was then computed by simply dividing the recorded time into the volume and normalizing to standard conditions.

IV. Results and Discussion

A comparison of the leak rates measured using the optical techniques and the direct manometer method is shown grapically in (Fig. 7). The 98% recovery time was measured for packages leaking at a rate of 10^{-3} atm cc/sec or greater. The leak rates of the remaining packages were computed by measuring the internal pressure after a 5-min dwell time at increased chamber pressure.

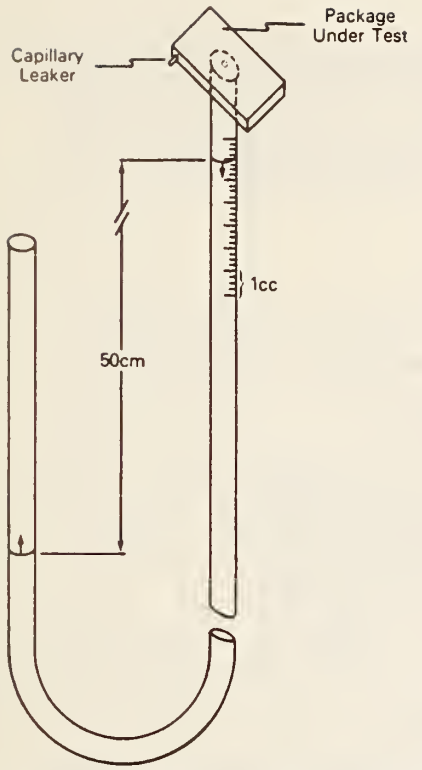

Fig. 6. Water manometer technique for measuring leak rates.

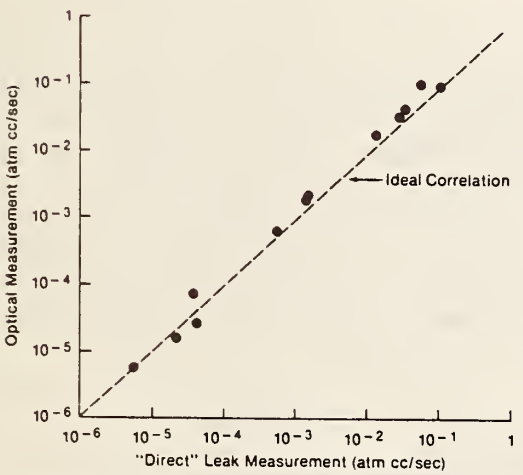

Fig. 7. Leak-rate data obtained optically and directly using the water manometer technique.

It should be noted that leak-rate data are usually assumed to indicate the rate of gas flow into a package at a 1-atm differential pressure. Bear in mind that the data presented here represent the leak conduction at only 50 cm H_2O or 1/20 of 1-atm differential pressure. To obtain standard leak values, the optical tests must be run again using $P_e = P_a + 1$ atm or $P_e = P_a - 1$ atm. Because of changes in flow modes at increased differential pressure, the lower-pressure data may not in general be directly extrapolated to give the higher-pressure values. Having previously obtained standard leak-rate values for all of the test packages, however, it was interesting to note that for those packages with leak rates below 10^{-4} atm cc/sec, there was a direct proportionality between the leak rate and the applied pressure. That is to say that leak rate of these packages at 1/20 atm (50 cm H_2O) was very nearly 1/20 of their measured leak rates at 1-atm differential pressure. This was not true for packages with larger leaks. This variation in leak-conduction rate with applied pressure may be useful in discerning flow modes, thereby providing some indication of the leak geometry.

Optical correlation has been shown to provide an accurate means for detecting and measuring leak rates in hybrid microcircuit packages in the range from 10^{-1} to 10^{-6} atm cc/sec. Using higher pressures and/or longer dwell times, there is every reason to believe that its accuracy may be extended further into the fine-leak range. With erasable, rapid-process storage media (thermoplastic film or Prom, etc.) and simple control circuitry, a fast automated system might be configured for quality-control applications.

References

1. S. Ruthberg, "A rapid cycle method for gross leak testing with the helium leak detector" IEEE Trans, Vol. CHMT-3 (4) December 1980.
2. S. B. Banks, R. E. McCullough, and E. G. Roberts, "Investigation of Microcircuit Seal Testing," Rome Air Development Center Tech. Rep. RADC-TR-75-89 (April 1975).
3. D. A. Howl and C. A. Mann, Vacuum 15, 347 (1965).
4. J. W. Goodman, *Introduction to Fourier Optics* (McGraw-Hill, New York, 1968), pp. 171–184.
5. R. J. Collier, C. B. Burckhardt, and L. H. Lin, *Optical Holography* (Academic, New York, 1971), pp. 206–210.
6. J. W. Wagner, "Final Segment Report: Characteristics of Optical Correlation Systems" CMDA80-009 (U.S. GPO, Washington, D.C., 1980).

6. SESSION V MOISTURE PHYSICS

6.1 THE PHYSISORPTION OF WATER ONTO INTEGRATED CIRCUIT PACKAGE COMPONENTS

by

James M. Ammons, Gerald R. Hoff and Michael Kovac
Center for Engineering Development and Research

and

Jack H. Linn and William E. Swartz, Jr.
Department of Chemistry

University of South Florida
Tampa, Florida 33620

ABSTRACT

The physisorption of water onto various substances commonly encountered in integrated circuits has been studied. Data were obtained for iron, nickel, gold, SiO_2, and polyimide using a commmercially available quartz crystal thickness monitor. Test gas mixtures containing 100 to 23000 ppmV water were prepared using nitrogen, hydrogen or helium. It was found that adsorption isotherms for most of the materials were similar to BET curves. Exceptions were those obtained for materials such as polyimide, which absorbs as well as adsorbs water. The quartz crystal oscillator technique is a powerful tool for characterizing the physisorption/disorption of water to package component materials. Since the technique can be employed at atmospheric pressure and not at high vacuum as do other surface techniques, it is possible to study materials under conditions which they may experience during processing and use.

INTRODUCTION

It is well known that moisture inside a microelectronic package can reside at a number of different locations. At any given time the location of the water is determined by the local temperature differential between competing surfaces and their adsorption/desorption properties as defined by their chemical and physical nature (1). This study is aimed at elucidating the intrinsic moisture uptake properties of materials commonly employed in component parts of microelectronic packages. These include gold, iron, nickel (2), silicon dioxide, silicon nitride, polyimide and others.

Previous work (2) has demonstrated that it was possible to study the physisorption of water onto various substances via a quartz crystal thickness monitor operated at atmospheric pressure. After coating with the substance of interest, the test crystal was exposed to a

controlled test gas containing known amounts of moisture. Water adsorption onto the various substrates was monitored by noting the resultant deviation of the frequency of the crystal. Most materials characterized appear to exhibit Brunauer, Emmett, and Teller (BET) (3) type adsorption curves.

EXPERIMENTAL

A. Equipment

Quartz crystal oscillator data were obtained using equipment described previously (2). This system consists of a Kronos QM 311 thickness monitor and FTT 350 detection head. The detector head was modified so as to allow unrestricted gas flow to both sides of the crystal and was housed in a stainless steel test chamber measuring 2" wide x 4" long x 1" deep. The analog output of the QM 311 was fed to a Hewlett-Packard 3465S strip chart recorder.

Controlled test gas mixtures containing 200 to 23000 ppmV water were prepared by dilution of water saturated carrier gas. Nitrogen (N_2) (boil off from liquid), dry compressed hydrogen (H_2) or helium (He) served as the carrier gas. The water content of the test gas stream was monitored via a General Eastern National Bureau of Standards (NBS) traceable optical dewpoint hygrometer.

B. Materials

Quartz crystals were obtained in plano-plano configuration from Phelps Electronics. These crystals were supplied with a nominal 1000Å layer of gold over a 1000Å chromium, both thermally evaporated. The base oscillating frequency was 4.73 MHz.

Nickel and iron were obtained with a minimum purity of 99.99% from Research Organics/Research Inorganics. Silicon monoxide was obtained from a commercial coating firm. DuPont Pyralin PI 2550 polyimide was obtained from Honeywell.

C. Procedures

Quartz Crystal Preparation. Water adsorption studies on gold were performed both on "as received" crystals and crystals which had been rinsed in isopropanol, or trichloroethylene under a blanket of dry nitrogen. Extreme care was exercised in removing all traces of isopropanol since, as was determined during the experiments, that the presence of even traces of a polar solvent led to greatly enhanced water uptake. Nickel and iron surfaces were prepared by thermal evaporation of the metal onto the existing gold/chrome surface of crystals which had been previously characterized for moisture uptake properties. Thicknesses ranged from 800Å to 1500Å. Silicon dioxide surfaces were prepared by thermal evaporation of silicon monoxide in a Drumheller (4) style source. Polyimide surfaces were prepared by spin coating the crystals and curing the material according to the procedures given by the manufacturer. All surfaces were analyzed via

X-ray photoelectron spectroscopy (XPS) for purity and composition. Nickel and iron were found to be present as a partially hydrated oxide. Evaporation of silicon monoxide yielded a surface which analyzed as silicon dioxide.

Water Adsorption Testing. Preliminary data were obtained by switching the moisture generation system to "drydown", waiting for the system to reach dry conditions as determined by the dewpoint hygrometer, zeroing the thickness monitor, and then stepping to a preselected moisture value of from 200 to approximately 24,000 parts per million by volume (ppmV). After equilibration (~15 min.) and subsequent data recording, the system was switched back to dry conditions. It was found that more rapid equilibration occured and equivalent data could be obtained if the system were first brought to dry conditions and then stepped sequentially from low to high moisture values. At the conclusion of the data gathering, the system was stepped dry. Drift in the instrumentation was found to be negligible over the time span of an experiment (~3 hours). The latter procedure was used in the majority of the work reported herein. Crystals were also stepped from wet to dry in order to demonstrate that the same equilibrium points were obtained. Generally, each crystal was allow to sit in "drydown" overnight before testing in order to ensure that equilibration with the dry carrier gas was achieved.

RESULTS AND DISCUSSION

A. Water Adsorption on Gold. Figure 1 presents data obtained for a typical gold coated crystal using nitrogen, hydrogen, and helium carrier gases containing up to approximately 23,000 ppmV water. The data have been corrected to account for only one side of the crystal (both sides are coated). This was done to facilitate comparison to other surfaces which were coated on only one side of the crystal. As can be seen, the shapes of the adsorption isotherms are quite similar for the three carrier gases and appear to be characteristically BET in nature. The onset of multilayer formation appears to occur at approximately 6000 ppmV. It would be expected that multilayer formation would start at the completion of one monolayer of water -- about 4.5 Å in thickness. Examination of the isotherms reveals that the inflection point at 5000-6000 ppmV water occurs at a 4 to 5 Å increase in thickness referenced to the zero point under dry conditions. The implication from this data is that a monolayer is formed at approximately 5000 ppmV water. It is possible that microcapillary condensation also occured, and, since this technique measures a change in mass , this water would also be detected. This seems unlikely since examination of the surface via scanning electron microscopy did not confirm the presence of significant numbers of capillaries. Therefore, fractional monolayers of water are probably present at ambient water concentrations less than 5000 ppmV. It should be noted that heating the crystal at 100° C for several hours in H_2 or N_2 had no effect on the shape or position of the isotherms.

The data have not been corrected for the difference in zero observed when changing from one carrier gas to another. This phenomenon is

believed to arise from a difference in packing and therefore condensed phase density of the carrier gas and not in water displacement or accumulation. The same relative change was observed no matter which order was used. With H_2 as zero reference, He was observed to have an increase in mass of 4.5Å, while N_2 was 22-24Å. The hydrogen carrier was found to have slightly more trace water contamination than the other two carriers. Repetitive experiments using only dry carriers failed to demonstrate that the differences arose from water adsorption/desorption.

Figure 2 shows a comparison between two gold crystals using an H_2 carrier. Similar curves were obtained with N_2 and He. As can be seen, there is a significant difference in moisture uptake between the two crystals. Scanning electron micrographs of the two crystals revealed that crystal 2, with the larger uptake, had an obvious and significantly rougher surface than crystal 1. Therefore, it is believed that the difference observed between these two crystals arises from a difference in surface areas. The crystal with the larger surface area exhibited greater water adsorption. While results from crystal to crystal varied, it was found that adsorption for a given crystal could be well characterized and was quite reproducible.

Figure 3 is a plot of water adsorption on iron (iron oxide) using H_2 and N_2. The plots have been corrected for a zero offset between the two carrier gases of approximately 24Å. As can be seen, there is a significant enhancement in water adsorption especially in the area of less than 3000 ppmV relative to the gold. This is undoubtedly due to the presence of the oxide. It was found during the course of this study, that oxide on a surface always lead to enhanced water adsorption. This confirms earlier observations (2). The shape of these curves is the same as that found in classical multilayer systems (5). The knee of the curve at approximately 2000 ppmV is traditionally taken to be the completion of one monolayer (5). In the present case, this corresponds to approximately 12-15Å of equivalent water. Since the instrumentation reading corresponds to mass, and not true thickness, this suggests that the oxide structure has significantly greater surface area than the gold.

An enlargement of the region of these curves from 0 to 6000 ppmV is shown in Figure 4. The displacement of the isotherm obtained in H_2 towards higher water content was reproducible on iron. A similar effect was not found in the case of gold or nickel. For iron, it appears that H_2 can cause a suppression of water adsorption at low moisture values. At values less than 3000 ppmV, the partial pressure of water does not seems to be sufficient to cause a full displacement of hydrogen.

Figure 5 shows the difference in water adsorption for two different iron crystals. The crystal termed "light oxide" was prepared by exposing a freshly evaporated iron film to air at room temperature, and is the same data as that presented in Figure 4. The "heavy oxide"

crystal was prepared by exposing a freshly deposited iron film to air while the crystal was at approximately 50° C for 10 minutes. The latter treatment resulted in a visible layer of oxide, which analyzed as an iron oxy-hydroxide by XPS. This is an extreme example of a trend noted repeatedly -- the more oxide present, the more water there is adsorbed, and the longer the time that is required for the surface to release the water and reach equilibrium with a dry carrier gas.

Figure 6 shows the results obtained for a nickel(oxide) surface. Again the nitrogen zero has been adjusted by 23Å. Both curves are classical multilayer formation curves. The similarity to the iron curves can be explained on the basis of the presence of an oxide surface. It should be noted that this crystal, like the iron crystal in Figure 3 was exposed only to air at room temperature. XPS analysis of this surface indicated that nickel is present as a mixture of oxide and water as was the case for iron. It has been shown previously (2) that this water is probably water of hydration and is therefore not physically adsorbed. Its presence, however, undoubtedly influences the physisorptive properties of both the nickel and iron surfaces. Oxides and water both are capable of forming associative bonds with water. Both the nickel and iron isotherms may be interpreted in terms of the BET equation or a modification (6).

The results obtained for SiO_2 are shown in Figure 7. The large amount of equivalent angstroms of water adsorbed illustrates the well known hydorscopicity of SiO_2 and glass in general. Undoubtedly the water significantly penetrated the upper layers of SiO_2 and formed a hydrated SiO_2 structure (7). Hydrated gel layers are known to exist and vary in depth from 50Å to 1000Å depending on the glass. As can be seen from the figure, relatively high levels of moisture (~10000ppmV) are required to initiate multilayer formation.

Figure 8 presents data obtained for polyimide. As can be seen, this material exhibits an enormous tendency to absorb and adsorb moisture. There is probably a multilayer structure formed on the surface but the amount of water required is insignificant compared to the amount of water absorbed by the polymer. Therefore the characteristically shaped BET curve is not readily seen overlaid onto the bulk adsorption curve. The time required for equilibration this material was approximately the same as for the other materials examined. This is probably due to the thickness of the material -- a few thousand angstroms.

SUMMARY AND CONCLUSION

It has been demonstrated that a quartz crystal thickness monitor may be adapted to measure the adsorption/desorption properties of various materials. It was found that materials which adsorb moisture through interaction with the surface atomic layer only (i.e., gold), exhibit a characteristic BET style adsorption isotherm. Materials which interact through the uppermost atomic layers, such as oxides, exhibit

enhanced BET type isotherms. It has been demonstrated that the amount of moisture adsorbed in this case is proportional to the amount of oxide present. Materials which absorb water as well as adsorb water (polyimide) are capable of retaining large amounts of water even under relatively dry conditions. In all cases studied, the adsorption process was found to be freely reversible in as much as desorption readily occured.

ACKNOWLEDGEMENT

This work was supported by Rome Air Development Center (RADC) under contract No. F30602-80-C-D169.

REFERENCES

1. G. A. Samorjai, Chemistry in Two Dimensions: Surfaces, Cornell University Press, Slhaca/London, 1981.

2. W. E. Swartz, Jr., J. H. Linn, J. M. Ammons, M. Kovac, and K. Wilson, Reliability Physics 21st Annual Proceedings, 52 (1983).

3. S. Brunauer, P. H. Emmett, and Teller, T. Amer. Chem. Soc., 60, 309 (1938).

4. C. E. Drumheller, Trans. 7th AVS Symp., Pergamon Press, New York, p. 306 (1960).

5. A. W. Adamson, Physical Chemistry of Surfaces, 4th Ed., Wiley Interscience, New York, Chapter 26 (1982).

6. L. E. Drain and J. A. Morrison, Trans. Faraday Soc., 49, 654 (1953).

7. H. H. Willard, L. L. Merritt, and J. A. Dean, Instrumental Methods of Analysis, 5th Ed., D. Van Nastrand Co., New York, Chapter 20 (1974).

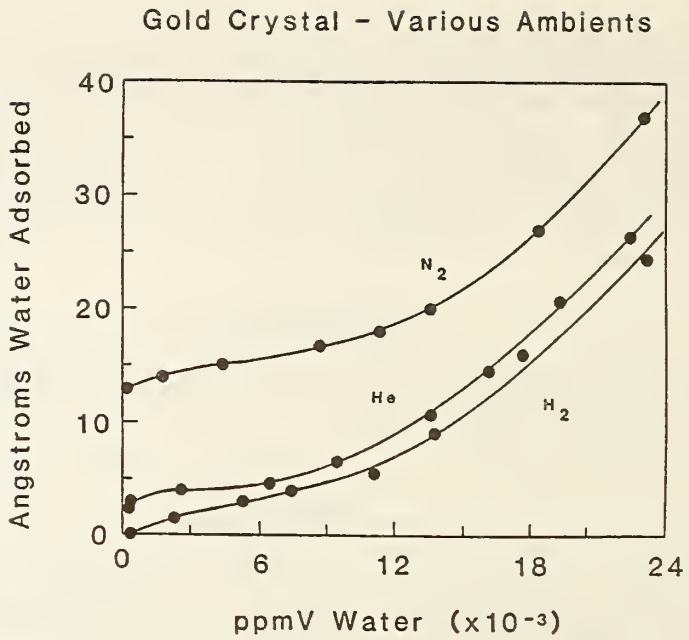

Figure 1. Water adsorption on Gold

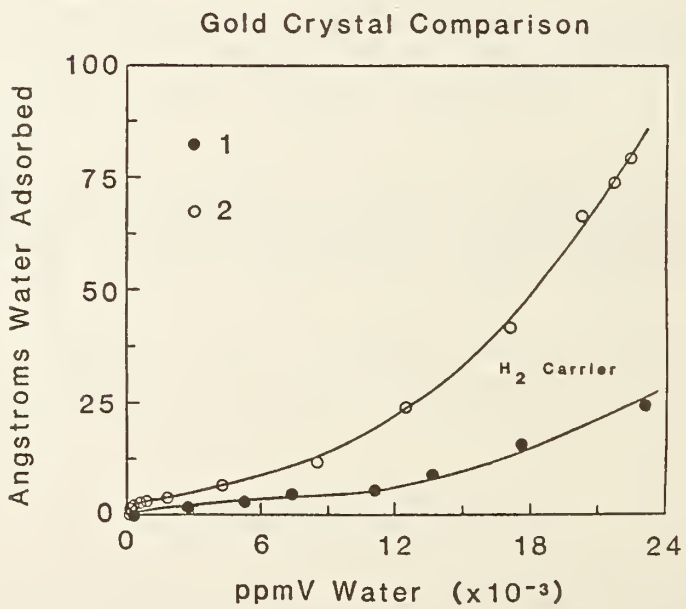

Figure 2.

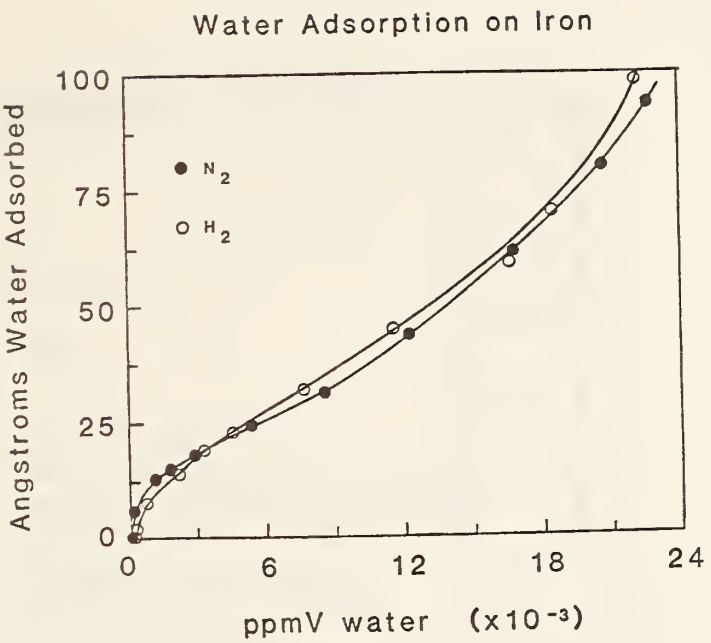

Figure 3.

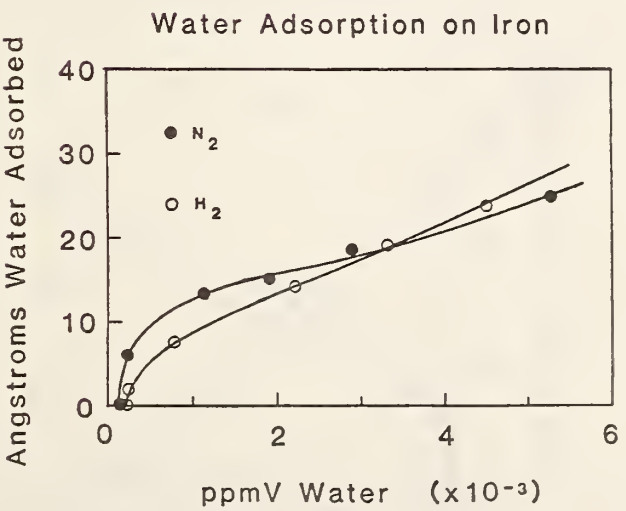

Figure 4.

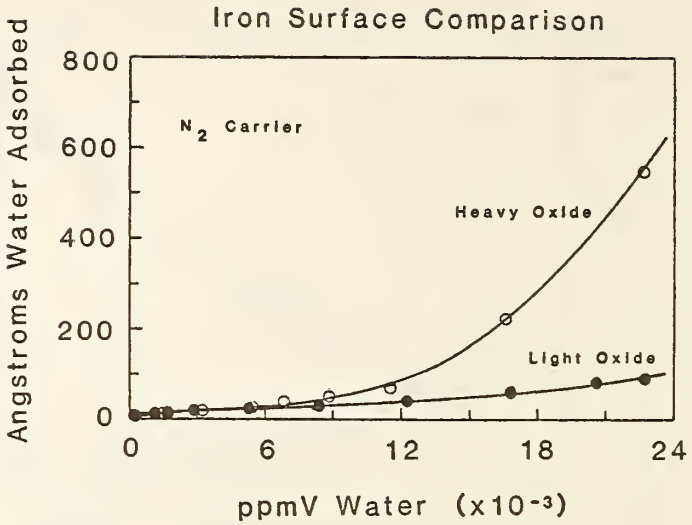

Figure 5.

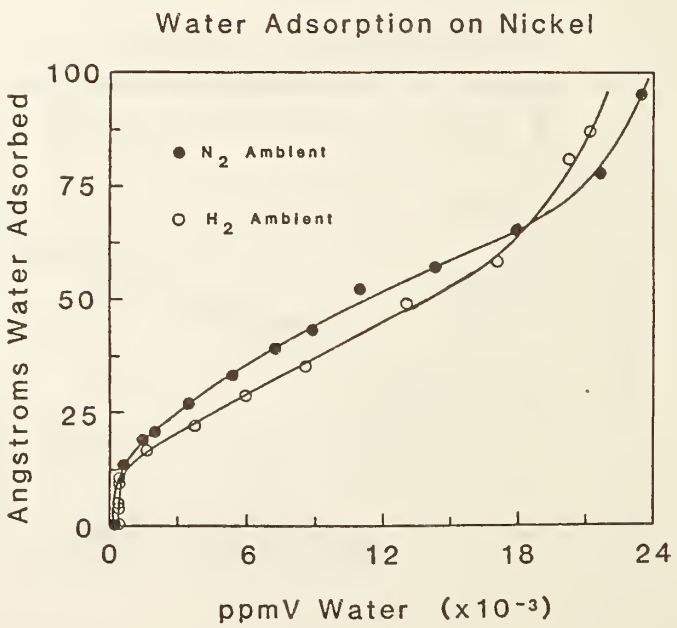

Figure 6.

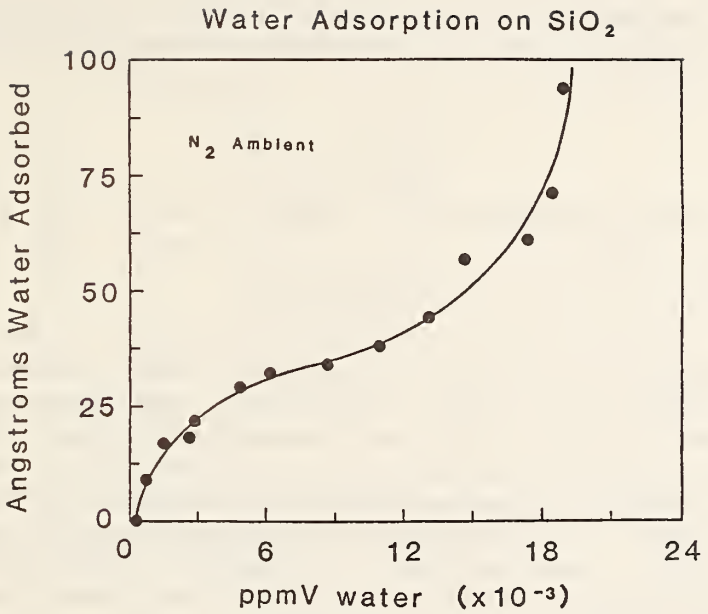

Figure 7.

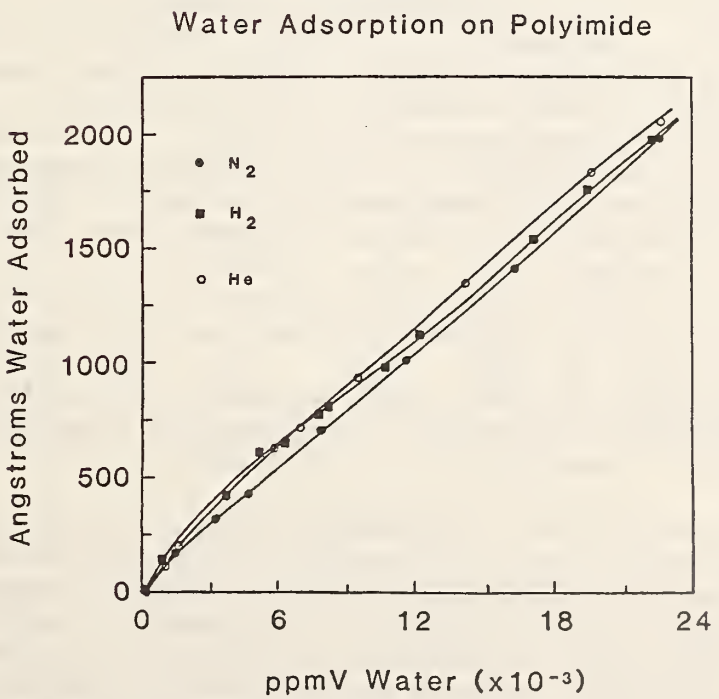

Figure 8.

6.2 SIMULATING THE CORROSION THRESHOLD OF LSI/VLSI DEVICES USING MOISTURE SENSITIVE TEST PATTERNS

John B. Kiely
Intel Corp.
3065 Bowers Ave., Santa Clara CA 95051

ABSTRACT

Two moisture sensitive test die, the Panametrics MM-HT and an Intel built interdigitated structure of aluminum lines on silicon oxide, have been used to simulate corrosive conduction. It is shown that an absolute minimum bound on the moisture limit for high reliability can be set by examining the moisture concentration threshold for conduction. A definitive value cannot be determined from this work, but for VLSI size CERDIP packages the industry standard 5000 ppma limit is probably sufficiently conservative. More investigations are necessary to quantify this value.

INTRODUCTION

The interest in measuring moisture concentrations of hermetic semiconductor packages arises from corrosion and metal migration reliability concerns. Both failure modes require a voltage, a reactive ion, and surface moisture to be present. Of these three, the package moisture level is the only realistically controllable attribute. Thus a measurement technology has been developed to quantify and control hermetic package moisture. The premier technique is residual gas analysis (RGA). Though powerful, it is expensive, slow, difficult to do, and under some circumstances the measurement can be erroneous [1,2]. Another technique is using surface moisture sensitive test die which can be calibrated to RGA [3,4]. The die are inexpensive and straightforward to use, but are not as sensitive as is RGA and are considered somewhat suspicious because of sensitivity, repeatibility, and calibration concerns.

It is interesting to compare the "measure and control the number of water molecules" philosophy of the hermetic package reliability workers to similar work in plastic package technology. Plastic semiconductor packages are often used in mild environments, such as air conditioned offices, or when high reliability is not a concern. The plastic technologists concern themselves with maximizing the time to failure of the packages in a harsh environment, eg. biased 85/85 (85°C/85% RH) or unbaised steam chambers. These difficult conditions act as accelerating factors

allowing the lifetime under normal use to be estimated. Test die are regularly used in plastic package corrosion investigations. This approach is not used with hermetic packages, mainly on the assumption that highest reliability is desired and (assuming the package is truely hermetic) accelerating techniques cannot be found to sufficiently quicken the failure rate for measurement in a reasonable time.

The only major pitfall with the philosophy of measuring package moisture is that the moisture level at which reliability is jeopardized is unknown. The industry standard of 5000 ppma is at best a guess [5], not an experimentally determined value. It is quite easy to make arguments that the standard has inaccuracies. For example, 5000 ppma of moisture in a 0.02 cc ceramic package corresponds to about two monolayers of water on the cavity surfaces. In a 10 cc metal package, 5000 ppma corresponds to tens of monolayers [6]. The discrepancy here is glaringly visible. The main problem with the fixed standard is that the industry uses a wide variety of hermetic packages, from large hybrid metal cans to small ceramic VLSI DIPs. A single reliability standard cannot span such a huge range. Unfortunately, there is no systematic way of determining the reliability standard moisture level for each package style; thus a best guess seems to be the only available solution.

This paper will illustrate a technique that can estimate the maximum moisture level for long term reliability in hermetic packages. The method involves low level leakage current measurements of moisture sensitive test die.

CORROSION CURRENTS

Corrosion or metal migration failure occurs due to a destructive ionic current. Estimates of current levels which jeopardize reliability can be made. For bondpad corrosion, failure will be defined as depletion of 30% of the bondpad metal. Also, the bondpad is assumed to be aluminum and there are three electrons conducted for each aluminum atom removed by corrosion. The time to failure (T) is

$$T > (V \times d \times 3 \times 0.3)/I = (V \times d)/I$$

where V is the bondpad volume (cc), d the aluminum density (atoms/cc), and I the corrosion current. For a bondpad (100 x 100 x 1) microns with a 1 pA corrosion current

$$T > 3 \text{ years.}$$

Thus, to assure a 30 year lifetime, the corrosion current should be below 0.1 pA in this example.

The significance of this example is that if one measured a current from the bondpad of this packaged device, THIS CURRENT IS GREATER THAN OR EQUAL TO THE CORROSION CURRENT. Consequently, an upper bound on the corrosion current can be determined. There-

fore, if the bondpad to bondpad current measured less than 0.1 pA in the above example the device would be reliable for the thirty year time period. One never knows the true corrosion current by this method, only the upper bound. Measuring less than one picoampere can be done, but it is not easy.

THE AMPLIFICATION FACTOR - PROPER TEST DIE DESIGN

It is quite simple to design a test die that amplifies the total current that would be observed on a real device. Take the previous example of the bondpad as an illustration. With a constant voltage, a larger current could be produced by using a pad with a larger perimeter. An example of exploiting geometries to amplify the measurable current are given in Figure 1.

This can be stated more analytically for both volume and surface conduction. An example of volume conduction is a current between two plates of a capacitor. Surface conduction is typified by current passing on a surface between two metal lines. Ohm's Law can be written for each case:

Volume Conduction: $I = \sigma \times (A/L) \times V$

Surface Conduction: $I = \sigma \times (P/L) \times V$

where σ is a conductivity, A an area, P a perimeter length, L the distance between conductors, and V the voltage. The conductivity is fixed by the type of material between the conductors, the moisture level, the number of available charge carriers, ect. The amplification factor is (A/L) or (P/L). Examples for surface conduction are given in Figure 1. Note that to quantify the amplification, the geometric configuration must be kept constant and only the dimensions scaled. Otherwise, the effects of fringing fields must be taken into account.

The methodology used in this work can now be stated. If one is concerned that 0.1 pA of corrosion from a bondpad is the maximum for adequate reliability, but the measurement accuracy is only 1.0 pA, then a test die with greater than 10X amplification using the same manufacturing technology can be used instead. It must be assembled and the leakage current measured under otherwise identical conditions.

CORROSION CURRENT THRESHOLDS

One more concept must be introduced before the experimental results are reviewed. If the material between the conductors is an "insulator" and no moisture is adsorbed, the conductivity is zero. As water molecules are added the conductivity does not immediately become nonzero. One water molecule cannot support conduction, nor can one monolayer (one monolayer of water is strongly bonded and has no mobility). As the number of water molecules increases a minimum conduction supporting film is

eventually formed. This is the moisture concentration threshold for conduction. Again, because the total current has the corrosion current as one of its components the previous rule can be restated as follows:

THE THRESHOLD FOR CORROSIVE CONDUCTION IS ALWAYS EQUAL TO OR GREATER THAN THE THRESHOLD FOR THE TOTAL CONDUCTION.

Physical models for conductive threshold effects abound in the literature such as percolation theories or domain growth theories. A very interesting physical example is the insulator to metal transition of doped polyacetylene. As the dopant concentration is increased a sharp increase in the conductivity occurs at 2 - 3 % doping. Resistivity changes of twelve orders of magnitude have been observed [7]. Which model most closely models the data in this work is indeed interesting, but not necessary for a first order analysis. An analogy will be given, though, to illustrate the dependent variables.

Consider a fish tank with perfectly insulating sides and bottom except for two opposite sides. An ohmmeter is connected to the two conductive sides such that there is an open circuit between the two plates. Now the tank is filled with glass balls. The measured resistance is infinite. Then remove all the balls and replace one glass ball with an iron ball, mix the balls up well and replace them in the tank. If this one ball replacement step is repeated over and over eventually the iron balls will form a closed circuit between the conductive sides and a finite resistance will be measured. During the step where the circuit is first completed the resistance will jump from infinite to some finite value. This quantum change marks the iron/glass percentage threshold for conduction.

This simple analogy illustrates the variables that determine the threshold value. The first variable is the percentage of water in the package, equivalent to the iron to glass ratio in the example. It is the water between the conductors that is important, but for both volume and surface conduction this should be proportional to the total moisture content. The second variable is a materials property, such as the hydrophobic or hydrophilic nature of the surface. The anology in the fishtank example is whether the iron balls tend to form clumps (they are magnetic) or be randomly but uniformly distributed.

The last variable is not obvious and requires some explanation. The threshold may or may not depend on the distance between the conductors. In the fishtank example, if the balls are infinitely small the threshold occurs at the same <u>percentage</u> regardless of the conductor spacing. However if the ball diameter is a significant fraction of the spacing, then varying the distance would change the threshold point. The similar situation for a device is whether the moisture builds up in consistent monolayers as the package moisture increases, or whether it forms nucleated clumps and the clumps grow with the increasing ambient moisture. If the

moisture forms clumps with mean diameters that are significant fractions of the conductor spacing then a distance dependence will occur.

The purpose of this paper is not to form a detailed theory of the conduction process. However in order to interpret the data a few assumptions must be made. Therefore, assume the threshold dependent variables are the moisture percentage in the package, the type of material between the conductors, and further assume the dependence on spacing is either weak or nonexistent. Consistent with these assumptions, one would expect the leakage current versus moisture content (as measured by RGA) to behave as in Figure 2.

EXPERIMENTAL TECHNIQUES

Two test die were used in these studies. The first was a structure of interdigitated aluminum lines on a thermal oxide grown on a silicon substrate. The conduction path was from one metal line, across the surface of the oxide to the other aluminum line. The line spacing was eight microns and the line periphery was about 64,000 microns. If compared to a typical device design rule for bonding pads of 100 x 100 microns with a 100 micron pad to pad spacing, the test die had an amplification factor of about 8000.

The second test die used was the Panametrics MM-HT Sensor die [8]. Because it is a gold/aluminum oxide/aluminum capacitor, it approximates a volume conductor more closely than a surface conductor. The conduction should be along the granular boundaries of the aluminum oxide; therefore it only closely approximates a true volume conductor. For the purposes of this paper, it is assumed that the die is a volume conductor with an area/thickness ratio around 10,000 cm. Relating this to a surface amplification factor is impossible. The Panametrics die had a capacitance about 50X greater than the interdigitated structure. One would expect that the amplification factor would be larger due to the more intense electric field. This is speculation though, subject to experimental verification. The conductor spacing of the MM-HT is roughly 100X smaller than the interdigitated spacing.

The most sensitive leakage current measurement technique is by DC methods. The capacitances involved are large enough that hundreds to thousands of picoamperes of displacement current will be conducted if AC detection is used. For example:

Die capacitance C = 50 pf
at a frequency f = 10 Hz
and a voltage V = 25 V
the displacement current is 80 nA .

Measurement resolution of better than 10 - 100 pA is difficult under these AC conditions, but with DC techniques resolution of

around one picoampere is possible.

There are serious disadvantages to using DC methods. Figure 3 illustrates the worst drawback - the leakage current has an initial decay that can last for many minutes. Figure 3 demonstrates the situation for the interdigitated die, the Panametrics die has a similar behavior. This decay phenomena is probably due to polarization effects. Any bound dipoles on the surfaces will align with the applied electric field. The long time decay is caused by the binding: the electric field has to break this force before the dipole can align. The primary evidence that this is the proper model is that the decay shows hysteresis with the field polarity. If the voltage is applied in one polarity and then repeated with the same polarity after a short rest, the second decay is very small. This is because the dipoles were already properly aligned for the second try. If the second application is at opposite polarity a large decay again occurs; the dipoles must be flipped this time. Though this polarization current is moisture dependent, it has nothing to do with the corrosion current. The corrosion current cannot cause serious damage if it is only a transient. The measuring circuit is shown in Figure 4.

Another DC measurement problem is parallel conduction in the package or the measurement circuit. If a leaky switch is used or the package material is slightly conductive, this circuit is in parallel with the die leakage route and could cause erronous readings. It is actually quite difficult to keep pin to pin leakage in a ceramic package below one picoampere at greater than 60% relative humidity in the room. The method for control under these circumstances is to do a differential measurement: measure the leakage for equivalently spaced open pins and then measure the pins attached to the die. For this work, units with open pin currents above one picoampere were discarded (less than 5% of the units were discarded). Therefore the differential technique was not needed. The resolution was 1 - 2 pA for the interdigitated die and 4 - 5 pA for the Panametrics die. The reason for the increased noise and drift on the Panametrics sensor was never determined, but both noise levels were sufficiently low for these investigations.

The packages used were 24 lead CERDIPs (a ceramic dual-in-line-package using a solder glass for the lid to base seal) with a vitreous sealing glass. The package was desiccant free and the die attach was gold/silicon eutectic. The method for generating wet packages was crude but effective. Packages were sealed on a heaterblock in room air at 40 - 50 % relative humidity. A nozzle of heated nitrogen was used to modulate the amount of room air in the package cavity, done by positioning the nozzle at varying distances from the package during seal. Though extremely crude, a range of 2000 to 16,000 ppma moisture could be obtained. More controlled methods exist [9] and are recommended over this technique for more quantitative studies. The Intel standard sealing process (<< 5000 ppma) was too dry for use in this work.

All the packages were electrically measured and sorted into groups of nearly identical leakage currents. A standard time of one and a half minutes was used for decay settling after a bias was applied to the die (ie. the reading was made 90 seconds after the bias was applied). The bias voltage was 25 VDC for the MM-HT and 40 VDC for the Intel interdigitated die. Random samples from each group were then measured for internal package moisture using the Intel RGA. The RGA readings were corrected as necessary for the oxygen content to null any spurious signals generated in the equipment [2]. After RGA, all die were tested for functionality.

EXPERIMENTAL RESULTS

The results are given in Figure 5 for the leakage current versus package moisture (as measured by RGA) for both test die. Figure 6 shows a more detailed analysis with linear and quadratic fits for the Panametrics die. The fits were done by ignoring the zero current data points. Therefore, the conduction thresholds shown in the fits are from fitting the nonzero data points. Note that the thresholds determined by fitting agree quite well with the "by eye" threshold. The Panametrics die was by far the most sensitive of the two. As shown in Figure 6, the threshold for conduction is 2100 ppma for the linear fit, 2800 ppma for the quadratic fit, and about 3000 ppma "by eye". The interdigitated structure is not sensitive below 9000 - 12,000 ppma and the data quality is not as good due to lower sensitivity to the moisture levels above 10,000 ppma (ie. the amplification factor is smaller).

Qualitatively the data fits the simple model quite well. The slope of the nonzero portion of the MM-HT plot is 30X - 60X larger than the equivalent interdigitated die region. This is strikingly close to the ratio of capacitances. Also, the 100X difference in conductor spacings made only a 3X - 4X shift in the threshold point. Finally, note that for the Panametrics die (the test die for which the data is the best) the threshold is a very sharp phenomena. If the conduction is supposed to suddenly turn on, as the model predicts, then this sharpness is expected.

Detailed quantitative conclusions cannot be drawn from these data. It was noticed that the MM-HT sensor leakage current increased with age as much as 50 % in a three month period for packages in the 4000 - 7000 ppma range. Whether the Panametrics die decreases in sensitivity with aging or the packages slowly getters moisture was not determined. All packages were verified to be hermetic, so ambient gas leakage could not be the cause. No similar shift with time was observed with the interdigitated structure, but the sensitivity cannot compare to the MM-HT.

CONCLUSIONS

The most outstanding conclusion of this work is that the conduc-

tion threshold for moisture dependent conduction does exist. The consequences of this fact is that a lower limit on the corrosion threshold for the test die can be set: it must be at a moisture level equal to or greater than the level for the total conduction threshold. This is because the total conduction must include the corrosion current as one of its many components. If the test die is properly designed (ie. it is identical in manufacturing technology as the real device, except that the conductor geometries are changed to take advantage of amplification) then the corrosion threshold of a real device can also be bounded.

To prove the model for the conduction threshold and amplification factor quantitatively, more detailed experiments are needed. The best experiments would characterize the threshold and amplification with a number of similar test die geometries where only the P/L or A/L of the die are allowed to change. A comparison with identical geometries but differing insulators (for example, thermal oxide versus silicon nitride versus CVD oxide) would also be useful.

An important conclusion shown by this work is that the Panametrics MM-HT is an extremely sensitive design. It is more sensitive in fact than anything normally designed into a semiconductor chip. These data have shown the MM-HT in CERDIPs to be insensitive below 3000 ppma. Furthermore, the Intel die more closely simulates MOS technologies and the threshold in this case is around 10,000 ppma. The result from all this is that the 5000 ppma reliability limit in CERDIPs is most likely correct or too conservative, but not too loose. The author's personal opinion is that for VLSI CERDIPs the proper reliability limit is in the 5000 to 15,000 ppma range. The "best guess" of 5000 ppma is probably a good safe limit. Note that more test die designs would have to be run to confirm this and that these results only hold for IC DIP type packages. The surface to volume ratio of the package cavity should greatly affect the results due to moisture gettering by the walls. Therefore, although the principles should be the same for larger packages, such as large hybrid circuits, the threshold point may shift for those packages. For LSI/VLSI type devices the safety of the 5000 ppma limit seems sensible: both makers and users of LSI/VLSI semiconductors have stated that moisture related reliability issues have evaporated since the enforcement of MIL STD 883 Method 1018. Regardless of whether the issues were real or perceived, the 5000 ppma limit seems to have settled them.

ACKNOWLEDGEMENTS

I would like to thank Dr. Richard Blish of Intel for many useful discussions over the last two years on the topics of corrosion and moisture sensors. Without his suggestions and tutoring I doubt the results would have been as successful as they were. I would also like to thank Dr. Paul Flinn of Intel for many similarly useful discussions.

REFERENCES

1. J.C. Pernicka; "Moisture Measurement By Mass Spectrometry", ARPA/NBS Moisture Measurement Workshop (March 1978), NBS Spec. Publ. 400-69; pg. 45.

2. J. Kiely, P. Flinn, and B. Sun; "A Mechanism For The Dependence Of Moisture Detection Sensitivity On Gas Composition In RGA", Int. Rel. Physics Symp. (April 1981); pg. 167.

3. M.G. Kovac; "Cross Correlation Experiments On Different Types Of Sensors", NBS/RADC Moisture Measurement Technology Workshop (Nov. 1980), NBS Spec. Publ. 400-72; pg. 76.

4. J.C. Hale and V. Fong; "Moisture Sensors, Mass Spectrometry, And MIL Standards", ibid (ref. 3); pg. 90.

5. R.W. Thomas; "Problems In Specifying And Measuring Moisture Content In Electronic Devices", ibid (ref. 1); pg. 179.

6. For example: assume a square volume, a microscopic roughness factor of 2 - 4, and a 5 A° water molecule spacing in a monolayer. These numbers are only approximate but they do illustrate the surface to volume effect quite well.

7. C.K. Chaing, C.R. Fincher, Y.W. Park, A.J. Heeger, H. Shirakawa, E.J. Louis, S.C. Gau, A.G. MacDiarmid; "Electrical Conductivity In Doped Polyacetylene", Phys. Rev. Lett. Vol. 39 (Oct. 1977); pg. 1098.

8. Panametrics Inc., 221 Crescent St., Waltham MA 02154

9. M.L. White and R.E. Sammons; "A Procedure For Preparing Hermetic Packages With Known Moisture Levels", ibid (ref. 3); pg. 49.

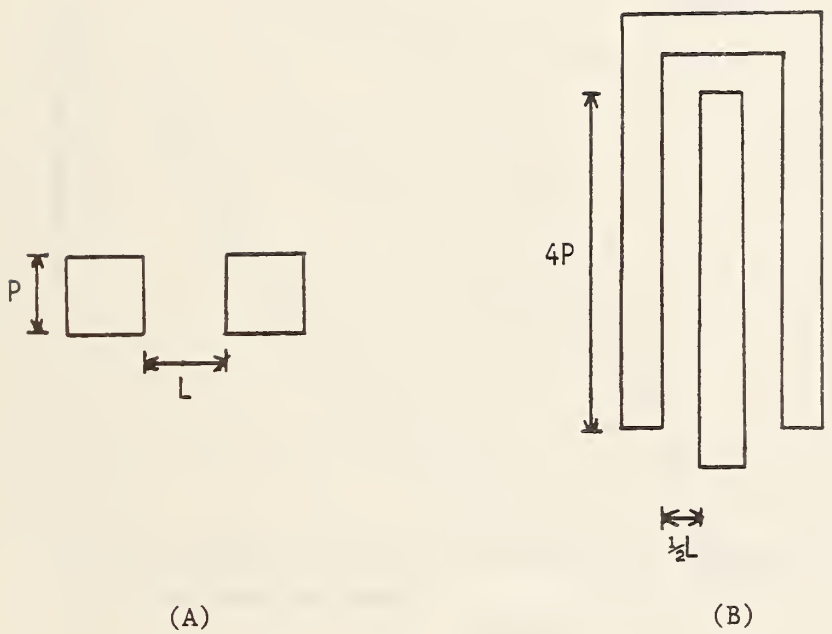

Figure 1 An example of using die design to amplify a surface current. In case (A) the conduction path size is P/L, whereas in (B) it is about 16 (P/L). Therefore, the current is amplified 16X by using (B) design.

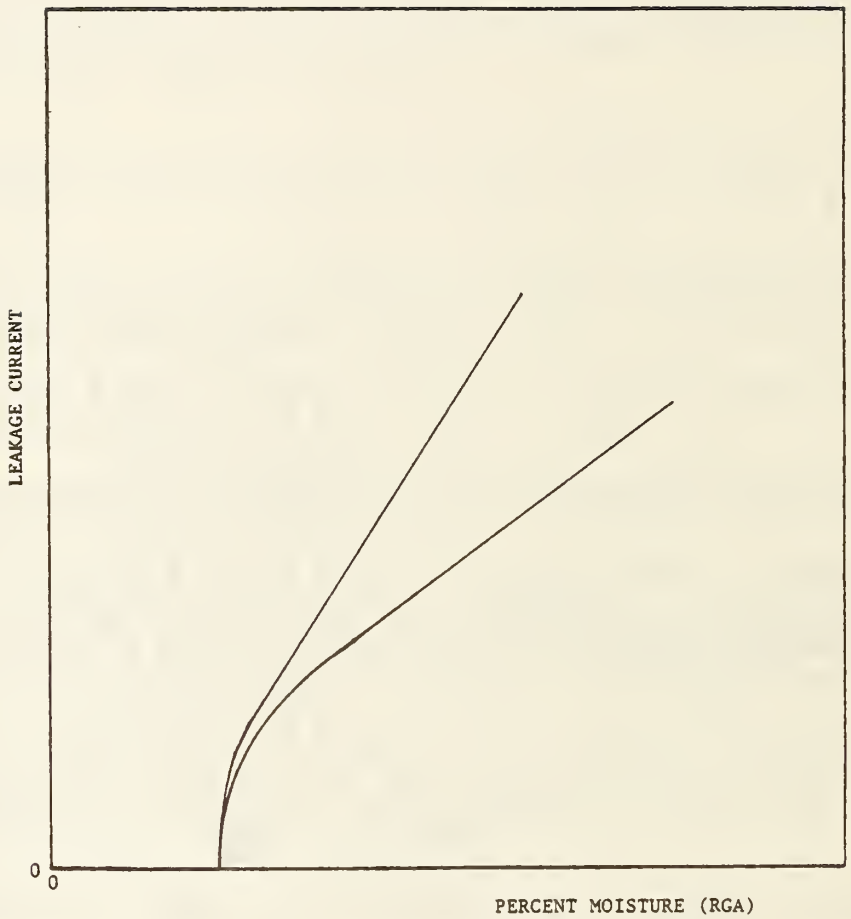

Figure 2 The expected behavior of the die leakage current versus ambient moisture in a hermetic package. Two examples are shown to illustrate the effect designed in amplification has. The lower curve has less amplification.

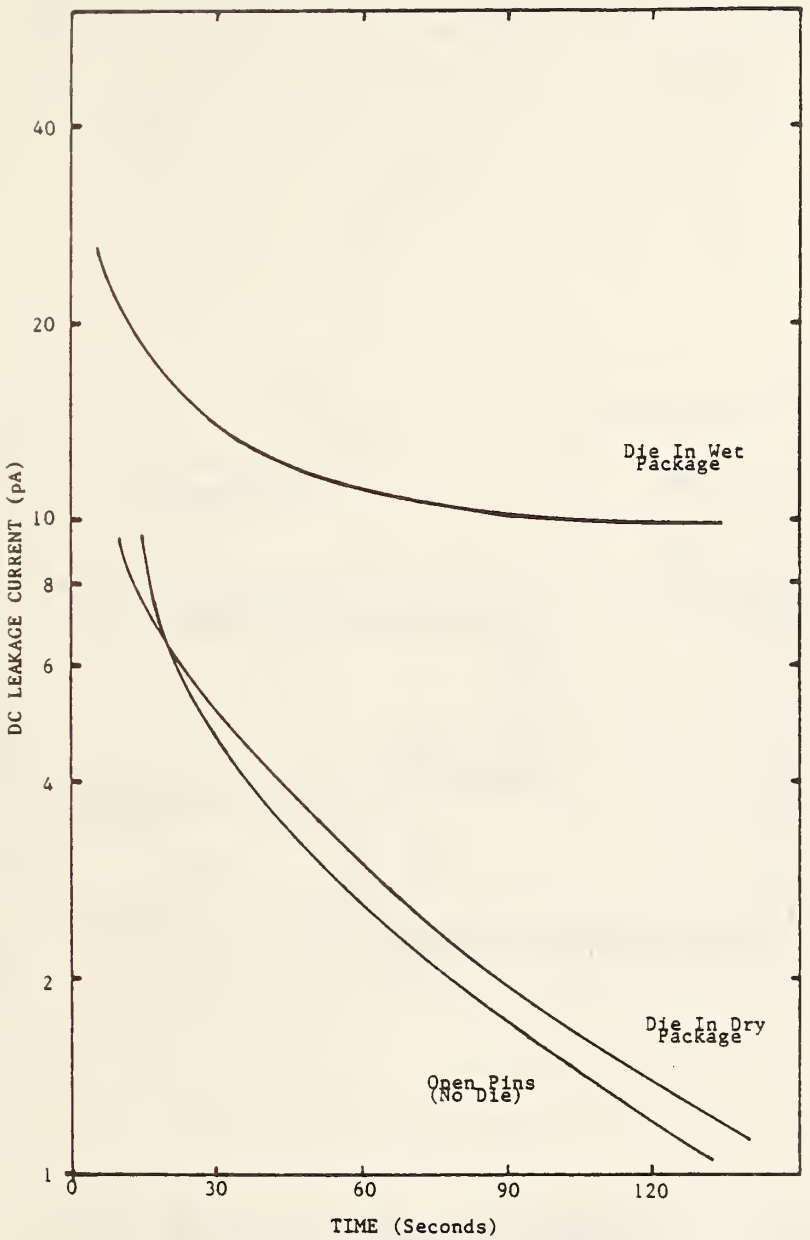

Figure 3 The measured DC leakage current versus time for the Intel interdigitated die. Time zero is when the DC bias is applied. The relevant current for this work is the value after about 90 to 100 seconds.

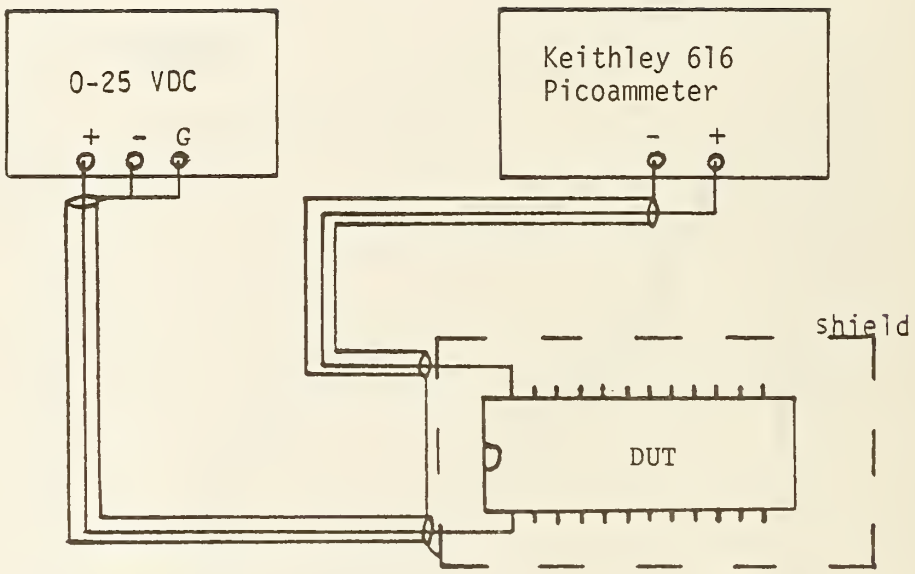

Figure 4 The measurement circuit used in this experiment

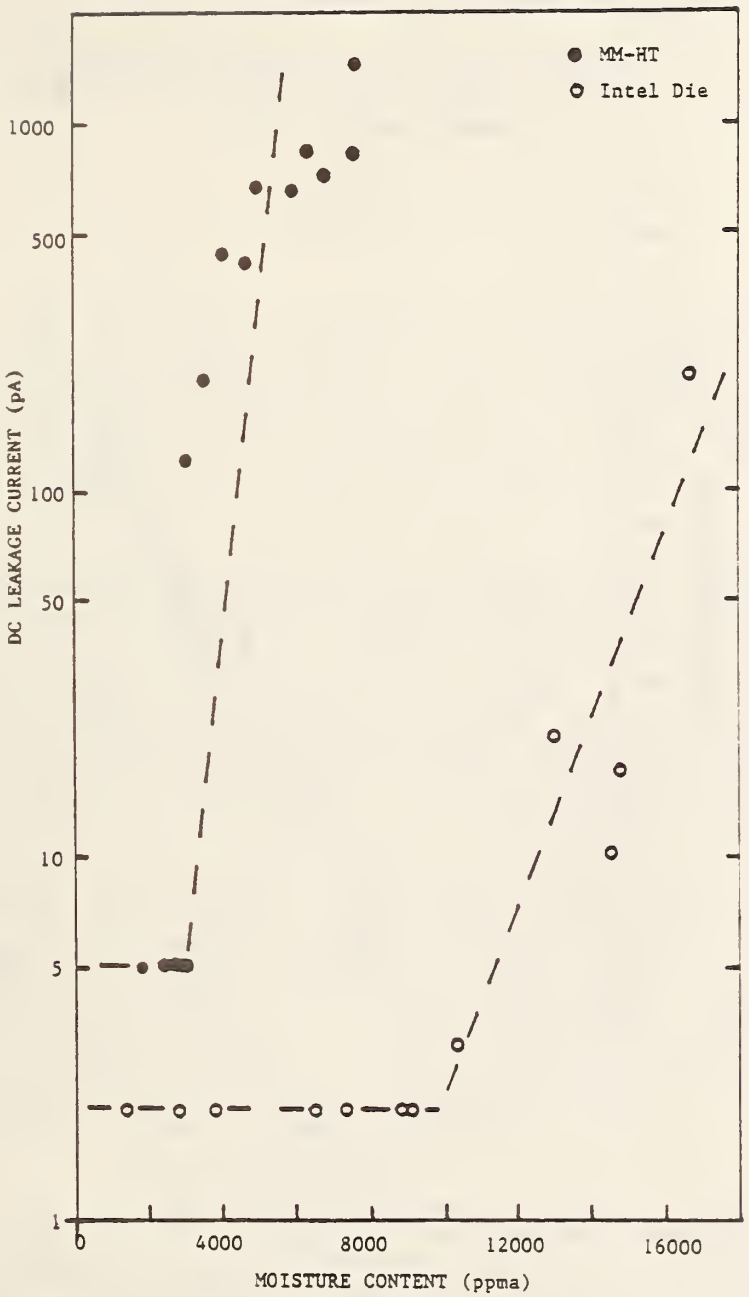

Figure 5 The DC leakage current versus internal moisture (measured by RGA) for the Panametrics MM-HT and the Intel die. The dotted lines are guides for the eye. The lowest current points for each die were actually fluctuating around zero. All such points were plotted at the measured noise level for graphical clarity.

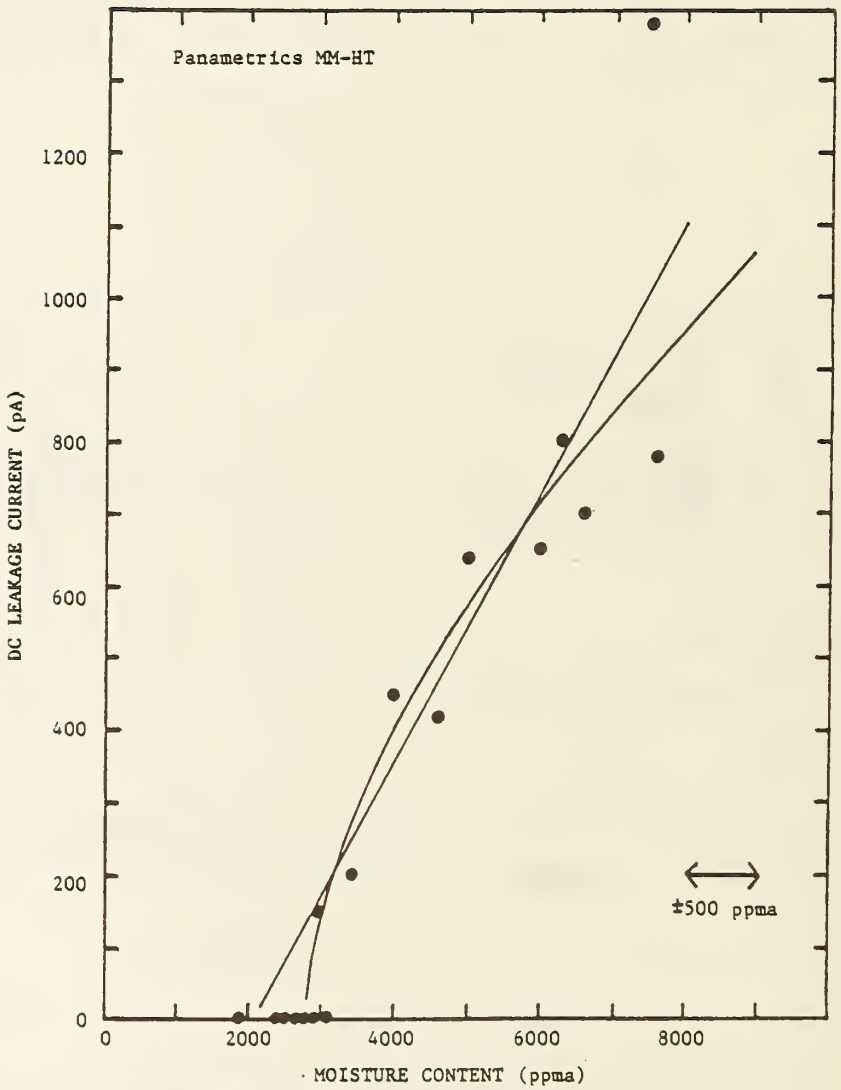

Figure 6 The same Panametrics MM-HT data as in Figure 5 with linear and quadratic data fits. The thresholds from the fits are 2100 ppma for the linear fit and 2800 ppma for the quadratic fit. A reasonable RGA uncertainty is ±500 ppma (shown).

6.3 THE EFFECT OF HUMIDITY ON CERMET RESISTORS

Thomas R. Homa and Phillip P. Vadala
IBM Corporation
Endicott, NY 13760

ABSTRACT

The development of the thin film Cermet (Cr Al O) resistor material involves assessing the product's stability to typical commercial computer environments. The standard package for these resistors is not hermetic. An epoxy seal is used in this package but it only delays moisture transport into the interior of the module. Therefore the resistors must be capable of operating in equilibrium with nominal humidity.

During accelerated testing it was learned that high resistance drift was occurring on samples that were operating at nominal power levels. Modules exhibited the problem after 400 hours in 85°C/80%RH with a 25mW load. The thin film resistors were visually changing from an opaque material to a transparent one around the laser trim areas. The conversion was accelerated when a conformal coating was applied to the resistors. When a thin epoxy layer from the encapsulation process seeped onto the resistors, or a corrosion inhibiting polyimide film covered the resistor, more drift was observed than when the resistors were uncoated. Stress tests on modules with normal ionic contamination levels were not significantly different than ultraclean samples. Different humidity levels were tested to see if a humidity acceleration factor could be defined, however, no drift was observed on modules exposed to conditions less severe than 85°C/80% RH. When a silicone coating was placed over the resistors, no drift or attack was observed at any humidity level. Parts with the coating stressed through 2000 hours of 85°C/80% RH had drifted less than 0.2%. All functional requirements were achieved with this coating.

INTRODUCTION

The rapid advance of computer technology is demanding novel packaging approaches to satisfy the aggressive system requirements. Each new generation of systems has become physically smaller, uses less power, and is significantly faster than its predecessor. One of the major items affecting performance in many computers is the time needed for a signal to pass from one chip to another.[1] In order to reduce this delay the chips must be placed closer together, or each chip must have more functions. When more circuits are placed on a single chip, more electrical contacts are usually required, but that is feasible only if the package can accommodate more connections and signal paths.

Paste thick film resistors have been successfully used in the computer industry for many years, however paste resistors require paste conductor lines which have density limitations. Line-to-line and line-to-contact tolerances are not sufficient to allow large output chips to be

connected in the most efficient pattern. In order to reduce package size and increase density, evaporated copper conductors have been developed. With this technology, high density packages can be achieved in a minimal amount of space.[2]

In high density packages there is still a critical need for precision resistors. The resistors must conform to the overall package strategy in that they must be compact, very reliable, capable of active adjustment, and indigenous within the package to minimize delay time. Finally, because of the intense competition, the package must be cost effective. For use in commercial systems, the trend has been away from strict hermetic packages and into various types of plastic encapsulations. Plastic packages should be classified as "quasi-hermetic" in that there are no direct free paths for contaminants to reach the chip area, but diffusion, especially of water vapor, readily passes through the seal area.[3]

PACKAGE DESCRIPTION

The package used by IBM many in its low and intermediate end systems may have between one to three chips in a pin grid array design whose physical dimensions range in size from 12 to 36mm. All connections are on the top surface and there are no interplanes within the ceramic. The chip is connected by reflow solder joints [4],then a conformal topseal is applied. The topseal on copper conductors is an amide-imide copolymer (AIP). The entire assembly is placed into an aluminum cap and sealed with epoxy.

The details regarding fabrication of the Cermet resistor have been published [5] previously and only a brief description of the product will be given here. Product specifications for this resistor are ±1% from trim to end-of-life. To facilitate testing, 0.6% has been apportioned between end-of-process and end-of-life. End-of-process is defined as a completed module mounted on a printed circuit carrier. Cermet is defined in the context of this paper as a thin film resistor originating from a Cr/SiO target. Depending upon deposition method and subsequent thermal treatments, the resistor material transforms to varying proportions of chrome silicides, SiO_2, and alpha chromium.

The bare alumina substrate is entirely covered by sputtering from a 62/38 (mole %) Cr-SiO target. Then the conductor material (copper) is blanket deposited over the surface. Circuitry is produced using conventional photoresist and etch wet processes. The copper conductor is then removed from the resistor locations to give a completed substrate. A schematic of the typical part is shown in Figure 1. Contact resistance is reduced because the resistor material underlays the circuitry and therefore provides a broad contact area in contrast to that for a paste resistor. A typical part is shown in Figure 2.

The substrates are next sent to chip join for the reflow operation. After this step the assembly is ready for trimming. The resistors can either be passively trimmed to a specific value or the chip powered and the signal adjusted to a specific output. Topseal and backseal are applied and the module is complete.

STRESS TESTS

When a new technology is proposed, a number of accelerated reliability tests are performed to determine how the product will withstand field conditions. The tests are similar to the MIL standards but are modified for commercial products.

Accelerated Stress Tests

Thermocycle	0-100°C 3 cycles/hr.
Thermal age	130°C
Temperature & Humidity	85°C/80%RH
Wet Sulfur	
Corrosive Gas	
Shipping Stress	-40 +65°C

The temperature and humidity stress is performed with and without a 10V bias to examine susceptibility to migration and corrosion failure mechanisms respectively. All tests were successfully completed.

During the 10V temperature and humidity bias test, an anomaly occurred on the Cermet package. There are instances where resistors are deleted from the circuit by simple complete cuts with the laser. To test the possibility of metal migrating back across the gap and shorting the deleted circuit, a simple bias test was initiated. The part was produced in the standard manner, and the AIP topseal placed on all resistors. After 1000 hours of stress with a 10 volt bias no shorting was observed and the test was considered successful. However, when the module was examined, the laser delete appeared to have grown in size as shown in Figure 3. Parts without bias were unaffected.

Such a change is not a problem with a delete, but what about a real part that has been trimmed? Figure 4 shows voltage distribution of a resistor trimmed to 7352 ohms with a total drop of 10 volts. At the start of either plunge cut, there is a potential of about 8 volts across the trim gap. Therefore if a resistor was trimmed to that specification and run at a nominal load, degradation may be observed.

CONTAMINATION

At this point it was felt that contamination was the major cause for the degration. In any failed temperature and humidity test, contamination is always suggested as the cause, especially when a bias is involved. A sample of 20 substrates were identically prepared with 10K ohm resistors, except 10 were cleaned in an ionograph [6] bath. [An ionograph bath is a mixture of isopropyl alcohol and water. The alcohol suppresses the ionization constant of water and allows the solution to remove more ionic material than possible with pure water]. The parts were then stressed for 1000 hours in 85/80 with a 10 volt bias. During readouts, the load was removed and the modules taken from the humidity chamber to a 100°C drying oven for 24 hours. Failed resistors are those that changed more than 0.6% from the initial value. The results are given in the following table

OUT OF TOLERANCE PERCENT vs. TIME

STRESS TIME (Hrs.)	528	816	1000
NORMAL HANDLING	3%	22%	25%
IONOGRAPH CLEANED	0	18%	25%

There appears to be a very slight difference between normal and ionograph cleaned parts, but clearly not enough to categorically define contamination as the major cause of resistor drift. Whatever is causing the resistance drift did not appear to be strongly dependent upon ionic contamination level and no further testing was performed with contamination as a variable.

A careful examination of the parts that had significant positive drift shows an attack of the resistor in the region of highest potential drop as mentioned earlier. An example of the degradation is shown in Figure 5. The resistor material appears to have been transformed in the attacked region from an opaque to a transparent film.

POLY AMIDE-IMIDE COATING COVERAGE

The next item to be investigated was the extent of topseal coverage. A test matrix was developed to stress parts with 100%, 50%, and no AIP topseal coverage with a 5 volt drop across the resistor. The 50% resistors were prepared by simply painting about half of the resistors with a brush. All resistors on the package were trimmed to 15K ohms, and backsealed with epoxy. After 1000 hours of 85°C/80%RH significant drift was observed on all modules. For each readout the modules were removed from the humidity chamber to a 100°C drying oven for 24 hours. The damage was again found in the regions predicted by the voltage distribution model.

Figure 6 shows a cumulative plot of the percent drift. From the graph we can see that the uncoated resistors drifted the least, 100% coverage drifted more, and the resistors with 50% coverage drifted the most. If the 0.6% drift criteria were used, the failure rate for 0, 50%, and 100% coverage would be 6%, 17% and 10% respectively.

POWER LEVELS

A test was designed to examine the effect of drift as a function of power level, temperature, humidity, and time. We were looking for a critical temperature and humidity below which no reaction occurred. Parts were produced to the following specifications: Six resistors per module, all trimmed to 15K ohms, no topseal or backseal, four modules per cell. Our intent was to start substrates at a low humidity level and record any changes for a fixed time, then the humidity would be increased and the process repeated. All readings were performed in-situ. A description of the matrix is given in Figure 7.

The results of the step stress may be summarized as follows. No significant drift was observed in the 70°C test regardless of relative humidity or power setting. In the 85°C cell, no drift was observed at relative humidities less than 80% RH. Modules were held at 80% RH for 400

hours to see if any drift could be induced. The results of this test are shown in Figure 8.

There was a slight increase in resistance for cells stressed in 85/80 as can be seen in Figure 8b. The results are not uniform because the most drift was observed on the 50mW cell and not the 200mW one. This may be explained by the fact that the surface temperature of a 200mW resistor is about 40°C above ambient which will reduce the relative humidity in the vicinity of the resistor from 80% to less than 20% RH. Conversely a 25mW load will only raise the surface temperature about 5°C. Therefore the 200 mW cell should not drift as much as the 25mW one if the reaction is dependent upon relative humidity.

RESISTOR LOCATION

When the raw data was examined it was observed that certain locations seemed to be more susceptible to drift than others even though all resistors were trimmed to the same final value. The high drift resistors were near the edge of the substrate on parts without topseal coating but were backsealed with epoxy. Closer examination showed that some of the epoxy had wicked between the cap and substrate and wet the suspect resistor.

SILICONE TOPSEAL

A number of moisture studies on this particular package have been performed [7] which revealed that the encapsulated package stored at 85°C/80%RH can contain about six times more moisture than expected from free volume condensation. This moisture must be adsorbed on the interior surfaces of the package. Because the drift was greater on coated resistors, more moisture must be adsorbed on them rather than on uncoated resistors. Very little drift was observed on coated resistors powered to 130°C.

A protective coating was necessary to prevent formation of the moisture film [8]. A simple barrier coating is not sufficient because given enough time, moisture will diffuse through the film, just delaying the inevitable reaction. The coating should form high energy bonds with the conductor which are not broken by moisture. It should have a low solubility of water to suppress conductivity in the film itself. The film should have a low sorption coefficient and be chemically stable. The material which can meet these requirements is a silicone topseal. Corrosion studies have been performed on other systems where the corrosion properties of AIP [9] and epoxy [10] were compared to silicon topseals. It was found that the electrodes were protected by the silicone but attacked under the other materials.

Several tests were initiated to study the effect of Cermet resistors under silicone in our particular IBM package. The first test was run with 10K ohm resistors at 85/80 with a 25mW bias. One set of substrates had silicone over all the resistors while the other set was not intentionally coated. All modules were sealed with epoxy. After stressing the results could be divided into three groups, 1) coated with silicone, 2) uncoated,

3) coated with accidental run-in from epoxy backseal process. The results are presented in below:

PERCENT FAILS AFTER 500 HOURS

Silicone Coating	Epoxy Coating	Uncoated
0%	27%	5%

As can be seen, there were no fails under the silicone. On the uncoated resistors, very few resistors failed, while on the resistors where run-in occurred, a much larger fraction was affected. The reduction of drift by the silicone on modules sealed with epoxy can be simply explained by the fact that when silicone is put on first, it will prevent wetting of any subsequent materials.

A second test was performed to determine what effect manufacturing variability and stress conditions would have on resistor reliability. It was intended to simulate the effect of partial resistor coverage due to equipment malfunction by producing samples with partial resistor and partial substrate coverage. These two parameters would simulate the effect a random bubble on the coating, or a malfunctioning dispense nozzle respectively. Epoxy backseal coating was used on all parts. Stress time was 500 hours except for the silicone parts which was 1000 hours. The stress conditions were the usual 85°C/80%RH, with 70°C/70% RH and 90°C/60°RH as additional conditions. The humidity cells were added to determine if there is any threshold for the corrosion reaction. Failures were considered to be those resistors which had drifted more than 0.6% percent. The results are summarized in the following table.

PERCENT FAILURES vs. STRESS

	85/80	70/70	90/60
Silicone	0	0	0
Partial Substrate	11	7	4
Partial Resistor	28	13	4
Uncoated	27	58	17

The above results repeat the previous observations that the silicone sealant prevents resistor drift.

DISCUSSION OF RESULTS

From the results of the previous tests one item is very clear. When silicone topseal is applied to Cermet resistors no significant drift is observed when the resistors were powered in a humid environment.
The picture is not quite as clear when the results of the resistors powered without silicone coating are reviewed. Where resistor drift was

observed during a particular test, it is not uniformly distributed in extent or location. The skewed behavior could not be attributed to resistor variation because all test samples were accurately trimmed to either 10K or 15K ohms and powered in parallel. Most of the drifted resistors appeared to be near the outer edge of the substrate. Resistors in this location are susceptible to epoxy run-in. The run-in is very light and has never affected performance of other products. The edge resistors are also more susceptible to inadvertent condensation. The aluminum cap is a good heat conductor and if a cool current of air struck the module during chamber entry, condensation would occur on the cap and run down to the perimeter of the module. In the presence of liquid water and biasm, the corrosion reaction occurs very rapidly.

The procedure followed during readouts may also contribute to the observed drift. The only test not to show any significant drift was the power step stress test. These were the only parts that were read in-situ, the rest were taken from the stress chamber and baked before measuring. This procedure has been used for many years without problems on other products but it may inadvertently contribute to damage on Cermet resistors.

The corrosion reaction seems to take place without much driving force. The as-deposited base material was identified as a mixture of chrome silicides, silicon dioxide, and alpha chrome. It is dark gray, which optically supports the composition argument because both chrome silicide (Cr_3Si) and chrome are gray. After the resistor has been attacked, a transparent glassy film remains. This indicates that chrome is being depleted from the clear region. Electron microprobe analysis confirms that fact because the clear region has less chrome that the opaque one. The transparent region would be the residual SiO_2 which is an insulator. Resistance on parts that are attacked always increases supporting the above arguments.

CONCLUSION

The addition of sputtered Cermet resistors on a metallized ceramic substrate provides a versatile packaging strategy. High circuit density modules can be produced with laser trimmed precision resistors.

During a powered high humidity stress test, a corrosion reaction was observed on trimmed Cermet resistors. There was an attack of the resistor material at the point of maximum voltage drop across the trim region. Microprobe analysis of the resistor show that there is a depletion of chrome in the afflicted region. The corrosion reaction must involve transport of free chrome, and chrome from the chrome silicide compounds on the resistor, leaving the glassy silicon dioxide phase unaltered. The resistance of the damaged resistor increases over its initial value, supporting this argument.

Resistor attack was definitely affected by topseal coverage. The amide-imide polymers and epoxy coatings accelerated damage while silicone prevented it. Data analysis was difficult because of the possible interaction of test variables that initially were not believed to affect results, but in retrospect may have contributed to the observed erratic

behavior. Inadvertent epoxy run-in and temperature-humidity fluctuations are candidates for stringent control in future experiments.

The application of complete silicone topseal coating on the Cermet resistors prevented any drift during testing. The coating stopped epoxy run-in by preventing the epoxy from wetting the resistor and also prevented water from forming a continuous film across the substrate surface. When a water film is present on the resistor, the corrosion rate is highly accelerated. The combination of Cermet resistors and silicone topcoating is a very stable resistor system that will perform well in commercial applications.

Acknowledgements

The authors would like to thank J. Elmgren, H. S. Hoffman, R. T. Howard, R. T. Huebner and A. J. Posocco for their critical contributions.

REFERENCES

1.) A. J. Blodgett, "Microelectronic Packaging", Scientific American, July 1983, p. 86.

2) T. R. Homa, "Substrate Reliability of Fine Line Metallized Ceramic Packages", Proceedings of the 1982 Electric Component Conference, San Diego, Ca., p. 91.

3) H. C. Barron, F. R. Moses, and J. Susko, "Internal Moisture Measurement of IBM Integrated Circuit Memory Package, Moisture Measurement and Control Workshop, National Bureau of Standards, Gaithersburg, Md., 1980.

4) L. S. Goldman, "Geometric Optimization of Controlled Collapse Interconnections," IBM Journal of Research and Development, May 1969, p. 251.

5) H. S. Hoffman and E. Stephans, "Cermet Resistors on Ceramic Substrates", Proceedings of the 1981 Electronic's Components Conference, Atlanta, Ga.

6) J. G. Ameen, "Ion Extraction Method Improves Reliability, ibid., p. 401.

7) F. R. Moses and H. C. Baron, "Internal Moisture Measurements of IBM Circuit Packages," Proceedings of the 1981 Electronic's Component Conference, San Diego, Ca., p. 406.

8) R. T. Howard, "Electrochemical Model for Corrosion of Conductors on Ceramic Substrates," Proceedings of the 1981 Electronic Components Conference. Atlanta, Ga.

9) M. L. White, "Encapsulation of Integrated Circuits," Proceedings of the IEEE, Vol. 57, No. 9, September 1969, p. 1610.

10) S. F. Sim and R. W. Lawson, "The Influence of Plastic Encapsulation and Passivation Layers in the Corrosion of Thin Aluminum Films Subject to Humidity Stress," 1979 International Reliability Physics Symposium.

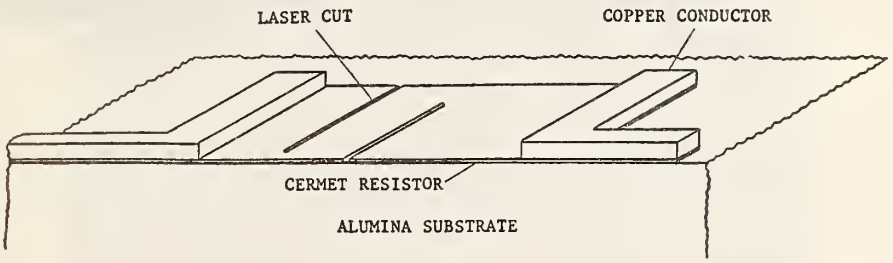

Figure 1. Schematic of Cermet Resistor on an Alumina Substrate

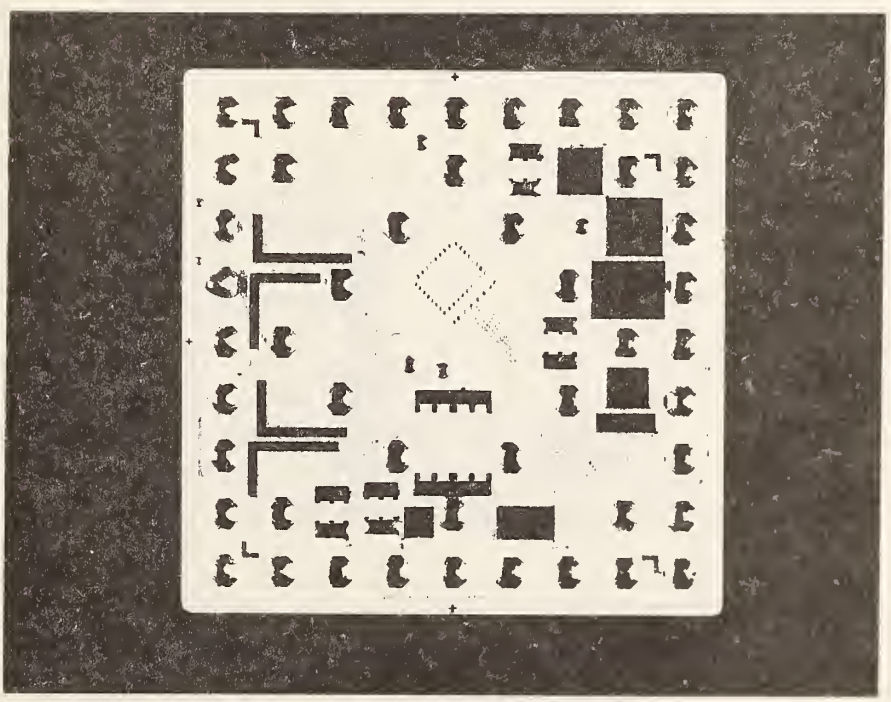

Figure 2. Photograph of a Typical Cermet Part. 2.7X

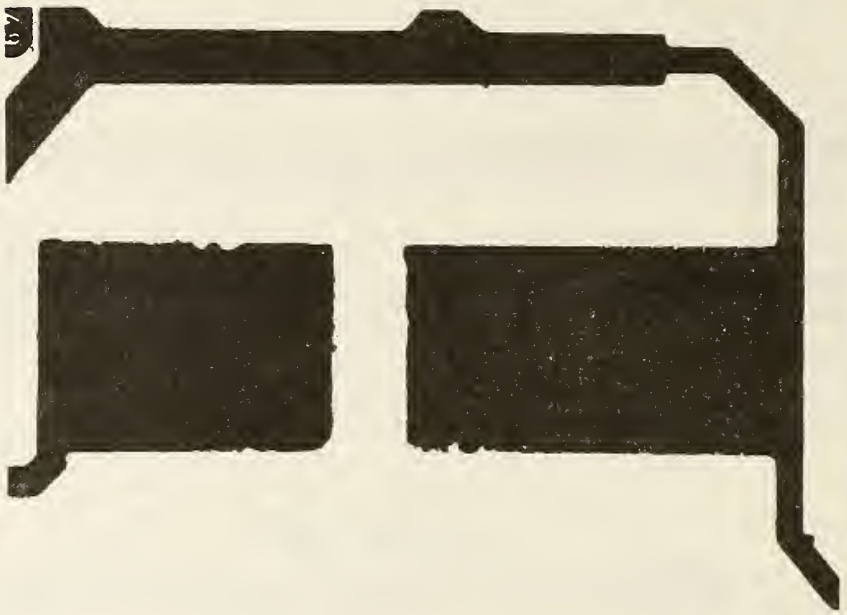

Figure 3 Damage Observed on a Deleted Cermet Resistor After 1000 Hours of 85/80

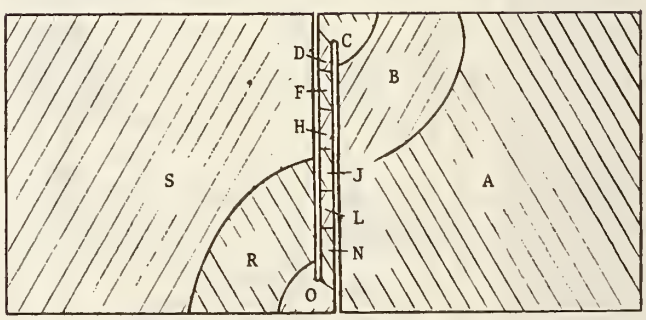

A	10.0	9.6	B	9.6	9.0
C	9.0	8.4	D	8.4	7.3
F	7.3	6.3	H	6.3	5.1
J	5.1	4.0	L	4.0	3.0
N	3.0	1.3	O	1.3	0.7
R	0.7	0.2	S	0.2	0.0

Figure 4. Voltage Distribution on a 7352 Ohm Cermet Resistor Ten Volt Total Drop

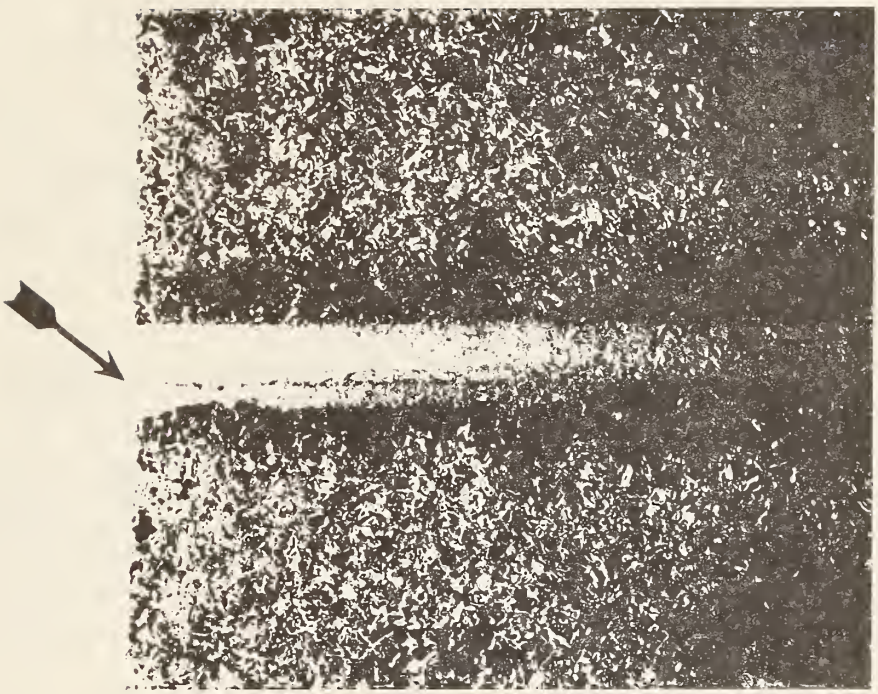

Figure 5. Cermet Degredation at Laser Trim 70X

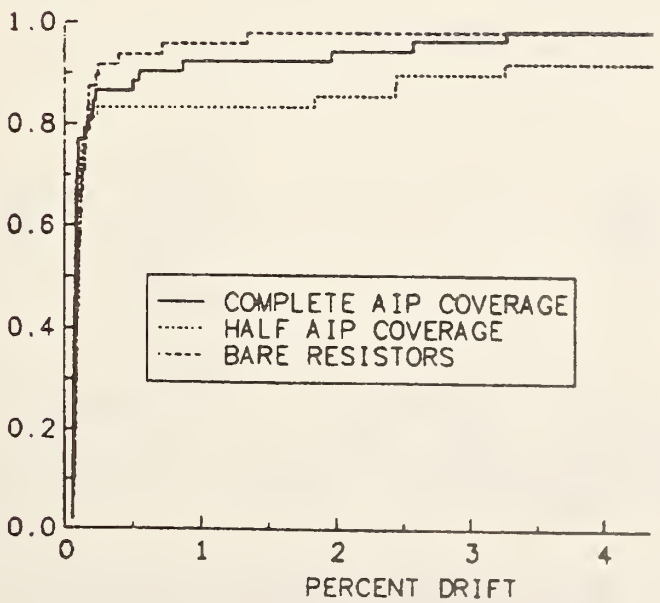

Figure 6. Percent Drift of Cermet Resistors Covered with AIP
0.6% Drift is Considered a Failure

Test Description

15 K ohms — Six Resistors / Module

No Topseal or Backseal — Stress Temperature 70°C, 85°C

Stress Times At Each Humidity (hours)

	Relative Humidity			
Power Level(mw)	35%	50%	65%	80%
25	96	96	96	400
50	96	96	96	400
200	96	96	96	400

Figure 7. Power Drift Step Stress Test

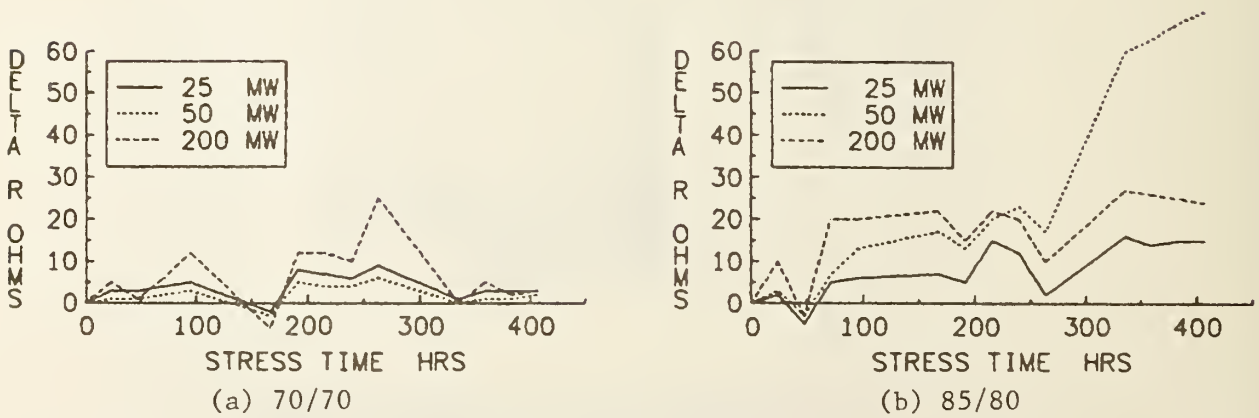

Figure 8. Drift with Time for 70/70 and 85/80 Stress. No Drift was Observed at Lower Humidities. Scatter in Readings is Due to TCR Effect During Powering. The 85/80 Cell Shows a Slight Increase with Time

6.4 MOISTURE EFFECTS ON PASSIVE HYBRID COMPONENTS

- 4 YEAR EXPOSURE TEST -

Jacob A. Ronning and Allan H. Jevne

Medtronic, Inc.
3055 Old Highway Eight
P.O. Box 1453
Minneapolis, Minnesota 55440

Abstract: Thick film hybrids with passive circuitry were constructed for humidity exposure tests at 0, 10, 30, and 85% RH at room temperature (21°C). Circuit components tested were thick film resistors, capacitors, and insulation resistances of various conductive paths and crossovers. Glass passivated circuits were compared with unglassed circuits. The effectiveness of coating the circuits with Parylene 'C' or Silicone QCF-3-6550, was compared to no coating. The circuits were powered at 3.5V D.C. Glass passivated circuits compared better than unglassed. Coated circuits exhibit real, but subtle advantages over uncoated circuits.

TEST DESCRIPTION

To evaluate conformal coatings as a protection for hybrid circuits against moisture and contamination, representative substrates were built.

Electrical resistor and capacitor shifts, insulation resistance reductions, and conductor path integrity were monitored for potential failure or changes during the four-year test period.

Design, materials, and processing of the test substrates were representative of actual product.

Test Conditions

1. Exposure to 0, 10, 30, and 85% relative humidities at room temperatures.

2. Circuit voltage, 3.5V D.C.

3. Controlled contamination.

Test Substrate Construction

The test substrates were ceramic (Al_2O_3), 1.12" x .63" x .025" thick. Eleven connector pins were attached for voltage application during the test and for parameter measurements.

Resistors were thick film, laser trimmed. Conductors were gold and platinum/gold. Solder dipping was used for capacitor attach pads, solder test pads, and lead frame attach points. One-half of the substrate (pins 1 through 6) was glass passivated over the resistors and conductor paths. The circuits from pins 6 to 11 were not glassed.

Figure 1 shows a schematic layout of the test substrate to better illustrate the physical nature of the test circuits under evaluation.

Circuit Coatings

Each of the test substrates had glass passivated and nonglassed construction to allow that comparison in the coated or uncoated condition. Initial screening resulted in the selection of two circuit coatings for the evaluation test. Forty substrates were uncoated; forty were coated with Parylene 'C', a Union Carbide vapor deposited product; and forty substrates were coated with QCF-3-6550, a Dow Corning silicone product.

The Parylene coating was clear and changed the appearance of the substrate very little. The Dow Corning QCF-3-6550 coating was grey and opaque. After coating, all resistor values, insulation resistance readings and capacitor values were recorded as reference parameters.

Contamination

Each of the test substrates was then contaminated by placing one cc of an $NaCl/H_2O$ solution on the circuit surface to dry. The contamination level was 0.44 equivalent microgram NaCl per cm^2 of surface.

Humidity Test Setup

Room temperature humidities for the exposure test were generated in sealed containers by the use of saturated salt solutions.

Salt	% Relative Humidity 20° - 50°C
$ZnCl_2 \circ x\ H_2O$	10 - 10
$MgCl_2 \circ 6H_2O$	33 - 30
KCl	86 - 81

The containers used were one-half gallon wide-mouth jars with 250 ml of the saturated salt solution in each jar. Feedthrough connector blocks were mounted on the jar lids.

The test circuits were plugged inside the jar lids for exposure to the humidity levels established by the saturated salts.

The 0% humidity test chamber was constructed in the same manner, but instead of a saturated salt solution, 250 grams of a desiccant (14 x 30 mesh, 4A LINDE-molecular sieve) plus 10 grams of a color indicating Drierite were put in the jar.

Ten uncoated circuits, ten coated with Parylene 'C', and ten coated with QCF-3-6550 silicone were exposed to each of the humidities (0, 10, 30, 85%) and powered at 3.5V D.C. for four years.

SUMMARY OF RESULTS

Abnormalities Over Four Years - 0, 10, 30% R.H.

Reference readings were taken after cleaning and coating applications. Zero time ("0") readings were taken after the contamination step, and placing in the controlled humidity jars.

Changes from the original reference readings for insulation resistance and resistors are plotted as "abnormalities" in Figures 2 and 3. A resistance change greater than 1/4% is defined as an abnormality. A reduction in insulation resistance to less than 2 x 10^{12} ohms (2TΩ) is defined as an abnormality.

Figure 2 shows abnormalities in the insulation resistance of conductive paths and the resistors plotted together for 0% and 10% humidities. Figure 3 shows abnormalities for the 30% humidity exposures over the four years. There are 80 readings for each point plotted in Figure 2 (0%, 10% R.H.) and 40 readings for each point in Figure 3 (30% R.H.).

These figures show fewer abnormalities for coated circuits. They also show an advantage for glass passivation over unglassed circuits. The initial number of abnormalities measured at the zero year point (after contamination and placing in the controlled humidity jars) did not change significantly over the years.

Insulation Resistance, Coating, and R.H. % at Three-Year Point

To look at performance of coatings versus relative humidity, data on insulation resistance at the three-year point was taken for all the coatings and humidity exposures.

Figure 4 shows the trend towards more abnormalities as humidity increases.

For insulation resistance, glass passivation is comparable to the coatings in the range 0-30% R.H. Both coatings were an improvement over uncoated circuits at 85% R.H.

Readings for the 0, 10, and 30% R.H. points were taken with the test substrates remaining in the humidity jars. The 85% R.H. jars were so wet that insulation resistance breakdowns in the connectors became a problem. For the 85% R.H. readings, the substrates were therefore removed from the connectors and air dried so that comparative readings could be taken.

A dendrite growth was found under the Parylene 'C' coating in an 85% R.H. test substrate. It was surrounded by a white appearing spot indicating spot contamination and loss of adhesion. The insulation resistance reduced to 2KΩ at three years and the dendrite was found. Visual examination of all 0, 10, and 30% R.H. test samples revealed no dendrites nor a start of dendrite growth on any substrate.

Capacitors

A .1μf ceramic capacitor and a 22 μf tantalum capacitor were mounted on each test substrate. The capacitors are constructed to be reflow solder attached to solder pads.

The ceramic capacitors exhibited value shifts less than 1% over time for most units. A few shifted up to 3½%. No correlation could be established between parameter shift and coating. Likewise the tantalum capacitors showed value shifts that did not correlate with coating. One manufacturer's lot shifted from -2½% to +3% as humidity increased and others shifted less than ±½% with humidity.

It appears that redundant coatings do not improve ceramic or tantalum capacitor stability over uncoated capacitors.

CONCLUSIONS FROM THE 4 YEAR TEST, CIRCUIT COATING EVALUATION FOR MOISTURE AND CONTAMINATION

1. Glass passivation is comparable to other coatings at relative humidities less than 30%.

2. Some contamination can be tolerated by glassed and coated circuits up to 30% R.H., (21°C) for the voltage and materials used.

3. The Silicone QCF-3-6550 and Parylene 'C' coatings improved insulation resistance stability in the 85% R.H. (21°C) test.

4. In the 0, 10, 30% R.H. tests, initial abnormalities did not increase significantly with time.

REFERENCES AND ACKNOWLEDGMENT

1. Complete data set is referenced in Medtronic Laboratory Notebook Number 341, page 51, Allan Jevne, Energy Technology Division.

2. A sincere thank you is extended to Eileen Schultz for her untiring dedication to the data acquisition and reduction efforts of this project.

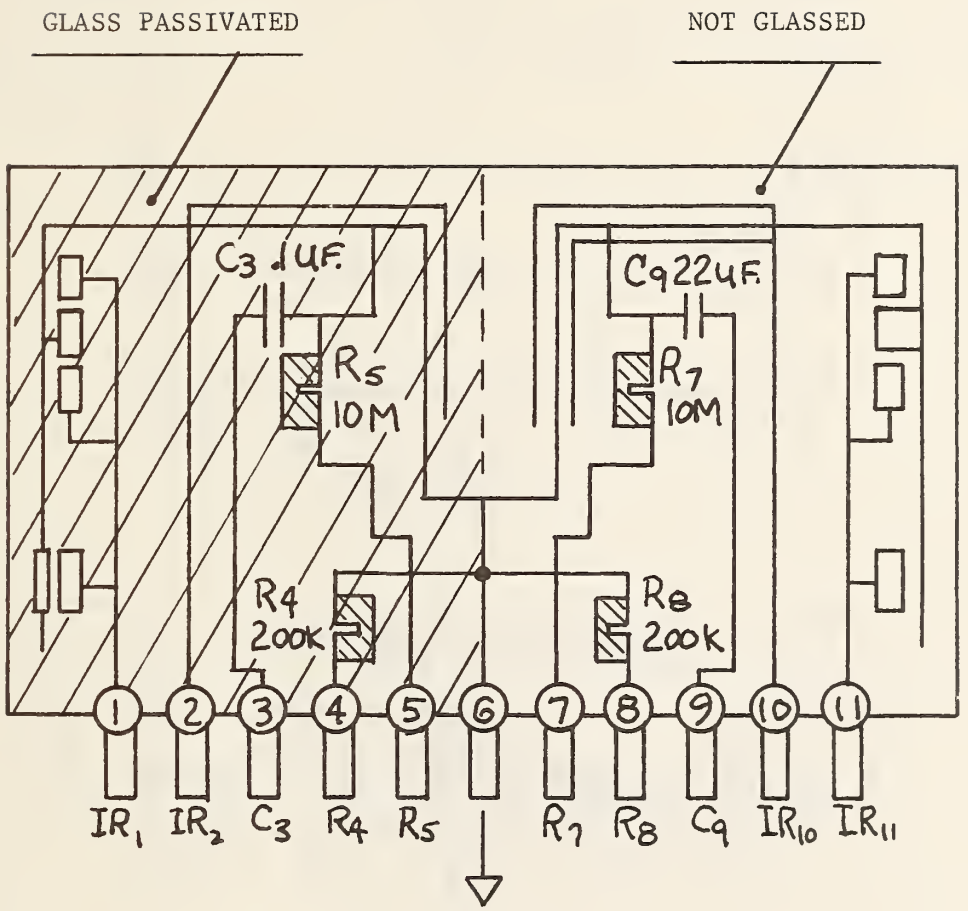

HYBRID TEST SUBSTRATE

4 YEAR COATING EVALUATION TEST FOR HUMIDITY AND CONTAMINATION

+3.5V D.C. PINS 1-5 AND 7-11 (Pin 6 NEG.)

FIGURE 1

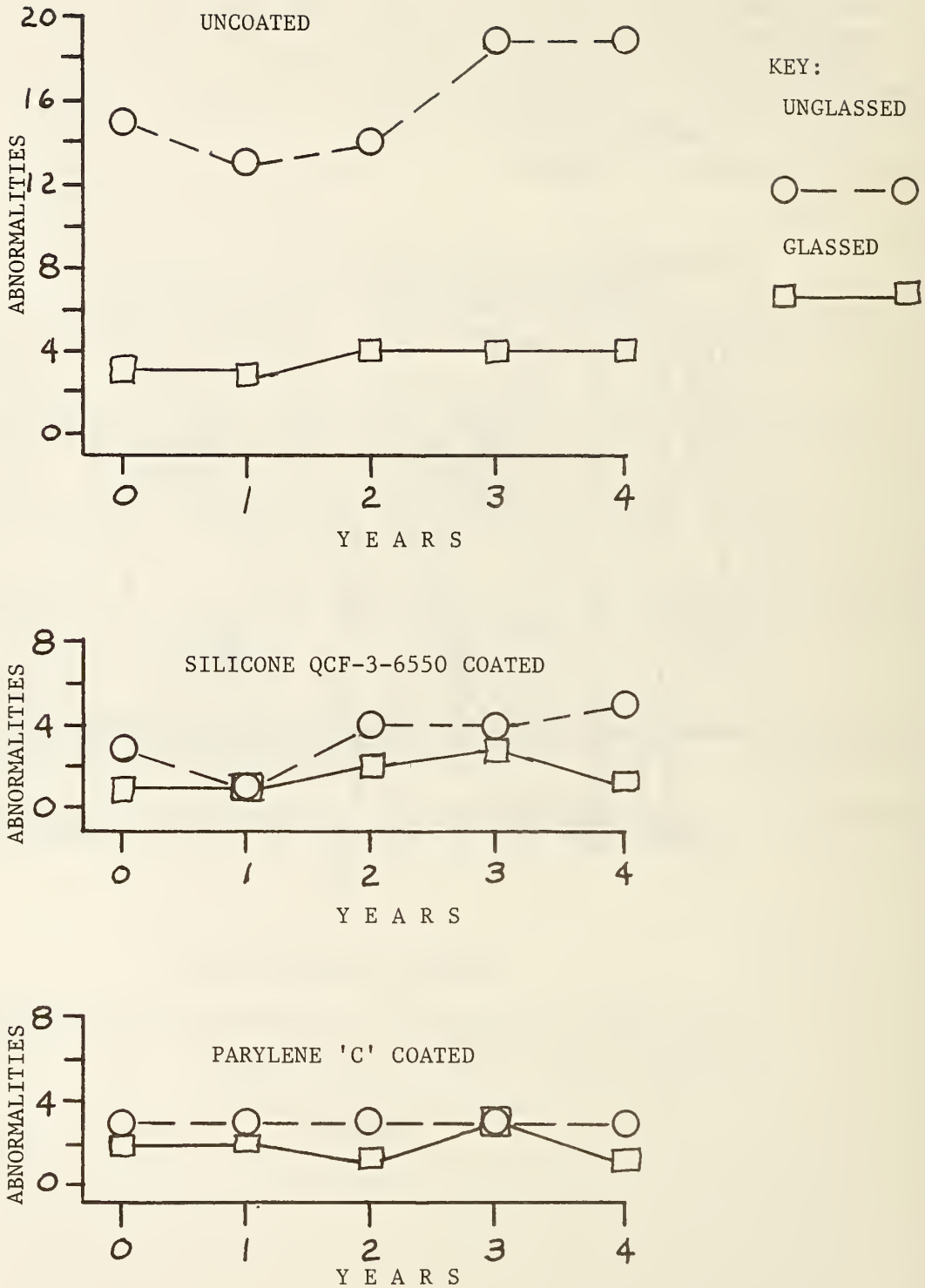

COMPONENT ABNORMALITIES

RESISTORS >¼%, INSULATION RESISTANCE $<2\times10^{12}\Omega(2T\Omega)$

0% & 10% RELATIVE HUMIDITY, 80 COMPONENTS PER DATA POINT

FIGURE 2

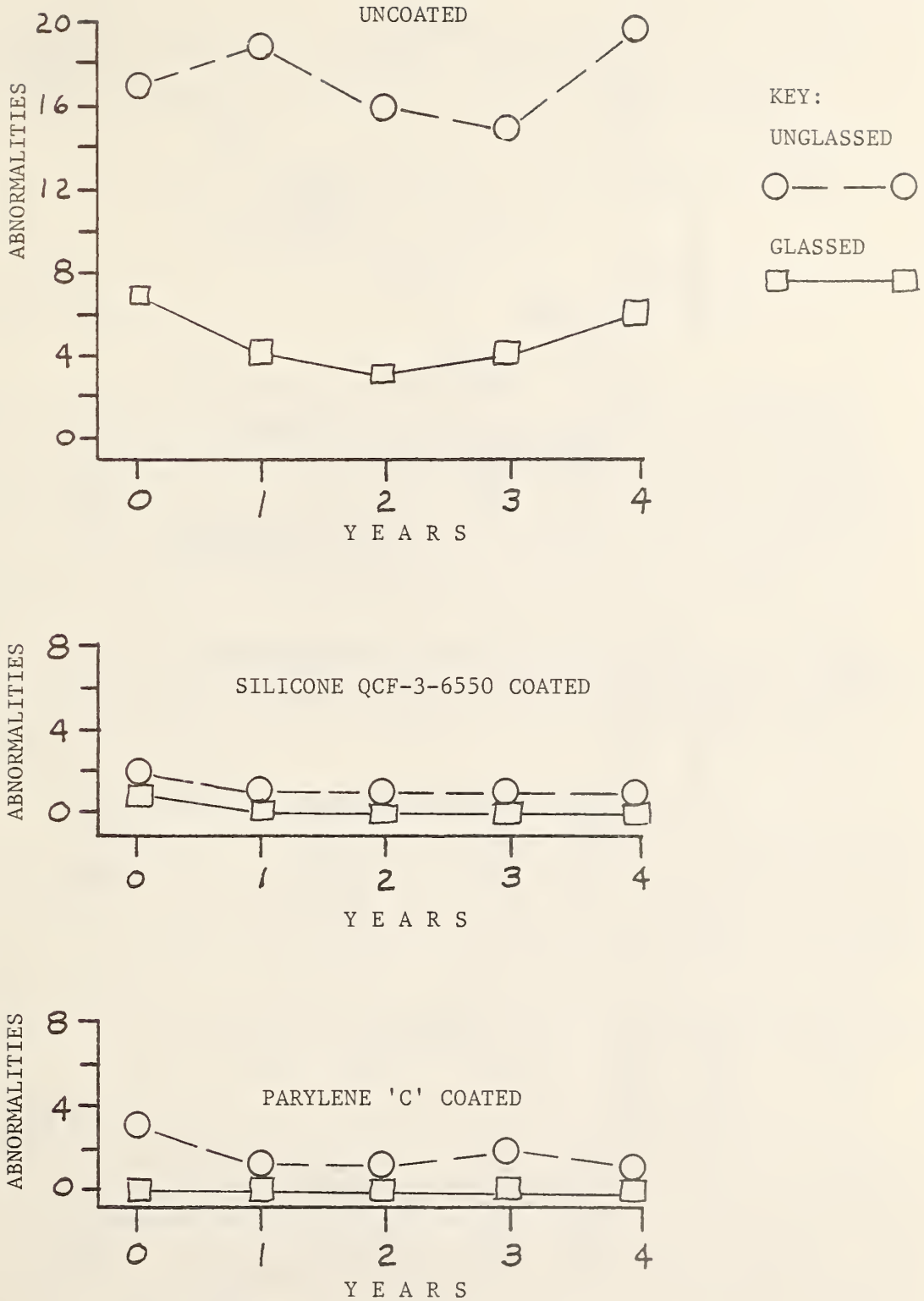

COMPONENT ABNORMALITIES

RESISTORS >¼%, INSULATION RESISTANCE $<2 \times 10^{12}\ \Omega$ (2T Ω)

30% RELATIVE HUMIDITY, 40 COMPONENTS PER POINT

FIGURE 3

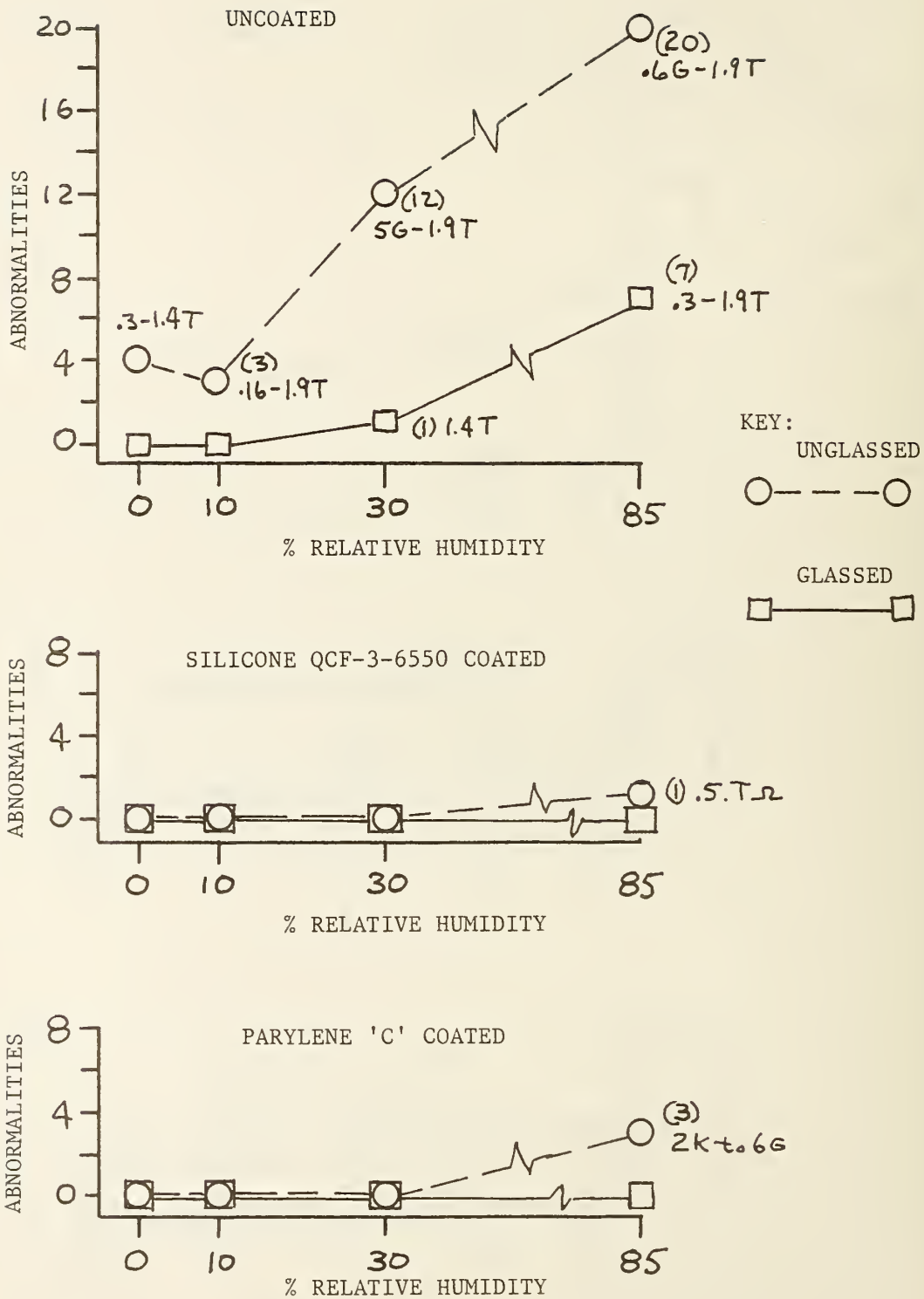

INSULATION RESISTANCE ABNORMALITIES
(Number $<2 \times 10^{12}\Omega$ or $2T\Omega$)

20 COMPONENTS PER DATA POINT, 3½ VOLTS D.C., 3 YEARS, 21°C

FIGURE 4

7. SESSION VI MOISTURE AND ORGANICS

7.1 MASS SPECTROMETRIC EVALUATION OF EPOXY ADHESIVE SYSTEMS

William Bardens
Beckman Instruments, Incorporated
2500 Harbor Boulevard
Fullerton, California 92634
(714) 773-8666

Abstract: Epoxy adhesives used for die and/or substrate attachment in hermetically-sealed packages can be a source of significant amounts of moisture, as well as other atmospheric contaminants. The level of moisture experienced is the result of many variables such as epoxy formulation, preseal bake conditions, sealing process, and post-seal temperature exposure. It is difficult to predict the magnitude of the effect of different combinations of these variables. The effects can, however, be determined by utilizing selected combinations of these variables.

This paper discusses the results of mass spectrometric analysis of the internal atmosphere of hermetically-sealed packages using various combinations of epoxy types, preseal bakes, and post-seal temperature exposure. The results demonstrate that this technique is, in fact, useful for evaluating such variables.

1. INTRODUCTION

In the course of manufacturing hybrid microcircuits, failure to conform to the water vapor requirement of 5,000 ppm maximum required by MIL-M-38510 occurred on a sporadic basis. Experience had shown that the epoxy adhesive used in the construction of the hybrids was the primary water vapor contributor. Furthermore, this same experience had shown that the problem occurred on units which utilized epoxy adhesives for attachment of the substrate to the header, but did not occur on units which omitted this attachment material even though both types of units utilized epoxy adhesive die attachment. It was thus assumed that the epoxy substrate attachment material was the primary source of the internal water vapor content, a not unreasonable conclusion considering the fact that the amount of substrate attachment material contained within the package cavity is generally 5 to over 100 times the amount of die mount material. It was felt that, at the present limit of 5,000 ppm water vapor content, effort should be concentrated on investigating the behavior of the substrate attachment adhesive to achieve the maximum benefit. The data discussed in this paper is the result of work done on the effects of material and process variation on water vapor content and illustrates the use of mass spectrometric analysis as an evaluation tool.

2. EXPERIMENTAL DESIGN

The goal of the experiment was to investigate a new material for substrate attachment, the use of which could result in a lower water vapor content. For the past several years, Ablefilm 529 adhesive has been the standard material in use for substrate attachment. As water vapor content limits were

imposed and proceeded to be lowered, it was found to be more and more difficult to meet these requirements. The experiment was designed to provide comparative data on the water vapor levels resulting from the use of Ablefilm 529 and a new attachment material, Ablefilm 555. Additionally, the effect of varying the preseal bake-out process was investigated as well as the effect of post-seal storage time.

The variables included in the experiment are as follows.

1. A comparison of two materials - Ablefilm 529 and Ablefilm 555.

2. Post-seal high temperature storage at two temperatures - 125°C. and 150°C. - for up to 1,000 hours.

3. Preseal bake-out at 150°C. for two different time periods - 16 hours prebake + 4 hours vacuum bake and 48 hours prebake + 4 hours vacuum bake.

This third variable needs some clarification as to the bake combination used. It is generally accepted that in order to obtain a dry package, some level of preseal baking is required. This bake could be performed entirely in the vacuum oven which is attached to and directly opens into the sealing chamber. A number of years ago, before the imposition of internal water vapor requirements, the preseal bakes used were only 1 or 2 hours in length and the vacuum oven was used exclusively. However, the need for longer preseal bake cycles to meet current requirements has made it impractical to utilize the vacuum oven for the total time period because of the severe limitation it places on production thru-put. Several alternative methods were considered, but the one adopted utilizes a first bake in a forced convection oven with nitrogen gas flow into the oven. This bake is identified by the term "prebake" and this identifier will be used in the balance of the paper. Following prebake, the parts were transferred to a vacuum oven for completion of the preseal bake cycle. Since the transfer between ovens results in exposure to room air- the transfer time was limited to a period of ten minutes to minimize diffusion of moisture back into the epoxy.

In order to make the results as meaningful as possible, conditions other than those previously discussed were kept as nearly identical as possible. To this end, the following conditions were observed for all samples.

1. The package style used was a TO-8 metal header with a nickel-plated body and gold-plated leads utilizing a solid nickel lid.

2. The lids were attached to the header by single shot resistance welding inside a glove box containing dry nitrogen atmosphere with less than 10 ppm water vapor content.

3. Internal volume of the sealed unit was approximately 0.65 cc.

4. The epoxy used to attach the substrate to the header came from the same manufacturing lot for each of the two materials tested.

5. The same volume of epoxy material was used in each test sample.

6. Blank alumina substrates the same size as the epoxy preform (.330" square) were bonded to the header using the same procedure and cure schedule for all samples of the same material.

7. All water vapor analysis was done by the same facility (Oneida Research Service) utilizing the procedure specified in MIL-STD-883, Method 1018.1 except that the bake required prior to puncture was specified as 20-24 hours at 125°C.

8. Timing of the testing of the samples was controlled such that puncture for mass spectrometric analysis occurred 4-7 days after the parts were removed from the post-seal bake oven.

3. EXPERIMENTAL RESULTS

Figures 1 and 2 show the results of the mass spectrometric data in graphic form. Each point on the curve represents the average of at least two samples which were tested after post-seal bake exposure of 168, 500 and 1,000 hours. The interval of 168 hours was chosen as the first test point because this represents the time required for burn-in on units built to conform to MIL-STD-883, Method 5008, and normally the requirement for water vapor content must be met after burn-in.

In order to avoid wasting test time and the unnecessary expense of analyzing units which exhibited unacceptable leak rates, a seal test per the requirements of MIL-STD-883, Method 1014, Conditions A,and C, was performed immediately after seal and just prior to sending any units to the testing facility. Even with this precaution, three of the units tested out of 128 samples were found to be leak test escapes when the mass spectrometric results were analyzed; i.e., units containing measurable helium or fluorocarbon materials were assumed to be leaking units. The results from these three units were considered invalid and were not included in the data presented.

In addition to the water vapor results shown in Figures 1 and 2, the mass spectrometric analysis gives information on other components of the gas contained within the sample. Although there is no specification limit on these other components, their presence or absence can aid in a better understanding of the systems under investigation. Out of the total 128 samples, the following was noted.

1. No ammonia was detected in samples built with either material.

2. Oxygen was detected in only 10 samples and had a high value of 800 ppm in those where it was detected.

3. M.E.K. was detected only in those samples utilizing Ablefilm 529 and was present up to a maximum level of 15,000 ppm.

4. Methane was detected in most samples, but was less than 4,000 ppm.

5. Other solvents and hydrocarbons were not detected or were less than 300 ppm.

6. Hydrogen was detected in approximately half of the samples, but at levels less than 400 ppm.

7. CO_2 was detected in varying amounts depending on the time and temperature of exposure the units had seen after sealing. Figure 3 gives the range of CO_2 seen for each substrate mount material.

4. CONCLUSIONS

Referring to Figure 1 and Figure 2, several conclusions can be reached concerning the performance of the two epoxy systems when stored at 125°C. or 150°C. after seal.

1. Storage at 150°C. after seal greatly increases the internal water vapor content over that reached at the same time period at 125°C. storage for both materials.

2. Given equivalent conditions of processing and temperature exposure, Ablefilm 555 resulted in a significantly lower internal water vapor level than did Ablefilm 529.

3. Increasing the duration of preseal baking will result in lower internal water vapor levels for both materials at all time periods tested. The degree of reduction is similar for both materials.

4. After 1,000 hours of post-seal baking, the internal water vapor content is still increasing at a rate which could have been predicted by the 168-hour and 500-hour levels and shows no indication of having reached a maximum value.

5. As indicated by the nearly identical slope of the curves, the rate of water vapor evolution is similar for both materials. The lower levels achieved by the use of Ablefilm 555 at any time during post-seal temperature storage appear to be the result of a lower level of absorbed water vapor remaining after preseal baking.

6. Given the observations as stated in paragraphs 4 and 5 preceding, it would be unreasonable to conclude that the increase in water vapor content is due solely to the release of absorbed or adsorbed water. When the additional observation concerning the large increase in CO_2 experienced during post-seal bake is considered, it would be reasonable to assume that some portion of the increase in water vapor is due to thermal breakdown of the epoxy system which results in the formation of water. It would require additional testing to prove this assumption, but analysis of the results of work to date point heavily in this direction.

5. SUMMARY

The work described in this paper has utilized the technique of mass spectrometric analysis as a method to provide useful data concerning the effect of multiple variables on the level of internal water vapor content inside hermetically-sealed packages. The data developed has proven useful and can be summarized as follows.

1. Differences in internal water vapor levels can result from the usage of different epoxy materials in the internal package cavity.

2. Of the two materials tested, the usage of Ablefilm 555 in place of Ablefilm 529 will result in lower water vapor levels.

3. When units contain epoxy materials, it is important to minimize the post-seal temperature exposure, particularly if the temperatures are in excess of 125°C.

4. The curves developed during the experiment have proven useful in predicting the internal water vapor levels for various combinations of post-seal elevated temperature exposure.

5. Materials with improved thermal resistance are needed if internal water vapor levels below 5,000 ppm are required after extended post-seal exposures to elevated temperatures of 125°C. or above.

FIG. 1

VARIATIONS IN WATER VAPOR VS POST SEAL TEMP. STORAGE

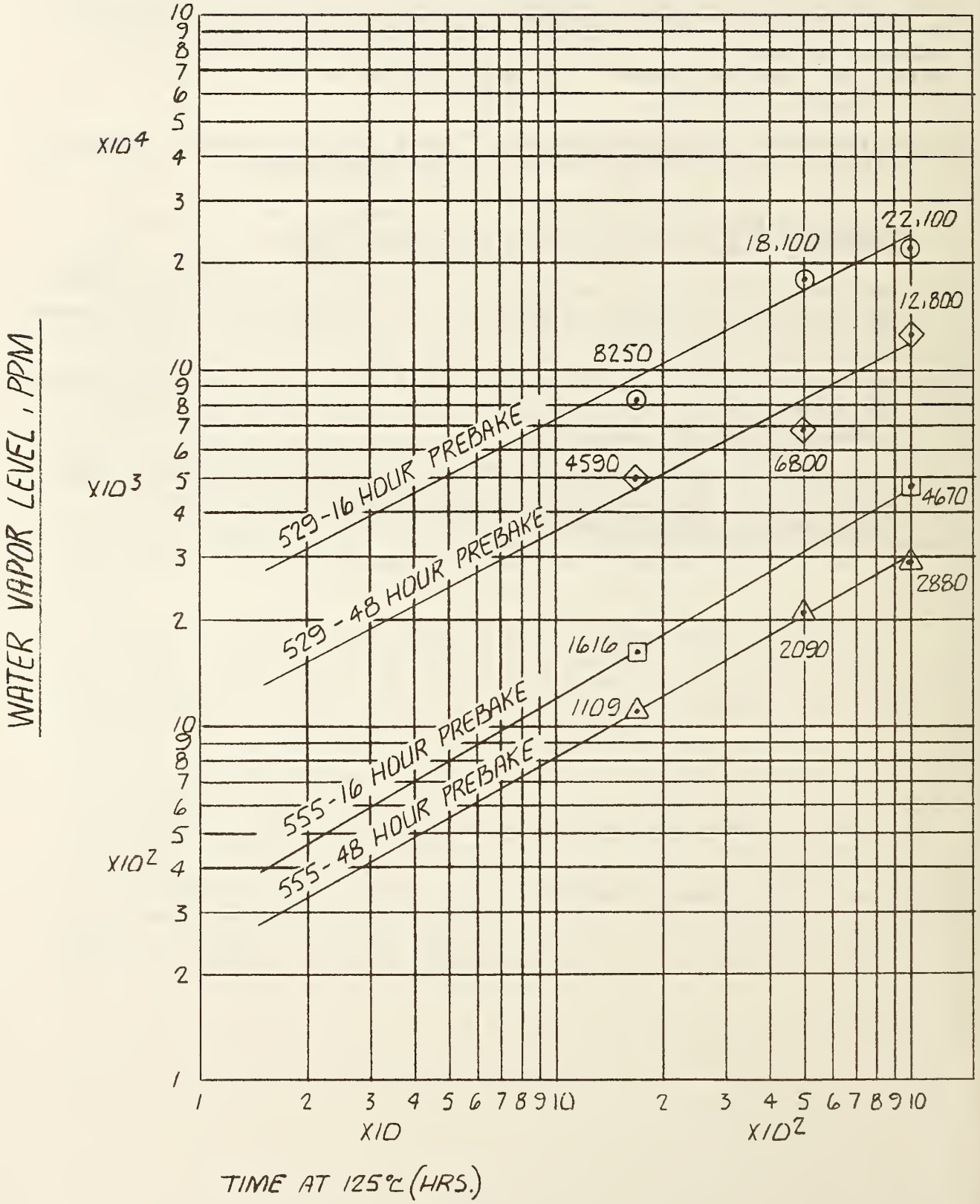

FIG. 2

VARIATIONS IN WATER VAPOR VS POST SEAL TEMP. STORAGE

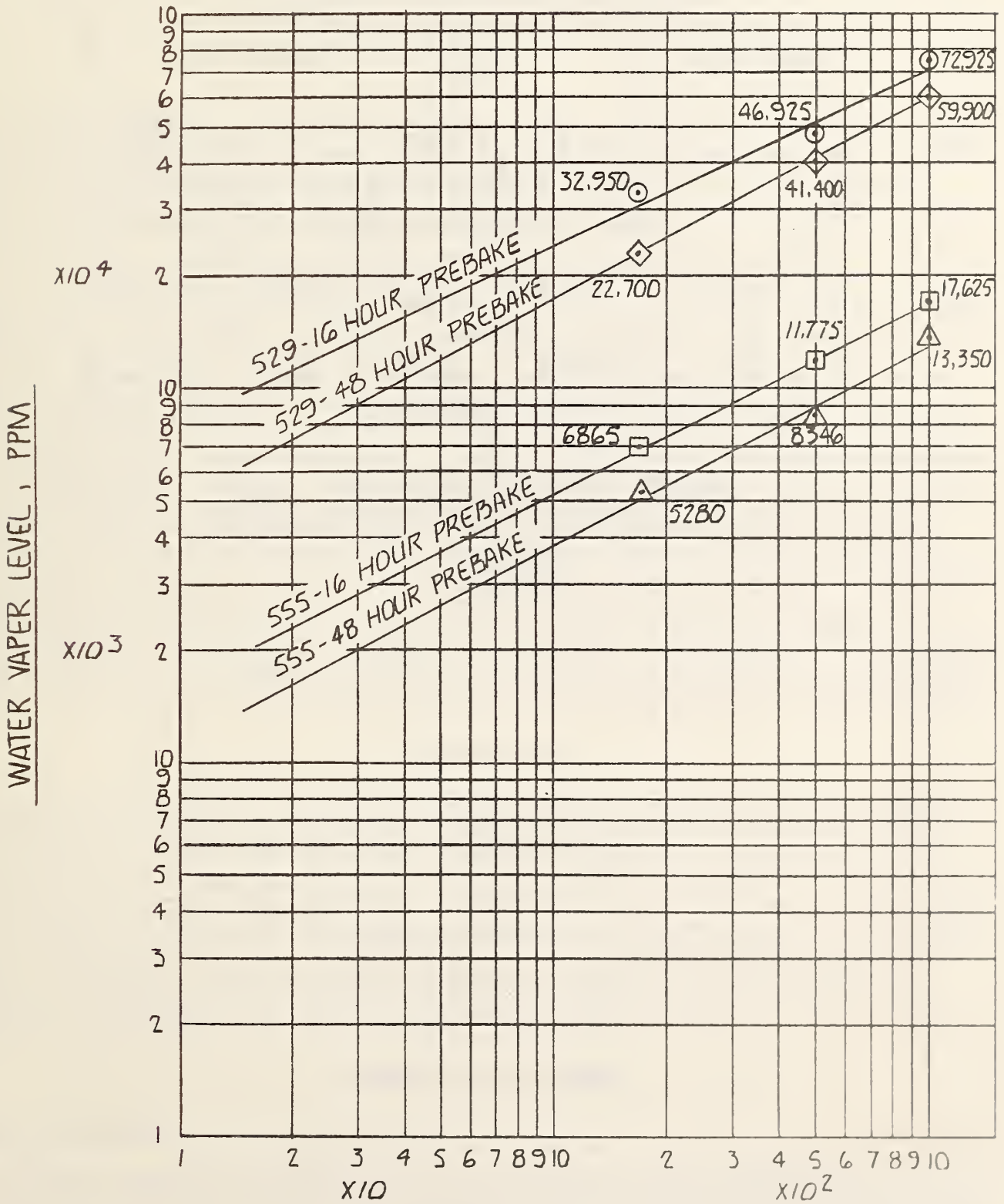

MATERIAL	TIME AT TEMPERATURE			
	125°C STORAGE		150°C STORAGE	
	168 HOURS	1000 HOURS	168 HOURS	1000 HOURS
529	930	2580	4880	12,400
555	4346	6600	7600	10,300

RANGE OF CO_2 CONTENT, PPM

FIG. 3

7.2 MOISTURE TRANSPORT IN POLYIMIDE FILMS: IMPLICATIONS FOR MOISTURE MEASUREMENT IN IC PACKAGES

Denice D. Denton, David R. Day, and Stephen D. Senturia
Department of Electrical Engineering and Computer Science, and
Center for Materials Science and Engineering
Massachusetts Institute of Technology
Cambridge, MA 02139

ABSTRACT

As organics such as polyimide (PI) find increasing use in integrated circuits, the fact that such materials can absorb moisture must be carefully examined. We have made in-situ measurements of the moisture uptake and moisture diffusion rate in thin PI films on integrated circuits. The samples consist of parallel-plate capacitors with aluminum electrodes in which the PI film (typical thickness 1 μm) is the dielectric. By comparing weight change with change in capacitance, it is found that the capacitance change on exposure to ambients with varying moisture can be used as a quantitative measure of moisture absorption. Furthermore, by monitoring capacitance versus time, the rate of diffusion of moisture in the thin sheet of PI between the electrodes can be determined. Principal experimental results are: (1) Moisture diffusion in PI is Fickian, with an activation energy of about 0.25 eV, and a diffusion constant at room temperature of about 5×10^{-9} cm^2/sec. For this activation energy, the diffusion constant at 100°C is about an order of magnitude larger than that at room temperature. (2) The equilibrium absorption of moisture in the temperature range 20 - 80°C follows the ambient relative humidity, although the adsorbed moisture - R.H. relation is not perfectly linear. Based on these results, a model is developed which shows that absorption of moisture by a PI passivation layer could greatly reduce the apparent dewpoint inside an IC package. In addition, attempts to measure moisture inside packages in which PI is used as an interlevel dielectric must take into account the time scale of absorption and desorption both from covered and uncovered PI regions, and must be related to the actual geometry of the device structure being tested. For example, a 1 μm thick PI film covered by 10 μm wide metalizations would required about 10 minutes to equilibrate, but a typical bonding pad of dimension 250 μm would require about one day.

INTRODUCTION

Because of its excellent thermal and chemical stability and its good dielectric properties, polyimide (PI) is finding increasing use in integrated circuit technology both as a passivant and as an interlevel dielectric. One property of PI that has caused concern is its strong interaction with moisture [1]. As part of a comprehensive study of the electrical properties of PI, we have developed a capacitance-based technique for the in-situ measurement of moisture uptake and transport in thin PI films. This paper presents the first quantitative results from this work, and discusses those results with particular emphasis on the problems of moisture measurement in integrated circuit packages within which PI may be used either as a passivant or as an interlevel dielectric.

EXPERIMENTAL PROCEDURES

Sample Preparation

All samples consisted of aluminum-PI-aluminum parallel-plate capacitance structures on silicon substrates. The fabrication procedure was as follows: A 0.75 μm pure aluminum lower electrode was evaporated onto a cleaned silicon wafer. Then a PMDA-

ODA polyamic acid precursor in NMP solvent was spin-coated onto the wafer. No adhesion promoter was used; spinning conditions were 6000 rpm for 30 sec in dry air. A cure sequence of 90°C for 30 minutes in dry air followed by 300°C for 1 hour in ambient air (i.e., nominal 40% R.H.at room temperature) was used for the results reported here. Other cure schedules have been examined, and will be reported in a later publication. Final PI thickness was 1 μm. Following cure, a 0.75 μm thick pure aluminum upper electrode was evaporated onto the sample, and patterned photolithographically using Shipley 1470J resist and 351 developer. The overall size and configuration of the upper electrode was varied. Figure 1 illustrates a typical sample used for electrical measurements. The stripe electrode pattern is chosen to permit moisture access, and to create a dominant shortest diffusion path for moisture equal to half the width of each stripe. This diffusion path is in the PI beneath the stripe, as illustrated schematically by the arrows in Fig. 1(b). Three different stripe and spacing widths, 13, 51, and 102 μm, were used for electrical measurements.

Two types of samples were used in weight uptake experiments. Al-PI-Al samples having 51 μm Al stripes and 5 μm spacings covering an entire wafer were used. In addition, some weight uptake experiments were performed on samples with PI on both sides of a silicon wafer, and no metallization.

Capacitance- and Weight-Versus-Moisture Measurements

Wafers were placed on a vacuum chuck covered by an enclosure through which air of known dew point was flowed. The air source was a compressor, followed by oil and water traps, a particle filter, and a molecular sieve dryer. The dry air stream was divided into two streams, one of which passed through a saturating bubbler at 22°C. Dewpoint control was achieved by mixing wet and dry streams. A General Eastern dew-point hygrometer was used to measure dew point of the final air stream.

Capacitance was monitored as a function of time using a GenRad 1689 Digibridge. It was determined that the capacitance did not depend on frequency in the range 1-100 kHz. Below 1 kHz, there was deterioration of signal-to-noise ratio. Except where noted, the results reported here are for measurements at 2 kHz.

Weight uptake versus time was followed in two different ways. First, a sample initially equilibrated at +18°C dewpoint was placed on the pan of a Mettler balance in lab air, and the weight loss monitored as a function of time, while a similarly equilibrated and exposed capacitance sample was monitored electrically. The second approach was to place a sample coated on both sides with PI and with no metallization in a Cahn microbalance, and heat it to above 100°C in dry air (dewpoint -11°C) until its weight stabilized. Then air of -20°C dewpoint was introduced into the microbalance and the weight and temperature of the sample were monitored during cooling, in effect monitoring the weight change against relative humidity.

EXPERIMENTAL RESULTS

Capacitance Versus Time

Figure 2(b) shows typical capacitance-versus-time behavior for a sample with L = 51 μm at room temperature for the dewpoint sequence of Fig. 2(a). The capacitance increases with increasing dewpoint, and the effect is large, ~15%. The moisture cycle is reversible on a time scale of hours, as shown. No investigation of long-term changes has been made.

That the capacitance change can be attributed directly to moisture uptake is shown in Fig. 3, in which the capacitance of a capacitor is plotted against weight of a similarly exposed sample, with time as a parameter. The nearly perfect linear correlation shows that the capacitance change is proportional to moisture uptake.

The shape of the capacitance transient can be analyzed with a simple one-dimensional model. We assume that vertical moisture transport in the exposed PI regions is so rapid compared to the lateral diffusion beneath the stripe that the exposed PI regions establish a constant moisture concentration boundary condition that is in equilibrium with ambient. Solution of the diffusion equation beneath the stripe is then obtained from standard methods [2], to yield an expression for the fractional moisture uptake versus time for the sample as a whole. Since capacitance and moisture uptake are proportional, we can write for the time dependent capacitance C(t):

$$C(t) = C_f + (C_i - C_f) \sum_{n=0}^{\infty} \frac{8e^{-\frac{D(2n+1)^2\pi^2 t}{L^2}}}{\pi^2(2n+1)^2} \qquad (1)$$

where D is the diffusion constant, L is the stripe width, and C_i and C_f are the initial and final capacitances, respectively.

Equation 1 is fitted to the capacitive transient data as follows: First, C_i and C_f are found from the endpoints of the transient. Then, the transient portion is plotted against $t^{1/2}$ with a scale factor that is adjusted so that the midpoint of the capacitive transient agrees with the midpoint of Eq. 1. The scale factor, then, for the known experimental value of L, yields the diffusion constant D.

Figure 4 illustrates a typical fit between theory and experiment for a dry-to-wet transient. There are some minor shape discrepancies which may mean that a somewhat more elaborate model may be required for a fully detailed interpretation of the data. That the diffusion model is reasonable, however, can be seen from Table I, which shows the D extracted at room temperature for samples of different L. The times to reach mid-point of the transient t_{mid} vary by a factor of 40, but the D values agree to within 25%.

The diffusion constant was also determined at 40, 60, and 80°C. The results are plotted in Ahrrenius form in Fig. 5. If this is a thermally activated process, then the activation energy is small, ~.25 eV. That is, D increases by only a factor of 10 between 22 and 80°C.

The <u>amount</u> of moisture uptake, however, as indicated by $(C_f - C_i)$, does depend on temperature via the relative humidity. Figure 6 shows $\Delta C/C$ versus ΔRH for dewpoint changes from -20°C to +20°C but measured at different temperatures. At 22°C, the ΔRH is 75%, while at 80°C, the same dewpoint change produces a ΔRH of only 3%. An approximately linearly correlation between $\Delta C/C$ and ΔRH is observed. However, corresponding studies of weight uptake versus temperature measured during a cooling experiment, show a small but distinct nonlinearity.

DISCUSSION

The implications of these results for moisture measurement in integrated circuit packages are several. When PI is used only as a passivant, and is therefore not covered by other layers, equilibration times with the ambient are quite rapid, on

the order of a few seconds for a 1 μm thick film. In test sequences in which the package is heated, moisture will desorb from the PI. If the package is then punctured while warm, the moisture can be expected to leave the package quantitatively. However, if the package is subsequently cooled, for example, in a dewpoint type test, rapid reabsorption of the moisture will occur, and the dewpoint measured will be an underestimate of the total moisture content of the package. That this could be a large effect is illustrated by the following simplified model:

Let $p_A(T)$ be the parts per million by volume (PPMV) of moisture in the air inside a TO-8 transistor package at temperature T, and let $p_S(T)$ be the corresponding PPMV at saturation. We have observed that the absorption of moisture by the PI is approximately proportional to relative humidity, i.e., to $p_A(T)/p_S(T)$. Based on this observation, it is easily shown that

$$p_A(T) = \frac{p_A(\infty)}{1 + \frac{K}{m p_S(T)}} \qquad (2)$$

where $p_A(\infty)$ is the high-temperature PPMV when all moisture is fully desorbed from the PI, K is a constant representing the maximum mass of water the PI can absorb at 100% R.H., and m is the mass of air inside the package.

If we assume that a 4x4 mm chip is covered with a 1 μm thick PI film, use the data of Fig. 3 to evaluate K, and use the volume of a TO-8 can at one atmosphere to evaluate m, we can plot $p_A(T)$ versus either T or $p_S(T)$, as in Fig. 7, for various values of $p_A(\infty)$. Note that at high T, all of the moisture is desorbed, but as the package is cooled, the PPMV in the package drops significantly due to absorption in the PI. In fact, this simple model predicts that for the geometry used in this example, the PPMV measured at high temperature would have to be about 20,000 before one would ever observe a dewpoint, as indicated by the crossing of the condensation line in Fig. 7. For less moisture than this value inside the package, the PI absorbs enough to prevent condensation at any temperature. While this fact could significantly interfere with the problem of measurement of moisture using dewpoint methods, the fact that PI suppresses condensation in all but the wettest packaging conditions may actually be a reliability benefit, provided that the moisture in the PI does not itself create reliability problems. These issues are the subject of our current research.

When PI is used as an interlevel dielectric, the diffusion of moisture beneath the areas covered by metal makes the overall rates of absorption and desorption depend strongly on geometry. For example, at room temperature, a 1 μm thick PI film covered by aluminum stripes 10 μm wide would require about 10 min to equilibrate with ambient, but a typical bonding pad of dimensions 250 μm would require about one day. At 100°C these times decrease by about a factor of 10, but bonding pads would still require several hours to equilibrate. Therefore, a puncture test with a heated package would yield too low a result unless adequate time at elevated temperature had been allocated for desorption. Furthermore, a heating cycle followed by cooling toward the dewpoint could yield extremely confusing results, depending on the precise intervals used for heating and cooling. If, for example, a 1 μm interlevel dielectric is 50% covered by metal, and the cooling is so rapid that even though adequate time was allowed for desorption on heating, re-equilibration with the 50% of the PI that is covered does not take place during cooling. Under these circumstances (full desorption followed by only partial reabsorption), each of the curves in Fig. 7 would have to be shifted up, meaning that condensation

on rapid cooling would occur for less total moisture in the package than on slow cooling.

ACKNOLWEDGEMENT

This work was sponsored in part by IBM. Extensive use ws made of the MIT Microelectronics Laboratory, a Central Facility of the Center for Materials Science and Engineering, which is supported in part by the National Science Foundation under Contract DMR-81-19295.

REFERENCES

1. E. Sacher and J. R. Susko, "Water Permeation of Polymer Films. III. High-Temperature Polyimides", J. Appl. Polymer Science, 26 679-686 (1981).

2. J. Crank, The Mathematics of Diffusion, Oxford, Clarendon Press, 1956, p. 54.

TABLE I

Room Temperature Moisture Diffusion Constant Determined from Capacitance Transients for Three Different Stripe Widths

Width L (μm)	Time to midpoint t_{mid} (sec)	Diffusion Constant D (cm^2/sec)
13	20	3.8×10^{-9}
51	300	4.0×10^{-9}
102	867	5.6×10^{-9}

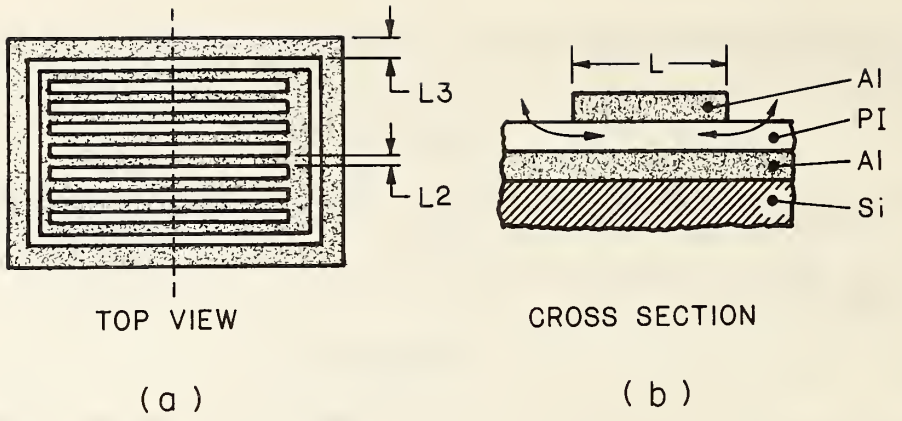

Figure 1. (a) Schematic top view of aluminum upper electrode with stripe width L2 = 56 μm and surrounded by guard ring of width L3 = 102 μm. An alternate electrode structure with stripe width L1 = 13 μm is not shown. (b) Schematic cross section through one stripe of the upper electrode or guard ring showing the aluminum-polyimide-aluminum parallel plate capacitor structure on a silicon substrate, where L = L1, L2, or L3. Arrow shows direction of dominant moisture diffusion assumed by the model.

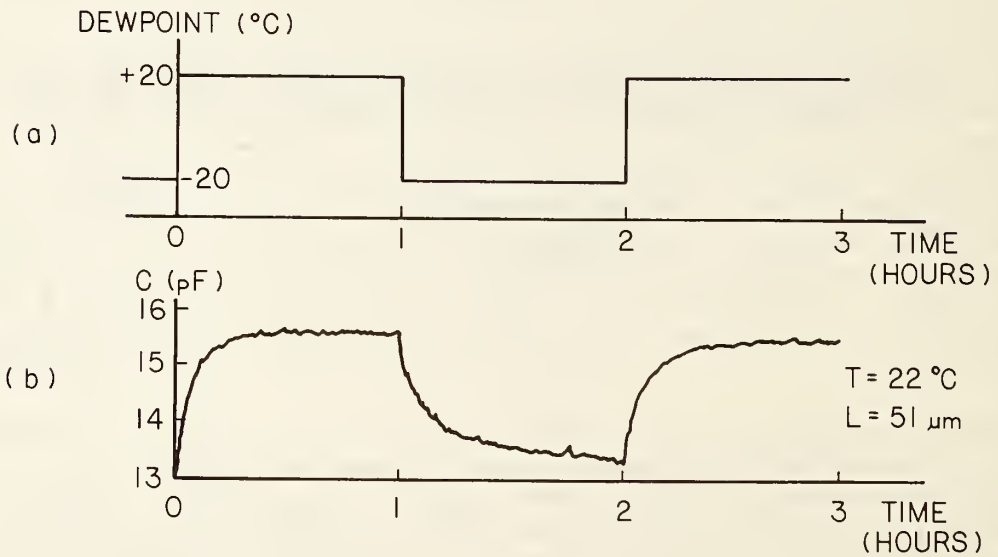

Figure 2. (a) Dewpoint versus time for a dry-wet-dry-wet cycle. (b) Typical capacitance versus time response to the dewpoint cycle of (a) for L = 51 μm.

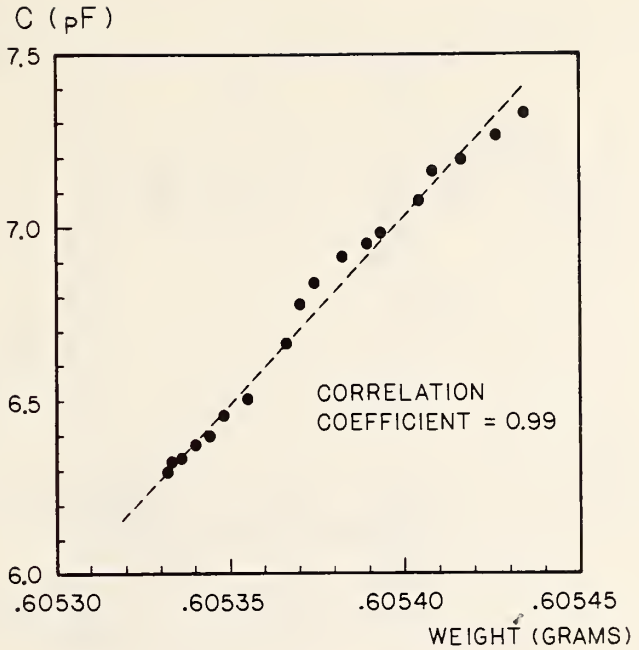

Figure 3. Correlation between capacitance change and moisture uptake measured gravimetrically.

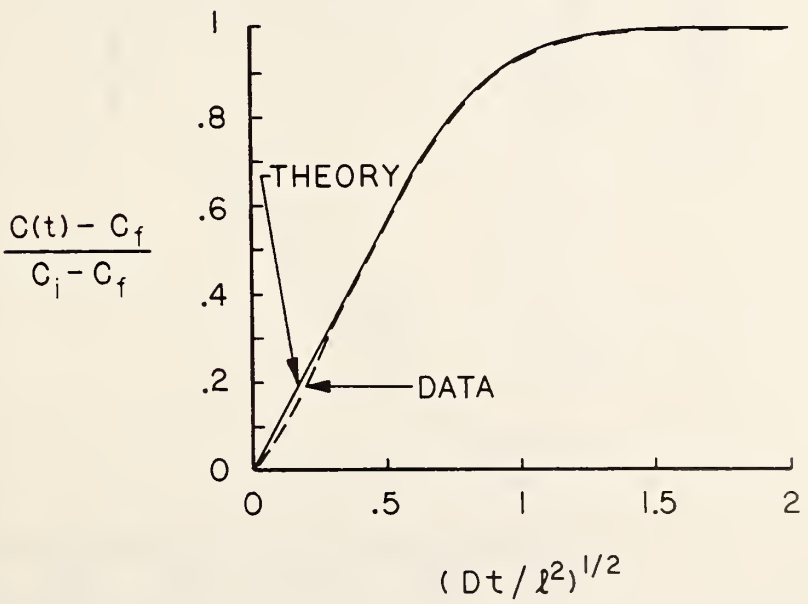

Figure 4. Comparison between experimental capacitance plotted versus $(\text{time})^{1/2}$ and the one-dimensional diffusion model for a dry-to-wet transient (data at 100 kHz). The diffusion constant can be extracted from the time axis scale factor required to fit the slope in the $t^{1/2}$ region.

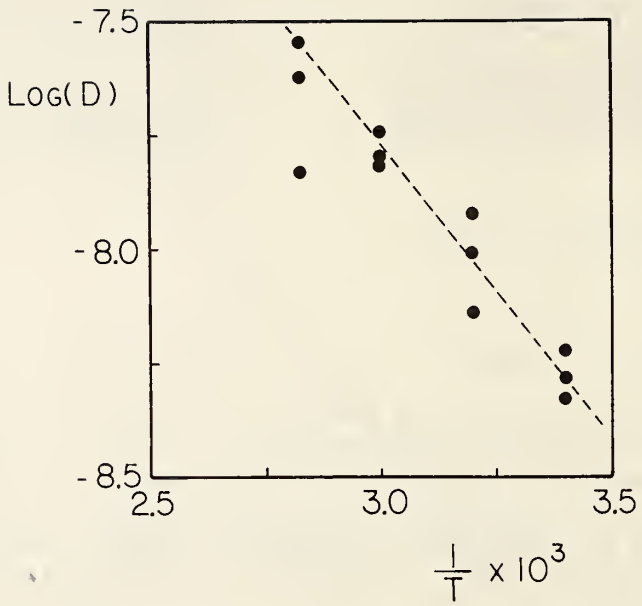

Figure 5. Arrhenius plot of moisture diffusion constant versus temperature.

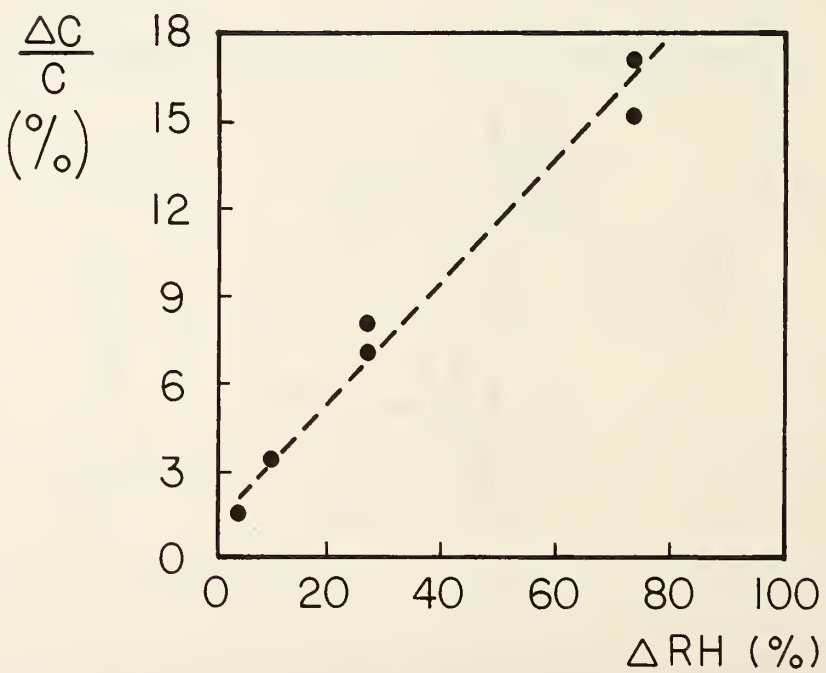

Figure 6. Correlation between the fractional capacitance change and the change in relative humidity.

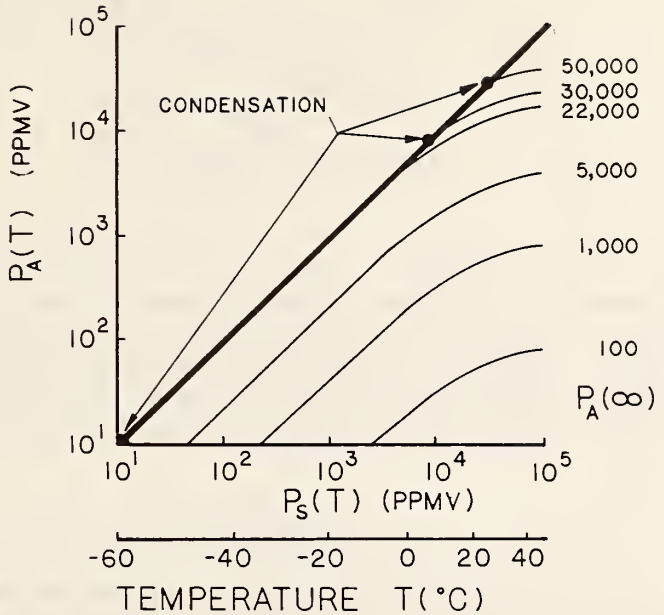

Figure 7. Effect of moisture absorption on the apparent PPMV of moisture inside a typical TO-8 transistor package, based on the assumptions of Equation 2.

7.3 MOISTURE CONTENT VARIATION IN A HIGH POLYMER CONTENT PACKAGE

Bruce Church
Medtronic, Inc.
6951 Central Avenue
Minneapolis, MN 55432
(612) 574-4761

The cardiac pacemaker is a high polymer content electronic package. Hermetically sealed, it must reliably operate for years in a hostile environment. Extensive testing has been performed to determine the moisture content and its distribution within the device.

This paper summarizes the moisture testing performed on Medtronic's pacemakers. The effects of configuration and processing are shown. Methods employed include analysis of total water per MIL-STD 883B, total water observed at other temperatures, and the use of Al_2O_3 sensors.

7.4 VOLATILITY BEHAVIOR OF ORGANIC DIE ADHESIVE MATERIALS

R. K. Lowry and K. L. Hanley
Harris Semiconductor
P. O. Box 883
Melbourne, FL. 32901

ABSTRACT

Mass spectrometry, surface conductivity moisture sensors, and thermal analysis were used to study volatility of three organic adhesives. Mass spectrometry and in-situ sensors verified the moisture-gettering property of polyimide material but not of epoxy. Agreement on general levels of moisture in package groups occurred between mass spectrometry and the in-situ sensors, though specific agreement on individual packages was poor. Mass spectrometry reveals interesting differences in the quantities of volatiles other than water vapor outgassed by the different adhesives.

INTRODUCTION

Organic adhesives for die attach of semiconductor devices in some hermetic package styles can offer distinct advantages in certain applications. These include:

- device thermal limits precluding eutectic die attach
- heat sinking
- cost reduction

Optimizing package technology with regard to moisture content has yielded some interesting data on the performance and properties of three adhesive systems chosen for study. All three were silver filled materials, as follows:

- Ablebond 843-1 epoxy
- Amicon C-860 XLC epoxy
- Ablebond 71-1 polyimide

EXPERIMENTAL

The test vehicle used for these adhesive studies was a 24-lead side braze package. This package utilizes a gold-filled die cavity and gold-plated Alloy 42 lids. One Harris surface conductivity moisture sensor chip [1-2] was mounted in each package with one of the adhesives of interest. Adhesives were then cured with slightly less than the optimum cures specified for each adhesive type. The purpose of less-than-optimum cure was to identify any unique characteristics imparted to the package cavity by the particular adhesive. Packages were then sealed and leak-tested. They were then analyzed for internal water vapor via Test Method 1018.2 Procedure 3 using the sensor chip. They were subsequently analyzed for moisture via Test Method 1018.2 Procedure 1 using mass spectrometry. No pre-analysis bake was used. Several packages with eutectically attached sensor chips were also prepared for reference.

In separate experiments, thermogravimetric analysis (TGA) was run on each adhesive. Carefully-weighed samples of cured material were baked at 150°C, cooled to room temperature, exposed to moist air, and then this cycle was repeated several times. Increases and decreases in adhesive mass were monitored as a function of time and temperature.

		°C	PPMV	PPMV	V%	PPMV	PPMV	V%	PPMV	PPMV	PPMV	PPMV	PPMV
		MOISTURE SENSOR PEAK	H_2O VIA SENSOR	AMU 18 H_2O	AMU 2 H_2	AMU 4 He	AMU 15 CH_3	AMU 29 N_2	AMU 32 O_2	AMU 40 Ar	AMU 44 CO_2	AMU 45 HC	AMU 69 FC
EUTECTIC	H	--	< 700	3200	5.20	NIL	373	93.8	NIL	165	5140	33	20
EUTECTIC	H	--	< 700	3900	5.11	NIL	308	94.2	NIL	174	1500	29	24
EUTECTIC	C	-10	2700	5220	5.76	NIL	644	93.5	NIL	NIL	1300	NIL	NIL
71-1	H	--	< 700	45300	.047	NIL	514	89.4	39800	8634	5880	25	2139
71-1	H	--	< 700	5390	4.90	NIL	299	93.6	NIL	166	8080	21	20
71-1	C	+4	7600	7530	4.60	NIL	NIL	94.3	NIL	NIL	2880	134	NIL
71-1	C	--	< 700	3550	5.50	NIL	NIL	94.0	NIL	NIL	760	190	NIL
71-1	H	--	< 700	7300	4.75	NIL	352	92.6	NIL	160	17090	39	26
71-1	H	--	< 700	7900	4.70	NIL	414	92.5	NIL	166	17260	50	30
843	H	+27	34000	NO ANALYSIS									
843	H	+20	22000	51500	3.30	NIL	5556	89.5	990	923	10530	1328	88
843	C	-8	3200	51300	5.95	NIL	5983	86.7	NIL	NIL	11000	2230	NIL
843	C	+40	>40000	63300	6.22	NIL	4837	85.3	NIL	NIL	12600	2079	NIL
860	C	> +40	>40000	30700	3.31	NIL	3894	92.1	NIL	NIL	5660	2528	NIL
860	C	+40	>40000	46200	2.90	NIL	4750	90.7	NIL	NIL	6630	3046	NIL
860	H	+18	19000	16000	2.04	NIL	3563	93.8	1540	392	16240	2274	33
860	H	+9	11000	13900	1.92	NIL	3992	90.5	110	392	54590	2373	40

DISCUSSION

Moisture cell and mass spectrometric findings are given in Table I. Discussion points include:

(1) Baseline H_2O in these packages is around 4000ppmv.

(2) Four of five 71-1 parts contain no H_2O detected by the sensor, which depends for its operation on controlled cooling of the specimen to -35°C. The first 71-1 specimen is discounted because it contains air.

(3) The five non-air containing 71-1 parts have 3500-7900ppmv H_2O when measured by mass spectrometry at 105°C.

(4) Inability to detect H_2O at the cold temperatures coupled with detection of H_2O at elevated temperatures in the same package suggests a temperature-dependent H_2O property of 71-1 polyimide. This is further explored in the TGA studies.

(5) 843 epoxy parts contained 2-4v% H_2O by sensor and 5-6v% H_2O by mass spectrometry.

(6) 860 epoxy contained either >4v% or 1-2v% H_2O by sensor and like amounts when measured by mass spectrometry.

(7) Sensor/mass spectrometer agreements are
- lacking in 71-1, see item (4)
- good for 860 epoxy
- poor for 843 epoxy

(8) The eutectic mount and the 843 samples contain about the same amount of H_2, about 5.2v%. But the 71-1 parts contain an average of 4.9v% H_2, and the 860 specimens contain an average of 2.5v% H_2. It is possible that these two materials consume H_2 from the package ambient.

(9) Relative to organic species
- 843 and 860 display about the same amounts of amu's 15 and 45.
- They display substantially more amu's 15 and 45 than 71-1 polyimide
- 71-1 polyimide is not much different than eutectic in organics content

(10) With regard to carbon dioxide, the adhesives parts usually contain more than eutectics, but amounts are highly variable.

(11) There are some interesting interlab measurement comparisons in the data in Table I. Specimens marked "H" in the left-hand column were analyzed in Harris' mass spectrometer. Those marked "C" were analyzed at a commercial DESC-certified laboratory. Again, none of the specimens received a pre-analysis bake.
- Eutectic mount: The relative difference between sensor and mass spec occurred at both H and C.
- 71-1 polyimide: C agreed exactly with the sensor on the one wet package. C and H alike found H_2O in all other parts measured dry by sensor.
- 843 epoxy: C had one serious discrepancy with the sensor. Otherwise both C and H measured somewhat higher than the sensor.

- 860 epoxy: Both C and H agree with the sensor.
- H_2: C and H are in general agreement on H_2 levels in the various groups.
- Organics: C reported no amu 15 but higher amu 45 than H in 71-1.

These data, which have been reproducible over years of experimentation with these adhesives, indicate the desiccating properties of some organic materials. Note the inability of the moisture sensor to detect >5000ppmv quantities of H_2O in the polyimide parts. In the 843 epoxy parts the sensor seems to detect substantially less H_2O than mass spectrometry. Only in the 860 epoxy did the sensor and mass spectrometry agree. Of these three materials, 71-1 epoxy is consistently dry at dewpoint temperatures. This has important implications, both for the operating reliability of the part as well as the moisture measurement technology used. Pre-analysis baking and/or measurement at elevated temperatures may cause detection of H_2O which, because of sorption properties of adhesives, is never available at the much lower dewpoint temperatures.

Thermal analyses were carried out to further investigate this behavior of organic adhesives. Fig. 1 is a thermogravimetric analysis (TGA) scan of a fully-cured 50mg sample of 71-1 polyimide. The left-hand vertical axis is weight percent, plotted by the solid line. The right-hand vertical axis is °C plotted by the dashed line. The polyimide, when baked in N_2 at 150°C for 20 mins., offgasses about 0.04% of its mass. When cooled to 35°C in N_2 the weight remains almost constant. But when moist air is admitted to the cell, the polyimide regains back to its original value in about 40 mins. Behavior is the same when this cycle is repeated, and is indicative of its moisture uptake properties at low temperatures. Similar scans of 843 and 860 epoxy, combined in Fig. 2, showed similar behavior. However, offgassed and resorbed quantities varied. These are summarized in Table 2. The polyimide lost the least mass on initial heat. And on subsequent coolings and heatings the sample mass change was exactly the same. Epoxies lost 4-6 times as much on initial heating, and resorbed only about one-fifth the offgassed material when exposed to moist air. Subsequent re-heating caused the epoxy to lose additional mass. However, by the second cooling step the epoxies have begun to resorb similar amounts as they out-gassed during the second heating.

Table 2

TGA HEAT/COOL CYCLES

SAMPLE	INITIAL MASS	1ST HEAT TO 150°C	1ST COOL TO 35°C	2ND HEAT TO 150°C	2ND COOL TO 35°C
71-1	50.45MG	- 0.03MG	+ 0.02MG	- 0.02MG	+ 0.02MG
843	62.85MG	- 0.18MG	+ 0.03MG	- 0.06MG	+ 0.05MG
860	52.50MG	- 0.13MG	+ 0.03MG	- 0.04MG	+ 0.04MG

The TGA data confirm the mass spectrometry data in these respects:
- 71-1 epoxy in general gave the driest packages, agreeing with the Table 2 information showing it had the least volatiles.
- H_2O was undetectable in the cooled 71-1 specimens by sensor. Uptake of all volatiles in 71-1 on cooling was confirmed by TGA.
- H_2O was detectable in the cooled 843 and 860 specimens by sensor. TGA showed these materials did in fact not resorb all offgassed products.

CONCLUSION

A unique combination of three diverse analytical techniques was used to study the volatility behavior of several organic adhesives intended for semiconductor packaging. Relative moisture-producing potential of sub-optimum cured material was defined, as was the potential to produce significant amounts of hydrogen and organic species. Mass spectrometry provides significant useful information on species other than moisture. The moisture sorption behavior of the polyimide suggests that when properly processed it will not contribute significant amounts of available moisture to a package cavity at dewpoint temperatures <10°C, while the epoxy materials do not exhibit the same desirable moisture removal effect.

REFERENCES

1. Lowry, R. K., Miller, L. A., Jonas, A. W., and Bird, J. M., "Characteristics of a Surface Conductivity Moisture Monitor for Hermetic Integrated Circuit Packages," in Proceedings of the 17th Annual Reliability Physics Symposium, April 24-26, 1979, San Francisco, CA., pp. 97-102.

2. Product Information Bulletin, Harris Semiconductor HIO-55001-6, Moisture Sensor Chip, March, 1979.

Figure 1

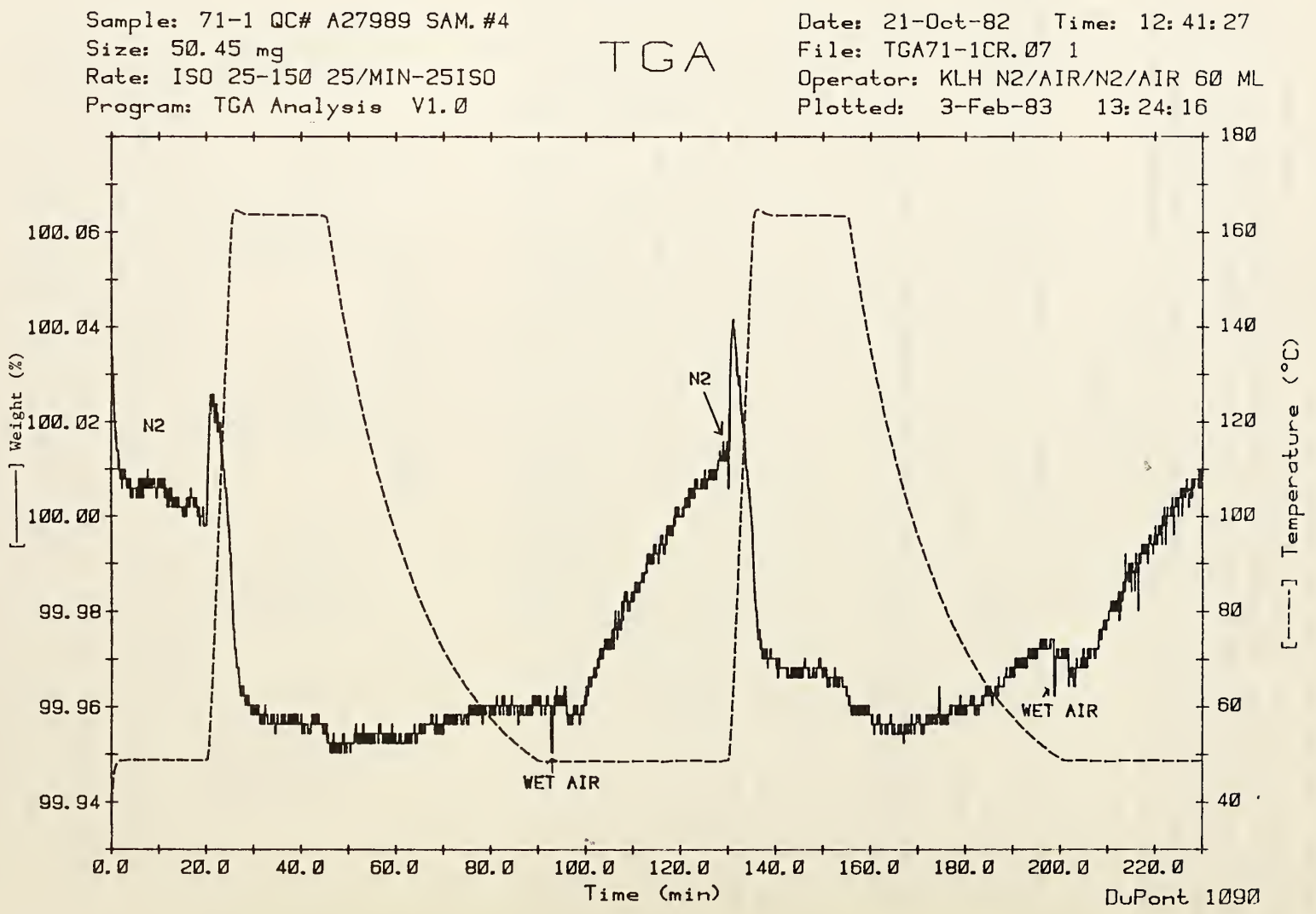
Sample: 71-1 QC# A27989 SAM.#4
Size: 50.45 mg
Rate: ISO 25-150 25/MIN-25ISO
Program: TGA Analysis V1.0
TGA
Date: 21-Oct-82 Time: 12:41:27
File: TGA71-1CR.07 1
Operator: KLH N2/AIR/N2/AIR 60 ML
Plotted: 3-Feb-83 13:24:16
[——] Weight (%)
[----] Temperature (°C)
100.06
100.04
100.02
100.00
99.98
99.96
99.94
180
160
140
120
100
80
60
40
N2
N2
WET AIR
WET AIR
0.0
20.0
40.0
60.0
80.0
100.0
120.0
140.0
160.0
180.0
200.0
220.0
Time (min)
DuPont 1090

Figure 2

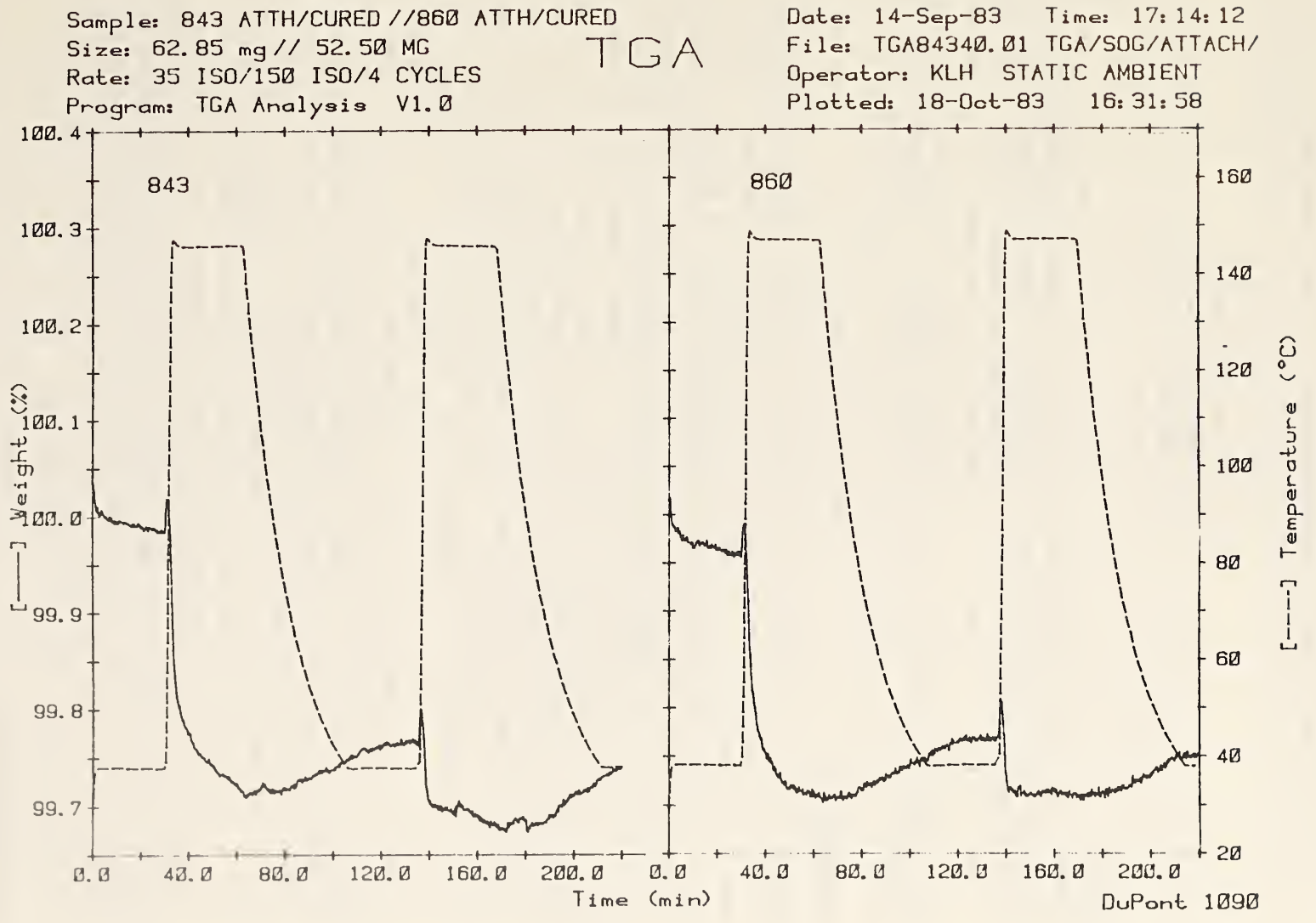
Sample: 843 ATTH/CURED //860 ATTH/CURED
Size: 62.85 mg // 52.50 MG
Rate: 35 ISO/150 ISO/4 CYCLES
Program: TGA Analysis V1.0
TGA
Date: 14-Sep-83 Time: 17:14:12
File: TGA84340.01 TGA/SOG/ATTACH/
Operator: KLH STATIC AMBIENT
Plotted: 18-Oct-83 16:31:58
843
860
100.4
100.3
100.2
100.1
100.0
99.9
99.8
99.7
[——] Weight (%)
160
140
120
100
80
60
40
20
[----] Temperature (°C)
0.0
40.0
80.0
120.0
160.0
200.0
Time (min)
DuPont 1090

8. SESSION VII MOISTURE CONTROL

8.1 MOISTURE IN ELECTRONIC PACKAGING: MEASUREMENT AND THE CONTROL OF IT

George B. Cvijanovich
AMP Incorporated Research
3441 Myer Lee Road
Winston-Salem, NC 27102

Summary

Review of origins of moisture in a sealed package. Systems of measurement of entrapped water (invasive and noninvasive). Possible new technologies for dealing with moisture residues. Suggested methods: accept some moisture, but immobilize ion migration by activation of getters; or use water consuming organic compounds. Use of catalysts to redirect the moisture activity. Importance of ultra-dry rooms in process control. Prospects for VLSI packaging.

Introduction

Several years of experimentation and of operation in the field, with sealed electronic packages, have clearly demonstrated the failure of these systems when the presence of moisture within the package was above a certain limit. The failure is defined here, as the final or the intermittent interruption of the functioning of the system due to the corrosion or electromigration of aluminum from the leads, pads, and other conducting sites located on the chip, or the chip-holding assembly. To quantify this type of failure, most of the people involved in the study of it are looking for some kind of accelerated life test under fairly exotic conditions. Then, most of the effort to solve this problem is directed toward designing a package for a so-called 85/85 test, rather than for a proper long lasting functioning of the device. In many instances not only aluminum is involved in the migration, but also other material such as silver, copper, etc. According to experimental evidence we must strive for essentially two principal design criteria in the packaging of ICs: thermohydrolytic stability and, if necessary, a predetermined oriented diffusion, i.e., a quasi directed corrosion (that will not affect the functioning of the device). The aim is to package a chip for a functional expectancy of about $10^{1 \cdot 2}$ years. This is an average time interval of the "modernity" of a device (about 15 years). This could mean a life time of about 20 years. To quantify such a concept we will adopt what is known as a Mean Time to Failure (MTF) concept. The MTF, at a given site, is proportional to the divergence (or the strength) of the migration ion flux. This definition is based on the assumption that, almost exclusively, the interruption of the functioning of a device occurs when a large portion or the whole of a conductor is removed from its design location. We have, therefore, to relate MTF to moisture and its corroding activity.

Design Criteria

At present we package, within a very small space, a plethora of elements and compounds together: silicon, aluminum, silver, gold, silicon oxide, nitride, assorted series of alloys, polymers, and special organic compounds. Some of

it is in monomolecular layer quantities. In addition, very limiting geometries are imposed on most of the structures designed, such as leads as small as one micrometer square, separated by completely heterogeneous materials. This necessarily complex design generates very hard physical and chemical conditions.

Some operational conditions are determined by the necessity to transport not more than 18,000 to 50,000 electrons from one place to another, or then to handle 10^5 to 10^6 Coulombs/sec/cm^2 per active site. This means that occasionally an active site must dissipate enormous quantities of heat. As an example, the volume resistivity of Al, at 100°C, is about 3.5×10^{-6} ohm cm. At a current density of 10^6 A/cm^2 such systems must dissipate almost 3.5×10^6 W/cm^3. In addition, very often, such leads have significant local microdefects. Therefore, local temperature and concentration gradients are extremely large.

Chemical parameters for the operation of VLSI are even more stringent. Due to high local temperatures and concentration gradients, electrochemical environment becomes especially severe. These conditions, coupled to a large surface to volume ratio, are of central importance in the role of electromigration and the ultimate failure of the device. We believe that, in essence, the local high "chemical temperature islands" represent the ultimate failure factories.

Observed consequences of these conditions are such processes as self diffusion, surface diffusion, electromigration, fast ion transport, thermohydrolysis and local corrosion, growth of material due to stress gradients, whiskers, etc. Almost all of these processes are greatly enhanced in the presence of moisture and operational currents. But, the main question is at what percentage of moisture, the really dramatic and final enhancement occurs. Based on several years of experimental work and field data (and after few thousand pages of print) a tentative limit of 4000 to 6000 ppm of H_2O at STP may be acceptable. We believe that even this amount of moisture, in certain restricted cases, may not be acceptable in local electromigration.

The methods of measurement of entrapped water in a chip are numerous and well known. All of these methods deal, however, with water extracted from the chip. Not all of that moisture is necessarily active in electromigration. We have seen that the ion flux strength is a highly local affair. After inspection of some chips, it was discovered that some of them, even slightly corroded, did not fail.

A new method to discover such active sites consists of using a tritium saturated water (1) in a 85/85 environment, and then take a radio assay print of the chip. The radio assay test, in conjunction with other measurements, shows that the water presence is due mostly to curing of epoxies, molecular flow through cracks and pinholes, to a possible surface catalysis of $2H_2 + 2H_2O$, and very often to careless manufacturing processes (need for ultra dry rooms). Also the main location of the corrosive action, almost always, is at the surface boundaries between the elements of the IC device and the potting compound, and at very sharp edges, where extremely high local fields can exist.

Directed Electromigration

The type of failures, leading to the interruption of functioning of the device, is recognized almost universally as due, at least to some degree, to electromigration.

Electromigration, at an active site, is a form of directed diffusion. A number of people (2, 3) have investigated microdiffusion processes, using Na22 and Cl36 isotopes (figures 1 and 2) in alkyd coatings. When a small potential was applied, an order of magnitude increase in diffusion occurred, as shown in figure 2. If we now consider the MTF as a consequence of locally directed electromigration (through self and surface diffusion), then let us establish the following:

1. The removal of material from a location on the chip through directed diffusion, and

2. The exchange of atomic species at a site is due to ion flux proportional to the current density at the site. In that case, the MTF becomes conveniently measurable, at least to some degree. Thus, we can write MTF α 1/current density = 1/J.

This model, corrected for temperature effects (temperature gradients), leads to an expression of the form MTF α $1/J^3$.

Experiments have shown that for aluminum these relations hold:

MTF α 1/J for J = 10^3-10^5 A/cm^2
MTF α $1/J^3$ for J = 10^5-10^6 A/cm^2

Why this discrepancy for different J?

The inspection of Al leads shows that the crystalites are relatively small compared to the lead structures. Therefore, the contribution to the diffusion from lattice grain boundaries and the surface geometry must be taken into account with more weight. Especially in the case of VLSI where the surface to volume ratio is very large for all leads, and therefore the conventional laws of conduction must be modified. In such cases the limit of bulk to grain conductivity must be redefined. Thus the overall diffusion coefficient D must be written as $D = D_s \cdot D_{gr} \cdot D_l$, i.e., as a combination of surface, grain, and lattice diffusion coefficients. The current density itself, in that case, becomes a nonlocal (4) quantity, as defined in figure 4. In this context, the problem of moisture and its impact on MTF can be related to two stages: the nonlocal, mostly D_s dependent migration, and at a later, catastrophic, stage, to the bulk electrolytic properties of the water.

Tentative Conclusion and Possible Remedies

Based on experimental work and some theoretical models, we think that a highly local electromigration occurs, under minimal presence of moisture, (less than 5000 ppm). According to that model it is more efficient to act locally to modify D_s, and to immobilize water, rather than to try to make a package absolutely dry. Thus, it seems that the use of titanates, or

vanadites is preferred to getters. Such compounds consolidate the local orientation of hydrophylic-hydrophobic chains. The use of these compounds does not exclude the application of moisture binding chemistry. However, the use of titanates makes the functioning of the chip less dependent of its state of dryness.

The application of "water-consuming" organic catalysts is another very intriguing idea.

To ascertain the functioning of a chip packaged in the above fashion, it is best to establish the presence of activity sites and their character by obtaining a tritium radio assay print for each design. Such a print will show the critical points in the packaging system.

Bibliography

1. A. Baily, G. B. Cvijanovich, to be published.

2. J. Bass, The Phil Magazine, Vol. 15, No. 136, pp 717, April, 1967.

3. J. Black, IEEE Trans. Electron Devices, Vol. ED-16, pp 338-347, April, 1969.

   J. Black, "Physics of Electromigration" RADC Tech. Rept. TR-68-243, October, 1969.

4. G. B. Cvijanovich, NBS/RADC Workshop, NBS Special Publication 400-72, April, 1982.

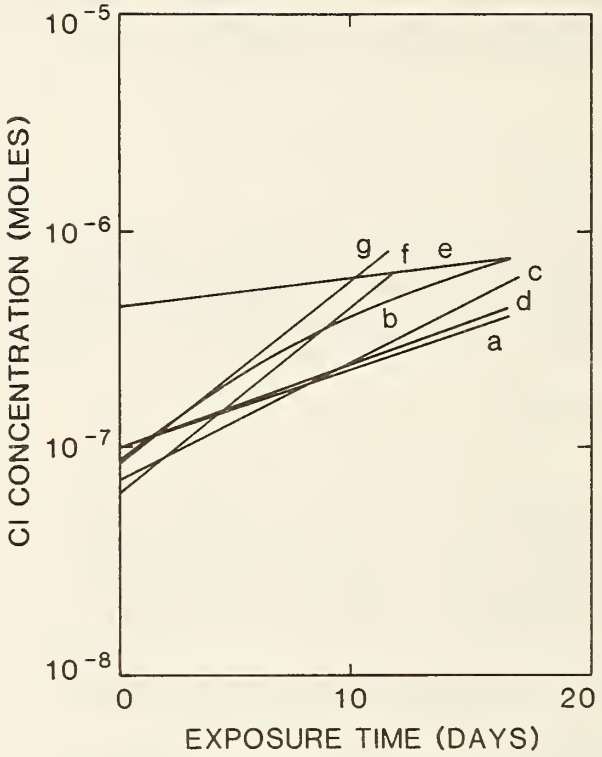

Fig. 1 Chlorine uptake as a function of time for seven different alkyd coatings. Measurements made using Cl-36 isotope. a to g from 25 to 58 microns.

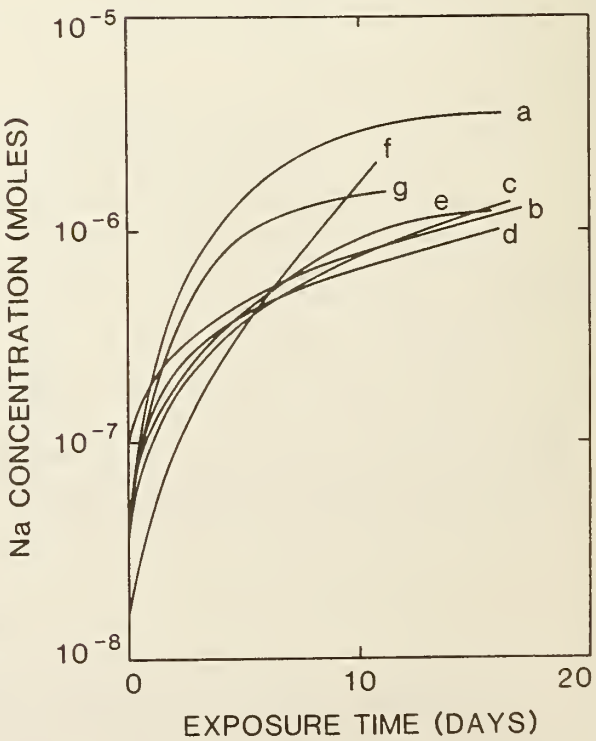

Fig. 2 Sodium uptake as a function of time for alkyd coatings (as in Fig. 1), exposed to 0.5 M NaCl. Measurements were made using Na-22 isotope. The values increase by an order of magnitude when only -0.8 V vs. SCE are applied. (H_3O^+ may play an important role.)

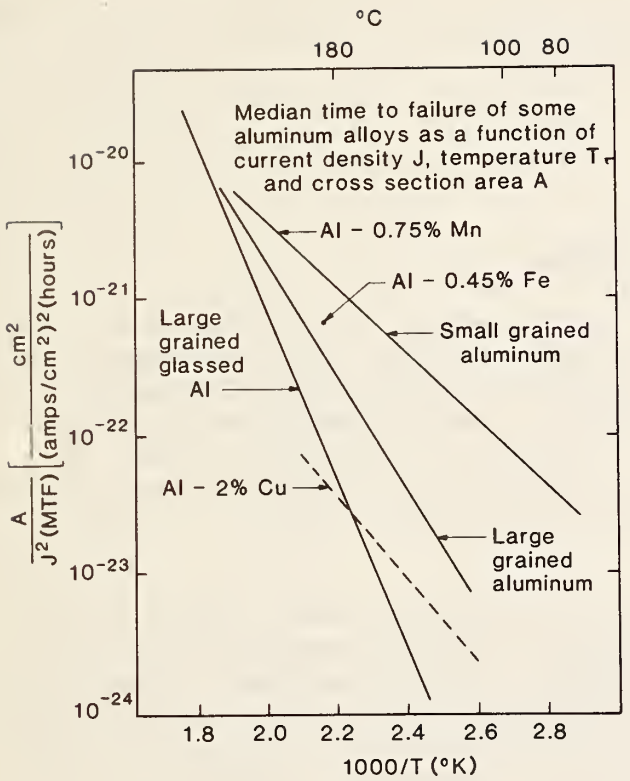

Fig. 3 MTF of some Al alloys as a function of J, T and cross sectional area A.

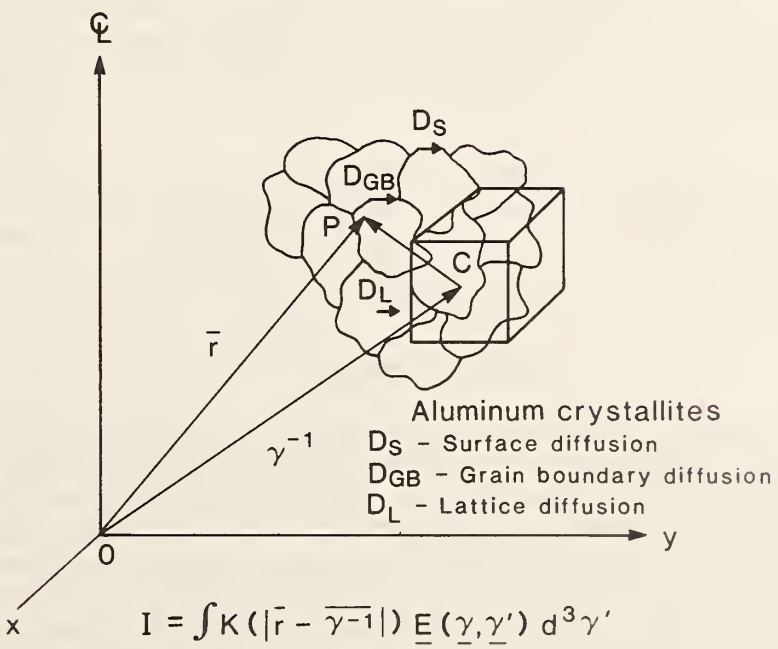

Fig. 4 Current density J as a function of a non-local field E distribution.

8.2 EVALUATION OF MOISTURE SOURCES IN HYBRID MICROCIRCUITS

George H. Ebel, Harry Hammer and Stephen Herman
Singer Company
Kearfott Division
1150 McBride Ave
Little Falls, NJ 07424
(201) 785-2982

ABSTRACT

An effort to evaluate polymeric substrate attachment in hybrid microcircuits led to the study of moisture sources in these devices. Over ten hybrid suppliers, three polymeric material suppliers, three package manufacturers, ROME Air Development Center and several users combined resources to gather the data reported in this paper. The observations presented are based on a comprehensive study of RGA tests on over 500 hybrids. Most of the packages in the study were square metal flatpacks in the range of 1 to 1-1/4 inch on a side.

Possible moisture sources discussed in this paper have been categorized into three basic areas. These are the packages, polymeric materials and processing. Packaging items that will be covered include 1) glass/lead/metal interfaces, 2) base-sidewall junction, 3) internal plating and 4) the advantages of using a special one piece package with no leads for evaluation of polymeric materials. A review of problems associated with the use of polymeric materials include 1) long time thermal decomposition, 2) trapped gasses under large area devices, 3) excess of curing agent, 4) moisture gettering and 5) material handling prior to the curing operation. Areas related to processing that will be discussed are 1) insufficient bakeout (time/temperature), 2) exposure to atmosphere between bakeout and sealing, 3) sealer drybox conditions, 4) rework of poor package seals and 5) necessity for having a flowing atmosphere during the curing and post curing bakes.

Throughout the testing programs, the RGA data were carefully studied to evaluate this method of locating possible moisture sources. Based on these data, recommendations for minimum sample sizes, the use of empty packages and other observations related to bake times and temperatures will be discussed. Also the effect of "rest time" between bake and RGA tests will be covered.

POSSIBLE SOURCES OF MOISTURE

In an earlier paper [1], the details of three groups of round robin testing were reported. Those tests led to the highlighting of most of the possible sources of moisture as listed above. As a result of these tests, particularly the observations made after dye penetrant tests of glass, lead, metal interfaces, it became apparent that a leadless one piece package was the best vehicle for evaluation of polymeric materials used in hybrid packages. Such a package was used for all tests starting with the third round robin. In that round robin, excessively high moisture levels were measured on an epoxy substrate evaluation group of electrolytic nickel plated packages. Moisture levels greater than 1 percent were measured for the evaluation group and for the

empty packages used as control samples in the evaluation. The data is shown in Figure [1] under the heading 'First Seal'. This round robin test included over 120 samples sealed by 8 hybrid suppliers who had, in the previous two round robins, demonstrated their ability to construct hybrid microcircuits with low moisture content. It was theorized that the high moisture levels measured were caused by the electrolytic plating on the cases. A decision was made to run an experiment using empty packages with different plating combinations to evaluate the effects of plating. At the same time, the electrolytic plated packages were delidded, baked out and resealed. RGA (residual gas analysis) measurements were repeated and the moisture content data is shown in Figure [1] under the heading 'Second Seal'. All the reseals showed significantly lower moisture levels. The empty package measurement of 400 PPMV reinforced the theory that plating was at least a partial cause of the 'First Seal' high moisture content.

Empty Package Experiment

Three package suppliers made up one piece leadless packages using the following plating configurations:

1) Electroless nickel over a kovar base

2) Electrolytic nickel over a kovar base

3) Gold plating over electroless nickel on a kovar base

4) Gold plating over electrolytic nickel on a kovar base

The packages were all processed and sealed as a batch. The parts were vacuum baked at 150 degrees C for 24 hours in an oven attached to the package sealer and were transferred directly to the sealer dry box without exposure to the external atmosphere. The packages were sealed as rapidly as possible to minimize dwell time in the dry box. Cell size for RGA analysis was set at eight parts. Two packages from each vendor lot by plating type formed the cell (one vendor had submitted two sets of packages). Four cells were baked at 150 degrees C for 24 hours and four cells were baked at 175 degrees C for 24 hours before RGA was performed. Figure [2] shows the results of this testing. Each line shows the range of moisture content for the eight packages in that cell. The range for the 64 parts was 25 to 600 PPMV. There was little difference between the parts baked at 150 degrees C and the parts baked at 175 degrees C. The best parts, both from the average moisture content and range were the gold over electrolytic nickel packages. The poorest were the electrolytic nickel plated parts. Looking back at the empty package data of Figure [1], the moisture level for the second seal falls in the range of the data for electrolytic nickel plated packages shown in Figure [2].

Round Robin No.4 Epoxy Evaluation

Based on the empty package experiment, the gold over electrolytic nickel package was selected for a new evaulation round of epoxies for substrate attach. Each participant in this test was supplied with all the materials including a sufficient number of packages to seal some empty packages as control samples. The test results are shown in Figure [3]. Evaluation packages as well as empty control samples showed high moisture content with the notable exception of the empty package that had been pre-seal baked in an oven not used for organics. That package showed a moisture level consistent with the data obtained in the empty package experiment.

Review of the data of Figure [3] with both round robin and general industry participants in the epoxy evaluation effort led to the theory of cross contamination (or "epoxy rain") for empty packages baked in the same oven used for curing the packages containing epoxy. The remaining data for the empty packages substantiates the "epoxy rain" theory since two units with flowing N2 in the bake out oven showed appreciably lower moisture levels (0.23 and 0.39 percent) than the all vacuum bake parts (1.08 percent). The parts with the 0.23 percent level were also capped with a loose lid during the bake which adds additional credence to the "epoxy rain" theory. The data for packages with epoxy mounted substrates still shows units with very high moisture levels. A comparison of the Ablestick 555 results in Figures 2 and 3 shows similar moisture levels. The data for Ablestick 555 with reduced curing agent in Figure 3 shows how excess curing agent can affect moisture levels. Comparision of these data in Figures [2 and 3] suggests the need to reduce curing agents in the epoxy formulations to the minimum consistent with maintaining the physical properties required for adhesion. A combination of limited curing agent and appropriate bakeout conditions should minimize this source of moisture in the package. The long term thermal decomposition was considered to be another major source for the high moisture levels measured in this group of tests. IR spectroscopy tests were performed on samples of uncured, cured and cured and baked 550 epoxy. The initial results qualitatively confirm thermal decomposition as a source of moisture. Further testing is necessary to define the effects of long term thermal decomposition. In the general discussions during the data review, the question of how precure handling of an epoxy (shipment, storage, exposure) affected post seal moisture levels was raised. It will be necessary to set up experiments to evaluate possible effects of handling. It should also be noted that in the first two round robins, the test cell size was set at 4 units while in the subsequent tests, cell size was 2 units. The cell sizes were set to provide qualitative results indicating direction of the measured test results.

Summary

While plating can be a source of moisture in a hybrid package, it can be controlled so that package contribution to moisture levels is negligible. Minimizing curing agent in the epoxy should also reduce moisture levels. The effect of long term thermal breakdown needs further evaluation as does the "epoxy rain" theory and the effects of pre-cure handling.

Acknowledgements

The work reported on in this paper represents the efforts of many people in the hybrid industry working together on a common industry problem. The authors wish to particularly acknowledge the following people for their efforts in the empty package experiment.

For supplying packages:

F. Vaccaro - Hermetite
S. Tower - Isotronics
R. Chalman - Tekform

For constructing the test samples:

C. Totten - Rockwell

For testing and control of the experiment:

W. Stewart - RADC

Many others were previously acknowledged [1] and we reaffirm our appreciation for their efforts. With so many participants, it is easy to err and omit a name. We therefore, wish to acknowledge all who have offered help, information and raised many questions in the pursuit of this effort.

REFERENCES

[1] G.H. Ebel, Application of 1018.2 to Hybrid and VLSI Devices Proceedings, Reliability Physics 1983, pp. 274-281.

COMPARISON OF MOISTURE CONTENT IN
ELECTROLYTIC NICKEL PLATED PACKAGES SEALED TWO TIMES

Substrate Attachment Material	Moisture Content,%		Ratio
	First Seal	Second Seal	
Amicon T-86	4.57	.94	4.86
Semi Alloys 915	9.20	3.09	2.98
Ablestik 555	5.88	1.60	3.67
Empty	2.55	0.04	58.6

Note: All parts baked for 100 hrs at 175 degrees C before running RGA.

Figure 1

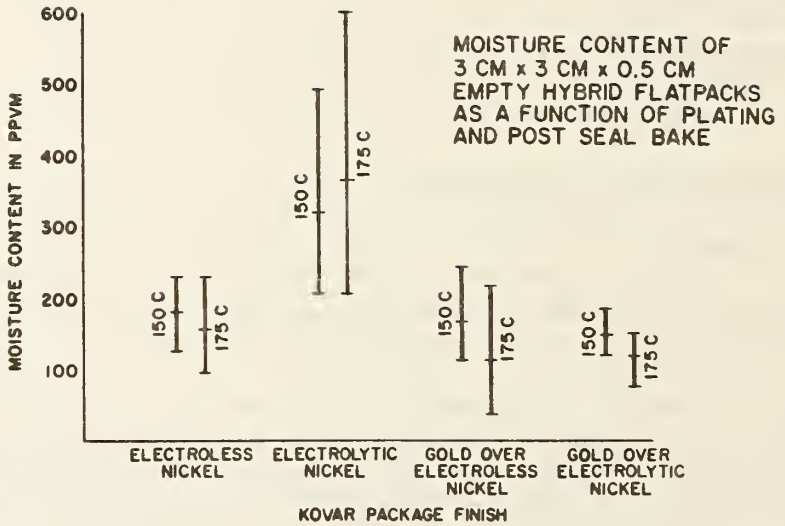

Figure 2

COMPARISION OF MOISTURE LEVEL IN PACKAGES
CONTAING SUBSTRATES MOUNTED WITH EPOXY
WITH EMPTY PACKAGES PROCESSED AT THE SAME TIME

Substrate Attachment Material	Moisture Content,%		Preseal Bake
	With Substrate	Empty Package	
Ablestik 555	4.24	1.08	All Vacuum
Ablestik 555 with reduced curing agent	2.68	0.06 *	All Vacuum
Ablestik 550	1.12	0.39	Flowing N2 followed by Vacuum Bake
Amicon TG-86	0.46	0.23	Flowing N2 followed by Vacuum Bake
Amicon TG-86	0.95	0.77	Vacuum with N2 bleed followed by Vacuum Bake

* Part baked in a separate oven not used for organics

Note: All parts baked 300 hours at 150 degrees C before RGA

Figure 3

8.3 IMPLANTABLE PACEMAKER MOISTURE CONTROL

Jacob A. Ronning, Jr.
Medtronic, Inc.
3055 Old Highway Eight
P.O. Box 1453
Minneapolis, Minnesota 55440

Abstract: Since 1976 Medtronic has been producing hermetically sealed heart pacemakers as its mainline product. The units operate for years in the totally wet environment of the human body, monitoring and pacing the heart when necessary. Moisture concerns for the hermetically sealed designs were different from moisture concerns for the epoxy encapsulated pacemakers that preceeded them. Hermetic sealing processes, cleanliness practice, and internal moisture levels are reviewed along with moisture related product performance.

EPOXY POTTED IMPLANTABLE PACEMAKERS

Older implantable pacemakers consisted of discrete component circuits and batteries encapsulated in epoxy resin potting compounds. After implantation in the body, the epoxy would become 100% moisture saturated.

Moisture related failures could occur if a sufficient size fluid film would develop between portions of the circuit so that unintended leakage currents would result. Adhesion of the epoxy resin to components and interconnecting wires would prevent this type of failure. Components were tested for suitability for epoxy potting. Semiconductors were hermetically sealed components. Moisture related failures were minimized by good cleaning practices to promote epoxy adhesion, by visual examination and rework to prevent circuit bridging bubbles or foreign material, and by maintenance of circuit spacing standards within the epoxy. See Figure 1, Epoxy Potted Pacemaker.

Batteries used were of Mercury-Zinc construction and outgassed hydrogen as their energy was depleted. The hydrogen permeated through the epoxy, minimizing pressure buildup.

HERMETICALLY SEALED IMPLANTABLE PACEMAKERS

Lithium iodide batteries, which are themselves hermetically sealed, brought the improved features of long life and no hydrogen outgassing. Pacemaker designs were then changed to incorporate hermetically sealed enclosures as protection for the circuits and battery. Design considerations in developing the hermetic enclosure were selecting a material to minimize corrosion as a concern and developing a design and processes that would allow virtually no moisture ingress over the life of the pacemaker. See Figure 2, Titanium Hermetically Sealed Pacemaker.

Hermetic Enclosure

Titanium was selected for the pacemaker enclosure. It is a body compatible material with negligible corrosion. In addition, titanium is light weight (about 55% the weight of stainless steel) and can be fabricated by standard

metalworking techniques. The titanium enclosure consists of high precision parts welded together. The parts are inspected and pre-tested to meet design requirements necessary for functionality and for high reliability welding practice. All welds are done with qualified processes and equipment. Each weld seam is visually inspected. Sample weld parts from each weld run are analyzed for acceptable weld penetration and hardness.

The pacemakers are backfilled with helium before the final weld so they can be reliably leak checked in a helium leak detector. They are tested to a 1×10^{-8} standard cc. helium/sec. fine leak rate. Because of helium sorbing materials within the pacemaker, a gross leak will not dissipate the entrapped helium immediately. A fine leak test done within a specified time of the helium backfill and final weld point will detect a gross leak as well as a fine leak. This helium leak test approach is a reliable quality control tool that has been used successfully for years at Medtronic.

Since going to the titanium welded design, over 500,000 units have been built with no returns for hermetic failure. This record was made possible by the use of high reliability parts and processes monitored by an excellent quality assurance program.

Internal Moisture Control

Hermetic sealing of the pacemaker locks in residual moisture and contaminants for the life of the device. "How clean?" and "how dry?" are reliability questions that are addressed by the design and processing of the pacemaker.

The most moisture sensitive circuit elements are the integrated circuit chips. These are mounted in I.C. chip carriers, hermetically sealed and high temperature processed. The I.C. chip carriers become part of a hybrid circuit. They are solder reflow attached to a ceramic thick film circuit along with capacitors and component attach pins. This subassembly is an open hybrid, with hermetically sealed I.C. carriers, ready for cleaning, electrical check and then assembly into pacemaker circuits. (Figure 3)

At the pacemaker assembly stage, discrete components such as a reed switch, diode, crystal oscillator and antenna are added by resistance spotwelding to the hybrid component pins. (Figure 4) Soldering is avoided to minimize flux contamination and cleaning problems. The hybrid with components attached are placed in a plastic assembly carrier with the battery for final cleaning. (Figure 5) The proprietary cleaning process used has been developed to improve cleanliness of parts and assemblies. A key to improving the cleaning process and monitoring its performance is the Ionograph. This measures the quantity of ions extracted from samples and gives a measure of cleanliness expressed in equivalent micrograms of NaCl. The cleanliness levels maintained then, are based on a process capability that has been optimized and monitored with the Ionograph.

After cleaning, the battery and pacemaker connections are made by resistance spotwelding, the titanium shields are closed around the assembly and the seam weld is made. A hole is left in one shield to allow vacuum drying. The vacuum bake process first heats the pacemakers to their maximum storage temperature range (125°F) and then applies a vacuum. After a vacuum of a

sufficiently low level is reached, the required vacuum bake time is started. At the end of the cycle, the vacuum chamber is filled with dry helium. This backfills the pacemakers with helium also. The pacemaker's fill hole is welded shut in a helium environment, preserving the helium within the pacemaker for subsequent hermeticity checking in a helium leak detector.

The effectiveness of the drying process is monitored on samples by measuring total water content in micrograms. Method 1018.2, Procedure 2 is used [1]. By experimentation it has been shown that the total water moisture content of a pacemaker varies with prior moisture exposure, vacuum bake time and temperature, and polymer (epoxy) content of the design [2].

Internal Moisture and Product Performance

Since the adoption of vacuum bake processing to achieve an acceptable internal dryness level, no internal moisture caused failures have been identified as a problem. Over 500,000 units have been produced with this process.

The Medtronic four year test of "Moisture Effects on Passive Hybrid Components" predicts no failure modes for the 0-30% relative humidity range [3]. Vacuum bake process results are in this range.

CONCLUSIONS - PACEMAKER MOISTURE CONTROL

1. The titanium welded hermetic enclosure meets reliability goals with thorough process and quality control.

2. The vacuum bake and proprietary cleaning processes have given the pacemakers sufficient cleanliness and dryness to meet reliability goals.

3. The acceptable dryness range within the pacemaker is probably 0% - 30%, or over, depending on materials and cleanliness.

4. New designs may have different acceptable dryness levels.

5. Internal relative humidity in relation to total water content is useful in comparing dryness between different designs and processes.

REFERENCES

[1] "Total Water Measurement Equipment and Process Using Method 1018.2, Procedure 2". C. Sloneker and B. Church, Moisture Measurement and Control Conference Paper, NBS, November 2-4, 1983.

[2] "Moisture Content Variation in a High Polymer Content Package". B. Church, Moisture Measurement and Control Conference Paper, NBS, November 2-4, 1983.

[3] "Moisture Effects on Passive Hybrid Components". Jacob A. Ronning, Jr. and Allan H. Jevne, Moisture Measurement and Control Conference Paper, NBS, November 2-4, 1983.

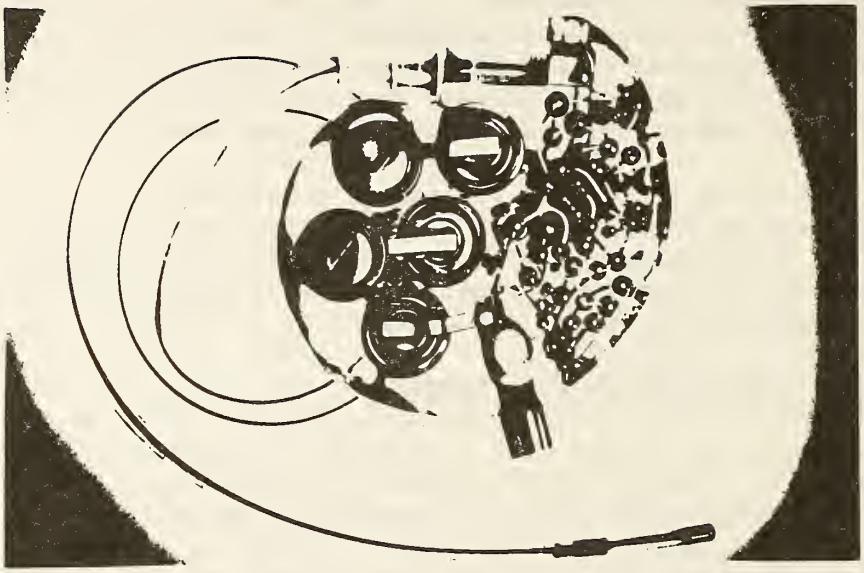

FIGURE 1

EPOXY POTTED PACEMAKER

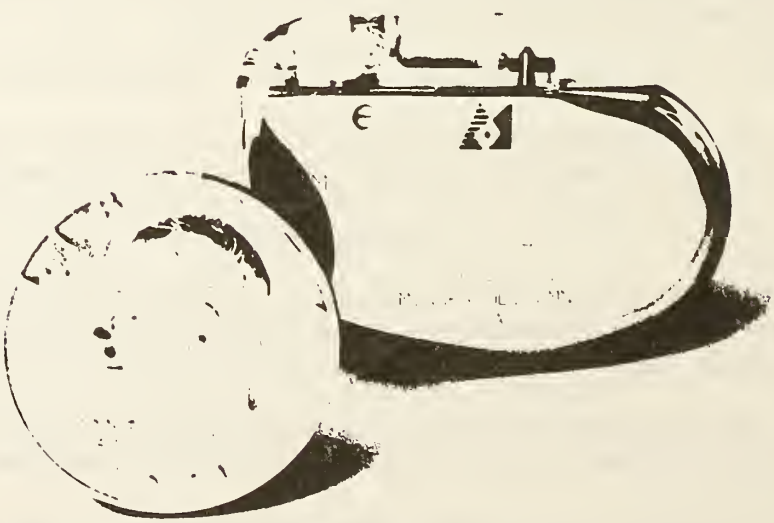

FIGURE 2

TITANIUM HERMETICALLY SEALED PACEMAKER

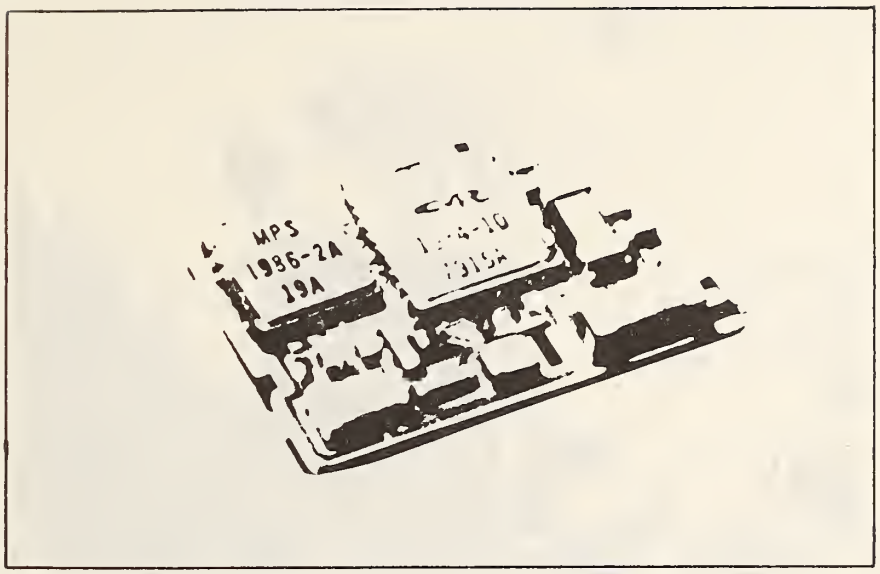

FIGURE 3

HYBRID CIRCUIT SHOWING I.C. CHIP CARRIERS

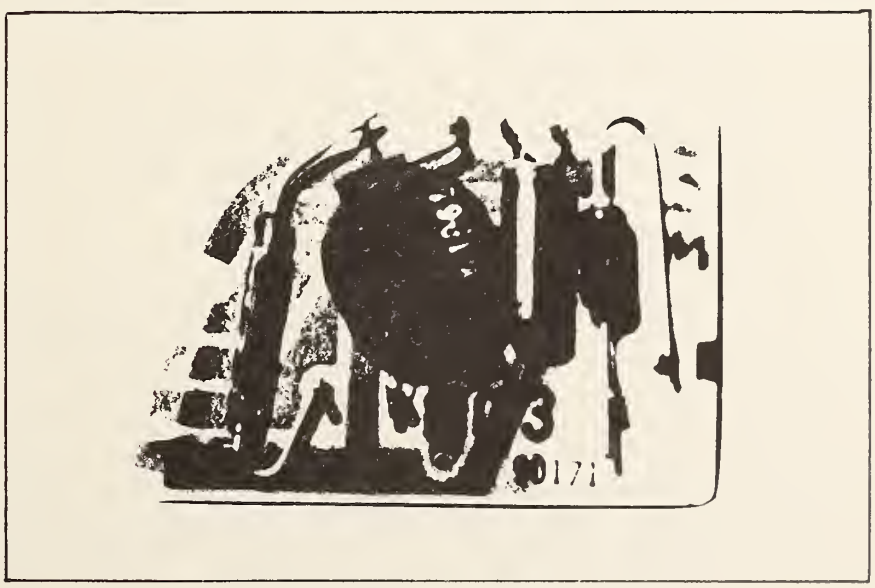

FIGURE 4

HYBRID CIRCUIT SHOWING COMPONENTS
ATTACHED BY RESISTANCE SPOTWELDING

FIGURE 5

HYBRID, BATTERY AND PLASTIC CARRIER

8.4 DETERMINATION OF RELIABLE MOISTURE LEVELS

Bruce Church
Medtronic, Inc.
6951 Central Avenue
Minneapolis, MN 55432
(612) 574-4761

The determination of a reliable moisture level for an electronic package is a difficult process. Many variables enter into the equation. This paper describes an undergoing procedure to evaluate the reliability of a hermetically sealed pacemaker regardless of the configuration. The method uses technology in a step-by-step approach.

The steps involve:

1. The use of an Al_2O_3 sensor mounted inside the device to determine the relative humidity seen by the components at the operating temperature.

2. The determination of the total free water available by heating the device to its maximum storage temperature.

3. Replacing the Al_2O_3 sensor with a surface conductivity sensor and subjecting the device to temperature excursions. This will demonstrate the possibility of reaching humidity levels that allow surface conductivity to begin.

4. Quantify the total water present in the device by Method 1018 or equivalent. This is used to determine the specification for moisture and for process control.

9. WORKSHOP PARTICIPANTS

9.1 List of Speakers

Moisture Measurement Workshop
November 2-4, 1983

James M. Ammons
University of South Florida
4202 Fowler Avenue
Tampa, FL 33620
(813) 974-3532

Naga K. Annamalai
RADC/RBRE
Griffiss Air Force Base
Rome, NY 13440
(315) 330-4055

Bill Bardens
Beckman Instruments, Inc.
2500 Harbor Boulevard
P.O. Box 3100
Fullerton, CA 92634
(714) 773-8666

Bruce Church
Medtronic Inc.
6970 Central Avenue N.E.
Findley, MN 55432
(612) 574-4486

George B. Cvijanovich
AMP Inc.
Myer-Lee Road
Winston-Salem, NC 27102
(919) 727-5298

J. Gordon Davy
Westinghouse
9200 Berger Road
Columbia, MD 21045
(301) 995-5825

Ray Denton
Naval Weapons Support Center
Code 6052
Crane, IN 47522
(812) 854-1338

Aaron DerMarderosian*
Raytheon Co.
528 Boston Post Road
Sudbury, MA 01776
(516) 443-9521 x2791

Diane Feliciano-Welpé
Oneida Research Services, Inc.
3 Ellinwood Court
New Hartford, NY 13413
(315) 736-3057

Victor Fong*
Panametrics, Inc.
221 Crescent Street
Waltham, MA 02254
(617) 899-2719

Paul R. Forant
Varian/Lexington Vacuum Div.
121 Hartwell Avenue
Lexington, MA 02173
(617) 861-7200

Fred Gollob
Gollob Analytical Service
47 Industrial Road
Berkeley Heights, NJ 07922
(201) 464-3331

Ray F. Haack
Jet Propulsion Laboratory
4800 Oak Grove Drive, MS 122-123
Pasadena, CA 91109
(213) 354-6568

Harry Hammer
Singer Company
1150 McBride Avenue
Little Falls, NJ 07424
(201) 785-2982

---

* Session Chairman

Kristen Hanley
Harris Semiconductor
P.O. Box 883
Melbourne, FL 32901
(305) 729-5535

Tom Homa
IBM
Dept. T66, Bldg. 619-1
1701 North Street
Endicott, NY 13760
(607) 755-8639

John Hunter
Advanced Micro Devices
901 Thompson Pl.
Sunnyvale, CA 94088
(408) 749-3089

Harold Joss
Coors Porcelain Company
17750 W. 32nd Avenue
Golden, CO 80401
(303) 277-4057

Dr. John Kiely*
Intel Corp.
3065 Bowers Avenue
Santa Clara, CA 95051
(408) 496-9549

Robert K. Lowry*
Harris Semiconductor
Box 883, MS PT-40
Melbourne, FL 32901
(305) 724-7566

Arnie M. Massoletti
American Microsystems, Inc.
3800 Homestead Road
Santa Clara, CA 95051
(408) 246-0330 x2758

Robert Merrett
British Telecoms Research Labs
Martlesham Heath
Ipswich, IPS 7RE
United Kingdom
473642309

Benjamin A. Moore
RADC/RBRE
Griffiss Air Force Base
Rome, NY 13440
(315) 330-4055

John A. Mucha
Bell Laboratories
Room ID-249
600 Mountain Avenue
Murray Hill, NJ 07940
(201) 582-3659

Louis C. Phillips
Johns Hopkins University
1024 E. 38th Street
Baltimore, MD 21218
(301) 338-8679

Dr. L. J. Rigby
Standard Telecommunication
Laboratories Limited
London Road
Harlow, Essex, England CM17 9NA
0279-29531

Carl Roberts, Jr.
Analog Devices, Semiconductor
804 Woburn Street
Wilmington, MA 01887
(617) 935-5565

Jack A. Ronning, Jr.
Medtronic, Inc. Company
6951 Central Avenue, N.E.
Minneapolis, MN 55432
(612) 574-4761

Thomas J. Rossiter*
Oneida Research Services, Inc.
3 Ellinwood Court
New Hartford, NY 13413
(315) 736-3057

Stanley Ruthberg*
National Bureau of Standards
A331/Bldg. 225
Washington, DC 20234
(301) 921-3625

Stephen D. Senturia
Massachusetts Institute of Technology
Room 13-3010, 77 Mass. Avenue
Cambridge, MA 02139
(617) 253-6869

Robert W. Thomas*
Rome Air Development Center
Griffiss AFB, NY 13441
(315) 330-3730

Judith Weiner
Thomson-CSF
2 Gannett Drive
White Plains, NY 10604
(914) 694-4450

Phillip Vadala
IBM Corp.
1701 North Street
Endicott, NY 13760
(607) 755-8638

Luc Van Beek
Bell Telephone Manufacturing Co.
Gasmeterlaan 106
900 Gent
Belgium
91/35 12 25

Moisture Measurement Workshop
November 2-4, 1983

ATTENDEES LIST

James M. Ammons
University of South Florida
4202 Fowler Avenue
Tampa, FL 33620
(813) 974-3532

David Angst
Bell Laboratories
555 Union Boulevard
Allentown, Pa 18103
(215) 439-5676

Naga K. Annamalai
RADC/RBRE
Griffiss Air Force Base
Rome, NY 13440
(315) 330-4055

Bernhard A. Bang
Westinghouse Electric Corp.
P.O. Box 1521
Baltimore, MD 21203
(301) 765-7340

Bill Bardens
Beckman Instruments, Inc.
2500 Harbor Boulevard
P.O. Box 3100
Fullerton, CA 92634
(714) 773-8666

Sandra Baumler
Westinghouse Electric Corp.
P.O. Box 746, MS V-14
Baltimore, MD 21203
(301) 765-4036

J. J. Bindell
Bell Laboratories
555 Union Boulevard
Allentown, PA 18103
(215) 439-6827

James C. Burrus
Texas Instruments Inc.
P.O. Box 6448, MS 3003
I20 and FM Road, 1788
Midland, TX 79711
(915) 561-6944

Steve Carvellas
Gollob Analytical Service
47 Industrial Road
Berkeley Heights, NJ 07922
(201) 464-3331

E. L. Chavez
Sandia National Laboratories
P.O. Box 5800
Albuquerque, NM 87185
(505) 844-8593

Bruce Church
Medtronic Inc.
6970 Central Avenue N.E.
Findley, MN 55432
(612) 574-4486

George B. Cvijanovich
AMP Inc.
Myer-Lee Road
Winston-Salem, NC 27102
(919) 727-5298

Demetrios Dalietos
Northrop Electronics Corp.
2301 West 120th Street
Hawthorne, CA 90250
(213) 418-4788

J. Gordon Davy
Westinghouse
9200 Berger Road
Columbia, MD 21045
(301) 995-5825

Gary Dency
Harris Corp.
Govt. Aerospace Systems Div.
P.O. Box 37, MS 16-308
Melbourne, FL 32901
(305) 727-4033

Ray Denton
Naval Weapons Support Center
Code 6052
Crane, IN 47522
(812) 854-1338

Aaron DerMarderosian
Raytheon Co.
528 Boston Post Road
Sudbury, MA 01776
(516) 443-9521 x2791

William D. Dorko
National Bureau of Standards
B-364/Bldg. 222
Washington, DC 20234
(301) 921-2886

Michael Ebert
Medtronic Inc.
6970 Central Avenue, N.E.
Fridley, MN 55432
(612) 574-6475

Leonid Finkelshteyn
Technology Glass (Div. of Demetron)
1643 27th Avenue
San Francisco, CA 94122
(415) 566-2928

Bill Fitch
Motorola
4629 E. Sunset Drive
Phoenix, AZ 85028
(602) 897-3331

Diane Feliciano-Welpé
Oneida Research Services, Inc.
3 Ellinwood Court
New Hartford, NY 13413
(315) 736-3057

Victor Fong
Panametrics, Inc.
221 Crescent Street
Waltham, MA 02254
(617) 899-2719

Paul R. Forant
Varian/Lexington Vacuum Div.
121 Hartwell Avenue
Lexington, MA 02173
(617) 861-7200

Dr. Gary T. Forrest
Spectra Physics
25 Wiggins Avenue
Bedford, MA 01730
(617) 275-2650

Peter J. Frasso
Varian/Lexington Vacuum Div.
121 Hartwell Avenue
Lexington, MA 02173
(617) 861-7200 x324

Fred Gollob
Gollob Analytical Service
47 Industrial Road
Berkeley Heights, NJ 07922
(201) 464-3331

Vince Green
Solid State Equipment Corp.
1015 Virginia Drive
Fort Washington, PA 19034
(215) 643-7900

T. F. Gukelberger
IBM Corp.
B/908 D/A29, Box 590
Poughkeepsie, NY 12602
(914) 432-7238

Ray F. Haack
Jet Propulsion Laboratory
4800 Oak Grove Drive, MS 122-123
Pasadena, CA 91109
(213) 354-6568

David C. Hackburth
Cardiac Pacemaker, Inc.
4100 N. Hamline
P.O. Box 43079
St. Paul, MN 55408
(612) 631-3000 x4376

Ronald Hall
Kyocera International Inc.
8611 Balboa Avenue
San Diego, CA 92123
(619) 576-2600

Orjan Hallberg
RIFA AB
S-16381
Stockholm, Sweden

Harry Hammer
Singer Company
1150 McBride Avenue
Little Falls, NJ 07424
(201) 785-2982

Kristen Hanley
Harris Semiconductor
P.O. Box 883
Melbourne, FL 32901
(305) 729-5535

George G. Harman
National Bureau of Standards
B344/Bldg. 225
Washington, DC 20234
(301) 921-3621

Lewis G. Harriman, III
Cargocaire Engineering Corp.
79 Monroe Street
Amesbury, MA 01913
(617) 388-0600

Sab Hasegawa
National Bureau of Standards
B250/Bldg. 221
Washington, DC 20234
(301) 921-3748

Tom Homa
IBM
Dept. T66, Bldg. 619-1
1701 North Street
Endicott, NY 13760
(607) 755-8639

Charles Hopkins
Cordis Corp.
10555 W. Flagler Street
Miami, FL 33174
(305) 551-2520

Nick Horvath
Cardiac Pacemakers, Inc.
4100 Hamline Avenue, North
St. Paul, MN 55164
(612) 631-4410

John Hunter
Advanced Micro Devices
901 Thompson Pl.
Sunnyvale, CA 94088
(408) 749-3089

Harold Joss
Coors Porcelain Company
17750 W. 32nd Avenue
Golden, CO 80401
(303) 277-4057

Ronald Kersey
Fairchild Camera & Instrument Corp.
333 Western Avenue
South Portland, ME 04106
(207) 775-8112

Dr. John Kiely
Intel Corp.
3065 Bowers Avenue
Santa Clara, CA 95051
(408) 496-9549

Allen I. Kine
Northrop Electronic Division
2301 W. 120th Street
Hawthorne, CA 90250
(213) 418-5469

Terry Layton
Burroughs Corp.
P.O. Box 28810
San Diego, CA 92128
(619) 451-4379

Kemp Lehmann
C. M. Kemp Mfg. Co.
Glen Burnie, MD 21061
(301) 761-5100 x333

Thomas E. Libbey
Fairchild
333 Western Avenue
South Portland, ME 04106
(207) 775-8012

Eric W. Lindsay
ITAS-West Coast Technical Service
17605 Fabrica Way
Cerritos, CA 90701
(213) 921-9831

Mike C. Loo
Advanced Micro Devices
901 Thompson Place
Sunnyvale, CA 94088
(408) 749-3847

Robert K. Lowry
Harris Semiconductor
Box 883, MS PT-40
Melbourne, FL 32901
(305) 724-7566

Nigel MacDonald
Cordis Corporation
- Implantables Div.
P.O. Box 525700
Miami, FL 33152
(305) 551-2232

Raymond M. Maffey
General Electric Co.
1 Neumann Way, M/S E7
P.O. Box 156301
Cincinnati, OH 45215
(513) 243-7291

Margie Marlow
Naval Surface Weapons Center
White Oak
Silver Spring, MD 20910
(202) 394-1295

Arnie M. Massoletti
American Microsystems, Inc.
3800 Homestead Road
Santa Clara, CA 95051
(408) 246-0330 x2758

Richard Merrell
ITAS-West Coast Technical Service
17605 Fabrica Way, Suite D
Cerritos, CA 90701
(213) 921-9831

Robert Merrett
British Telecoms Research Labs
Martlesham Heath
Ipswich, IPS 7RE
United Kingdom
473642309

Dr. John Meyer
Raychem Corporation
66 Blauvelt Road
Monsey, NY 10952
(914) 425-9452

Benjamin A. Moore
RADC/RBRE
Griffiss Air Force Base
Rome, NY 13440
(315) 330-4055

Hayden Morris
U. S. Naval Surface Weapons Center
Code U-14, Rm. 2-249
Silver Spring, MD 20910
(202) 394-1295

John A. Mucha
Bell Laboratories
Room ID-249
600 Mountain Avenue
Murray Hill, NJ 07940
(201) 582-3659

Ed Murphy
Pall Pneumatic Products Corp.
4647 S.W. 39th Avenue
Ocala, FL 32674
(904) 237-1220

Wolfgang H. Penzel
Honeywell, Inc.
MN11-1812
600 2nd St., N.E.
Hopkins, MN 55343
(612) 931-6983

Louis C. Phillips
Johns Hopkins University
1024 E. 38th Street
Baltimore, MD 21218
(301) 338-8679

Arthur L. Poole
Pall Pneumatic Products Corp.
4647 S.W. 39th Avenue
Ocala, FL 32674
(904) 237-1220 x126

Frank C. Quinn
10911 Bornedale Drive
Adelphi, MD 20783
(301) 937-6435

Dr. L. J. Rigby
Standard Telecommunication
Laboratories Limited
London Road
Harlow, Essex, CM17 9NA
United Kingdom
0279-29531

Carl Roberts, Jr.
Analog Devices, Semiconductor
804 Woburn Street
Wilmington, MA 01887
(617) 935-5565

James A. Rogowski
Analog Devices Semiconductor
804 Woburn Street
Wilmington, MA 01887
(617) 658-8313 x2362

Jack A. Ronning, Jr.
Medtronic, Inc.
6951 Central Avenue, N.E.
Minneapolis, MN 55432
(612) 574-4761

Harry P. Ross
Western Electric
Dept. 1910
555 Union Boulevard
Allentown, PA 18052
(215) 770-3169

Thomas J. Rossiter
Oneida Research Services, Inc.
3 Ellinwood Court
New Hartford, NY 13413
(315) 736-3057

Stanley Ruthberg
National Bureau of Standards
A331/Bldg. 225
Washington, DC 20234
(301) 921-3625

Stephen D. Senturia
Massachusetts Institute of Technology
Room 13-3010, 77 Mass. Avenue
Cambridge, MA 02139
(617) 253-6869

Christopher T. Shillito
Defense Electronics Supply
Center - EQM
Wilmington Pike
Dayton, OH 45444
(513) 296-6259

Rod Steward
Honeywell Inc.
13350 U.S. Highway 19S
Clearwater, FL 33546
(813) 531-4611 x2676

Milton Stoll
Research Instrument Co., Inc.
36 Mascolo Road
So. Windsor, CT 06074
(203) 528-9625

Bradford L. Sun
Intel Corp.
2896 Kingsgate Ct.
San Jose, CA 95132
(408) 263-3076

Robert W. Thomas
Rome Air Development Center
Griffiss AFB, NY 13441
(315) 330-3730

Phillip Vadala
IBM Corp.
1701 North Street
Endicott, NY 13760
(607) 755-8638

Leopoldo Valero
Zilog Corporation, Dept. 537
1315 Dell Avenue
Campbell, CA 95008
(408) 370-8000 x4866

Luc Van Beek
Bell Telephone Manufacturing Co.
Gasmeterlaan 106
900 Gent
Belgium
91/35 12 25

Danny R. Walker
Defense Electronics Supply
Center - EQM
Wilmington Pike
Dayton, OH 45444
(513) 296-6259

Tom Walker
Naval Weapons Support Center
Code 6052
Crane, IN 47522
(812) 854-1338

Judith Weiner
Thomson-CSF
2 Gannett Drive
White Plains, NY 10604
(914) 694-4450

Stephen Weisskoff
Phys-Chemical Research Corp.
36 West 20th Street
New York, NY 10011
(212) 924-2070

Bob Woodwell
Honeywell Inc.
13350 U.S. Highway 19S
Clearwater, FL 33546
(813) 531-4611 x3516

NBS-114A (REV. 2-8C)

U.S. DEPT. OF COMM. BIBLIOGRAPHIC DATA SHEET (See instructions)	1. PUBLICATION OR REPORT NO. NBSIR 84-2852	2. Performing Organ. Report No.	3. Publication Date May 1984

4. TITLE AND SUBTITLE

RADC/NBS Workshop, Moisture Measurement and Control for Semiconductor Devices, III

5. AUTHOR(S)

B. A. Moore and S. Ruthberg, Editors

6. PERFORMING ORGANIZATION (If joint or other than NBS, see instructions)

NATIONAL BUREAU OF STANDARDS
DEPARTMENT OF COMMERCE
WASHINGTON, D.C. 20234

7. Contract/Grant No.

8. Type of Report & Period Covered

9. SPONSORING ORGANIZATION NAME AND COMPLETE ADDRESS (Street, City, State, ZIP)

10. SUPPLEMENTARY NOTES

☐ Document describes a computer program; SF-185, FIPS Software Summary, is attached.

11. ABSTRACT (A 200-word or less factual summary of most significant information. If document includes a significant bibliography or literature survey, mention it here)

The workshop, one of a series concerned with measurement problems in integrated circuit processing and assembly, served as a forum to examine the continuing progress that has been made in the measurement and control of moisture in hermetically packaged semiconductor devices. Thirty-four presentations are included which contain detailed information for securing hermetic packages with low moisture content. Agreement in measurement has been obtained with the mass spectrometer for cerdip and metal packages at the 5000 ppmv level of moisture through the use of suitable moisture generators, a 3-volume calibrator, calibrated dewpoint hygrometers, and appropriate operational procedures. An approach is given for a reproducible and reliable transfer package. However, the increased use of organic materials in new and rapidly expanding technologies such as VLSI/VHSIC and hybrid packaging presents new and more complex challenges to accurate measurement of interior moisture.

12. KEY WORDS (Six to twelve entries; alphabetical order; capitalize only proper names; and separate key words by semicolons)

Analysis of moisture content; hermetically packaged semiconductor devices; hybrid packages; mass spectrometer measurements; moisture; organic package materials; moisture generators; moisture sensors; quality control; reliability of semiconductor devices; semiconductor devices.

13. AVAILABILITY

☒ Unlimited

☐ For Official Distribution. Do Not Release to NTIS

☐ Order From Superintendent of Documents, U.S. Government Printing Office, Washington, D.C. 20402.

☒ Order From National Technical Information Service (NTIS), Springfield, VA. 22161

14. NO. OF PRINTED PAGES

328

15. Price

$36.50

☆ U.S. GOVERNMENT PRINTING OFFICE: 1984-420-997:149